8-31-2015 12:00 AM

Functional –ESiMe3 Containing Reagents: From Organo-polychalcogenolates to NHC Ligated M-E-SiMe3

Mahmood Azizpoor Fard
The University of Western Ontario

Supervisor
John F. Corrigan
The University of Western Ontario

Graduate Program in Chemistry
A thesis submitted in partial fulfillment of the requirements for the degree in Doctor of Philosophy

Functional –$ESiMe_3$ Containing Reagents: From Organo-polychalcogenolates to NHC Ligated M-E-$SiMe_3$

by

Mahmood Azizpoor Fard

Graduate Program in Chemistry

A thesis submitted in partial fulfillment
of the requirements for the degree of
Doctor of Philosophy

The School of Graduate and Postdoctoral Studies
The University of Western Ontario
London, Ontario, Canada

Abstract

The reaction of M[ESiMe$_3$] (M = Li/Na; E = S, Se) with polyorganobromides, has afforded polychalcogenotrimethylsilane complexes Ar(CH$_2$ESiMe$_3$)$_n$: 1,4-(Me$_3$SiECH$_2$)$_2$(C$_6$Me$_4$) (E = S, **1**; E = Se, **2**), 1,3,5-(Me$_3$SiECH$_2$)$_3$(C$_6$Me$_3$) (E = S, **3**; E = Se, **4**) and 1,2,4,5-(Me$_3$SiECH$_2$)$_4$(C$_6$H$_2$)(E = S, **5**; E = Se, **6**). The powerful potential of these complexes as precursor to combine with other organic reagents such as acyl halides (here ferrocenoyl chloride) lead to polyferrocenylchalcogenoesters: [1,4-{FcC(O)ECH$_2$}$_2$(C$_6$Me$_4$)] (E = S, **7**; E = Se, **8**), [1,3,5-{FcC(O)ECH$_2$}$_3$(C$_6$Me$_3$)] (E = S, **9**; E = Se, **10**) and [1,2,4,5-{FcC(O)ECH$_2$}$_4$(C$_6$H$_2$)] (E = S, **11**; E = Se, **12**).

Two new dichalcogenotrimethylsilane reagents 1,2-(Me$_3$SiSCH$_2$)$_2$(C$_6$H$_4$), **13** and 1,2-(Me$_3$SiSeCH$_2$)$_2$(C$_6$H$_4$), **14** were prepared to further expand the series above. These two new reagents were prepared from 1,2-(BrCH$_2$)$_2$(C$_6$H$_4$) and Li[ESiMe$_3$]. Their reactivity towards metal salts and M-E bond formation was demonstrated when **13** and **14** were reacted with [PdCl$_2$(dppp)] to give two analogous dinuclear organochalcogenolate-bridged complexes [(dppp)$_2$Pd$_2$-μ-κ^2S-{1,2-(SCH$_2$)$_2$C$_6$H$_4$}]X$_2$, [**15**]X$_2$ and [(dppp)$_2$Pd$_2$-μ-κ^2Se-{1,2-(SeCH$_2$)$_2$C$_6$H$_4$}]X$_2$, [**16**]X$_2$ (X = Cl, Br) respectively. To expand this methodology, the tetranuclear palladium complex [(dppp)$_4$Pd$_4$-μ-κ^4S-{1,2,4,5-(SCH$_2$)$_4$C$_6$H$_2$}]X$_4$, [**17**]X$_4$ (X = Cl, Br) was isolated when complex **5** was reacted with a suspension of [PdCl$_2$(dppp)] in the presence of LiBr, as a source of counter ion.

The reactivity of the polychalcogenotrimethylsilanes was developed with a different coordination chemistry system, namely the addition of [(IPr)CuOAc] (IPr = 1,3-bis(2,6-diisopropylphenyl)imidazol-2-ylidene) to solutions of **1**, **2**, **3**, **4** and **6** and the previously reported 1,1´-fc(CH$_2$ESiMe$_3$)$_2$ to yield the poly(NHC)-copper-chalcogenolate complexes, 1,4-[{(IPr)CuECH$_2$}$_2$(C$_6$Me$_4$)] (E = S **18**, E = Se **19**), 1,1'-[fc{CH$_2$ECu(IPr)}$_2$] (E = S **20**,

E = Se **21**), 1,3,5-[{(IPr)CuECH$_2$}$_3$(C$_6$Me$_3$)] (E = S **22**, E = Se **23**) and 1,2,4,5-[{(IPr)CuSeCH$_2$}$_4$(C$_6$H$_2$)] (**24**).

The copper-chalcogenolate [(IPr)Cu-ESiMe$_3$] (E = S **25**, Se **26**, Te **27**) have been prepared from [(IPr)CuOAc] and E(SiMe$_3$)$_2$. Single crystal X-ray analysis illustrates that the structures of complexes **25**-**27** exhibit a pendant –SiMe$_3$ group bonded to a chalcogen atom with a near linear coordination geometry about the copper centre. Reaction of Hg(OAc)$_2$ with freshly prepared **25** [(IPr)Cu-SSiMe$_3$] yielded the ternary cluster [{(IPr)CuS}$_2$Hg], **28** via activation of the S-Si bonds.

This straightforward approach has also been extended by i) substituting copper(I) with silver(I) and ii) by using the smaller NHC ^{i}Pr$_2$-bimy (1,3-diisopropylbenzimidazolin-2-ylidene) instead of IPr.

The reaction of [(IPr)AgOAc] with one equivalent of E(SiMe$_3$)$_2$ (E = S, Se) yielded [(IPr)Ag-ESiMe$_3$] (E = S **29**, Se **30**). The addition of two equivalents of [(IPr)Ag-SSiMe$_3$] to a solution of one equivalent of Hg(OAc)$_2$ in THF led to the first example of a Ag-Hg-sulfide cluster [{(IPr)CuS}$_2$Hg], **31**, which is isostructure with **28**.

Similar reactions between [(^{i}Pr$_2$-bimy)CuOAc] and E(SiMe$_3$)$_2$ (E = S, Se) led to the formation of two new metal-chalcogen complexes, [(^{i}Pr$_2$-bimy)Cu-ESiMe$_3$] (E = S **32**, Se **33**). Unlike the IPr containing complexes **25**-**27**, **29** and **30**, [(^{i}Pr$_2$-bimy)Cu-ESiMe$_3$] exist as dimers in the solid state; this can be attributed to the smaller size of the coordinated ^{i}Pr$_2$-bimy compared to IPr. One consequence of the varying ligand size is demonstrated with the reaction between [(^{i}Pr$_2$-bimy)Cu-SSiMe$_3$] and Hg(OAc)$_2$ which leads to the formation of a ternary cluster with a Cu$_{10}$S$_8$Hg$_3$ core surrounded by six ^{i}Pr$_2$-bimy ligands, [(^{i}Pr$_2$-bimy)$_6$Cu$_{10}$S$_8$Hg$_3$], **34**.

Keywords

chalcogen, polydentate, chalcogenoester, ferrocene, silylchalcogenolate, metal-chalcogen, bridging ligand, palladium, trimethylsilyl chalcogenolate, N-heterocyclic carbene, ternary cluster, copper, silver, precursor, X-ray crystallography,

Co-Authorship Statement

The research discussed in chapters 2, 3, 4, 5 and 6 of this dissertation are the results of major contributions from the author, Mahmoood Azizpoor Fard, under the supervision of Prof. John F. Corrigan. Coworkers from the University of Western Ontario and their detailed contribution are described here.

Chapter 2 describes work published in *Chem. Eur. J.*, **2014**, *20*, 7037-7047 coauthored by Mahmood Azizpoor Fard, Bahareh Khalili Najafabadi, Dr. Mahdi Hessari, Prof. Mark S. Workentin and Prof. John F. Corrigan.

Bahareh Khalili Najafabadi instructed the author on the crystal structure analyses. Dr. Mahdi Hessari instructed the author on cyclic voltammetry of the ferrocene containing complexes. All synthesis, characterizations, and analysis were done by the author under the supervision of Prof. Corrigan. The manuscript was drafted by the author and Prof. Corrigan provided great assistance with editing it.

Chapter 3 describes work published in *Dalton Trans.*, **2015**, *44*, 8267–8277 coauthored by Mahmood Azizpoor Fard, Mathew J. Willans, Bahareh Khalili Najafabadi, Tetyana I. Levchenko and Prof. John F. Corrigan.

Dr. Mathew J. Willans instructed the author on some of the 2D NMR experiments, Bahareh Khalili Najafabadi instructed the author on the crystal structure analyses. Tetyana I. Levchenko instructed the author on TGA experiments, requested by the referees. All synthesis, characterizations, and analysis were done by the author under the supervision of

Prof. Corrigan. The manuscript was drafted by the author and Prof. Corrigan provided great assistance with editing it.

Chapter 4 describes work proposed by the author. All the synthetic and characterization work was performed by the author under the supervision of Prof. Corrigan. The manuscript was drafted by the author and Prof. Corrigan provided great assistance with editing.

Chapter 5 describes work published in *Chem. Commun.*, **2015**, *51*, 8361-8364 coauthored by Mahmood Azizpoor Fard, Prof. Florian Weigend, and Prof. John F. Corrigan.

Prof. Florian Weigend instructed the author on DFT calculation on complex **28**. All synthesis, characterizations, and analysis were done by the author under the supervision of Prof. Corrigan. The manuscript was drafted by the author and Prof. Corrigan provided great assistance with editing it.

Chapter 6 describes work proposed by the author. All the synthetic and characterization work was performed by the author under the supervision of Prof. Corrigan. The manuscript was drafted by the author and Prof. Corrigan provided great assistance with editing.

Acknowledgments

These past four years have been an enormous period of growth in my life. I am finally finishing my PhD degree. However, I would like to express my thanks to some people for their support, assistance and friendship.

First and foremost I would like to thank my supervisor and mentor Professor John F. Corrigan for his non-wavering guidance and support over my attendance in graduate school. His patience, support, knowledge and kindness really helped me through the trials and tribulations of scientific research.

I would like to thank the Department of Chemistry at The University of Western Ontario. Everyone, including support staff, technicians, secretaries, chemistry store staff, faculty members, fellow research associate, undergraduate student and classmate, have made my time in Chemistry more enjoyable. Also I would also like to take this opportunity to thank some of the other people who have made academic or collaborative contributions to this research. Specifically, I would like to thank Dr. Mathew J. Willans, for all of his assistance with my NMR experiments. Dr Paul D. Boyle, for for his operation of the X-ray diffraction facility at Western.

A great deal of thanks goes to my lab mates past and present for their disruptions in the daily laboratory routine that make life interesting. Also thanks to all my friends in the department.

This thesis could not be completed without the support, constant encouragement, and enthusiasm that are beyond comparison, which I have received from my loving wife. I want to thank her for believing in me and giving me much courage and strength. I would like thank my parents for their love and support. To my parents, in particular, you are the two hardest working people I know, and you have sacrificed so much for your children. I thank you for being there for all of us.

Table of Contents

List of Tables

List of Figures

List of Schemes

List of Abbreviations

µL	Microliter
Å	Angstrom
br	Broad
^{n}Bu	*n*-Butyl
^{t}Bu	*t*-Butyl
CCDC	Cambridge Crystallographic Data Centre
°C	Degree Celsius
d	Doublet
dppp	Diphenylphophinopropane
E	Chalcogen Atom
Fc	Ferrocene
FT-IR	Fourier Transform Infrared
g	Gram
GC/MS	Gas Chromatography/Mass Spectroscopy
HMBC	Heteronuclear Multi-Bond Coupling
h	Hour
HOMO	Highest Occupied Molecular orbital
L	Ligand
LMCT	Ligand to Metal Charge Transfer
HSQC	Heteronuclear Single Quantum Spectroscopy
LUMO	Lowest Unoccupied Uolecular Orbital
M	Metal Atom
Me	Methyl
min	Minute
mL	Millilitre
mmol	Millimole
nm	Nanometer
NMR	Nuclear Magnetic Resonance
OAc	Acetate
Ph	Phenyl
PL	Photoluminescence
PLE	Photoluminescence Excitation
ppm	Parts Per Million
^{i}Pr	*Iso*-Propyl
R	Organic Side Group
s	Singlet (NMR)
THF	Tetrahydrofuran
TGA	Thermogravimetric Analysis
TMS	Tetramethylsilane
UV	Ultraviolet
vis	Visible
vt	Virtual Triplet

Chapter 1

1.1 Introduction

It is common that the three heavy elements of the oxygen sub-group, namely sulfur, selenium and tellurium, be collectively referred to as the "chalcogens".[1] The chalcogens have a rich metal chemistry both in molecular compounds and in the solid state, on account of their ability to catenate and to bind to multiple metal centers. The early progress in the identification of the many possible coordination modes available for sulfide ligands was summarized neatly by Vahrenkamp.[2] The coordination modes and structural types of soluble metal selenides and tellurides, synthesized in solution or in the solid state, have been classified and described in the seminal review by Ansari and Ibers.[3] A large number of metal-chalcogenide solids are known to exhibit semiconducting behavior and excellent thermoelectric properties. They have been the focus of solid state research due to their potential for widespread applications, including rechargeable batteries,[4] thermoelectric energy converters,[5] and phase memory devices.[6] Furthermore the interest in metal–chalcogen complexes is further enhanced due to the significant role that they play in bioinorganic chemistry and in hydrodesulfurization and other catalytic processes.[7] Finally, the nanomaterials chemistry of metal-chalcgoenide has kept this class of compounds at the fore of chemical and materials research.[8]

The rich synthesis and structural chemistry of molecular, metal-chalcogen compounds developed due to the flexibility of chalcogen ligands in adopting several bridging coordination modes. To prevent extensive condensation reactions and the formation of bulk solids, metal-chalcogen assemblies must typically be kinetically stabilized.

Organochalcogenolate ligands RE^- are often being used in conjunction with chalcogenide ligands E^{2-} in the synthesis of metal-chalcogen complexes.[9]

1.2 Chalcogen Containing Ligands

There is a wide structural diversity in the coordination number and coordination geometry of chalcogenide (E^{2-}) and chalcogenolate (RE^-) ligands (E = S, Se, Te) that is rooted in the bonding flexibility of chalcogen atoms. This is demonstrated by their strong tendency to bridge two or more metal centers. This feature plays a significant role in the structural diversity in metal-chalcogen chemistry. Flexible coordination modes of chalcogenide and chalcogenolate ligands can be attributed to their high polarizability and the anionic nature of these ligands. Consequently, E^{2-} and RE^- ligands, compared to neutral chalcogen containing ligands such as H_2E, R_2E and REH, form more stable metal-chalcogen complexes in both bridging and terminal modes.

1.2.1 Chalcogenide Ligands

The most typical bonding modes of chalcogenide ligands are μ_2-, μ_3- and μ_4-, while the other higher coordination numbers are also observed (Figure 1.1). Among the reported metal-chalcogenide cluster complexes, the μ_3- and μ_4- coordination modes are more common in chalcogenide ligands. Going from S→Se→Te, with increasing ionic radii and polarizability, their ability to bridge a larger number of metal centres increases. Therefore heavier chalcogen atoms exhibit higher diversity of coordination modes in chalcogen-metal clusters.[10]

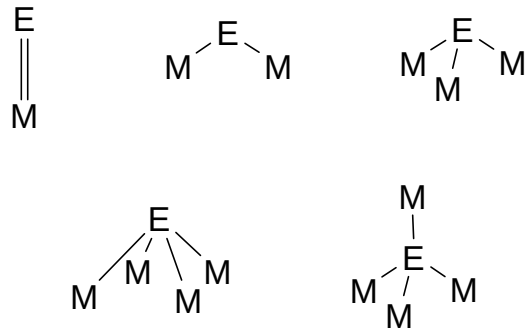

Figure 1.1. Common coordination modes of chalcogenide (E^{2-}) ligands.[10]

1.2.2 Chalcogenolate Ligands

Organochalogenolate ligands (RE^-) play an important role in metal-chalcogen cluster chemistry. Despite many examples of terminal coordination of organochalogenolate, they tend to bridge metal centers as well. In contrast to chalcogenides, the coordinating ability of organochalogenolate can be modified by changing the organic substituent "R". Organochalogenolate ligands are also able to adopt a terminal coordination mode on metal-chalcogen clusters. This has allowed access to metal chalcogenolate/chalcognide clusters that are not available in metal chalcogenide chemistry.

1.3 Synthesis of Metal-Chalcogen Complexes

A variety of synthetic strategies have been designed to access metal chalcogenide assemblies. One of these methods involves the reaction of a metal salt and an alkali-metal chalcogen source M_2E (M = alkali metal, E = S, Se).[11] As an example, the reaction of $CuCl_2 \cdot H_2O$ with EtS^- in the presence of Li_2S led to the copper(I) sulfide cluster $[Cu_{12}S_8]^{4+}$. The insolubility of alkali-metal chalcogen salt limits the ability to carry out this type of reaction in homogeneous solutions.

Other techniques involve the reaction between a metal salt and chalcogenols, REH (R = alkyl, aryl; E = S, Se, Te) (eq 1.1).[12] This method is also is also known to introduce difficulty, especially in the case of tellurium chemistry, where tellurols are thermally unstable and light sensitive starting materials.[13]

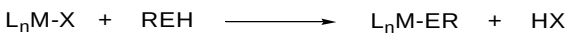

(eq. 1.1)

Direct insertion of chalcogen into metal-carbon bond (eq. 1.2, E = elemental chalcogen) has also been reported. This reaction normally happens at elevated temperatures due to the insolubility of the chalcogen.[14]

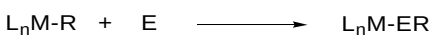

(eq. 1.2)

Oxidative addition (eq. 1.3) has also been employed in the synthesis of chalcogenolate complexes,[15] although, bulky dichalcogenide proceed too slowly in oxidation process and may not be applicable in this procedure.

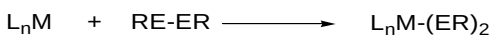

(eq. 1.3)

Silylated chalcogen reagents are valuable precursors for the synthesis of metal-chalcogen containing materials (eq. 1.4-1.6).[16] Silylated chalcogen reagents display two advantages in metal-chalcogen bond formation reactions. First, the lability of E-Si bond

leads to cleavage under mild conditions, and second the reactivity of this bond can be controlled by steric and electronic effects of substituents on the silyl group.[17]

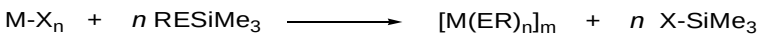

(eq. 1.4)

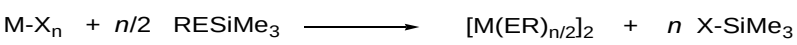

(eq. 1.5)

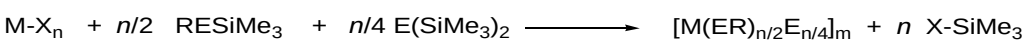

(eq. 1.6)

The driving force for such reactions is the formation of a X-Si bond and elimination of the X-$SiMe_3$ (X = OAc, halide) as the side product. As an additional benefit, the solubility, stability and volatility of X-$SiMe_3$ allows the clean isolation of the products.[18]

1.4 Trimethylsilyl Chalcogenoether Reagents

As described above, trimethylsilyl chalcogenoethers of the general formula $RESiMe_3$ or $ArESiMe_3$ (R = alkyl, Ar = aryl, E = S, Se, Te) offer a convenient, easily handled source of organo-chalcogenolate and are a powerful class of reagents due to their demonstrated ability to react smoothly with metal salts MX (X = halide, acetate) to form metal chalcogenolate cluster and nanocluster complexes $(M–ER)_x$, through the thermodynamically favourable elimination of $XSiMe_3$.[9, 19] This includes their use in nanoparticle chemistry, where silylated reagents have been utilized to passivate the surface of metal chalcogenide cores.[20] The 'tunability' of the substituent R- and Ar- gives the opportunity to introduce different characteristic to metal chalcogenolates and nanoclusters through these ligands. Despite their wide ranging utility, only a relatively limited number

of polychalcogenotrimethylsilane reagents have been reported, which is confined to a few bidentate aryl-chalcogenotrimethylsilane complexes.[21]

There are different possible approaches to form a silylated chalcogen group (E-$SiMe_3$) on an organic framework. The synthesis of $Ar(ESiMe_3)_n$ (Ar = aryl, E = S, Se) reagents can be readily carried out by insertion of elemental sulfur or selenium into C-Li bonds, followed by reaction with $ClSiMe_3$ to yield aryltrimethylsilylchalcogenoethers, $Ar(ESiMe_3)_n$.[22] Such reaction is driven by the thermodynamically favourable formation of an alkali metal halide (LiCl).[23] It is shown that the silylation of $Li[Se(C_6H_4)_nSe]Li$ (n = 0, 1) complexes with chlorotrimethylsilane $ClSiMe_3$ affords $Me_3SiSe(C_6H_4)_nSeSiMe_3$, which possesses two functionalized Se centres (Scheme 1.1). The reactivity of bidentate $Me_3SiSe(C_6H_4)_nSeSiMe_3$ toward metal salts and their ability to link metal centres with the facile formation of diselenolate complexes $^-Se(C_6H_4)_nSe^-$ of Pd(II) and Au(I) have been demonstrated (Scheme 1.2).[24]

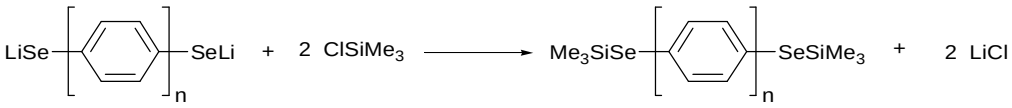

Scheme 1.1. Silylation of $Li[Se(C_6H_4)_nSe]Li$ complexes with chlorotrimethylsilane

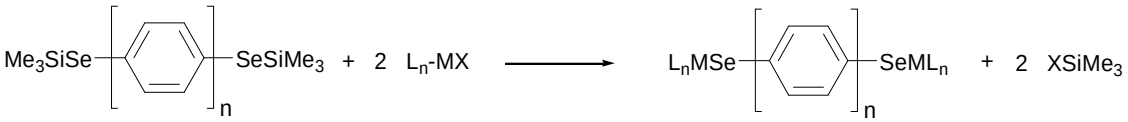

Scheme 1.2. Reactivity of bidentate $Me_3SiSe(C_6H_4)_nSeSiMe_3$ toward metal salts

In a similar procedure 1,1´-bis(trimethylsilylseleno)ferrocene, 1,1´-$fc(SeSiMe_3)_2$ was prepared via the reaction of chlorotrimethylsilane and $[Fe(\eta^5\text{-}C_5H_4SeLi)_2(tmeda)]$.[25] The reagent 1,1´-$fc(SeSiMe_3)_2$ was used for the assembly of high nuclearity metal clusters

containing multiple ferrocenyl units arranged around a central metal chalcogen core.[26] It was communicated that the surfaces of binary metal-chalcogen clusters can be passivated and functionalized through the use of the ferrocenyl reagent 1,1´-fc$(SeSiMe_3)_2$, which serves as a soluble source of ($fcSe_2^{2-}$) during cluster forming reactions. Furthermore, the incorporation of 1,1´-ferrocenyldiselenolate ($fcSe_2^{2-}$) in the synthesis of palladium and platinum complexes from 1,1´- bis(trimethylsilylseleno)ferrocene was reported.[27]

Li[$ESiMe_3$] is also used to prepare Ar-$ESiMe_3$ and R-$ESiMe_3$ via nucleophilic displacement reactions with organo halides. Utilizing this methodology to prepare bidentate organo trimethylsilyl chalcogenides, 1,1´-fc$(CH_2Cl)_2$ can also be readily converted to 1,1´-fc$(CH_2ESiMe_3)_2$ by nucleophilic displacement of Cl^- with $[ESiMe_3]^-$ (Scheme 1.3).[28]

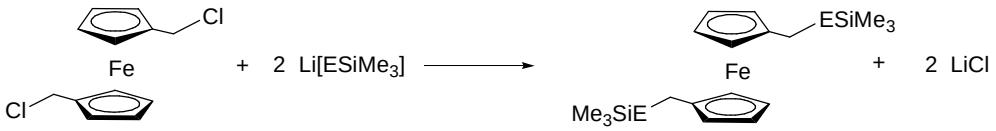

Scheme. 1.3 Synthesis of 1,1´-fc$(CH_2ESiMe_3)_2$

The bidentate ligand precursor 1,1´-fc$(CH_2SeSiMe_3)_2$ leads to dimeric [{Zn(fc$(CH_2Se)_2$)(tmeda)}$_2$] with two bridging 1,1´-fc$(CH_2Se)_2^{2-}$ versus a chelated [Zn(fc$(CH_2Se)_2$)(tmeda)] via reaction with [$Zn(OAc)_2$(tmeda)] (Scheme 1.4).[28]

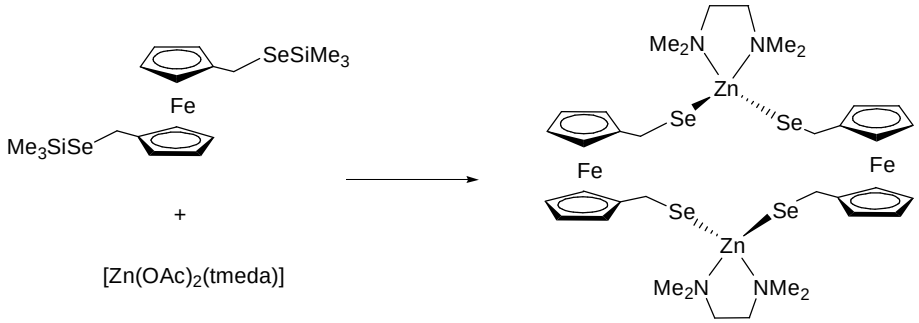

Scheme 1.4. Synthesis of [{Zn(fc$(CH_2Se)_2$)(tmeda)}$_2$]

1,4-bis(trimethylsilylthio)-2-butyne and 1,4-bis(trimethylsilylseleno)-2-butyne are two other rare examples of polychalcogenotrimethylsilane complexes, synthesized via the reaction between $Li[ESiMe_3]$ (E = S, Se, respectively) and the corresponding dibromide reagent.[21c]

1.5 Chalcogeno esters

Trimethylsilyl chalcogenoethers can play a significant role in development of convenient and efficient methods for the synthesis of chalcogenoesters. Trimethylsilyl chalcogenoethers are able to react with reactive organic precursors such as acyl halides to form chalcogenoesters (eq. 1.7).[29]

$$(R/Ar)\text{-}ESiMe_3 + (R/Ar)\text{-}C(O)Cl \longrightarrow (R/Ar)\text{-}E\text{-}C(O)\text{-}(R/Ar) + ClSiMe_3$$

(eq. 1.7)

Capperucci and Degl'Innocenti demonstrated that phenylselenotrimethylsilanes can behave as an efficient transfer agent of selenolate groups, affording a general access to selenoesters in good yields. They used nucleophilic fluoride anion to increase the reactivity of $PhSeSiMe_3$ in the reaction with acid chlorides.[29b]

Chalcogenoesters (also known as acyl chalcogenides) have attracted considerable attention, due to the importance of these S and Se systems in organic synthesis.[30] Chalcogenoesters are also useful synthetic intermediates and are employed as building blocks for the synthesis of a large variety of organic complexes.[31] Other common methods to prepare selenoesters include the reaction of acyl halides with selenols, or alkali metal selenide salts,[32] transition-metal catalyzed carbonylation,[33] and the Pd-catalyzed coupling of stannyl/silyl selenide and acyl halides.[34] They have also been prepared by the reaction of aldehydes, acyl halides, or esters with organoselenolato reagents, such as C_6H_5SeTl,[35] $Hg(SeR)_2$ (R = alkyl, aryl),[36] and $Me_2AlSeMe$,[31a, 37] as well as reactions between acyl chlorides and $C_6H_5SeSeC_6H_5$ mediated by indium iodide[38] or $RhCl(PPh_3)_3$.[39] Zhang and

co-workers have also reported novel syntheses of selenoesters by using SmI_2,[40] $Sm/TMSCl/H_2O$,[41] $TiCl_4$-Sm,[42] $Sm/CrCl_3$,[43] and $Sm/CoCl_2$[44] as reducing agents. Other methods include treating aryl selenocyanates with carboxylic acids,[45] and α,β-unsaturated selenoesters can be prepared by the reaction of acylzirconocene chlorides with electrophilic selenium bromides.[46]

Bidentate trimethylsilylselenide complexes of the type Me_3SiSe-Ar-$SeSiMe_3$ and 1,1´-$fc(SeSiMe_3)_2$ have also been employed for the formation of diselenoester complexes (Scheme 1.5 and 1.6).[29a]

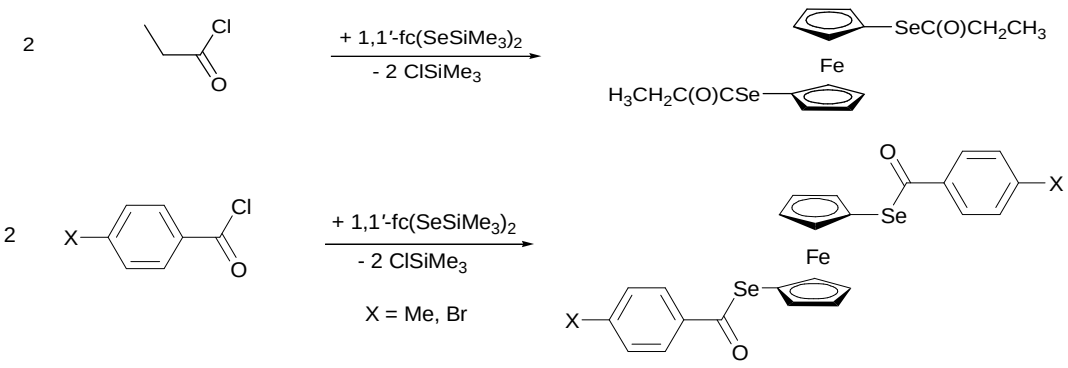

Scheme. 1.5 Synthesis of diselenoester complexes via 1,1´-$fc(SeSiMe_3)_2$ and RC(O)Cl

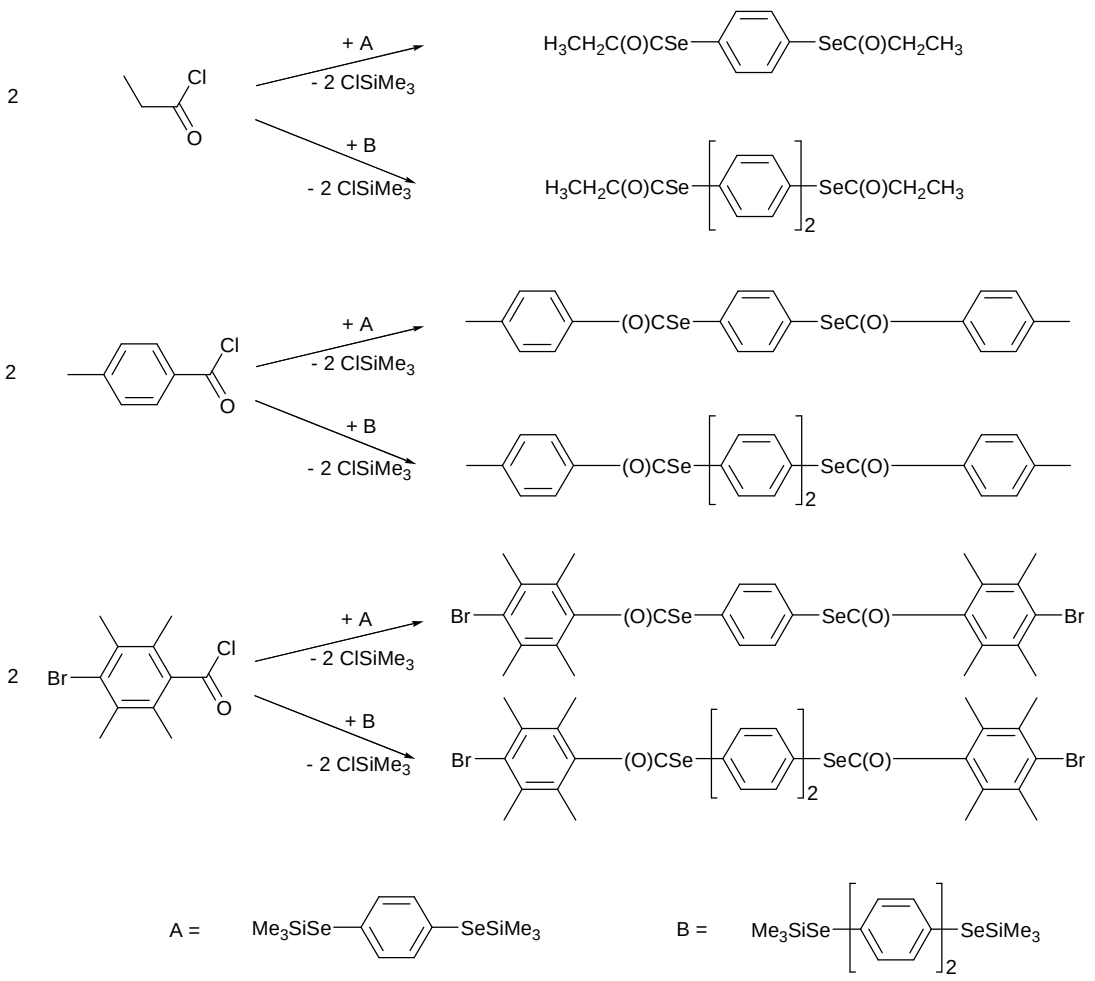

Scheme 1.6. Synthesis of diselenoester complexes via Me_3SiSe-Ar-$SeSiMe_3$ and RC(O)Cl

1.6 M-$ESiMe_3$ Precursors

Trying to find a general strategy for the controlled synthesis of mixed metal MM´E compounds has directed research efforts toward the synthesis of a reactive metal-chalcogen precursors with the general formula of [$L_nM(ESiMe_3)$] (E = S, Se, Te). This type of complex is synthesized via the reaction of L_nMX (X = Cl, AOc; L = ancillary ligand) and bis(trimethylsilyl chalcogenide) $E(SiMe_3)_2$, under mild conditions. $E(SiMe_3)_2$ (E = S, Se, Te) has already been widely used in the synthesis of binary metal-chalcogen clusters through the replacement of both –$SiMe_3$ groups with the same metal to form M-E-M

moieties.[47] Here, under appropriate conditions, one of the -$SiMe_3$ groups of $E(SiMe_3)_2$ is selectively eliminated via reaction with a L_nMX salt, to form a silyl-functionalized metal chalcogenolate complex, L_nM-E-$SiMe_3$. Various type of ancillary ligands "L", such as amines and phosphines, have been used to induce terminal coordination of –$ESiMe_3$ on a single metal centre.

This class of complex was first reported by Yu in the synthesis of the complex $[(PEt_3)_2Mo_2(OAc)_2(SSiMe_3)_2]$ (eq. 1.8)[48] and has been expanded greatly by the Corrigan group by introducing a wide range of d-block metals and ancillary ligand types to this area of chemistry.[49]

$$Mo(OAc)_4 + 2.2\ PEt_3 + 2.2\ E(SiMe_3)_2 \longrightarrow [(PEt_3)_2Mo_2(OAc)_2(SSiMe_3)_2]$$

(eq. 1.8)

In this regard the coinage metal precursors $[L_nCuESiMe_3]$ and $[L_nAgESiMe_3]$ have received considerable attention due to their specific role in ternary polynuclear cluster assembly.[50] The size and the number of ancillary ligands "L" about the metal centre can determine the reactivity and stability of $[L_nCuESiMe_3]$ and $[L_nAgESiMe_3]$ complexes and influence the size and stability of the final ternary clusters.[50a, 50c, 50e]

Applying four different tertiary phosphines in order to synthesize various silyl-functionalized copper and silver chalcogenolates, sixteen complexes of $[L_nMESiMe_3]$ (L = tertiary phosphine, E = S, Se, Te) have been reported.[50a, 50d, 50e] The melting points of these complexes range between -50 to 10°C. Such low melting points and a corresponding thermal instability of these type of complexes $[L_nM$-$ESiMe_3]$ have made them relatively difficult to handle and store them for longer periods of time. The phosphine ligands are released during the thermal decomposition process, producing polynuclear clusters of the corresponding binary systems (eg. Cu_2S).[47a]

Employing the stronger σ donor N-heterocyclic carbenes (NHCs) as the ancillary ligand provides thermodynamically stronger copper- and silver-ligand interaction versus tertiary phosphines.[51] This could provide a route to more thermally stable silyl chalcogenolate precursors. The steric properties of the NHC can be another key component in the stability of L-M-ESiMe$_3$ due to the ability to block additional coordination sites around the metal centre, forcing terminal coordination of the –ESiMe$_3$. An investigation of this hypothesis represents a significant component of this thesis.

1.7 Binary Cu-E and Ag-E clusters

The chemistry of chalcogenide-bridged molecular clusters of the coinage metal elements represents an ever-developing area in chemical and materials science research. This can be due to, in part, the fact that binary coinage metal-chalcogenides exhibit relatively high ionic and even higher electric conductivity in the solid state, leading to properties intermediate between those of semiconducting and metallic phases.[52] Secondly, the size-dependence of the chemical, physical, and structural properties of substances on going from small molecules to bulk materials is of general interest.[53] Colloid nanoparticles with narrow cluster size distributions[54] and crystalline cluster compounds suitable for single-crystal X-ray diffraction analysis are the two main interesting categories in this area. In both cases, the molecules have to be kinetically protected from further reaction to the thermodynamically favoured extended solids.

A ligand sphere coordinating to the outer metal or chalcogen atoms is therefore required to prevent uncontrolled oligomerization, and the formation of bulk material, and to also provide solubility in organic solvent. It has been shown that in most cases the polynuclear core of the clusters is surrounded by tertiary phosphine molecules or a combination of phosphines and organic groups.[47b, 55]

As mentioned earlier, a general route to copper–chalcogenide–phosphine clusters has been developed.[19a] The reactions of metal halide or carboxylate with bis(trimethyl)chalcogenide in the presence of phosphine leads to the formation of metal-

chalcogenide clusters under the elimination of trimethylsilyl-halide or -carboxylate (eq. 1.9).

$$CuX + n\ PR_3 \xrightarrow{+\ E(SiMe_3)_2} [(PR_3)_xCu_yE_z] + XSiMe_3 \qquad (X = Cl, OAc)$$

(eq. 1.9)

The driving force of the reaction is the elimination of thermodynamically favourable side product, $XSiMe_3$. The formation of the specific cluster complexes depends very much on the size and the nature of the ancillary ligand, the reaction conditions, as well as the solvent used for the synthesis.[47a, 47c]

Fenske and co-workers have employed $RESiMe_3$ and/or $E(SiMe_3)_2$ with phosphine ligated metal salts to produce a wide range of binary metal-chalcogen clusters. By varying the nature of the surface-stabilizing phosphine ligands together with reaction conditions, one can isolate a large variety of core sizes ranging from the molecular to the nanoscale in single-crystalline form.[19a, 56] The optical and electronic properties of these Cu_2E clusters can be tuned by controlling the assembly of these monodisperse systems. A systematic colour change is observed from red (Cu_{12})[57] through brown (Cu_{36})[58] and dark brown (Cu_{70})[59] to black (Cu_{146}).[60] Preliminary studies also show a relationship between size and conductivity of the clusters.

Due to the stronger σ-donating property of N-heterocyclic carbene with coinage metals compared with tertiary phosphines, applying them in the synthesis of new coinage metal clusters may improve their stabilization.[61] Khalili Najafabadi and Corrigan have recently found that the N-heterocyclic carbene $^{i}Pr_2$-bimy ($^{i}Pr_2$-bimy = 1,3-di-isopropylbenzimidazole-2-ylidene) can be used as an excellent ligand for the stabilization of silver–phosphorus polynuclear complexes. They showed that the reaction of [($^{i}Pr_2$-bimy)$_2$AgOAc] and $P(SiMe_3)_3$ in two different ratios (2:1 and 2:0.9) leads to the first examples of using NHCs to stabilize the AgP nanoclusters [$Ag_{12}(PSiMe_3)_6(^{i}Pr_2\text{-bimy})_6$] and [$Ag_{26}P_2(PSiMe_3)_{10}(^{i}Pr_2\text{-bimy})_8$], respectively) (Figure 1.2).[62]

Obviously the steric requirements of the NHC $^{i}Pr_2$-bimy is not large enough to limit the coordination number around the metal centres to prevent cluster formation.

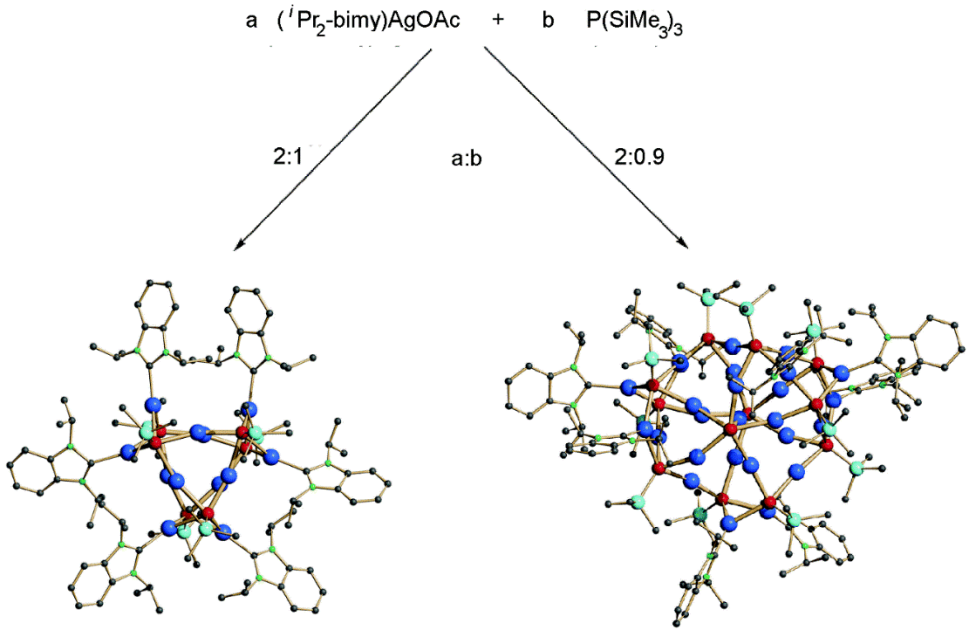

Figure 1.2. Molecular structures of the AgP nanoclusters, stabilized via NHC[62]

1.8 N-Heterocyclic Carbenes (NHCs)

A carbene is a neutral molecule that has an electron deficient divalent carbon atom. In N-heterocyclic carbenes the carbenic carbon atom assumes a bent geometry where this arrangement suggests a sp^2 hybrid orbital on the carbon. The steric and electronic effects of the substituents around the carbenic carbon play a very significant role in the ground-state spin multiplicity of the non-bonding electrons of divalent carbon and in stability of N-heterocyclic carbenes. In 1962 Wanzlick and co-workers showed that the stability of carbenes could be dramatically enhanced by having strong electron donor groups around the carbene centre, such as amine substituents. Electronic effects can be divided into two parts inductive effects and mesomeric effects.

In the inductive effect, the σ electron withdrawing substituent around the carbene centre stabilizes a singlet state over a triplet state, which is due to increasing the *s* character of *σ* non-bonding orbitals. Consequently it increases the gap between *σ* and *pπ* orbitals in the singlet state.

Having a *σ* donor substituent will reduce this energy gap (*σ-pπ*), as *σ* is destabilized which will favour the triplet state.[63] Mesomeric effects influence the multiplicity of a carbene as well.

Most of the substituents around the carbene centre have greater electronegativity values than does carbon and act as *σ*-acceptors to stabilize the carbene lone pair. Increasing the steric bulk of the substituents will cause smaller carbene bond angle N-C-N or longer carbene bond lengths N-C. This increases the *pπ* character and favors the triplet state carbene. Bulky substituents adjacent to the carbenic carbon also sterically disfavour dimerization to the corresponding olefin. In general these electronic and steric effects go a long way to explain the stability of N-heterocyclic carbenes. These general principles can be applied to all N-heterocyclic carbenes, but the relative importance of each effect varies for different carbene systems (Figure 1.3).[51]

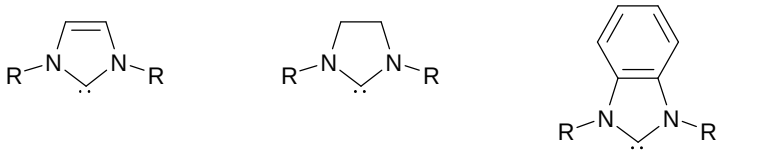

Fig. 1.3. Structures of some of the most commonly applied classes of NHCs. Ad, adamantyl; Mes, mesityl; tBu, tert-Butyl; iPr, iso-propyl; Ph, phenyl.[51]

N-heterocyclic carbenes have played a significant role in organometallic chemistry wherein the majority of applications of NHCs involve their coordination to transition metals. As already mentioned, the suitability of NHCs as ligands for transition metals can be rationalized by their donor ability with a lone pair available for donation into the σ-accepting orbital of the transition metals. While σ-donation is the most important component of NHC-metal bond, the contribution of both π back bonding into the carbene orbital and π-donation from the carbene p orbital is not negligible. In 1968, the first N-heterocyclic carbene (NHC) transition metal complexes were reported independently by Wanzlick et al.[64] and Öfele et al.[65]

The Wanzlick group showed that the direct treatment of 1,3- diphenylimidazolium salt with mercuric(II) acetate leads to deprotonation of the imidazolium salt, generating the NHC ligated mercury complex (Scheme 1.7).[64] This method expanded to became a general route for the synthesis of several NHC transition metal complexes.

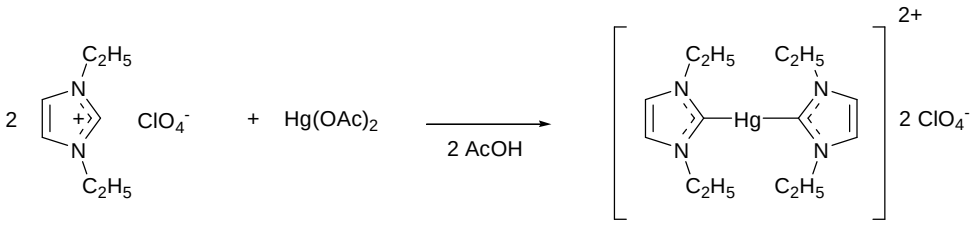

Scheme 1.7. NHC mercury complex synthesized by Wanzlick group

Ofele and co-workers found that heating the imidazolium salts of chromium can lead to a N-heterocyclic carbene chromium complex (Scheme 1.8).[65]

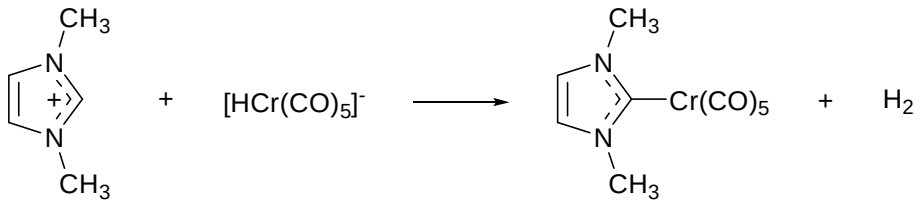

Scheme 1.8. NHC chromium complex synthesized by Ofele group

NHCs show similar behaviour to phosphine ligands in that they are neutral ligands and two electron σ donors. The structural versatility and the stability of the NHC complexes are the two key factors that have contributed towards the fast growth of NHC chemistry compared to ubiquitous trialkyl- and triarylphosphine ligands. Coordinated NHCs reveal a fan- or fence-like shape and form a pocket-like structure around the metal centre, while phosphines are cone-like ligands pointing away from the coordinated metal. Due to the good σ-donating property of NHCs, they can form stable metal–NHCs and stronger metal–carbon bonds with most metals compared with phosphine ligands.[66] The unique ligation properties of NHCs have been exploited even for the preparation and stabilization of polynuclear main group cluster complexes.[67]

In this regard, investigations on coinage metal-NHC complexes have increased substantially due to their interesting structural properties which come from the coordination flexibility of the coinage metal atoms. Their utility in transition metal mediated catalysis has also led to a rapid and continuous development in this area of inorganic chemistry. Taking advantage of N-heterocyclic carbene ligands, the Corrigan group has shown the role of $^{i}Pr_2$-bimy (1,3-di-isopropylbenzimidazole-2-ylidene) as the ancillary ligand in Cu(I) and Ag(I) metal–chalcogenolate clusters. The reaction of ($^{i}Pr_2$-bimy)CuCl and ($^{i}Pr_2$-bimy)AgOAc with $PhESiMe_3$ leads to formation of the polynuclear metal–chalcogenolates $[Cu_3(\mu\text{-}EPh)_3(^{i}Pr_2\text{-bimy})_3]$ and $[Ag_4(\mu\text{-}EPh)_4(^{i}Pr_2\text{-bimy})_4]$, respectively (Scheme 1.9 and 1.10, respectively). [68]

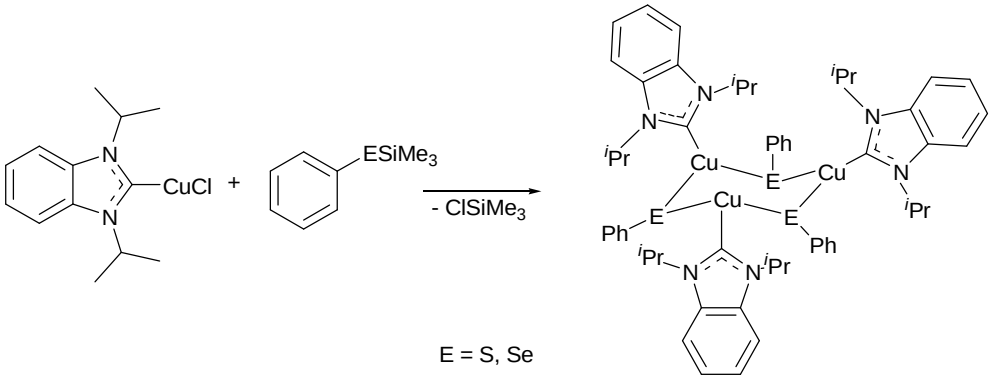

Scheme 1.9. Formation of the polynuclear metal–chalcogenolates $[Cu_3(\mu\text{-EPh})_3(^i Pr_2\text{-bimy})_3]$

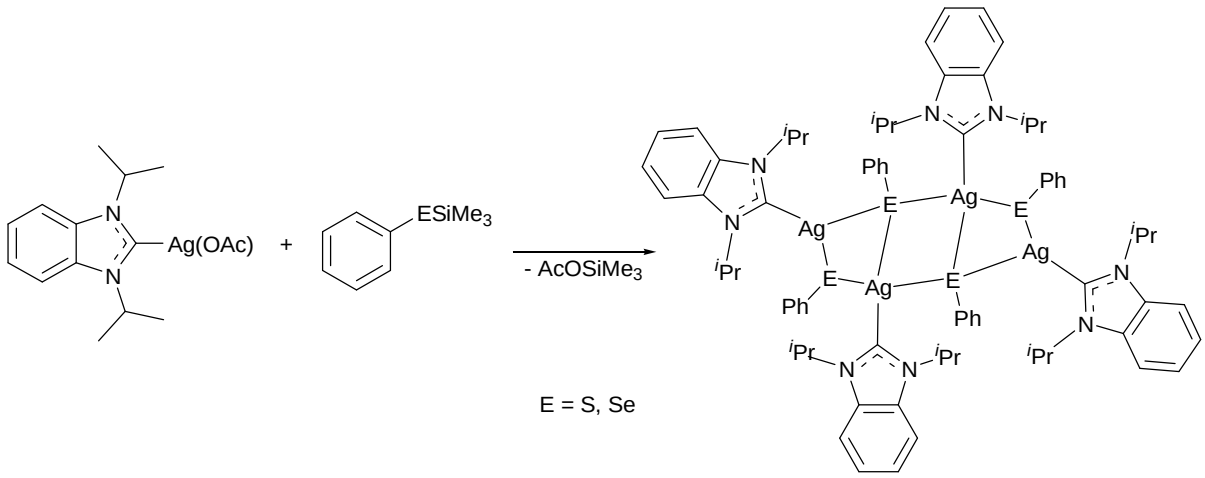

Scheme 1.10. Formation of the polynuclear metal–chalcogenolates $[Ag_4(\mu\text{-EPh})_4(^i Pr_2\text{-bimy})_4]$

These reactions illustrate that NHCs can be considered as a substitute for PR_3 ligands in the formation of polynuclear, group 11 metal–chalcogenolate complexes, which have already been used extensively in this type of chemistry.[66, 69]

1.9 Ternary M-E-M´ Clusters

The synthesis of ternary metal-chalcogenide clusters and nanoparticles has recently attracted considerable interest due to the importance of related ternary semiconductor solids.[70] Ternary systems show broader tunable properties and applications compared to their binary counterparts. In this regard coinage metal-chalcogen ternary clusters attained considerable attention as well, due to their potential application in light-absorbing materials.[71] As was mentioned, tertiary phosphine stabilized coinage metal silyl chalcogenolates $[(R_3P)_nCu–ESiMe_3]$ are efficiently used as the source of "cuprachalcogenolate" moieties when these complexes are reacted with a second metal salt (eq. 1.10).[50c, 50e, 72]

$$CuX + n\ PR_3 \xrightarrow{+\ E(SiMe_3)_2} (R_3P)_nCu\text{-}ESiMe_3 \xrightarrow{+\ M'X} [(PR_3)_XCu_yE_zM'_w] + XSiMe_3$$

X = Cl, OAc; E = S, Se, Te

(eq. 1.10)

The preformed metal-chalcogen bond in this precursor, the high solubility in common organic solvents, coupled with the reactivity of the $-ESiMe_3$ ligands toward other metal salts, makes them useful as precursors for the formation of M-E-M′ bonding interactions and entry point into ternary d-block MM′E clusters and nanoclusters.[73]

Only two CuHgE (E = S, Se) nanoclusters are reported via the reaction between $[(R_3P)CuESiMe_3]$ complexes and mercuric salts. As an example the treatment of $[(^nPr_3P)CuSSiMe_3]$ with half an equivalent of $[(^nPr_3P)_2Hg(OAc)_2]$ at -30°C formed the ternary CuHgS nanocluster of $[Hg_{15}Cu_{20}S_{25}(^nPr_3P)_{18}]$ (eq 1.11, Figure 1.4).

$$[(^nPr_3P)_3CuSSiMe_3] + 2\ {}^nPr_3P + 0.5\ Hg(OAc)_2 \longrightarrow [Hg_{15}Cu_{20}S_{25}(^nPr_3P)_{18}]$$

(eq. 1.11)

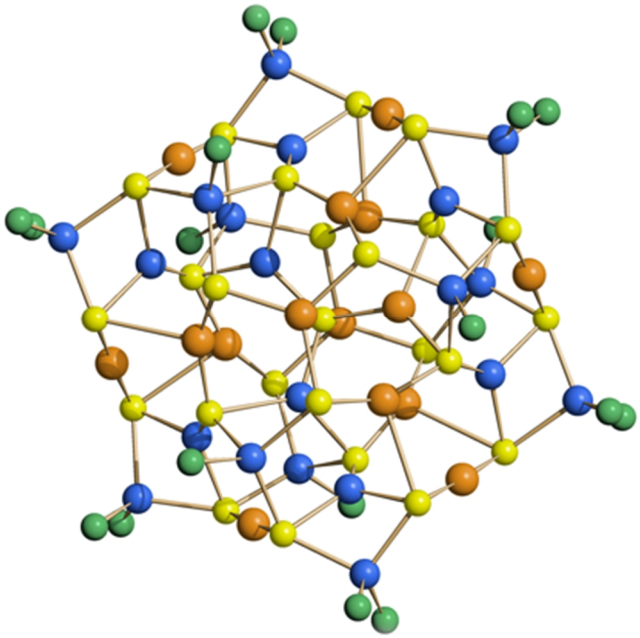

Figure 1.4. The molecular structure of $[Hg_{15}Cu_{20}S_{25}(^{n}Pr_3P)_{18}]$ (carbon and hydrogen atoms omitted).[50e] (Hg = orange, Cu = blue, S = yellow, P = green)

Applying this synthetic method to provide "argentachalcogenolate" moiety to a ternary cluster has not yet proven successful. This prompted us to investigate a new strategy to synthesise such ternary systems.

1.10 Project Summary

In Chapter 2 of this thesis, the synthesis and characterization of a new series of poly trimethylsilyl chalcogenoethers with two, three and four trimethylsilylchalcogenolate-CH_2- groups around an aromatic spacer has been successfully prepared and characterized. These complexes are the first examples of such poly(chalcogeno)silane groups on an organic spacer.

In order to take advantage of the reactivity of such polysilylchalcogenolate complexes to develop the chemistry of polychalcogenoesters, the facile preparation of di-, tri- and tetra polychalcogenoester frameworks via the reaction between ferrocenyl acid chloride and these di-, tri- and tetra- silyl chalcogen complexes is demonstrated.

In Chapter 3, two new bidentate trimethylsilylchalcogenolate reagents with the general formula of 1,2-$(Me_3SiECH_2)_2C_6H_4$ (E = S, Se) are reported. The adjacent positions of $–ESiMe_3$ groups in these reagents yield dinuclear organochalcogenolate-bridged complexes in reaction with (1,3-bis(diphenylphosphino)propane)palladium(II) chloride, $[PdCl_2(dppp)]$. The results of the reaction between 1,2,4,5-$(Me_3SiSCH_2)_4(C_6H_2)$ and $[PdCl_2(dppp)]$ to yield a "double-butterfly" Pd_4 complex is also decribed.

In Chapter 4, the reactivity of the polychalcogenolate precursors described in Chapter 2, 1,4-$(Me_3SiECH_2)_2(C_6Me_4)$, 1,3,5-$(Me_3SiECH_2)_3(C_6Me_3)$ (E = S, Se), 1,2,4,5-$(Me_3SiSeCH_2)_4(C_6H_2)$ is further demonstrated via reaction with two, three and four equivalents of [(IPr)CuOAc], respectively (IPr = 1,3-bis(2,6-diisopropylphenyl)imidazol-2-ylidene). IPr is one of the very well-known N-heterocyclic carbenes that has attracted considerable attention due to its stability, structural features and straightforward synthesis. Also the reaction between [(IPr)CuOAc] and 1,1´-$fc(CH_2ESiMe_3)_2$ (E = S, Se) is detailed.

As was mentioned above, the substitution reaction between the silylated metalchalcogenolate reagents $[L_nM\text{-}ESiMe_3]$ with the second metal salt is one of the most powerful approaches in the synthesis of ternary clusters of late d-block metals. The lability of phosphine ligands in systems reported to date prompted the development of a new strategy to synthesize these precursor types. In Chapter 5, a series of thermally stable $[L\text{-}Cu\text{-}ESiMe_3]$ complexes was synthesized by using IPr as the ancillary ligand. This is the first example of utilizing N-heterocyclic carbene ligands in the synthesis of such of copper-chalcogenolate complexes, $[(IPr)Cu\text{-}ESiMe_3]$ (E = S, Se, Te). By changing the metal centre from copper to silver, it was demonstrated a similar improvement in the thermal stability of silver-chalcogenolates $[(IPr)Ag\text{-}ESiMe_3]$ (E = S, Se). This work is detailed in Chapter 6. Also described is the effect of alternating IPr with the less sterically demanding NHC ($^iPr_2$-bimy) in the formation of $[(^iPr_2\text{-bimy})Cu\text{-}ESiMe_3]$ (E = S, Se).

Ternary nanoclusters MEM′ show optical, electronic and physical properties that might fall between the properties of corresponding binary clusters.[74] In Chapter 5 and 6, with the aim to synthesize novel ternary clusters and apply the new NHC stabilized precursors, [NHC-M-SSiMe$_3$] (NHC = IPr, ^{i}Pr$_2$-bimy; M = Cu, Ag) were reacted with mercuric(II) acetate. This provides an effective synthetic route to more size controlled ternary coinage metal-sulfide–mercury clusters.

1.11 References

[1] Bouroushian, M., Chalcogens and Metal Chalcogenides. In *Electrochemistry of Metal Chalcogenides*, Springer Berlin Heidelberg: 2010; pp 1-56.
[2] Vahrenkamp, H., *Angew. Chem. Int. Ed.* 1975, *14*, 322-329.
[3] Ansari, M. A.; Ibers, J. A., *Coord. Chem. Rev.* 1990, *100*, 223-266.
[4] Tarascon, J. M.; Armand, M., *Nature* 2001, *414*, 359-367.
[5] (a) Venkatasubramanian, R.; Siivola, E.; Colpitts, T.; O'Quinn, B., *Nature* 2001, *413*, 597-602; (b) Snyder, G. J.; Toberer, E. S., *Nat. Mater.* 2008, *7*, 105-114.
[6] Atwood, G., *Science* 2008, *321*, 210-211.
[7] (a) Liu, C.; Liu, H.; Yin, C.; Zhao, X.; Liu, B.; Li, X.; Li, Y.; Liu, Y., *Fuel* 2015, *154*, 88-94; (b) Niefind, F.; Bensch, W.; Deng, M.; Kienle, L.; Cruz-Reyes, J.; Del Valle Granados, J. M., *Appl. Catal., A* 2015, *497*, 72-84; (c) Oviedo-Roa, R.; Martínez-Magadán, J.-M.; Illas, F., *J. Phys. Chem. B* 2006, *110*, 7951-7966; (d) Ishii, A.; Nakata, N., The Mechanism for Transition-Metal-Catalyzed Hydrochalcogenation of Unsaturated Organic Molecules. In *Hydrofunctionalization*, Ananikov, V. P.; Tanaka, M., Eds. Springer-Verlag Berlin: Berlin, 2013; Vol. 43, pp 21-50.
[8] Gao, M.-R.; Xu, Y.-F.; Jiang, J.; Yu, S.-H., *Chem. Soc. Rev.* 2013, *42*, 2986-3017.
[9] Dehnen, S.; Eichhöfer, A.; Fenske, D., *Eur. J. Inorg. Chem.* 2002, *2002*, 279-317.
[10] MacDonald, D. G.; Corrigan, J. F., *Phil. Trans. R. Soc. A* 2010, *368*, 1455-1472.
[11] (a) Komuro, T.; Kawaguchi, H.; Tatsumi, K., *Inorg. Chem.* 2002, *41*, 5083-5090; (b) Hammerschmidt, A.; Lindemann, A.; Döch, M.; Krebs, B., *Z. Anorg. Allg. Chem.* 2003, *629*, 1249-1255.
[12] (a) Gysling, H. J., *Coord. Chem. Rev.* 1982, *42*, 133-244; (b) Zhao, D.-W.; Liu, X.-L.; Zhang, X.-Y.; Tang, L.-F., *J. Organomet. Chem.* 2015, *780*, 56-62; (c) Pearson, S.; Lu, H.; Stenzel, M. H., *Macromolecules* 2015, *48*, 1065-1076; (d) Maiti, B. K.; Avilés, T.; Moura, I.; Pauleta, S. R.; Moura, J. J. G., *Inorg. Chem. Commun.* 2014, *45*, 97-100.
[13] (a) Sink, C. W.; Harvey, A. B., *J. Chem. Phys.* 1972, *57*, 4434-4442; (b) Hamada, K.; Morishita, H., *Jpn. J. Appl. Phys.* 1976, *15*, 748-748.
[14] (a) Piers, W. E., *J. Chem. Soc., Chem. Commun.* 1994, 309-310; (b) Piers, W. E.; MacGillivray, L. R.; Zaworotko, M., *Organometallics* 1993, 4723-4725; (c) McGregor, K.; Deacon, G. B.; Dickson, R. S.; Fallon, G. D.; Rowe, R. S.; West, B. O., *J. Chem. Soc., Chem. Commun.* 1990, 1293-1294.
[15] (a) Canich, J. A. M.; Cotton, F. A.; Dunbar, K. R.; Falvello, L. R., *Inorg. Chem.* 1988, *27*, 804-811; (b) Cotton, F. A.; Dunbar, K. R., *Inorg. Chem.* 1987, *26*, 1305-1309.
[16] Fenske, D.; Ohmer, J.; Hachgenei, J.; Merzweiler, K., *Angew. Chem. Int. Ed.* 1988, *27*, 1277-1296.
[17] Semmelmann, M.; Fenske, D.; Corrigan, J. F., *J. Chem. Soc.-Dalton Trans.* 1998, 2541-2545.
[18] App, U.; Merzweiler, K., *Z. Anorg. Allg. Chem.* 1997, *623*, 478-482.
[19] (a) Zhu, N.; Fenske, D., *J. Chem. Soc., Dalton Trans.* 1999, 1067-1076; (b) Fenske, D.; Zhu, N., *J. Cluster Sci.* 2000, *11*, 135-151; (c) DeGroot, M. W.; Corrigan, J. F., *J. Chem. Soc., Dalton Trans.* 2000, 1235-1236; (d) F. Corrigan, J., *Chem. Commun.* 1997, 1837-1838; (e) Behrens, S.; Bettenhausen, M.; Deveson, A. C.; Eichhöfer, A.; Fenske, D.; Lohde, A.;

Woggon, U., *Angew. Chem., Int. Ed.* 1996, *35*, 2215-2218; (f) DeGroot, M. W.; Cockburn, M. W.; Workentin, M. S.; Corrigan, J. F., *Inorg. Chem.* 2001, *40*, 4678-4685.
[20] (a) Fenske, D.; Zhu, N.; Langetepe, T., *Angew. Chem., Int. Ed.* 1998, *37*, 2639-2644; (b) Steigerwald, M. L.; Alivisatos, A. P.; Gibson, J. M.; Harris, T. D.; Kortan, R.; Muller, A. J.; Thayer, A. M.; Duncan, T. M.; Douglass, D. C.; Brus, L. E., *J. Am. Chem. Soc.* 1988, *110*, 3046-3050.
[21] (a) Khalili Najafabadi, B.; Hesari, M.; Workentin, M. S.; Corrigan, J. F., *J. Organomet. Chem.* 2012, *703*, 16-24; (b) Wrackmeyer, B.; Klimkina, E. V.; Milius, W., *Z. Anorg. Allg. Chem.* 2011, *637*, 1895-1902; (c) Taher, D.; Wallbank, A. I.; Turner, E. A.; Cuthbert, H. L.; Corrigan, J. F., *Eur. J. Inorg. Chem.* 2006, *2006*, 4616-4620.
[22] Klapotke, T. M.; Krumm, B.; Mayer, P., *Z.Naturforsch.(B)* 2004, *59*, 547-553.
[23] Roof, L. C.; Kolis, J. W., *Chem. Rev.* 1993, *93*, 1037-1080.
[24] (a) Wallbank, A. I.; Brown, M. J.; Nitschke, C.; Corrigan, J. F., *Organometallics* 2004, *23*, 5648-5651; (b) Taher, D.; Taylor, N. J.; Corrigan, J. F., *Can. J. Chem.-Rev. Can. Chim.* 2009, *87*, 380-385.
[25] Wallbank, A. I.; Corrigan, J. F., *Chem. Commun.* 2001, 377-378.
[26] (a) Nitschke, C.; Wallbank, A.; Fenske, D.; Corrigan, J., *J. Cluster Sci.* 2007, *18*, 131-140; (b) Wallbank, A.; Corrigan, J., *J. Cluster Sci.* 2004, *15*, 225-232; (c) Wallbank, A. I.; Borecki, A.; Taylor, N. J.; Corrigan, J. F., *Organometallics* 2005, *24*, 788-790; (d) Nitschke, C.; Fenske, D.; Corrigan, J. F., *Inorg. Chem.* 2006, *45*, 9394-9401.
[27] Brown, M. J.; Corrigan, J. F., *J. Organomet. Chem.* 2004, *689*, 2872-2879.
[28] Ahmar, S.; Nitschke, C.; Vijayaratnam, N.; MacDonald, D. G.; Fenske, D.; Corrigan, J. F., *New J. Chem.* 2011, *35*, 2013-2017.
[29] (a) Taher, D.; Corrigan, J. F., *Organometallics* 2011, *30*, 5943-5952; (b) Capperucci, A.; Degl'Innocenti, A.; Tiberi, C., *Synlett* 2011, 2248-2252; (c) Taher, D.; Awwadi, F. F.; Pfaff, U.; Speck, J. M.; Rüffer, T.; Lang, H., *J. Organomet. Chem.* 2013, *736*, 9-18; (d) Sasaki, K.; Aso, Y.; Otsubo, T.; Ogura, F., *Chem. Lett.* 1986, *15*, 977-978.
[30] Fujiwara, S.; Kambe, N., In *Chalcogenocarboxylic Acid Derivatives*, Kato, S., Ed. Springer-Verlag Berlin: Berlin, 2005; Vol. 251, pp 87-140.
[31] (a) Kozikowski, A. P.; Ames, A., *J. Org. Chem.* 1978, *43*, 2735-2737; (b) Back, T. G.; Kerr, R. G., *Tetrahedron Lett.* 1982, *23*, 3241-3244; (c) Kuniyasu, H.; Ogawa, A.; Higaki, K.; Sonoda, N., *Organometallics* 1992, *11*, 3937-3939; (d) Petasis, N. A.; Lu, S. P., *Tetrahedron Lett.* 1995, *36*, 2393-2396.
[32] (a) Segi, M.; Kato, M.; Nakajima, T.; Suga, S.; Sonoda, N., *Chem. Lett.* 1989, 1009-1012; (b) Nishiyama, Y.; Katsuura, A.; Negoro, A.; Hamanaka, S.; Miyoshi, N.; Yamana, Y.; Ogawa, A.; Sonoda, N., *J. Org. Chem.* 1991, *56*, 3776-3780; (c) Reinerth, W. A.; Tour, J. M., *J. Org. Chem.* 1998, *63*, 2397-2400.
[33] (a) Nishiyama, Y.; Tokunaga, K.; Kawamatsu, H.; Sonoda, N., *Tetrahedron Lett.* 2002, *43*, 1507-1509; (b) Kuniyasu, H.; Ogawa, A.; Miyazaki, S.; Ryu, I.; Kambe, N.; Sonoda, N., *J. Am. Chem. Soc.* 1991, *113*, 9796-9803; (c) Takahashi, H.; Ohe, K.; Uemura, S.; Sugita, N., *J. Organomet. Chem.* 1987, *334*, C43-C45; (d) Uemura, S.; Takahashi, H.; Ohe, K.; Sugita, N., *J. Organomet. Chem.* 1989, *361*, 63-72.

[34] (a) Nishiyama, Y.; Kawamatsu, H.; Funato, S.; Tokunaga, K.; Sonoda, N., *J. Org. Chem.* 2003, *68*, 3599-3602; (b) Beletskaya, I. P.; Sigeev, A. S.; Peregudov, A. S.; Petrovskii, P. V., *Russ. J. Organ. Chem.* 2001, *37*, 1703-1709.
[35] Detty, M. R.; Wood, G. P., *J. Org. Chem.* 1980, *45*, 80-89.
[36] Silveira, C. C.; Braga, A. L.; Larghi, E. L., *Organometallics* 1999, *18*, 5183-5186.
[37] Inoue, T.; Takeda, T.; Kambe, N.; Ogawa, A.; Ryu, I.; Sonoda, N., *J. Org. Chem.* 1994, *59*, 5824-5827.
[38] (a) Nóbrega, J. A.; Gonçalves, S. M. C.; Peppe, C., *Tetrahedron Lett.* 2000, *41*, 5779-5782; (b) Ranu, B. C.; Mandal, T., *J. Org. Chem.* 2004, *69*, 5793-5795.
[39] Ajiki, K.; Hirano, M.; Tanaka, K., *Org. Lett.* 2005, *7*, 4193-4195.
[40] Zhang, Y. M.; Yu, Y. P.; Lin, R. H., *Synth. Commun.* 1993, *23*, 189-193.
[41] Wang, L.; Zhang, Y. M., *Synth. Commun.* 1999, *29*, 3107-3115.
[42] Zhou, L.-H.; Zhang, Y.-M., *J. Chem. Res., Synop.* 1999, 28-29.
[43] Liu, Y. K.; Zhang, Y. M., *Synth. Commun.* 1999, *29*, 4043-4049.
[44] Chen, R.; Zhang, Y. M., *Synth. Commun.* 2000, *30*, 1331-1336.
[45] Grieco, P. A.; Yokoyama, Y.; Williams, E., *J. Org. Chem.* 1978, *43*, 1283-1285.
[46] Huang, X.; Liang, C.-G., *J. Chem. Res., Synop.* 1999, 634-635.
[47] (a) Fuhr, O.; Dehnen, S.; Fenske, D., *Chem. Soc. Rev.* 2013, *42*, 1871-1906; (b) Fu, M.-L.; Issac, I.; Fenske, D.; Fuhr, O., *Angew. Chem., Int. Ed.* 2010, *49*, 6899-6903; (c) Corrigan, J. F.; Fuhr, O.; Fenske, D., *Adv. Mater.* 2009, *21*, 1867-1871; (d) Fernandez-Recio, L.; Fenske, D.; Fuhr, O., *Z. Anorg. Allg. Chem.* 2008, *634*, 2853-2857; (e) Sevillano, P.; Fuhr, O.; Hampe, O.; Lebedkin, S.; Neiss, C.; Ahlrichs, R.; Fenske, D.; Kappes, M. M., *Eur. J. Inorg. Chem.* 2007, *2007*, 5163-5167; (f) Yang, X.-X.; Issac, I.; Lebedkin, S.; Kuhn, M.; Weigend, F.; Fenske, D.; Fuhr, O.; Eichhofer, A., *Chem. Commun.* 2014, *50*, 11043-11045.
[48] Yu, S.-B., *Polyhedron* 1992, *11*, 2115-2117.
[49] DeGroot, M. W.; Corrigan, J. F., *Z. Anorg. Allg. Chem.* 2006, *632*, 19-29.
[50] (a) Borecki, A.; Corrigan, J. F., *Inorg. Chem.* 2007, *46*, 2478-2484; (b) Wallbank, A. I.; Corrigan, J. F., *Can. J. Chem.-Rev. Can. Chim.* 2002, *80*, 1592-1599; (c) Tran, D. T. T.; Beltran, L. M. C.; Kowalchuk, C. M.; Trefiak, N. R.; Taylor, N. J.; Corrigan, J. F., *Inorg. Chem.* 2002, *41*, 5693-5698; (d) Tran, D. T. T.; Corrigan, J. F., *Organometallics* 2000, *19*, 5202-5208; (e) Tran, D. T. T.; Taylor, N. J.; Corrigan, J. F., *Angew. Chem., Int. Ed.* 2000, *39*, 935-937.
[51] Hopkinson, M. N.; Richter, C.; Schedler, M.; Glorius, F., *Nature* 2014, *510*, 485-496.
[52] (a) Schmid, G., *Nanoparticles : from Theory to Application*. 2nd ed.; Wiley-VCH: Weinheim, 2010; p xiii, 522 p; (b) Vucic, Z.; Milat, O.; Horvatic, V.; Ogorelec, Z., *Phys. Rev. B* 1981, *24*, 5398-5401.
[53] (a) Morse, M. D., *Chem. Rev.* 1986, *86*, 1049-1109; (b) Nimtz, G.; Marquardt, P.; Gleiter, H., *J. Cryst. Growth* 1988, *86*, 66-71; (c) Koutecky, J.; Fantucci, P., *Chem. Rev.* 1986, *86*, 539-587; (d) Kappes, M. M., *Chem. Rev.* 1988, *88*, 369-389.
[54] (a) Weller, H., *Angew. Chem., Int. Ed.* 1998, *37*, 1658-1659; (b) Alivisatos, A. P., *Science* 1996, *271*, 933-937; (c) Weller, H., *Angew. Chem.-Int. Edit. Engl.* 1996, *35*, 1079-1081.

[55] (a) Anson, C. E.; Eichhöfer, A.; Issac, I.; Fenske, D.; Fuhr, O.; Sevillano, P.; Persau, C.; Stalke, D.; Zhang, J., *Angew. Chem., Int. Ed.* 2008, *47*, 1326-1331; (b) Dehnen, S.; Schäfer, A.; Fenske, D.; Ahlrichs, R., *Angew. Chem., Int. Ed.* 1994, *33*, 746-749.
[56] Fuhr, O.; Fernandez-Recio, L.; Fenske, D., *Eur. J. Inorg. Chem.* 2005, *2005*, 2306-2314.
[57] Deveson, A.; Dehnen, S.; Fenske, D., *J. Chem. Soc., Dalton Trans.* 1997, 4491-4498.
[58] Fenske, D.; Krautscheid, H.; Balter, S., *Angew. Chem., Int. Ed.* 1990, *29*, 796-799.
[59] Dehnen, S.; Fenske, D., *Chem.-Eur. J.* 1996, *2*, 1407-1416.
[60] Krautscheid, H.; Fenske, D.; Baum, G.; Semmelmann, M., *Angew. Chem., Int. Ed.* 1993, *32*, 1303-1305.
[61] (a) Rit, A.; Pape, T.; Hahn, F. E., *J. Am. Chem. Soc.* 2010, *132*, 4572-4573; (b) Rit, A.; Pape, T.; Hepp, A.; Hahn, F. E., *Organometallics* 2011, *30*, 334-347.
[62] Khalili Najafabadi, B.; Corrigan, J. F., *Chem. Commun.* 2015, *51*, 665-667.
[63] (a) Bourissou, D.; Guerret, O.; Gabbaï, F. P.; Bertrand, G., *Chem. Rev.* 2000, *100*, 39-92; (b) Irikura, K. K.; Goddard, W. A.; Beauchamp, J. L., *J. Am. Chem. Soc.* 1992, *114*, 48-51.
[64] Wanzlick, H. W.; Schönherr, H. J., *Angew. Chem., Int. Ed.* 1968, *7*, 141-142.
[65] Öfele, K., *J. Organomet. Chem.* 1968, *12*, P42-P43.
[66] Lin, J. C. Y.; Huang, R. T. W.; Lee, C. S.; Bhattacharyya, A.; Hwang, W. S.; Lin, I. J. B., *Chem. Rev.* 2009, *109*, 3561-3598.
[67] Quillian, B.; Wei, P.; Wannere, C. S.; Schleyer, P. v. R.; Robinson, G. H., *J. Am. Chem. Soc.* 2009, *131*, 3168-3169.
[68] Humenny, W. J.; Mitzinger, S.; Khadka, C. B.; Najafabadi, B. K.; Vieira, I.; Corrigan, J. F., *Dalton Trans.* 2012, *41*, 4413-4422.
[69] Garrison, J. C.; Youngs, W. J., *Chem. Rev.* 2005, *105*, 3978-4008.
[70] Dehnen, S.; Melullis, M., *Coord. Chem. Rev.* 2007, *251*, 1259-1280.
[71] (a) Rockett, A. A., *Curr. Opin. Solid State Mater. Sci.* 2010, *14*, 143-148; (b) Klenk, R.; Klaer, J.; Köble, C.; Mainz, R.; Merdes, S.; Rodriguez-Alvarez, H.; Scheer, R.; Schock, H. W., *Sol. Energy Mater. Sol. Cells* 2011, *95*, 1441-1445.
[72] Kluge, O.; Biedermann, R.; Holldorf, J.; Krautscheid, H., *Chem.-Eur. J.* 2014, *20*, 1318-1331.
[73] Khadka, C. B.; Eichhöfer, A.; Weigend, F.; Corrigan, J. F., *Inorg. Chem.* 2012, *51*, 2747-2756.
[74] DeGroot, M. W.; Taylor, N. J.; Corrigan, J. F., *Inorg. Chem.* 2005, *44*, 5447-5458.

Chapter 2

New Polydentate Trimethylsilyl Chalcogenide Reagents for the Assembly of Polyferrocenyl Architectures

(Mahmood Azizpoor Fard, Bahareh Khalili Najafabadi, Mahdi Hesari, Mark S. Workentin, and John F. Corrigan, *Chem. Eur. J.* **2014**, *20*, 7037 – 7047)

2.1 Introduction

The chemistry of ferrocene (Fc) containing molecules and materials continues to develop due to the favourable electronic (redox) properties of ferrocene and its ease of functionalization.[1-3] Such systems have a wide range of applications in materials science including use as sensors,[4] catalysts,[4a,5] electroactive materials[6] and aerospace materials,[7] in cancer therapeutics[8] and other medicinal applications,[9] and as a smokeless fuel additive.[10]

Much research focus has been placed on polyferrocene architectures where the organometallic units are linked with different organic spacers such as alkenes,[11] alkynes,[12] arenes,[13] heterocycles,[14] annulenes[15] and even larger molecules such as C_{60}.[16] These types of complexes are suitable for investigating intra-molecular electronic interactions in the corresponding mixed-valent species between the ferrocenyl units through the organic backbone.[14a-e, 17] Efforts have also been devoted to the incorporation of multiple ferrocene units into polymers,[18] dendrimeric frameworks[19] and inorganic nanoclusters.[20]

In a complementary vein for this work, the preparation of poly ferrocenylthio- and selenoesters has been pursued.[21] The chemistry of chalcogenoesters has had a strong development, due to the importance of these type of compounds as intermediates in synthetic organic chemistry.[22-24] Chalcogenoesters have been employed as acylating reagents in synthesis of corresponding acids,[25] esters,[25] amides,[25a,b,26] ketones[27, 28] and aldehydes.[29, 30] Acyl chalcogenides are also employed as building blocks for the synthesis of asymmetric aldols[31] and heterocyclic compounds such as oxazoles[32] and β-lactone.[33]

Chalcogenoesters also have been applied to the synthesis of natural compounds such as proteins[34] and alkaloids.[35]

Developed methodologies for the incorporation of these molecules into organic compounds generally involve the preparation of acyl radicals[36, 37] and anions[38] under mild conditions. New methods for the synthesis to thio- and selenoesters are still being developed and organo(trimethylsilyl) chalcogenides have been shown to be a convenient source of organo chalcogenide (RE^-) in the synthesis of chalcogenoesters,[39] and are of course well developed for the preparation of metal chalcogen complexes.[20d, 40] The preparation of new frameworks with multiple $–ESiMe_3$ moieties would offer routes to the assembly of poly thio- and selenoesters. Rimpler first reported that the sulfur silane reagent $Me_3SiOC(O)CH_2SSiMe_3$ reacts directly with acyl chloride under ambient conditions to yield the corresponding thioester $Me_3SiOC(O)CH_2SC(O)R$ via the formation of Me_3SiCl.[41] Aryl- and alkyl(trimethylsilyl)chalcogenides offer a convenient, easily handled source of "ArE" and "RE" (E = S, Se, Te) respectively. Ogura and co-workers demonstrated a similar methodology for the heavier congener tellurium reagent $PhTeSiMe_3$.[42] Twelve years later, reductive cleavage of the Se-Si bond in arylselenotrimethylsilane $PhSeSiMe_3$ was reported by Zhang and Zhang as a novel method for the synthesis of selenoesters.[43]

In contrast to sulfur and tellurium, the chemistry of selenium Ar-/R-$SeSiMe_3$ has not been as extensively developed for the preparation of chalcogenoesters. Recently the use of nucleophilic fluoride anion to increase the reactivity of $PhSeSiMe_3$ in the reaction with acid chloride has been demonstrated.[44] Concomitantly, we reported a new series of diselenoesters from the simple reaction of mono- or di(acid chlorides) with di- or monosubstituted organochalcogen-silane reagents in both solvent and under solvent-free conditions.[21a] The synthesis of an oligoselenoester complex in this work outlined the potential of this chemistry for the formation of polyselenoester complexes, including small oligomers. Herein we describe the preparation of a new class of di- tri- and tetrasubstituted thio- and selenotrimethylsilanes and demonstrate their utility for the assembly of a series of polysubstituted ferrocenylthio- and selenoesters, respectively, via their reaction with ferrocenoyl chloride.

2.2 Results and discussion

Various synthetic methods for chalcogenoesters have been reported and are usually based on the reactions of acyl chloride or acid anhydrides with a source of chalcogenide anion such as chalcogenols (via deprotonation),[45] dichalcogenides (via reduction)[46] or alkali metal chalcogenolates.[47, 48] Additional methods including metal-catalyzed reactions have also been reported.[49-57] The demonstrated reactivity of disubstituted 1,1´-bis(trimethylsilylseleno)ferrocene and related reagents for the preparation of diselenoesters[58] suggests that polychalcogenosilanes could behave efficiently in transferring chalcogeno moieties for the formation the polychalcogenoesters.[20a, b, 59]

The polychalcogenosilanes of the general formula $Ar(CH_2ESiMe_3)_n$ (Ar = aryl; E = S, Se; n = 2 – 4) **1**-**6** are readily prepared in good yield via the reaction of lithium (trimethylsilyl) chalcogenolate $Li[ESiMe_3]$ with the corresponding di-, tri- and tetra-bromobenzyl arene (Scheme 2.1). $Li[ESiMe_3]$ is first prepared in situ through the addition of bis(trimethylsilyl)chalcogenide $E(SiMe_3)_2$ to a stirred solution of *n*BuLi in tetrahydrofuran at 0º.[60] The portion-wise addition of organobromine reagents to the solution of $Li[ESiMe_3]$ in Et_2O at room temperature, followed by stirring for 12 hours, yielded **1**, **3** and **5** (white powders) and **2**, **4** and **6** (pale yellow powders) upon extraction with a hydrocarbon solvent. Similar reactions to substitute the bromine centers by using $Na[ESiMe_3]$[61] are equally effective in the formation of **1**-**6**. The addition of the organobromine reagents to a suspension of $Na[ESiMe_3]$ in tetrahydrofuran at room temperature, and production of NaBr, makes the extraction of **1**-**6** somewhat easier, with comparable yields of products. All six compounds are highly air sensitive; however, they are stable for several days in solution at room temperature under an inert atmosphere.

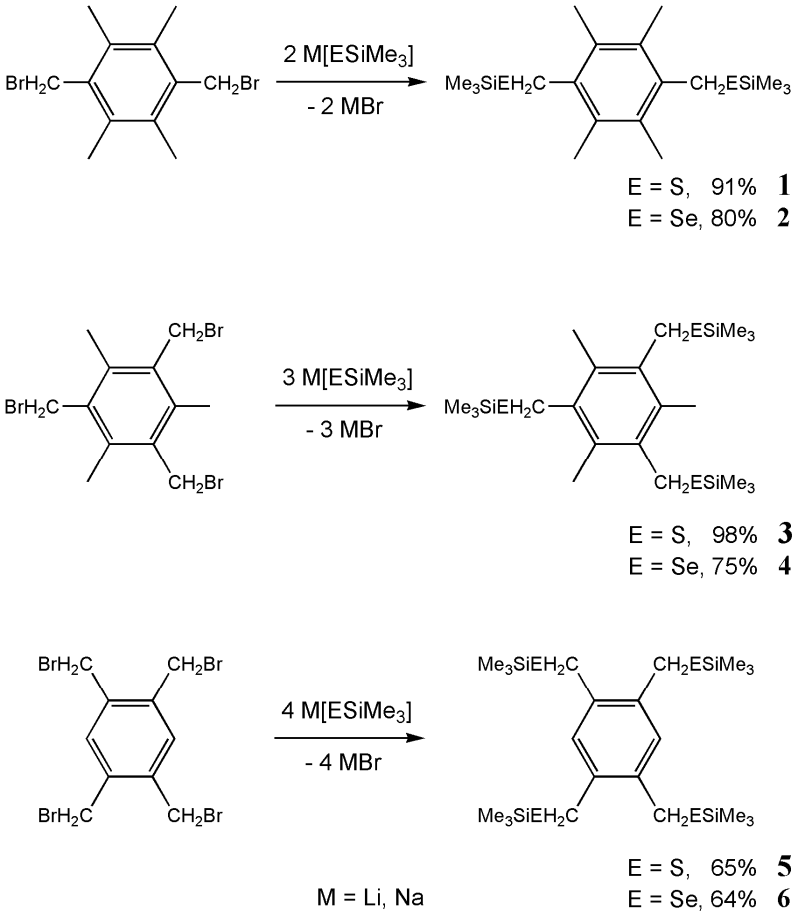

Scheme 2.1. Synthesis of **1**-**6**.

The solution NMR chemical shifts of **1**-**6** are reported in Table 2.1. The chemical shift values of the di- and tri- substituted complexes **1**-**4** are similar although they differ slightly compared to those of the corresponding tetrasubstituted aromatics **5**-**6**. The chemical shifts of the $Si(CH_3)_3$ moieties in the selenium complexes appear to lower field in both ^1H and ^{13}C $\{^1H\}$ NMR spectra versus the corresponding sulfur complexes. The ^1H NMR spectra display the expected singlet for the equivalent methylene groups. All $-CH_2-$ groups in analogous compounds show similar chemical shift values in their ^1H NMR spectra (**1**, **2** = 3.75 ppm; **3**, **4** = 2.46, 2.42 ppm; and **5**, **6** = 3.83 ppm) but the corresponding resonances in the ^{13}C $\{^1H\}$ NMR spectra of the selenides have lower chemical shift values (**1**, **3** and **5** = 25.9 - 27.5 ppm; **2**, **4** and **6** = 18.0 - 18.7 ppm). The $^{77}Se\{^1H\}$ chemical shift for

tetrasubstituted **6** is significantly upfield (-19.0 ppm) compared to the corresponding values for the di- and trisubstituted complexes **2** and **4** (-70.2 and -70.7 ppm, respectively); this is likely to be due to interamolecular Se…Se nonbonding interactions in solution, as described for complementary systems.[62]

To date, only a few crystal structures with -CESiMe$_3$ group have been reported[59a, 63] although the structural chemistry of Ar(CH$_2$ER)$_n$ in general is more mature.[64] The structures of **1**-**4** and **6** were confirmed by X-ray crystallographic analyses. Crystallographic data and data collection parameters are summarized in Tables 2.2.1 and 2.2.2. Complexes **1**-**4** crystallized in the tricilinic space group $P\bar{1}$. Complex **6** crystallized in the space group $P2_1/c$. The molecular structures of **1**-**4** and **6** and some of the selected intermolecular bond distances and angles are provided in Figures 2.1, 2.2, 2.3, 2.4 and 2.5. The S-Si [2.1387(7) - 2.1553(7) Å], Se-Si [2.276(2) - 2.287(2) Å], S-C [1.837(2) – 1.852(2) Å] and Se-C [1.982(5) – 1.997(6) Å] distances in these four compounds are typical for the sulfur-silicon, selenium-silicon, sulfur-carbon and selenium-carbon single bonds.[65]

Table 2.1. NMR spectroscopic data for **1**-**6** in CDCl$_3$. Chemical shifts are in ppm.

		^{1}H				^{13}C				^{77}Se
		Si(C**H**$_3$)$_3$	C**H**$_3$	C**H**$_2$	C**H**	Si(**C**H$_3$)$_3$	**C**H$_3$	**C**H$_2$	**-C-**	
Sulfides	**1**	0.41	2.32	3.72		0.7	16.1	26.1	132.7, 135.1	
	3	0.40	2.46	3.72		0.7	15.6	25.9	134.2, 134.7	
	5	0.34		3.83	7.21	0.9		27.5	131.8, 137.4	
Selenides	**2**	0.49	2.32	3.75		1.6	16.1	18.4	132.6, 135.2	-70.7
	4	0.47	2.42	3.72		1.6	16.0	18.0	133.6, 134.9	-70.2
	6	0.44		3.83	7.09	1.8		18.7	132.1, 137.5	- 19.0

Table 2.2.1. Crystallographic data and parameters for compounds **1**-**4**.

	1	**2**	**3**	**4**
Formula	$C_{18}H_{34}S_2Si_2$	$C_{18}H_{34}Se_2Si_2$	$C_{21}H_{42}S_3Si_3$	$C_{21}H_{42}Se_3Si_3$
formula Weight	370.75	464.55	475.00	615.70
crystal System	Triclinic	Triclinic	Triclinic	Triclinic
space group	*P*ī	*P*ī	*P*ī	*P*ī
a (Å)	6.4020(5)	6.2310(3)	10.0634(1)	10.125(2)
b (Å)	7.3238(4)	7.5548(4)	11.5851(2)	11.630(2)
c (Å)	11.9751(9)	12.1830(7)	13.0520(2)	13.257(3)
α (º)	103.313(4)	103.265(2)	86.4372(9)	87.81(3)
β (º)	97.665(3)	97.939(3)	68.2215(9)	67.71(3)
γ (º)	92.821(5)	93.901(3)	79.5821(9)	82.00(3)
V (Å^3)	539.64(7)	549.88(5)	1389.75(4)	1430.2(6)
Z	1	1	2	2
ρ_{cal} (g cm^{-3})	1.141	1.403	1.135	1.430
μ (Mo Kα) (mm^{-1})	0.354	3.468	0.402	3.990
F(000)	202	238	516	624
temperature (K)	150	150	150	150
θ_{min}, θ_{max} (º)	3.0, 27.8	2.8, 27.7	1.7, 39.8	2.2, 27.6
total reflns	4614	4460	90834	11696
unique reflns	2492	2510	16840	6548
R(int)	0.025	0.024	0.071	0.034
*R*1	0.0405,	0.0397,	0.0543,	0.0496,
w*R*2 [$I \geq 2\sigma(I)$]	0.0932	0.1021	0.1269	0.1198
*R*1 (all data)	0.0551	0.0470	0.1550	0.0816
w*R*2 (all data)	0.1007	0.1051	0.1736	0.1360
GOF	1.046	1.173	0.992	1.042
min peak	-0.298	-0.596	-0.626	-0.687
max peak	0.284	0.546	1.012	1.494

$R_1 = \sum(|F_o| - |F_c|)/\sum F_o$, $wR_2 = [\sum(w(F_o^2 - F_c^2)^2)/\sum(wF_o^2)]^{1/2}$, GOF = $[\sum(w(F_o^2 - F_c^2)^2)/(N_{observns} - N_{params})]^{1/2}$

Table 2.2.2. Crystallographic data and parameters for compounds **6**-**8** and **11**.

	6	**7**	**8**	**11**
Formula	$C_{22}H_{46}Se_4Si_4$	$C_{34}H_{34}Fe_2O_2S_2$	$C_{34}H_{34}Fe_2O_2Se_2$	$C_{54}H_{46}Fe_4O_4S_4$
formula Weight	738.79	650.43	744.23	1110.55
crystal System	Monoclinic	Triclinic	Monoclinic	Triclinic
space group	$P2_1/c$	$P\bar{1}$	$P2_1/c$	$P\bar{1}$
a (Å)	11.5701(11)	8.0896(16)	5.748(2)	5.7476(5)
b (Å)	6.5046(5)	10.354(2)	23.046(10)	13.3324(12)
c (Å)	21.8713(18)	18.010(4)	21.718(8)	14.9342(13)
α (º)	90	94.803(15)	90	91.675(4)
β (º)	95.733(5)	100.219(10)	95.791(10)	100.183(4)
γ (º)	90	98.517(14)	90	93.298(4)
V (Å^3)	1637.8(2)	1458.8(5)	2862.3(19)	1123.60(17)
Z	2	2	4	1
ρ_{cal} (g cm^{-3})	1.498	1.481	1.727	1.641
μ (Mo Kα) (mm^{-1})	4.636	1.168	3.588	1.501
F(000)	740	676	1496	570
temperature (K)	150	110	110	110
θ_{min}, θ_{max} (º)	1.8, 25.0	1.2, 28.0	2.8, 26.4	1.4, 27.5
total reflns	47682	20483	47265	21808
unique reflns	2880	20483	5860	5171
R(int)	0.252	0.000	0.094	0.061
$R1$	0.0438,	0.0525,	0.0415,	0.0639
w$R2$ [$I \geq 2\sigma(I)$]	0.0714	0.0952	0.0838	0.1683
$R1$ (all data)	0.1195	0.1081	0.0754	0.0904
w$R2$ (all data)	0.0856	0.1138	0.0955	0.1935
GOF	0.913	1.008	1.016	1.079
min peak	-0.601	-0.534	-0.562	-0.699
max peak	0.134	0.529	0.855	2.064

$R_1 = \sum(|F_o| - |F_c|)/\sum F_o$, $wR_2 = [\sum(w(F_o^2 - F_c^2)^2)/\sum(wF_o^2)]^{1/2}$, GOF $= [\sum(w(F_o^2 - F_c^2)^2)/(N_{observns} - N_{params})]^{1/2}$

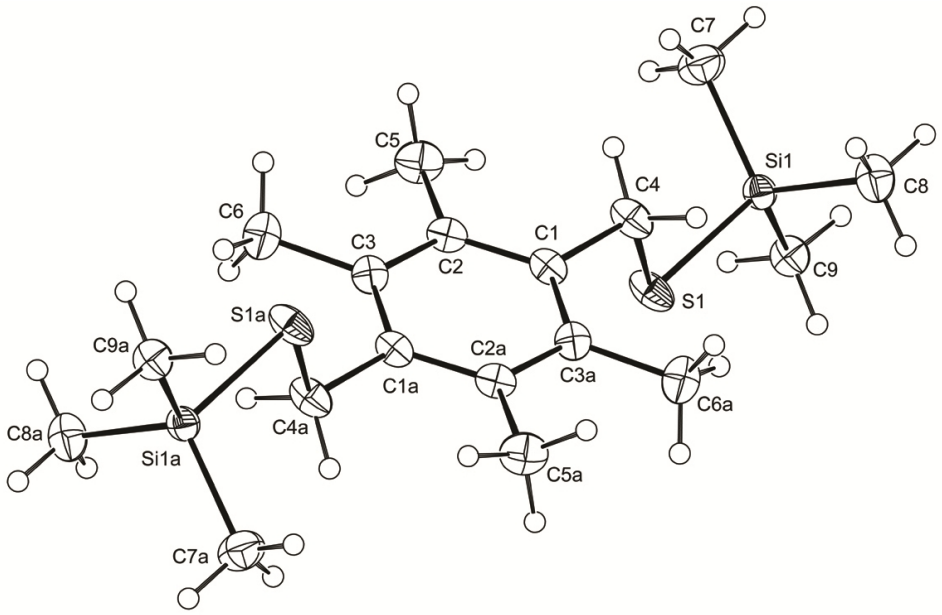

Figure 2.1. Thermal ellipsoid plot (40% probability level) of **1** with the atom numbering scheme. The thioether resides about crystallographic inversions center relating the two halves of the molecule. Selected bond distances (Å) and angles (º): C(4)-S(1) 1.852(2), S(1)-Si(1) 2.1553(7), C(4)-S(1)-Si(1) 99.84(7).

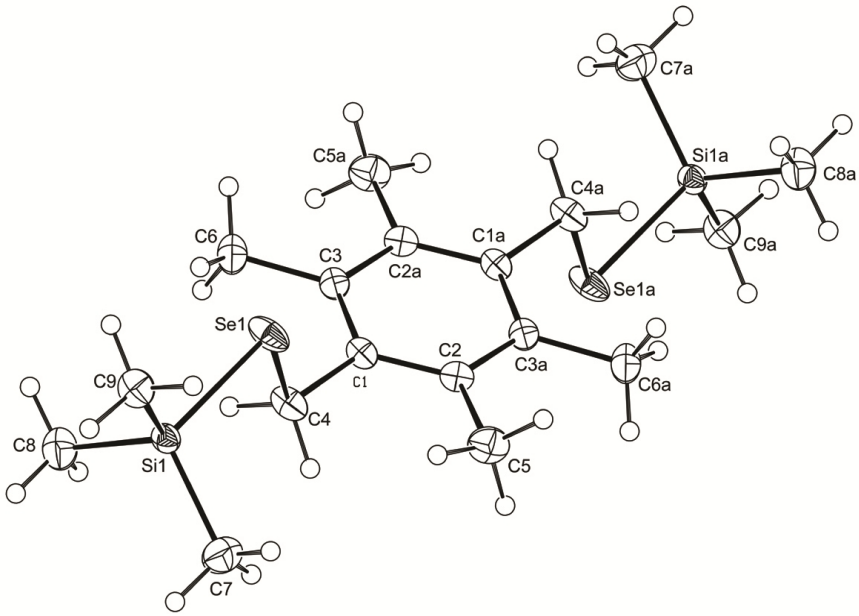

Figure 2.2. Thermal ellipsoid plot (40% probability level) of **2** with the atom numbering scheme. The chalcogenoesters reside about crystallographic inversions center relating the two halves of the molecules. Selected bond distances (Å) and angles (º): C(4)-Se(1) 1.995(4), Se(1)-Si(1) 2.285(1), C(4)-Se(1)-Si(1) 97.5(1).

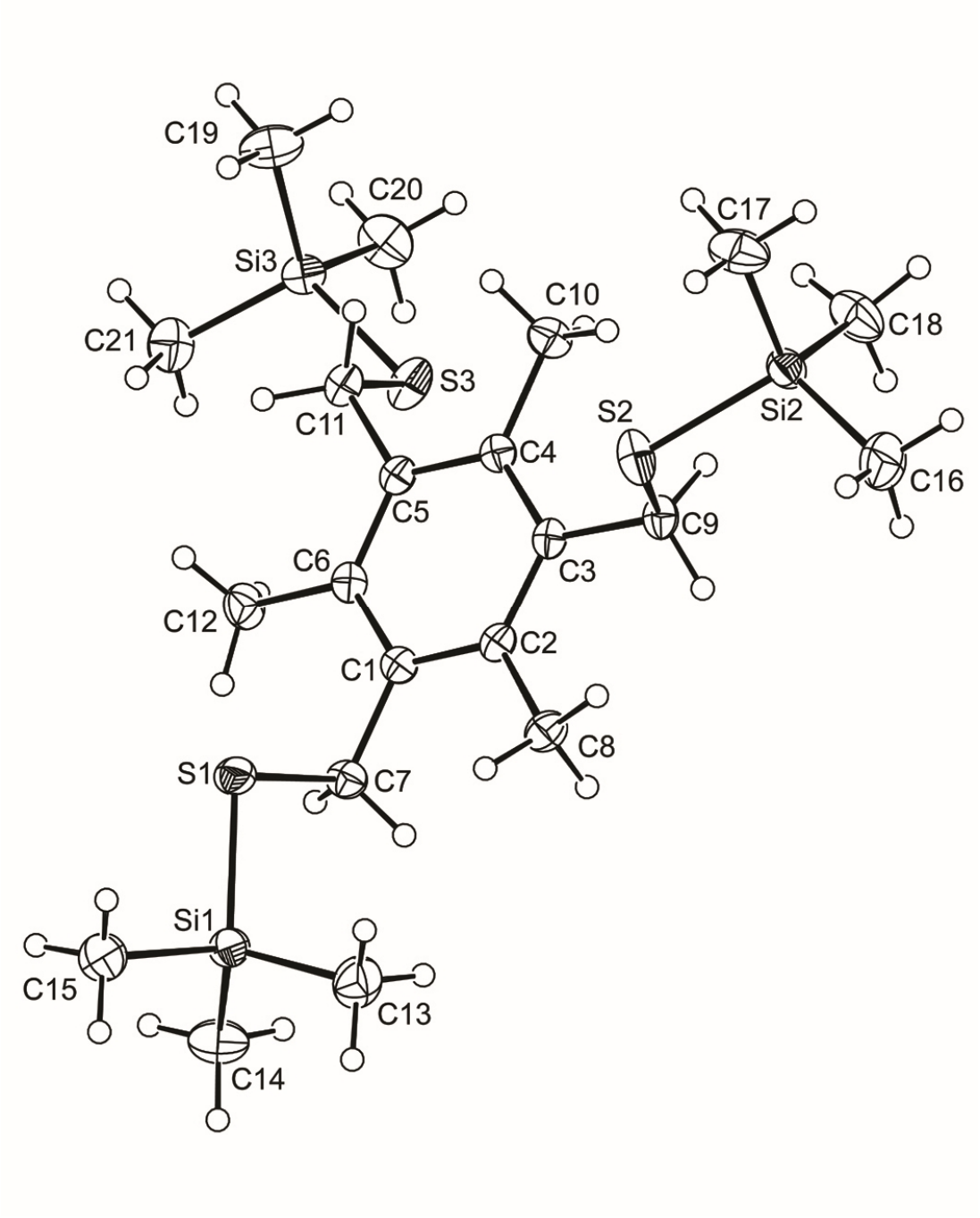

Figure 2.3. Thermal ellipsoid plot (40% probability level) of **3** with the atom numbering scheme. Selected bond distances (Å) and angles (º): C(7)-S(1) 1.846(2), C(9)-S(2) 1.837(2), C(11)-S(3) 1.849(2), S(1)-Si(1) 2.1430(6), S(2)-Si(2) 2.1387(7), S(3)-Si(3) 2.1426(6), C(7)-S(1)-Si(1) 101.71(6), C(9)-S(2)-Si(2) 104.98(6), C(11)-S(3)-Si(3) 103.15(6).

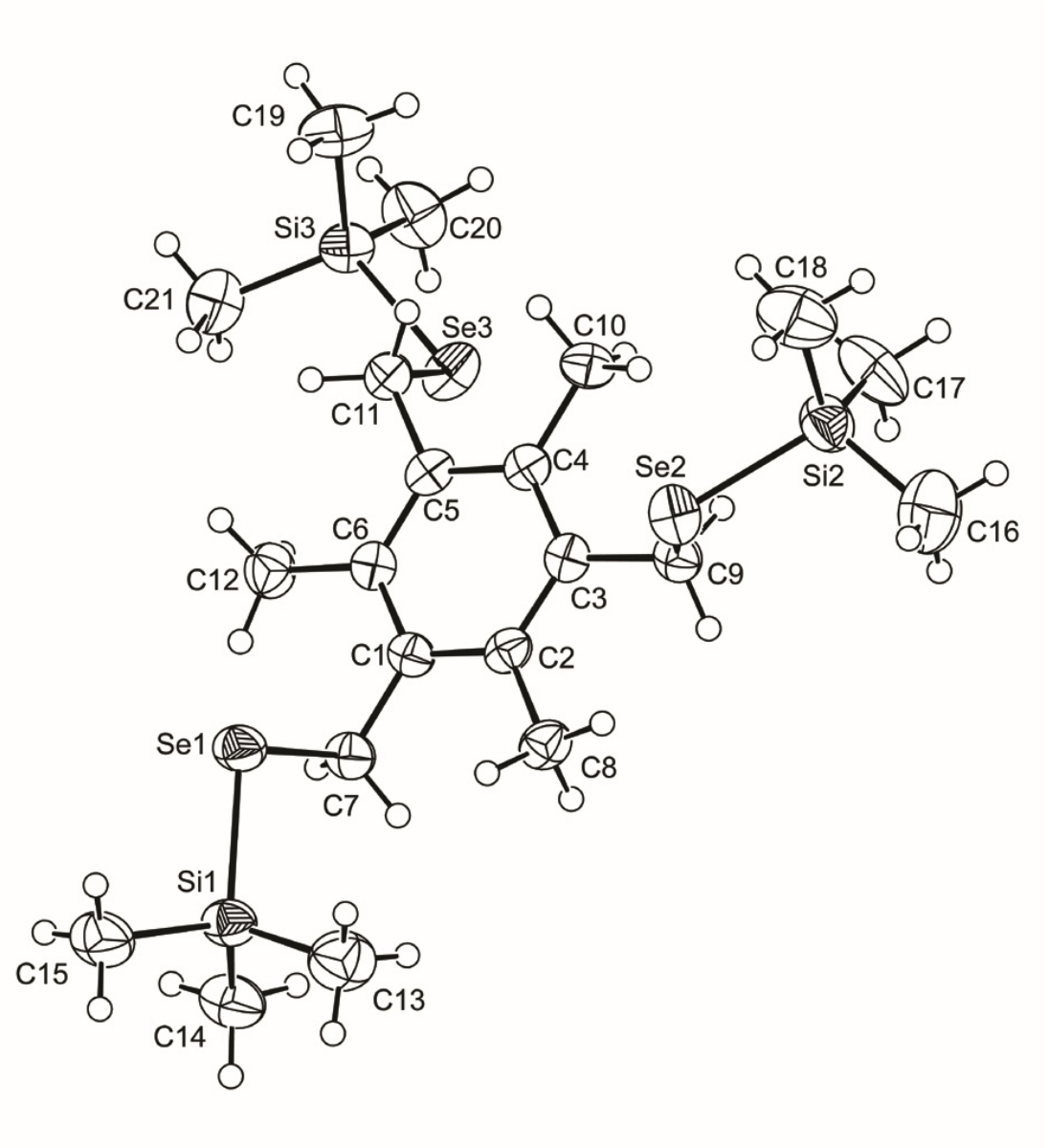

Figure 2.4. Thermal ellipsoid plot (40% probability level) of **4** with the atom numbering scheme. Selected bond distances (Å) and angles (º): C(7)-Se(1) 1.997(6), C(9)-Se(2) 1.982(5), C(11)-Se(3) 1.994(5), Se(1)-Si(1) 2.283(2), Se(2)-Si(2) 2.276(2), Se(3)-Si(3) 2.287(2), C(7)-Se(1)-Si(1) 98.7(1), C(9)-Se(2)-Si(2) 102.2(1), C(11)-Se(3)-Si(3) 100.4(1).

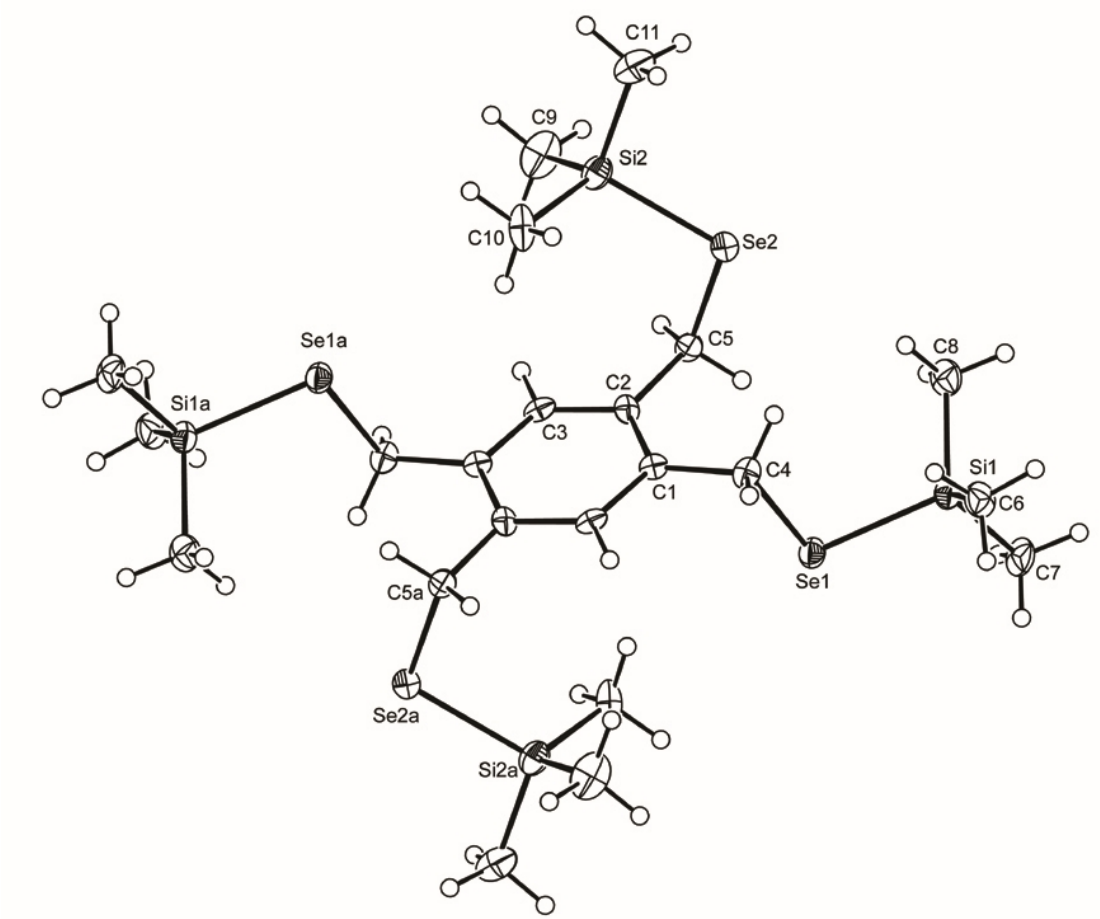

Figure 2.5. Thermal ellipsoid plot (40% probability level) of **6** with the atom numbering scheme. Selected bond distances (Å) and angles (º): C(4)-Se(1) 1.9839(1), C(5)-Se(2) 1.9849(2), Se(1)-Si(1) 2.2873(2), Se(2)-Si(2) 2.2857(2), C(4)-Se(1)-Si(1) 97.64(14), C(5)-Se(2)-Si(2) 102.85(16).

Examination of the structures of **1** and **2** shows that they have a crystallographic center of symmetry. The two -$ESiMe_3$ groups are held in *trans* configuration in the crystalline state and the C-E-Si moieties are approximately perpendicular to the central C_6 plane (**1** 87.89º, **2** 88.85º). In the crystal structures of **3** and **4**, two –$ESiMe_3$ groups lie on one side of the aromatic ring with the third group on the opposite face. These patterns mirror the structural features of $ArMe_{6-x}(CH_2ER)_x$ (R = alkyl, aryl).[66] The structure of **6** also has a center of symmetry; in this case adjacent -$SeSiMe_3$ groups are on opposite site of the C_6 ring;[64a] this conformation minimizes steric constraints.

The demonstrated reactivity of $-SeSiMe_3$ moieties towards acid chlorides suggested a facile route for the formation of poly-ferrocenylchalcogenoesters using **1**-**6**. In the first attempt to synthesize polyferrocene based chalcogenoesters, 1,4-$[(CH_3)_3SiSeCH_2]_2(C_6Me_4)$ **2** was reacted with ferrocynoyl chloride at room temperature in tetrahydrofuran. After stirring for six hours, workup and purification yielded 1,4-$[FcC(O)SeCH_2]_2(C_6Me_4]$ **8** in 40% yield (Scheme 2.2). The reaction of ferrocenoyl chloride with the other silyl-selenium complexes required more forcing conditions. Thus, compound **6**, with four $-SeSiMe_3$ groups about the aryl ring, reacted cleanly with four equivalents of FcC(O)Cl at 40-45 ºC to form the corresponding 1,2,4,5-$[FcC(O)SeCH_2]_4(C_6H_2)$ **12** in 45% yield. Similar reaction conditions with the sulfur complexes **1**, **3** and **5** did not lead to the formation of thioesters; higher reaction temperature yielded only modest evidence of S-Si activation, as indicated by ^1H NMR spectroscopy.

However, when reactions were performed by heating the silyl chalcogen reagents at 60-65 ºC in the presence of ferrocenoyl chloride (solvent free conditions), both seleno- and thioesters proved readily accessible. Using this methodology, the polyferrocenyl complexes 1,4-$[FcC(O)ECH_2]_2(C_6Me_4)$ (E = S, **7**; E = Se, **8**), 1,3,5-$[FcC(O)ECH_2]_3(C_6Me_3)$ (E = S, **9**; E = Se, **10**) and 1,2,4,5-$[FcC(O)ECH_2]_4(C_6H_2)$ (E = S, **11**; E = Se, **12**) were prepared (Scheme 2.2).

The NMR chemical shifts for the chalcogeno esters **7**-**12** are listed in Table 2.3. The ^1H NMR spectra show one singlet (4.17-4.24 ppm) and two virtual triplets (4.48-4.87 ppm) assigned to the C_5H_5 and substituted Cp rings of ferrocene, respectively. The chemical shift values of the CH_2 groups are shifted downfield (4.31-4.38 ppm) compared to the corresponding silyl-chalcogen precursor (3.72-3.83 ppm). Unlike the downfield shift of arene CH resonance **11** and **12** ($\delta\Delta \sim 0.2$ ppm) there is no considerable change in the chemical shifts of the arene CH_3 groups in **7**, **8**, **9** and **10**. The chemical shift values in the ^{13}C NMR spectra of the methylene groups for the selenoesters generally appear downfield of their respective $-SeSiMe_3$ precursor, with smaller changes observed for the thioesters. The large downfield shifts in ^{77}Se NMR of the selenoesters compared to **2**, **4** and **6** may be explained with the introduction of withdrawing >C=O group bonded to the selenium atom

versus Me_3Si. The carbonyl carbon chemical shifts are observed between 192-195 ppm in their respective ^{13}C NMR spectra.

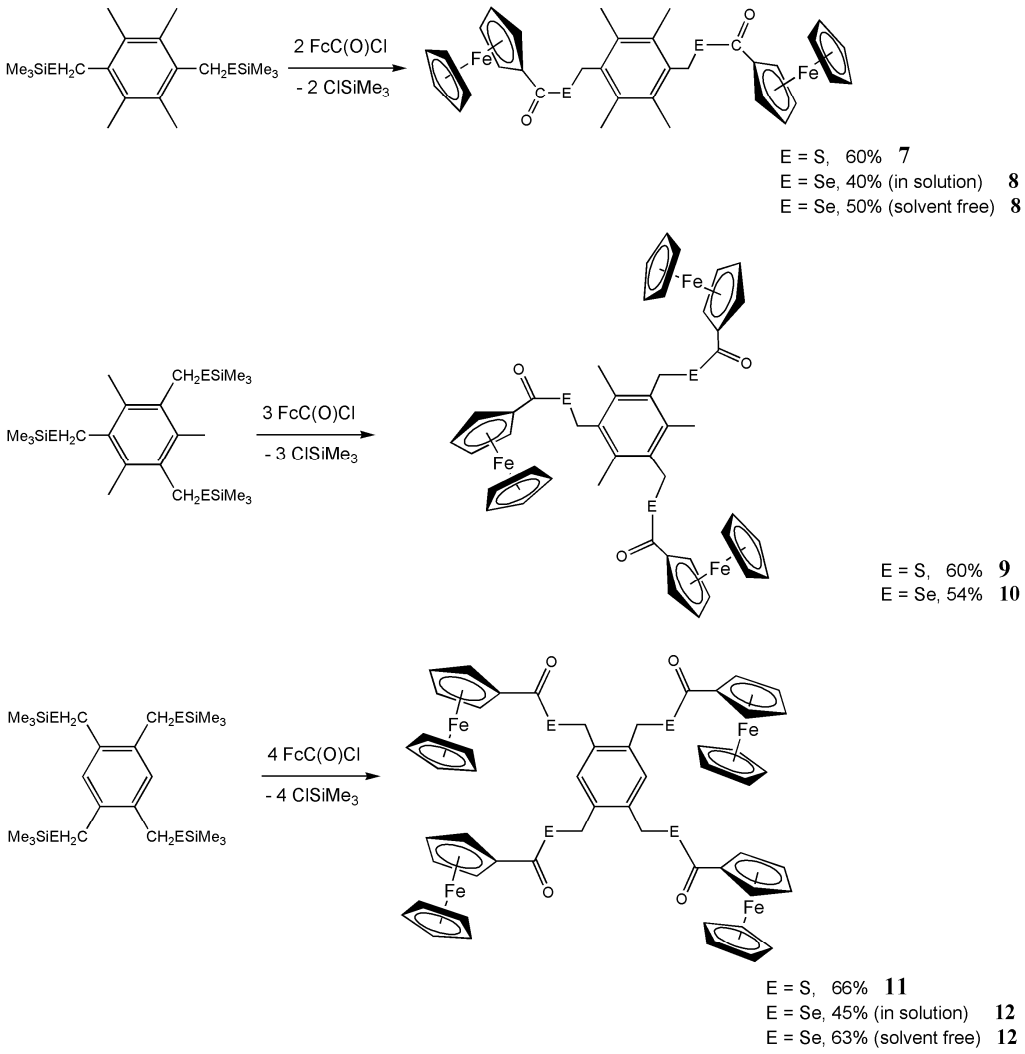

Scheme 2.2. Synthesis of **7-12**.

Table 2.3. NMR spectroscopic data for **7-12** in $CDCl_3$. Chemical shifts are reported in ppm.

		^{1}H				^{13}C				
		Fc	C**H**$_3$	C**H**$_2$	C**H**	Fc	**C**H$_3$	**C**H$_2$	**-C-**	**C**=O
Sulfides	**7**	4.24, 4.49, 4.87	2.34	4.37		68.7, 70.4,71.6, 79.0	16.5	29.2	132.0, 133.5	193.8
	9	4.24, 4.51, 4.83	2.43	4.37		68.9, 70.8, 72.0, 81.4	16.6	25.3	133.1, 135.2	195.0
	11	4.17, 4.45, 4.83		4.33	7.45	69.0, 70.6, 71.8, 79.0		29.8	132.9, 135.8	192.8
Selenides	**8**	4.24, 4.51, 4.84	2.31	4.38		68.9, 70.8, 72.0, 81.5	17.0	25.6	133.3, 133.4	195.2
	10	4.22, 4.48, 4.86	2.46	4.37		68.9, 70.6, 71.8, 79.1	16.5	29.2	131.8, 136.3	193.9
	12	4.20, 4.48, 4.81		4.31	7.36	69.0, 70.8, 72.0, 81.2		25.3	132.8, 136.8	194.0

The structure of 1,4-[FcC(O)SCH$_2$]$_2$(C$_6$Me$_4$) **7** was solved and refined in the triclinic space group *P*$\bar{1}$, while 1,4-[FcC(O)SeCH$_2$]$_2$(C$_6$Me$_4$) **8** crystallizes in monoclinic space group *P*2$_1$/*c*. The molecular structure in the crystal together with selected bond lengths and angles for complexes **7** and **8** are presented in Figures 2.6 and 2.7, respectively. The C=O [1.205(6)-1.216(5) Å] and E-C [E = S; 1.782(3)-1.821(4) Å, E = Se; 1.957(5)-1.975(5) Å] distances are in the range observed for thio- and selenoester complexes.[67, 68] Like their corresponding silylated precursors, the chalcogenoester groups are oriented in a *trans* configuration; in both complexes, the cyclopentadienyl rings adopting a staggered conformation.

In complex **7** the two ferrocenoyl groups are nearly perpendicular, with an angle of 88.09º between C$_5$-Fe-C$_5$ vectors. The central arene C$_6$ is not parallel with either of the two substituted C$_5$H$_4$ rings (rotated 60.46º and 65.12º). With dihedral angles C13-C12-S1-C11 and C16-C23-S2-C24 of 173.56º and 132.45º, respectively, one of the thioester groups is perpendicular to the central C$_6$ whereas the other is rotated by ~40º. The analogous configuration for complex **8** is not observed in the solid state; here the two selenoester groups are held in a *trans* configuration but with the two ferrocenoyl groups nearly parallel, with an angle of only 11.74º between planes defines by the C$_5$ rings.

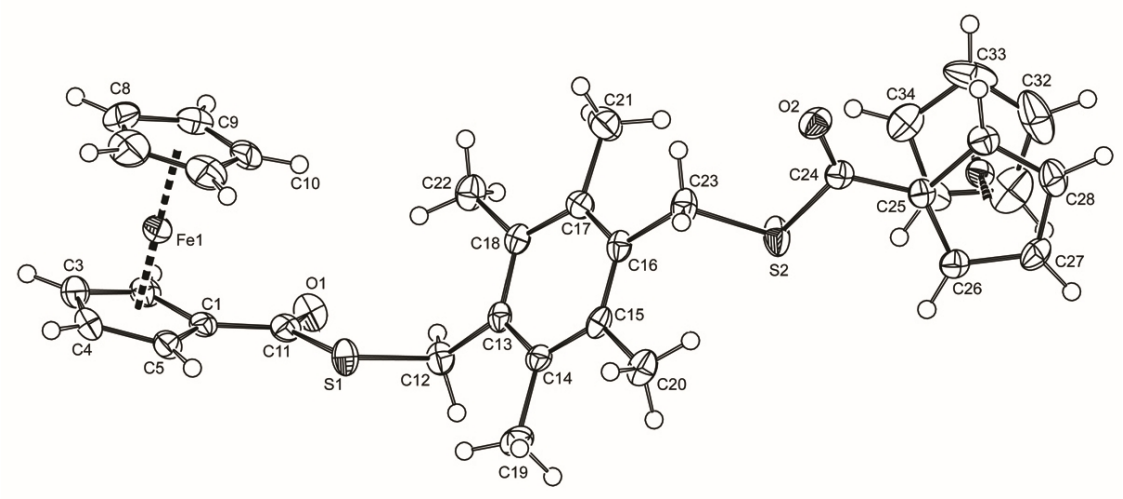

Figure 2.6. Thermal ellipsoid plot (40% probability level) of **7** with the atom numbering scheme. Selected bond distances (Å) and angles (º): C(12)-S (1) 1.821(4), C(11)-S(1) 1.780(4)**,** C(1)-C(11) 1.469(5), C(23)-S(2) 1.821(4), C(24)-S(2) 1.782(3)**,** C(24)-C(25) 1.470(5), C(11)-S(1)-C(12) 101.7(2), C(1)-C(11)-S(1) 113.2(3), C(23)-S(2)-C(24) 101.7(2), C(25)-C(24)-S(2) 114.0(3), C(1)-C(11)-S(1)-C(12) 178.1(3), C(25)-C(24)-S(2)-C(23) 169.8(3), C(13)-C(12)-S(1)-C(11) 132.4(3), C(16)-C(23)-S(2)-C(24) 173.6(3).

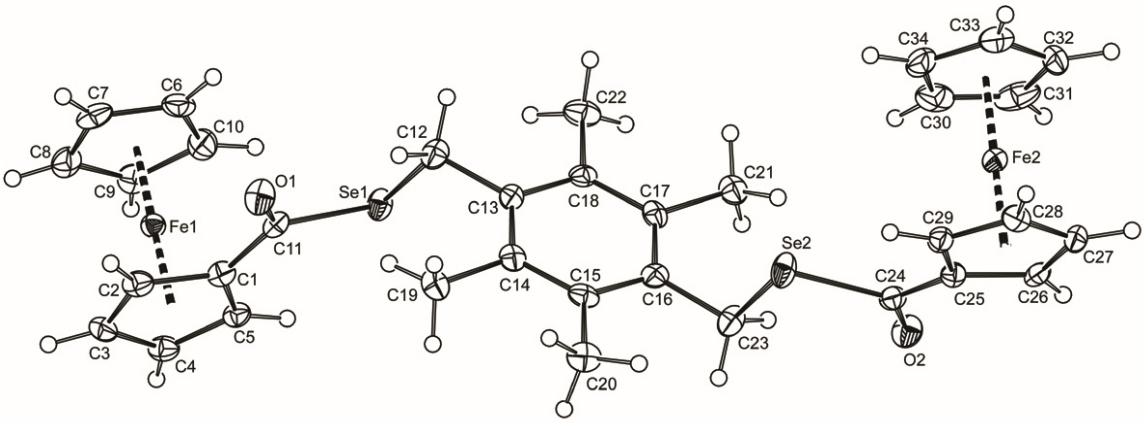

Figure 2.7. Thermal ellipsoid plot (40% probability level) of **8** with the atom numbering scheme. Selected bond distances (Å) and angles (º): C(12)-Se(1) 1.975(5), C(11)-Se(1) 1.961(4)**,** C(11)-C(1) 1.458(6), C(23)-Se(2) 1.957(5), C(24)-Se(2) 1.947(4)**,** C(24)-C(25) 1.461(6), C(11)-Se(1)-C(12) 98.0(2), C(1)-C(11)-Se(1) 113.9(3), C(23)-Se(2)-C(24) 96.2(2), C(25)-C(24)-Se(2) 113.8(3), C(1)-C(11)-Se(1)-C(12) 171.1(3), C(25)-C(24)-Se(2)-C(23) 175.9(3), C(13)-C(12)-Se(1)-C(11) 124.5(3), C(16)-C(23)-Se(2)-C(24) 150.0(3).

1,2,4,5-[FcC(O)SCH$_2$]$_4$(C$_6$H$_2$) **11** crystallized in the triclinic space group *P*$\bar{1}$ with a centre of inversion relating two halves of the molecule. The molecular structure and some of the selected intermolecular bond distances and angles are provided in Figure 2.8. As expected the large, adjacent ferrocenylthioester groups reside on opposite sides of the C$_6$ ring. Two of the equivalent C$_5$H$_4$ rings (bonded to Fe1/Fe1A) are rotated 61.67º out of the plane defined by the central C$_6$, while the other two are nearly perpendicular, twisted by 88.31º.

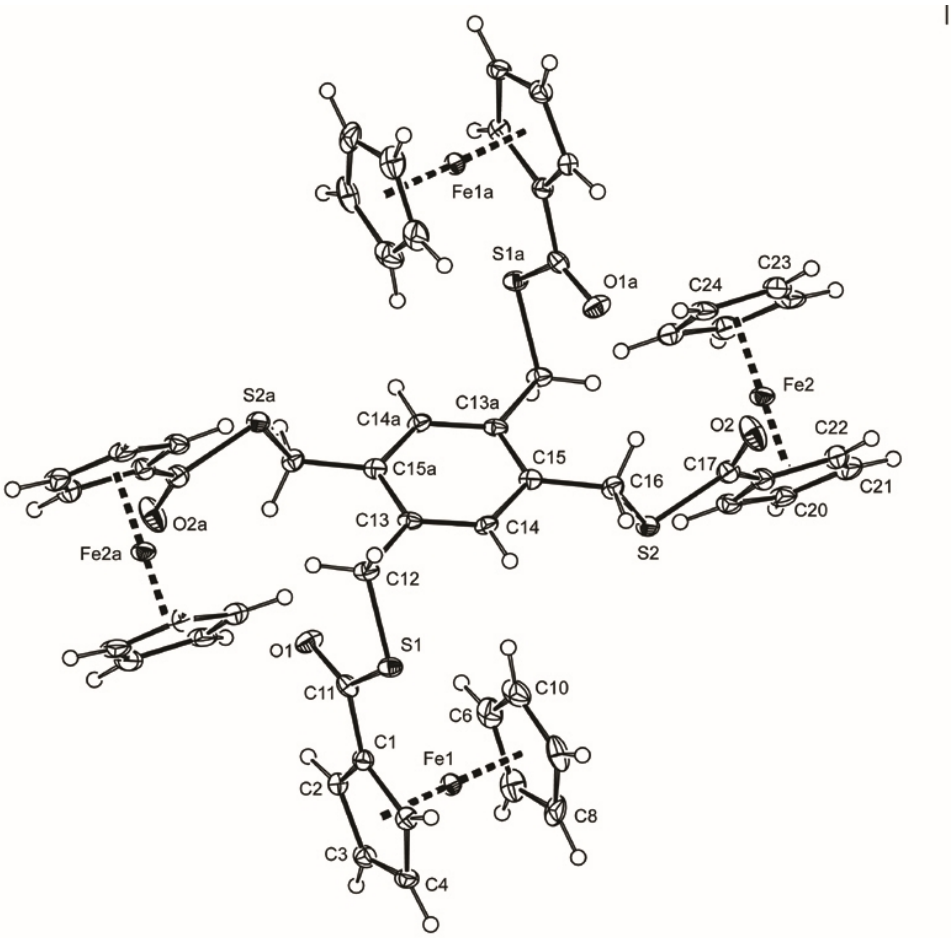

Figure 2.8. Thermal ellipsoid plot (40% probability level) of **11** with the atom numbering scheme. Selected bond distances (Å) and angles (º): C(11)-S(1) 1.7634(2), C(12)-S(1) 1.8067(1)**,** C(12)-C(13) 1.5225(1), C(17)-S(2) 1.7765(1), C(16)-S(2) 1.8293(1)**,** C(15)-C(16) 1.5013(1), C(11)-S(1)-C(12) 98.66(2), C(1)-C(11)-S(1) 114.6(3), C(16)-S(2)-C(17) 99.8(2), C(18)-C(17)-S(2) 113.6(3), C(1)-C(11)-S(1)-C(12) 172.9(3), C(13)-C(12)-S(1)-C(11) 74.0(4), C(18)-C(17)-S(2)-C(16) 168.9(3), C(15)-C(16)-S(2)-C(17) 138.9(3).

2.3 Electrochemistry Studies

Given the incorporation of the ferrocene units onto complexes **7**-**12**, it was incumbent to measure their electrochemical behavior of using cyclic voltammetry. To this end, 1 mM solutions of each polyferrocenyl complex **7**-**12** in acetonitrile containing 0.1 M tetrabutylammonium hexafluorophosphate ($TBAPF_6$) were prepared. The cyclic voltammograms were measured under inert atmosphere using a glassy carbon working electrode and the potentials were calibrated using ferrocene as an internal standard (0.34 V vs. SCE).[69] Figure 2.9 shows cyclic voltammograms (CVs) of ferrocene and complexes **7**-**11**.

The CVs of **7**-**10** (Figure 2.9 B, C), show what appears to be single chemically reversible oxidation process with an anodic to cathodic peak current ratios (I_{pa}/I_{pc}) for all four complexes **7**-**10** near unity. These are due to the reversible oxidation of the ferrocene moieties incorporated on these complexes. The current increases with the increasing ferrocene content of each of the complexes, with the integrated current area proportional to the number of ferrocene units in each of the complexes, relative to ferrocene. The apparent single, chemically reversible oxidation for each complex indicates that the ferrocenyl moieties on them oxidize at the same (or very similar potential) with little or no interaction between them.[70] The oxidation potentials of **7**-**12** are shifted to more positive potentials with Ep of ca. 0.68 V (E = S) and ca. 0.72 V (E = Se) than that observed for ferrocene (E_o = 0.34V vs SCE) under the same conditions, due to the presence of the electron withdrawing chalcogenoester groups on the C_5H_4 rings.[68b] The CVs for complexes **11** and **12** also show a single oxidation for the oxidation of the ferrocene moiety, but the reverse scan shows evidence for adsorption of these compounds onto the electrode (Figure 2.9 D), likely do to their limited solubility in this solvent, particularly upon oxidation.

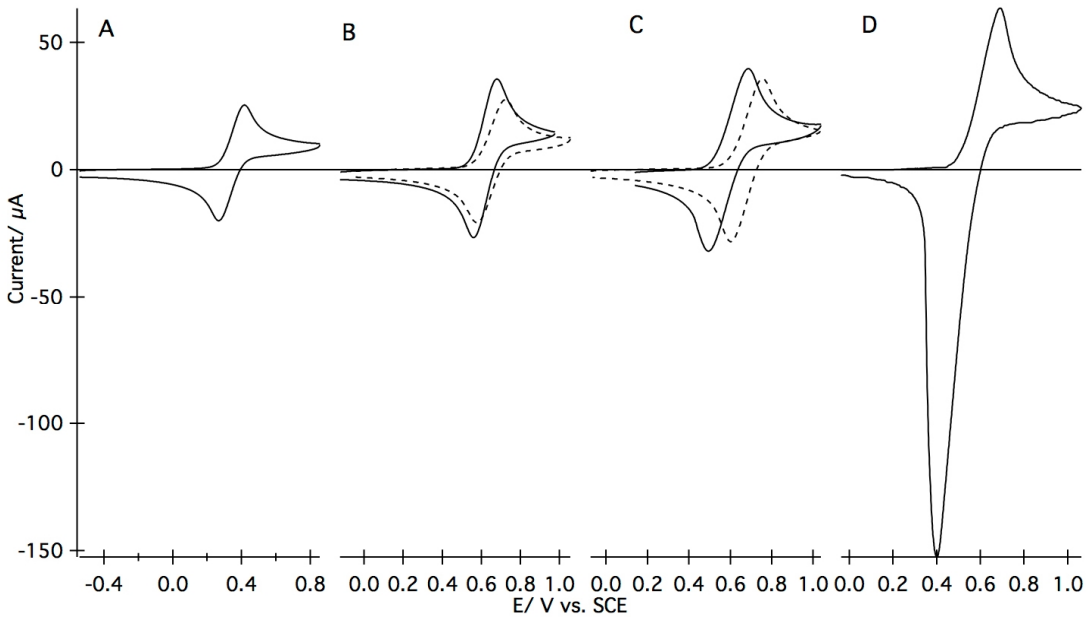

Figure 2.9. Cyclic voltammograms (CVs) of 1mM solutions of (A) ferrocene, (B) compound **7** (solid) **8** (dashed), (C) compound **9** (solid) and **10** (dashed), and (D) compound **11** in acetonitrile with 0.1 M $TBAPF_6$ as supporting electrolyte. All the CVs shown are recorded at 100 mV/s and are referenced to ferrocene at 0.34 V vs SCE.

2.4 Experimental Section

All syntheses were carried out under an atmosphere of high-purity dried nitrogen using standard double-manifold Schlenk line techniques and nitrogen-filled glove boxes unless otherwise stated. Solvents were dried and collected using an MBraun MB-SP Series solvent purification system with tandem activated alumina (tetrahydrofuran) and an activated alumina/copper redox catalyst (pentane).

Chlorinated solvents (dichloromethane, chloroform and chloroform-d) were dried and distilled over P_2O_5. Chemicals were used as received from Alfa Aesar and/or Aldrich. FcC(O)Cl,[71] 1,3,5-tris(bromomethyl)-2,4,6-trimethylbenzene,[72] 1,2,4,5-tetrakis(bromomethyl)benzene,[73] $Li[ESiMe_3]$[60] and $Na[ESiMe_3]$[61] (E = S, Se) were synthesized according to literature procedures. 1,4-bis(bromomethyl)-2,3,5,6-

tetramethylbenzene was prepared according to similar procedure for 1,3,5-tris(bromomethyl)-2,4,6-trimethylbenzene.[72] ^{1}H NMR ($CDCl_3$, 23 °C): δ 4.61 (s, 4H, CH_2), 2.34 (s, 12H, Ar-CH_3); ^{13}C {^{1}H} NMR ($CDCl_3$, 23 °C): δ 134.6, 134.0 (C6), 31.0 (CH_2), 15.9 (Ar-CH_3).

A BAS 100B\W Electrochemical Analyzer was used for cyclic voltammetry (CV) experiments. A homemade glassy carbon (GC, Tokai GC-20) working-electrode 3 mm in diameter was prepared by polishing over silicon carbide papers (500, 1200, 2400 and 4000) followed by diamond paste (Struers, 1 and 0.25 mm). The GC electrodes were stored in ethanol and polished before each set of experiments with the 0.25 mm diamond paste (Struers), rinsed with dry ethanol (Commercial Alcohols) and sonicated in dry ethanol for 5 min. Platinum wires served as the reference and counter electrodes. Electrochemical experiments were carried out in dry CH_2Cl_2 (Caledon) containing 0.1 M tetrabutylammonium hexa- fluorophosphate ($TBAPF_6$) as the supporting electrolyte. Potentials are referenced internally to ferrocene (0.342 V *vs*. SCE) added at the end of the experiments.

NMR spectra were recorded on Varian Mercury 400, Inova 400 and Inova 600 NMR spectrometers. ^{1}H and ^{13}C chemical shifts are referenced to $SiMe_4$, using solvent peak as a secondary reference, ^{77}Se chemical shifts are referenced to Me_2Se. Mass spectra and exact mass determinations were performed on a Bruker micrOTOF II instrument or Finningan MAT 8400. Elemental analysis was performed by Laboratoire d′Analyze Élementaire de l′Université de Montréal, Montréal, Canada, and Chemisar Laboratories, Guelph, Canada.

Single-crystal X-ray diffraction measurements were completed on Enraf-Nonius KappaCCD (**1**, **2** and **4**) and Bruker APEX-II CCD (**3**, **4**, **7**, **8** and **11**) diffractometers equipped with graphite-monochromated Mo Kα (λ = 0.71073 Å) radiation. Single crystals of the complexes were carefully selected, immersed in paraffin oil and mounted on MiteGen micromounts. The structures were solved using direct methods and refined by the full-matrix least-squares procedure of SHELXTL.[74] All non-hydrogen atoms, with the exception of disordered carbon centers, were refined with anisotropic thermal parameters. Hydrogen atoms were included as riding on their respective carbon atoms. For **7**, the TWIN

command in SHELXTL was used to refine the structure. Files CCDC 978321-978328 contain the supplementary crystallographic data for this paper. These data can be obtained free of charge from The Cambridge Crystallographic Data Centre via www.ccdc.cam.ac.uk/data_request/cif.

2.4.1 Synthesis of 1,4-$(Me_3SiSCH_2)_2(C_6Me_4)$ **1**

Method 1 1,4-bis(bromomethyl)-2,3,5,6-tetramethylbenzene (0.500 g, 1.56 mmol) and freshly prepared Li[$SSiMe_3$] (3.13 mmol) were each dissolved in anhydrous diethyl ether (30 mL and 15 mL respectively) and cooled to 0 °C. The solutions were mixed and stirred for 1 h at this temperature and overnight at room temperature resulting in an opaque suspension. The solvent was removed in vacuum and 30 mL chloroform and 15 mL of pentane were added to solubilize the product **1**. The solid LiBr was removed by twice passing the mixture through a sintered glass frit packed with Celite. The solvent was removed *in vacuo* yielding an off-white solid. **Method 2** 0.322g (2.51 mmol) of Na[$SSiMe_3$] was added portion wise to a solution of (0.400 g, 1.25 mmol) 1,4-bis(bromomethyl)-2,3,5,6-tetramethylbenzene in 40 mL tetrahydrofuran at room temperature followed by stirring overnight. The product was extracted as described above. Plate-like, colorless single crystals suitable for X-ray crystallography were obtained from slow evaporation of **1** in heptane (91% yield); m.p. 122-126 °C.

- ^{1}H NMR ($CDCl_3$, 23 °C): δ 3.72 (s, 4H, CH_2), 2.32 (s, 12H, Ar-CH_3), 0.41 (s, 18H, Si-CH_3) ppm.
- ^{13}C {^{1}H} NMR ($CDCl_3$, 23 °C): δ 135.1, 132.7 (*C*6), 26.1 (*C*H_2), 16.1 (Ar-*C*H_3), 0.7 (Si-*C*H_3) ppm.
- Anal. Calcd for $C_{18}H_{34}S_2Si_2$: C, 58.31; H, 9.24; S, 17.30. Found: C, 58.12; H, 9.30; S, 17.05.
- [M^+] for $C_{18}H_{34}S_2Si_2$: found (calculated) at *m/z* = 370.1645 (370.1640).

2.4.2 Synthesis of 1,4-($Me_3SiSeCH_2)_2(C_6Me_4$) **2**

0.500 g of 1,4-bis(bromomethyl)-2,3,5,6-tetramethylbenzene (1.56 mmol) in 30 mL of tetrahydrofuran was reacted with 3.12 mmol, 0.547 g of Na[$SeSiMe_3$] which was added portion wise. The suspension was stirred for 12 h at room temperature resulting in a white cloudy suspension. The solvent was removed in vacuum and 50 mL of pentane was added to solubilize **2**. NaBr was removed by passing the mixture through a sintered glass frit packed with Celite. The solvent was removed *in vacuo* yielding an off-white solid (80% yield); m.p. 151-152 °C. Colorless plate like single crystals suitable for X-ray diffraction were obtained by slow evaporation of **2** in hexanes.

- ^{1}H NMR ($CDCl_3$, 23 °C): δ 3.75 (s, 4H, CH_2), 2.32 (s, 12H, Ar-CH_3), 0.49 (s, 18H, Si-CH_3) ppm.
- ^{13}C {^{1}H} NMR ($CDCl_3$, 23 °C): δ 135.2, 132.6 (*C*6), 18.4 (*C*H_2), 16.1 (Ar-*C*H_3), 1.6 (Si-*C*H_3) ppm.
- ^{77}Se {^{1}H} NMR ($CDCl_3$, 23 °C): δ -70.7 ppm.
- [M^+] $C_{18}H_{34}$[^{76}Se] [^{80}Se]Si_2: found (calculated) at *m/z* = 464.0555 (464.0556).

2.4.3 Synthesis of 1,3,5-($Me_3SiSCH_2)_3(C_6Me_3$) **3**

0.500 g of 1,3,5-tris(bromomethyl)-2,4,6-trimethylbenzene (1.25 mmol) in 30 mL tetrahydrofuran was reacted with 3.76 mmol, 0.482 g of Na[$SSiMe_3$] as described for the preparation of **2** (98% yield); m.p. 134-137 °C. Colorless cubic prism single crystals suitable for X-ray diffraction were obtained by slow evaporation of **3** in hexanes.

- ^{1}H NMR ($CDCl_3$, 23 °C): δ 3.72 (s, 6H, CH_2), 2.46 (s, 9H,Ar-CH_3), 0.40 (s, 27H, Si-CH_3) ppm.
- ^{13}C {^{1}H} NMR ($CDCl_3$, 23 °C): δ 134.7, 134.2 (*C*6), 25.9 (*C*H_2), 15.6 (Ar-*C*H_3), 0.7 (Si-*C*H_3) ppm.
- Anal. Calcd for $C_{21}H_{42}S_3Si_3$: C, 53.10; H, 8.91; S, 20.25. Found: C, 52.94; H, 8.67; S, 20.01.
- [M^+] $C_{21}H_{42}S_3Si_3$: found (calculated) at *m/z* = 474.1766 (474.1756).

2.4.4. Synthesis of 1,3,5-($Me_3SiSeCH_2)_3(C_6Me_3$) **4**

0.500 g of 1,3,5-tris(bromomethyl)-2,4,6-trimethylbenzene (1.25 mmol) was reacted with 3.76 mmol, 0.658 g of Na[$SeSiMe_3$] (in 80 mL tetrahydrofuran) as described for the preparation of **2** (75% yield); m.p. 129-132 °C. Single crystals suitable for X-ray diffraction were obtained by slow evaporation of **4** in hexanes.

- ü ^{1}H NMR ($CDCl_3$, 23 °C): δ 3.72 (s, 6H, C*H*$_2$), 2.42 (s, 9H, Ar-C*H*$_3$), 0.47 (s, 27H, Si-C*H*$_3$) ppm.
- ü ^{13}C {^{1}H} NMR ($CDCl_3$, 23 °C): δ 134.9, 133.6 (*C*6), 18.0 (*C*H_2), 16.0 (Ar-*C*H_3), 1.6 (Si-*C*H_3) ppm.
- ü ^{77}Se {^{1}H} NMR ($CDCl_3$, 23 °C): δ -70.2 ppm.
- ü [M^+] $C_{21}H_{42}[^{78}Se][^{80}Se]_2Si_3$: found (calculated) at *m/z* = 616.0084 (616.0098).

2.4.5 Synthesis of 1,2,4,5-($Me_3SiSCH_2)_4(C_6H_2$) **5**

0.700 g of 1,2,4,5-tetrakis(bromomethyl)benzene (1.56 mmol) in 20 mL of diethyl ether was reacted with 6.22 mmol of freshly prepared Li[$SSiMe_3$] (in 50 mL diethyl ether) as described for **1** (65% yield); m.p. 104-107 °C.

- ü ^{1}H NMR ($CDCl_3$, 23 °C): δ 7.21 (s, 2H, *H*-Ar), 3.83 (s, 8H, C*H*$_2$), 0.34 (s, 36H, Si-C*H*$_3$) ppm.
- ü ^{13}C {^{1}H} NMR ($CDCl_3$, 23 °C): δ 137.4, 131.8 (*C*6), 27.5 (*C*H_2), 0.9 (Si-*C*H_3) ppm.
- ü [M^+] $C_{22}H_{46}S_4Si_4$: found (calculated) at *m/z* = 550.1552 (550.1559).

2.4.6 Synthesis of 1,2,4,5-($Me_3SiSeCH_2)_4(C_6H_2$) **6**

0.600 g of 1,2,4,5-tetrakis(bromomethyl)benzene (1.33 mmol) was reacted with 5.34 mmol) of freshly prepared Li[$SSiMe_3$] as described for **1** (in 70 mL diethyl ether) (64% yield); m.p. 104-107 °C. Colorless needle-like single crystals suitable for X-ray diffraction were obtained by slow evaporation of **6** in heptane.

- ü ^{1}H NMR ($CDCl_3$, 23 °C): δ 7.09 (s, 2H, *H*-Ar), 3.83 (s, 8H, C*H*$_2$), 0.44 (s, 36H, Si-C*H*$_3$) ppm.

- ü ^{13}C {^{1}H} NMR ($CDCl_3$, 23 °C): δ 137.5, 132.1 (*C*6), 18.7 (*C*H_2), 1.8 (Si-*C*H_3) ppm.
- ü ^{77}Se {^{1}H} NMR ($CDCl_3$, 23 °C): δ -19.0 ppm.

2.4.7 Synthesis of [1,4-{FcC(O)SCH$_2$}$_2$(C$_6$Me$_4$)] **7**

1,4-(Me_3SiSCH_2)$_2$(C_6Me_4) (0.186 g, 0.502 mmol) was mixed with 2 equiv of FcC(O)Cl (0.249 g, 1.00 mmol) as solids in an evacuated Schlenk tube. The sample was placed in a preheated (65 °C) oven, whereupon the reagents formed a dark red solid. After 10 h the mixture was cooled to room temperature. $ClSiMe_3$ was removed *in vacuo*, and the residue was washed with *n*-pentane. The crude compound was then purified by column chromatography and eluted using 25:75 acetonitrile:dichloromethane (60% yield); m.p. 206-209 °C. Small orange plate-like single crystals of **7** were obtained by slow evaporation of 1:20 acetonitrile:dichloromethane solution.

- ü ^{1}H NMR ($CDCl_3$, 23 °C): δ 4.87 (vt, 4H), 4.49 (vt, 4H), 4.37 (s, 4H, C*H*$_2$), 4.24 (s, 10H, Cp), 2.37 (s, 12H, C*H*$_3$) ppm.
- ü ^{13}C {^{1}H} NMR ($CDCl_3$, 23 °C): δ 193.8 (*C*=O), 133.5, 132.0 (*C*6), 79.0, 71.6, 70.4, 68.7 (Fc), 29.2 (*C*H_2), 16.5 (*C*H_3) ppm.
- ü Anal. Calcd for $C_{34}H_{34}Fe_2O_2S_2$: C, 62.78; H, 5.27; S, 9.86. Found: C, 62.89; H, 5.44; S, 9.86.
- ü [M^+] $C_{34}H_{34}Fe_2O_2S_2$: found (calculated) at *m/z* = 650.0700 (650.0699).

2.4.8 Synthesis of [1,4-{FcC(O)SeCH$_2$}$_2$(C$_6$Me$_4$)] **8**

Method 1 To 1,4-($Me_3SiSeCH_2$)$_2$(C_6Me_4) (0.093 g, 0.200 mmol) in 10 mL of tetrahydrofuran, a solution of 2 equiv of FcC(O)Cl (0.100 mg, 0.401 mmol) in 10 mL tetrahydrofuran was mixed at 25 °C. After 2 h of stirring at room temperature, the solvent and volatile $ClSiMe_3$ were removed under vacuum. After washing the residue with *n*-pentane, the remaining dark red solid was purified by column chromatography and eluted using 25:75 acetonitrile:dichloromethane (40% yield); m.p. 187-190 °C. **Method 2** 1,4-($Me_3SiSeCH_2$)$_2$(C_6Me_4) (0.220 g, 0.473 mmol) was mixed with 2 equiv of FcC(O)Cl

(0.235 g, 0.947 mmol) as solids in a Schlenk tube under vacuum. The sample was placed in a preheated (65 °C) oven, whereupon the reagents formed a dark red solid. After 12 h the mixture was cooled to room temperature. $ClSiMe_3$ was removed *in vacuo*, and the residue was washed with *n*-pentane. The residue was purified by column chromatography and eluted using 25:75 acetonitrile:dichloromethane (50% yield). Orange plate-like single crystal of **8** was obtained by diffusing *n*-pentane onto dichloromethane solution.

- ^1H NMR ($CDCl_3$, 23 °C): δ 4.84 (vt, 4H), 4.51 (vt, 4H), 4.38 (s, 4H, CH_2), 4.24 (s, 10H, Cp), 2.31 (s, 12H, CH_3) ppm.
- ^{13}C {^1H} NMR ($CDCl_3$, 23 °C): δ 195.2 (*C*=O), 133.4, 133.3 (*C*6), 81.5, 72.0, 70.8, 68.9 (Fc), 25.6 (*C*H_2), 17.0 (*C*H_3) ppm.
- ^{77}Se {^1H} NMR ($CDCl_3$, 23 °C): δ 528.4 ppm.
- Anal. Calcd for $C_{34}H_{34}Fe_2O_2Se_2$: C, 54.87; H, 4.60. Found: C, 54.59; H, 4.70.
- [M^+] $C_{34}H_{34}Fe_2O_2[^{78}Se][^{80}Se]$: found (calculated) at *m/z* = 743.9604 (743.9596).

2.4.9 Synthesis of [1,3,5-{FcC(O)SCH$_2$}$_3$(C$_6$Me$_3$)] **9**

A 0.116 g portion of 1,3,5-(Me_3SiSCH_2)$_3$(C_6Me_3) (0.244 mmol) was reacted with 0.182 mg (0.732 mmol) of FcC(O)Cl in solvent free conditions, as described for the preparation of **8** (see above). After appropriate workup, **9** was isolated as a dark red solid (60% yield); m.p. 208-210 °C.

- ^1H NMR ($CDCl_3$, 23 °C): δ 4.83 (vt, 6H), 4.51 (vt, 6H), 4.37 (s, 6H, CH_2), 4.24 (s, 15H, Cp), 2.43 (s, 9H, CH_3) ppm.
- ^{13}C {^1H} NMR ($CDCl_3$, 23 °C): δ 195.0 (*C*=O), 135.2, 133.1 (*C*6), 81.4, 72.0, 70.8, 68.9 (Fc), 25.3 (*C*H_2), 16.6 (*C*H_3) ppm.
- Anal. Calcd for $C_{45}H_{42}Fe_3O_3S_3$: C, 60.42; H, 4.73; S, 10.75. Found: C, 59.75; H, 4.80; S, 10.86.
- [M^+] $C_{45}H_{42}Fe_3O_3S_3$: found (calculated) at *m/z* = 894.0356 (894.0344).

2.4.10 Synthesis of [1,3,5-{FcC(O)SeCH$_2$}$_3$(C$_6$Me$_3$)] **10**

A 0.294 g portion of 1,3,5-(Me$_3$SiSeCH$_2$)$_3$(C$_6$Me$_3$) (0.478 mmol) was reacted with 0.356 g (1.43 mmol) of FcC(O)Cl as described for the preparation of **8** (see above). After appropriate workup, **10** was isolated as dark red solid (45% yield); m.p. 209-211 °C.

- ^{1}H NMR (CDCl$_3$, 23 °C): δ 4.86 (vt, 6H), 4.48 (vt, 6H), 4.37 (s, 6H, C*H*$_2$), 4.22 (s, 15H, Cp), 2.46 (s, 9H, C*H*$_3$) ppm.
- ^{13}C {^{1}H} NMR (CDCl$_3$, 23 °C): δ 193.9 (*C*=O), 136.3, 131.8 (*C*6), 79.1, 71.8, 70.6, 68.9 (Fc), 29.2 (*C*H$_2$), 16.5 (*C*H$_3$) ppm.
- ^{77}Se{^{1}H} NMR (CDCl$_3$, 23 °C): δ 528.2 ppm.
- Anal. Calcd for C$_{45}$H$_{42}$Fe$_3$O$_3$Se$_3$: C, 52.21; H, 4.09. Found: C, 52.41; H, 4.23.

2.4.11 Synthesis of [1,2,4,5-{FcC(O)SCH$_2$}$_4$(C$_6$H$_2$)] **11**

1,2,4,5-(Me$_3$SiSCH$_2$)$_4$(C$_6$H$_2$) (0.183 mmol, 0.101 g) was mixed with FcC(O)Cl (0.731 mmol, 0.182 g) at 25 °C in a Schlenk tube under vacuum. The sample was placed in a preheated (60-65 °C) oven. After 14 h, the mixture became solid. ClSiMe$_3$ was removed *in vacuo*, and the residue was washed with *n*-pentane. After appropriate workup, **11** was isolated as a dark red solid (66% yield); m.p. 185-189 °C. The residue was purified in two steps by silica and alumina column chromatography and eluted using 25:75 acetonitrile:dichloromethane and 12.5:87.5 heptane:dichloromethane, respectively. Small orange needle-like single crystals of **11** were obtained by slow evaporation of 1:5 heptane:dichloromethane solution. (50% yield).

- ^{1}H NMR (CDCl$_3$, 23 °C): δ 7.45 (s, 2H, Ar-*H*), 4.83 (vt, 8H), 4.45 (vt, 8H), 4.33 (s, 8H, C*H*$_2$), 4.17 (s, 20H, Cp) ppm.
- ^{13}C {^{1}H} NMR (CDCl$_3$, 23 °C): δ 192.8 (*C*=O), 135.8, 132.9 (*C*6), 79.0, 71.8, 70.6, 69.0 (Fc), 29.8 (*C*H$_2$) ppm.
- Anal. Calcd for C$_{54}$H$_{46}$Fe$_4$O$_4$S$_4$: C, 58.40; H, 4.17; S, 11.55. Found: C, 57.29; H, 3.96; S, 11.83.
- [M$^+$] C$_{54}$H$_{46}$Fe$_4$O$_4$S$_4$: found (calculated) at *m/z* = 1109.9655 (1109.9676).

2.4.12 Synthesis of [1,2,4,5-{FcC(O)SeCH$_2$}$_4$(C$_6$H$_2$)] **12**

Method 1 To 1,2,4,5-(Me$_3$SiSeCH$_2$)$_4$(C$_6$H$_2$) (0.111 g, 0.150 mmol) in 15 mL of tetrahydrofuran, a solution of four equiv of FcC(O)Cl (0.150 g, 0.601 mmol) in 10 mL tetrahydrofuran was mixed at 25 °C. After 4 h of stirring at room temperature, the solvent and ClSiMe$_3$ were removed under vacuum. The red solid was washed with *n*-pentane and the product was purified by column chromatography, eluted using 25:75 acetonitrile:dichloromethane (45% yield); m.p. 198-201 °C. **Method 2** 1,2,4,5-(Me$_3$SiSeCH$_2$)$_4$(C$_6$H$_2$) (0.174 g, 0.236 mmol) was mixed with four equiv of FcC(O)Cl (0.234 g, 0.943 mmol) as solids in an evacuated Schlenk tube. The sample was placed in a preheated (60-65 °C) oven, whereupon the reagents formed a dark red solid. After 14 h the mixture was cooled to room temperature. ClSiMe$_3$ was removed *in vacuo* and after appropriate workup, **12** was isolated as a dark red solid (63% yield).

- ^{1}H NMR (CDCl$_3$, 23 °C): δ 7.36 (s, 2H, Ar-*H*), 4.81 (vt, 8H), 4.48 (vt, 8H), 4.31 (s, 8H, C*H*$_2$), 4.20 (s, 20H, Cp) ppm.
- ^{13}C {^{1}H} NMR (CDCl$_3$, 23 °C): δ 194.0 (*C*=O), 136.8, 132.8 (*C*6), 81.2, 72.0, 70.8, 69.0 (Fc), 25.3 (*C*H$_2$) ppm.
- ^{77}Se{^{1}H} NMR (CDCl$_3$, 23 °C): δ 528.4 ppm.
- Anal. Calcd for C$_{54}$H$_{46}$Fe$_4$O$_4$Se$_4$: C, 49.96; H, 3.57. Found: C, 49.11; H, 3.80.
- [M$^+$] C$_{54}$H$_{46}$Fe$_4$O$_4$[^{78}Se][^{80}Se]$_3$: found (calculated) at *m/z* = 1299.7465 (1299.7462).

2.5 Conclusion

In summary, we have demonstrated a straightforward synthesis of a novel series of di-tri- and tetra- poly-chalcogenotrimethylsilanes Ar(CH$_2$ESiMe$_3$)$_n$ (n = 2-4). These have been used as "protected chalcogenides" for the facile preparation of poly ferrocenylseleno- and thioester assemblies via reaction with ferrocene acid chloride. The synthetic methodology is likely to be useful in the synthesis of other chalcogenoesters, and Ar(CH$_2$ESiMe$_3$)$_n$ themselves hold enormous potential for the assembly of polynuclear metal-chalcogen (cluster) architectures. We are currently developing this reaction chemistry.

2.6 References

[1] Rosenblum, M., *Chemistry of the iron group metallocenes: ferrocene, ruthenocene, osmocene*, Interscience Publishers, New York,, **1965**.

[2] Togni, A. and Hayashi, T., *Ferrocenes : homogeneous catalysis, organic synthesis, materials science*, VCH Publishers, Weinheim ; New York, **1995**.

[3] Adams, R. D., *J. Organomet. Chem.* **2001**, *637*, 1-1.

[4] (a) Astruc, D.; Ornelas C.; Aranzaes, J. R., *J. Inorg. Organomet. Polym.* **2008**, *18*, 4-17; (b) Armada, M. P. G.; Losada, J.; Zamora, M.; Alonso, B.; Cuadrado, I.; Casado, C. M., *Bioelectrochemistry* **2006**, *69*, 65-73; (c) Hendry, S. P.; Cardosi, M. F.; Turner, A. P. F., Neuse, E. W., *Anal. Chim. Acta* **1993**, *281*, 453-459.

[5] (a) Wei, B. Q.; Vajtai, R.; Choi, Y. Y.; Ajayan, P. M.; Zhu, H. W., Xu C. L.; Wu, D. H., *Nano Lett.* **2002**, *2*, 1105-1107; (b) Zhang, X. F.; Cao, A. Y.; Wei, B. Q.; Li, Y. H.; Wei, J. Q.; Xu, C. L.; Wu, D. H., *Chem. Phys. Lett.* **2002**, *362*, 285-290.

[6] (a) Ornelas, C.; Ruiz, J.; Belin, C.; Astruc, D., *J. Am. Chem. Soc.* **2009**, *131*, 590-601; (b) Megiatto, J. D.; Li, K.; Schuster, D. I., Palkar, A., Herranz, M. A., Echegoyen, L. Abwandner, S.; de Miguel, G.; Guldi, D. M., *J. Phys. Chem. B* **2010**, *114*, 14408-14419.

[7] Neuse, E. W.; Woodhouse, J. R.; Montaudo, G.; Puglisi, C., *Appl. Organomet. Chem.* **1988**, *2*, 53-57.

[8] (a) van Staveren, D. R.; Metzler-Nolte, N., *Chem. Rev.* **2004**, *104*, 5931-5985; (b) Allardyce, C. S.; Dorcier, A.; Scolaro, C.; Dyson, P. J., *Appl. Organomet. Chem.* **2005**, *19*, 1-10; (c) Neuse, E. W., *J. Inorg. Organomet. Polym.* **2005**, *15*, 3-32; (d) Fouda, M. F. R.; Abd-Elzaher, M. M.; Abdelsamaia, R. A.; Labib, A. A., *Appl. Organomet. Chem.* **2007**, *21*, 613-625; (e) Ornelas, C., *New J. Chem.* **2011**, *35*, 1973-1985; (f) Nguyen, A.; Vessieres, A.; Hillard, E. A.; Top, S.; Pigeon, P.; Jaouen, G., *Chimia* **2007**, *61*, 716-724.

[9] (a) Biot, C.; Francois, N.; Maciejewski, L.; Brocard, J.; Poulain, D., *Bioorg. Med. Chem. Lett.* **2000**, *10*, 839-841; (b) Zhang, J., *Appl. Organomet. Chem.* **2008**, *22*, 6-11; (c) Biot, C.; Glorian, G.; Maciejewski, L. A.; Brocard, J. S.; Domarle, O.; Blampain, G.; Millet, P.; Georges, A. J.; Abessolo, H.; Dive, D. Lebibi, J., *J. Med. Chem.* **1997**, *40*, 3715-3718; (d) Delhaes, L.; Biot, C.; Berry, L.; Maciejewski, L. A.; Camus, D.; Brocard, J. S.; Dive, D., *Biorg. Med. Chem.* **2000**, 2739-2745; (e) Itoh, T.; Shirakami, S.; Ishida, N.; Yamashita, Y.; Yoshida, T.; Kim, H. S.; Wataya, Y., *Bioorg. Med. Chem. Lett.* **2000**, *10*, 1657-1659; (f) Kondapi, A. K.; Satyanarayana, N.; Saikrishna, A. D., *Arch. Biochem. Biophys.* **2006**, *450*, 123-132.

[10] (a) Marsh, N. D.; Preciado, I.; Eddings, E. G.; Sarofim, A. F.; Palotas, A. B.; Robertson, J. D., *Combust. Sci. Technol.* **2007**, *179*, 987-1001; (b) Smith, C. S.; Metcalfe, E., *Polym. Int.* **2000**, *49*, 1169-1176; (c) Bruno, T. J.; Baibourine, E., *Energy Fuels* **2010**, *24*, 5508-5513.

[11] (a) Bildstein, B.; Malaun, M.; Kopacka, H.; Fontani, M.; Zanello, P., *Inorg. Chim. Acta* **2000**, *300*, 16-22; (b) Mathur, P.; Chatterjee, S.; Das, A.; Lahiri, G. K.; Maji, S.; Mobin, S. M., *J. Organomet. Chem.* **2007**, *692*, 1601-1607; (c) Berestneva, T. K.; Klimova, E. I.; Stivalet, J. M. M.; Hernandez-Ortega, S.; Garcia, M. M.; *Eur. J. Org. Chem.* **2005**,

4406-4413; (d) Liu, W. Y.; Xu, Q. H.; Ma, Y. X.; Liang, Y. M.; Dong, N. L.; Guan, D. P.; *J. Organomet. Chem.* **2001**, *625*, 128-131.

[12] (a) Wu, K. Q.; Guo, J.; Yan, J. F.; Xie, L. L.; Xu, F. B.; Bai, S.; Nockemann, P.; Yuan, Y. F., *Dalton Trans.* **2012**, *41*, 11000-11008; (b) Kramer, J. A.; Hendrickson, D. N.; *Inorg. Chem.* **1980**, *19*, 3330-3337.

[13] (a) Diallo, A. K.; Daran, J. C.; Varret, F.; Ruiz, J.; Astruc, D., *Angew. Chem. Int. Edit.* **2009**, *48*, 3141-3145; (b) Patoux, C.; Coudret, C.; Launay, J. P.; Joachim, C.; Gourdon, A., *Inorg. Chem.* **1997**, *36*, 5037-5049; (c) Santi, S.; Orian, L.; Durante, C.; Bencze, E. Z.; Bisello, A.; Donoli, A.; Ceccon, A.; Benetollo, F.; Crociani, L., *Chem. Eur. J.* **2007**, *13*, 7933-7947; (d) Yu, Y.; Bond, A. D.; Leonard, P. W.; Lorenz, U. J.; Timofeeva, T. V.; Vollhardt, K. P. C.; Glenn, D. W.; Yakovenko, A. A.. *Chem. Commun.* **2006**, 2572-2574.

[14] (a) Pfaff, U.; Hildebrandt, A.; Schaarschmidt, D.; Hahn, T.; Liebing, S.; Kortus, J.; Lang, H., *Organometallics* **2012**, *31*, 6761-6771; (b) Kowalski, K.; Winter, R. F., *J. Organomet. Chem.* **2009**, *694*, 1041-1048; (c) Ogawa, S.; Muraoka, H.; Kikuta, K.; Saito, F.; Sato, R., *J. Organomet. Chem.* **2007**, *692*, 60-69; (d) Speck, J. M.; Claus, R.; Hildebrandt, A.; Ruffer, T.; Erasmus, E.; van As, L.; Swarts, J. C.; Lang, H., *Organometallics* **2012**, *31*, 6373-6380; (e) Hildebrandt, A.; Lang, H., *Dalton Trans.* **2011**, *40*, 11831-11837; (f) Taher, D.; Awwadi, F. F.; Pfaff, U.; Speck, J. M.; Ruffer, T.; Lang, H., *J. Organomet. Chem.* **2013**, *736*, 9-18; (g) Thomas, K. R. J.; Lin, J. T., *J. Organomet. Chem.* **2001**, *637*, 139-144.

[15] (a) Bruce, M. I.; Costuas, K.; Gendron, F.; Halet, J. F.; Jevric, M.; Skelton, B. W., *Organometallics* **2012**, *31*, 6555-6566; (b) Nievas, A.; Gonzalez, J. J.; Hernandez, E.; Delgado, E.; Martin, A.; Casado, C. M.; Alonso, B., *Organometallics* **2011**, *30*, 1920-1929.

[16] Spanig, F.; Kovacs, C.; Hauke, F.; Ohkubo, K.; Fukuzumi, S.; Guldi, D. M.; Hirsch, A., *J. Am. Chem. Soc.* **2009**, *131*, 8180-8195.

[17] (a) Kaleta, K.; Hildebrandt, A.; Strehler, F.; Arndt, P.; Jiao, H. J.; Spannenberg, A.; Lang, H.; Rosenthal, U., *Angew. Chem. Int. Edit.* **2011**, *50*, 11248-11252; (b) Speck, J. M.; Schaarschmidt, D.; Lang, H., *Organometallics* **2012**, *31*, 1975-1982; (c) Kowalski, K.; Winter, R. F., *J. Organomet. Chem.* **2008**, *693*, 2181-2187.

[18] (a) Amer, W. A.; Wang, L.; Amin, A. M.; Ma, L. A.; Yu, H. J., *J. Inorg. Organomet. Polym.* **2010**, *20*, 605-615; (b) Chuo, T.-W.; Wei, T.-C.; Liu, Y.-L., *J. Polym. Sci., Part A: Polym. Chem.* **2013**, *51*, 3395-3403; (c) Kim, B. Y.; Ratcliff, E. L.; Armstrong, N. R.; Kowalewski, T.; Pyun, J., *Langmuir* **2010**, *26*, 2083-2092; (d) Kurane, R.; Gaikwad, V.; Jadhav, J.; Salunkhe, R.; Rashinkar, G., *Tetrahedron Lett.* **2012**, *53*, 6361-6366; (e) Nishihara, H.; Murata, M., *J. Inorg. Organomet. Polym.* **2005**, *15*, 147-156.

[19] (a) Astruc, D., *Nature Chemistry* **2012**, *4*, 255-267; (b) Kim, C.; Park, E.; Song, C. K.; Koo, B. W., *Synth. Met.* **2001**, *123*, 493-496; (c) Ong, W.; Gomez-Kaifer, M.; Kaifer, A. E., *Chem. Commun.* **2004**, 1677-1683; (d) Sengupta, S., *Tetrahedron Lett.* **2003**, *44*, 7281-7284; (e) Sengupta, S.; Sadhukhan, S. K., *Tetrahedron Lett.* **2001**, *42*, 3659-3661.

[20] (a) Nitschke, C.; Wallbank, A. I.; Fenske, D.; Corrigan, J. F., *J. Cluster Sci.* **2007**, *18*, 131-140; (b) Wallbank, A. I.; Corrigan, J. F., *J. Cluster Sci.* **2004**, *15*, 225-232; (c) Ahmar, S.; MacDonald, D. G.; Vijayaratnam, N.; Battista, T. L.; Workentin, M. S.; Corrigan, J. F., *Angew. Chem. Int. Edit.* **2010**, *49*, 4422-4424; (d) MacDonald, D. G.; Corrigan, J. F., *Phil.*

Trans. R. Soc. A **2010**, *368*, 1455-1472; (e) MacDonald, D. G.; Eichhofer, A.; Campana, C. F.; Corrigan, J. F., *Chem. Eur. J.* **2011**, *17*, 5890-5902; (f) Ruffer, T.; Jakob, A.; Swarts, J. C.; Lang, H., *J. Coord. Chem.* **2013**, *66*, 329-333.

[21] (a) Taher, D.; Corrigan, J. F., *Organometallics* **2011**, *30*, 5943-5952; (b) Takahashi, T.; Niyomura, O.; Kato, S.; Ebihara, M., *Z. Anorg. Allg. Chem.* **2013**, *639*, 108-114.

[22] Fujiwara, S.; Kambe, N., *Top. Curr. Chem.* **2005**, *251*, 87-140.

[23] (a) Boger, D. L.; Mathvink, R. J., *J. Org. Chem.* **1992**, *57*, 1429-1443; (b) Kozikowski, A. P.; Ames, A., *Tetrahedron* **1985**, *41*, 4821-4834; (c) Pfenninger, J.; Heuberger, C.; Graf, W., *Helv. Chim. Acta* **1980**, *63*, 2328-2337; (d) Schwartz, C. E.; Curran, D. P., *J. Am. Chem. Soc.* **1990**, *112*, 9272-9284.

[24] (a) Dheur, J.; Ollivier, N.; Melnyk, O., *Org. Lett.* **2011**, *13*, 1560-1563; (b) Suh, K. H.; Choo, D. J., *Tetrahedron Lett.* **1995**, *36*, 6109-6112; (c) Syu, S. E.; Lee, Y. T.; Jang, Y. J.; Lin, W. W., *Org. Lett.* **2011**, *13*, 2970-2973; (d) Zeysing, B.; Gosch, C.; Terfort, A., *Org. Lett.* **2000**, *2*, 1843-1845.

[25] (a) Tiecco, M.; Testaferri, K.; Temperini, A.; Bagnoli, L.; Marini, F.; Santi, C.; Terlizzi, R., *Eur. J. Org. Chem.* **2004**, 3447-3458; (b) Kozikowski, A. P.; Ames, A., *J. Org. Chem.* **1978**, *43*, 2735-2737; (c) Clericuzio, M.; Degani, I.; Dughera, S.; Fochi, R., *Synthesis* **2002**, 921-927; (d) Dabdoub, M. J.; Viana, L. H., *Synth. Commun.* **1992**, *22*, 1619-1625; (e) Um, P. J.; Drueckhammer, D. G., *J. Am. Chem. Soc.* **1998**, *120*, 5605-5610.

[26] (a) Wang, F.; Liu, H. X. ; Fu, H.; Jiang, Y. Y.; Zhao, Y. F., *Adv. Synth. Catal.* **2009**, *351*, 246-252; (b) Wehofsky, N.; Koglin, N.; Thust, S.; Bordusa, F., *J. Am. Chem. Soc.* **2003**, *125*, 6126-6133.

[27] (a) Anderson, R. J.; Henrick, C. A.; Rosenblu, L. D., *J. Am. Chem. Soc.* **1974**, *96*, 3654-3655; (b) Araki, M.; Sakata, S.; Takei, H.; Mukaiyam, T., *Bull. Chem. Soc. Jpn.* **1974**, *47*, 1777-1780; (c) Cama, L.; Christensen, B. G., *Tetrahedron Lett.* **1980**, *21*, 2013-2016; (d) Liebeskind, L. S.; Srogl, J., *J. Am. Chem. Soc.* **2000**, *122*, 11260-11261.

[28] (a) Back, T. G.; Kerr, R. G., *Tetrahedron* **1985**, *41*, 4759-4764; (b) Conrow, R.; Portoghese, P. S., *J. Org. Chem.* **1986**, *51*, 938-940; (c) Mcgarvey, G. J., Williams, J. M.; Hiner, R. N.; Matsubara, Y.; Oh, T., *J. Am. Chem. Soc.* **1986**, *108*, 4943-4952.

[29] (a) Fukuyama, T.; Lin, S. C.; Li, L. P., *J. Am. Chem. Soc.* **1990**, *112*, 7050-7051; (b) Miyazaki, T.; Han-ya, Y.; Tokuyama, H.; Fukuyama, T., *Synlett* **2004**, 477-480; (c) Wolfrom, M. L.; Karabinos, J. V., *J. Am. Chem. Soc.* **1946**, *68*, 1455-1456.

[30] Kuniyasu, H.; Ogawa, A.; Higaki. K.; Sonoda, N., *Organometallics* **1992**, *11*, 3937-3939.

[31] (a) Hirai, T.; Kuniyasu, H.; Kato, T.; Kurata, Y.; Kambe, N., *Org. Lett.* **2003**, *5*, 3871-3873; (b) Kobayashi, S.; Uchiro, H.; Fujishita, Y.; Shiina, I.; Mukaiyama, T., *J. Am. Chem. Soc.* **1991**, *113*, 4247-4252.

[32] (a) Kozikowski, A. P.; Ames, A., *J. Am. Chem. Soc.* **1980**, *102*, 860-862; (b) Subramanyam, C.; Noguchi, M.; Weinreb, S. M., *J. Org. Chem.* **1989**, *54*, 5580-5585.

[33] Danheiser, R. L.; Nowick, J. S., *J Org Chem* **1991**, *56*, 1176-1185.

[34] (a) Inoue, M.; Yamashita, S.; Ishihara, Y.; Hirama, M., *Org. Lett.* **2006**, *8*, 5805-5808; (b) Baca, M.; Muir, T. W.; Schnolzer, M.; Kent, S. B. H., *J. Am. Chem. Soc.* **1995**, *117*, 1881-1887.

[35] Martin, S. F.; Chen, K. X.; Eary, C. T., *Org. Lett.* **1999**, *1*, 79-81.

[36] (a) Keck; G. E., Grier, M. C., *Synlett* **1999**, 1657-1659; (b) Chen, C.; Crich, D.; Papadatos, A., *J. Am. Chem. Soc.* **1992**, *114*, 8313-8314; (c) Bachi, M. D.; Denenmark, D., *J. Am. Chem. Soc.* **1989**, *111*, 1886-1888; (d) Berlin, S.; Ericsson, C.; Engman, L., *Org. Lett.* **2002**, *4*, 3-6.

[37] (a) Penn, J. H., Liu, F., *J. Org. Chem.* **1994**, *59*, 2608-2612; (b) Crich, D.; Yao, Q. W., *J. Org. Chem.* **1996**, *61*, 3566-3570; (c) Benati, L.; Leardini, R.; Minozzi, M.; Nanni, D.; Spagnolo, P.; Strazzari, S.; Zanardi, G., *Org. Lett.* **2002**, *4*, 3079-3081; (d) Blakskjaer, P.; Hoj, B.; Riber, D.; Skrydstrup, T., *J. Am. Chem. Soc.* **2003**, *125*, 4030-4031; (e) Chatgilialoglu, C.; Crich, D., Komatsu, M.; Ryu, I., *Chem. Rev.* **1999**, *99*, 1991-2069.

[38] (a) Hiiro, T.; Morita, Y.; Inoue, T.; Kambe, N.; Ogawa, A.; Ryu, I. H.; Sonoda, N., *J. Am. Chem. Soc.* **1990**, *112*, 455-457; (b) Penn, J. H.; Owens, W. H., *Tetrahedron Lett.* **1992**, *33*, 3737-3740.

[39] (a) DeGroot, M. W.; Corrigan, J. F., *J. Chem. Soc., Dalton Trans.* **2000**, 1235-1236; (b) Zhu, N. Y.; Fenske, D., *J. Chem. Soc., Dalton Trans.* **1999**, 1067-1075.

[40] (a) Arnold, J., *Prog. Inorg. Chem.* **1995**, *43*, 353-417; (b) Fuhr, O.; Dehnen, S.; Fenske, D., *Chem. Soc. Rev.* **2013**, *42*, 1871-1906; (c) Roof, L. C.; Kolis, J. W., *Chem. Rev.* **1993**, *93*, 1037-1080.

[41] Rimpler, M., *Chem. Ber. Recl.* **1966**, *99*, 1528-1531.

[42] Sasaki, K.; Aso, Y., Otsubo, T.; Ogura, F., *Chem. Lett.* **1986**, 977-978.

[43] Zhang, S. L.; Zhang, Y. M., *Synth. Commun.* **1998**, *28*, 3999-4002.

[44] Capperucci, A.; Degl'Innocenti, A.; Tiberi, C., *Synlett* **2011**, 2248-2252.

[45] (a) Renson, M.; Draguet, C., *Bull. Soc. Chim. Belg.* **1962**, *71*, 260-275; (b) Bonner, W. A., *J. Am. Chem. Soc.* **1950**, *72*, 4270-4271; (c) Schleppnik, A. A.; Zienty, F. B., *J. Org. Chem.* **1964**, *29*, 1910-1915.

[46] (a) Ren, K.; Wang, M.; Liu. P.; Wang, L., *Synthesis* **2010**, 1078-1082; (b) Movassagh, B.; Mirshojaei, F., *Monatsh. Chem.* **2003**, *134*, 831-835; (c) Jia, X. S., Zhang, Y. M., Zhou, X. J., *Synth. Commun.* **1994**, *24*, 387-392.

[47] Reinerth, W. A.; Tour, J. M., *J. Org. Chem.* **1998**, *63*, 2397-2400.

[48] (a) Herberhold, M.; Leitner, P.; Dornhofer, C.; Ottlastic, J., *J. Organomet. Chem.* **1989**, *377*, 281-289; (b) Broussier, R.; Abdulla, A.; Gautheron, B., *J. Organomet. Chem.* **1987**, *332*, 165-173.

[49] (a) Ranu, B. C.; Mandal, T.; Samanta, S., *Org. Lett.* **2003**, *5*, 1439-1441; (b) Nobrega, J. A., Goncalves, S. M. C.; Peppe, C., *Tetrahedron Lett.* **2000**, *41*, 5779-5782; (c) Ajiki, K.; Hirano, M.; Tanaka, K., *Org. Lett.* **2005**, *7*, 4193-4195.

[50] (a) Schiesser, C. H.; Skidmore, M. A., *J. Org. Chem.* **1998**, *63*, 5713-5715; (b) Nishiyama, Y.; Tokunaga, K.; Kawamatsu, H.; Sonoda, N., *Tetrahedron Lett.* **2002**, *43*, 1507-1509; (c) Wallner, O. A.; Szabo, K. J., *J. Org. Chem.* **2005**, *70*, 9215-9221.

[51] Detty, M. R.; Wood, G. P., *J. Org. Chem.* **1980**, *45*, 80-89.

[52] Silveira, C. C.; Braga, A. L.; Larghi, E. L., *Organometallics* **1999**, *18*, 5183-5186.

[53] Inoue, T.; Takeda, T.; Kambe, N.; Ogawa, A.; Ryu, I.; Sonoda, N., *J. Org. Chem.* **1994**, *59*, 5824-5827.

[54] Dan, W. X.; Deng, H. J.; Chen, J. X.; Liu, M. C.; Ding, J. C.; Wu, H. Y., *Tetrahedron* **2010**, *66*, 7384-7388.

[55] (a) Zhang, Y. M.; Yu, Y. P.; Lin, R. H.; *Synth. Commun.* **1993**, *23*, 189-193; (b) Wang, L.; Zhang, Y. M., *Synth. Commun.* **1999**, *29*, 3107-3115; (c) Chen, R.; Zhang, Y. M., *Synth. Commun.* **2000**, *30*, 1331-1336; (d) Liu, Y. K.; Zhang, Y. M., *Synth. Commun.* **1999**, *29*, 4043-4049.

[56] Sheng, S. R.; Liu, X. L., *Org. Prep. Proced. Int.* **2002**, *34*, 499-502.

[57] (a) Godoi, M.; Ricardo, E. W.; Botteselle, G. V.; Galetto, F. Z.; Azeredo, J. B.; Braga, A. L., *Green Chemistry* **2012**, *14*, 456-460; (b) Santi, C.; Battistelli, B.; Testaferri, L.; Tiecco, M., *Green Chemistry* **2012**, *14*, 1277-1280.

[58] Tahert, D.; Corrigan, J. F., *Organometallics* **2011**, *30*, 5943-5952.

[59] (a) Wallbank, A. I.; Corrigan, J. F., *Chem. Commun.* **2001**, 377-378; (b) Nitschke, C.; Fenske, D.; Corrigan, J. F.. *Inorg. Chem.* **2006**, *45*, 9394-9401.

[60] (a) Taher, D.; Wallbank, A. I.; Turner, E. A.; Cuthbert, H. L.; Corrigan, J. F., *Eur. J. Inorg. Chem.* **2006**, 4616-4620; (b) Segi, M., Nakajima, T., Suga, S.; Murai, S.; Ryu, I.; Ogawa, A.; Sonoda, N., *J. Am. Chem. Soc.* **1988**, *110*, 1976-1978.

[61] (a) Schmidt, M.; Kiewert, E.; Lux, H.; Sametschek, C., *Phosphorus, Sulfur, and Silicon* **1986**, *26*, 163-167; (b) Do, Y.; Simhon, E. D.; Holm, R. H., *Inorg. Chem.* **1983**, *22*, 3809-3812.

[62] (a) Fujihara, H.; Yabe, M.; Chiu, J. J.; Furukawa, N., *Tetrahedron Lett.* **1991**, *32*, 4345-4348; (b) Fujihara, H.; Tanaka, H.; Furukawa, N., *J. Chem. Soc. Perkin Trans. 1* **1995**, 2375-2377; (c) Mugesh, G.; Panda, A.; Singh, H. B.; Butcher, R. J., *Chem. Eur. J.* **1999**, *5*, 1411-1421.

[63] (a) Becker, G.; Massa, W.; Schmidt, R. E.; Uhl, G., *Z. Anorg. Allg. Chem.* **1984**, *517*, 75-88; (b) Fuhr, O.; Fenske, D., *Z. Anorg. Allg. Chem.* **2004**, *630*, 1607-1612; (c) Ren, W. S.; Zi, G. F., Fang, D. C.; Walter, M. D., *J. Am. Chem. Soc.* **2011**, *133*, 13183-13196; (d) Schulz, A.; Villinger, A., *Chem. Eur. J.* **2010**, *16*, 7276-7281; e) Weber, L.; Uthmann, S.; Bogge, H.; Muller, A.; Stammler, H. G.; Neumann, B., *Organometallics* **1998**, *17*, 3593-3598; (f) Weber, L.; Uthmann, S.; Torwiehe, B.; Kirchhoff, R.; Boese, R.; Blaser, D., *Organometallics* **1997**, *16*, 3188-3193.

[64] (a) Gormley, F. K.; Gronbach, J.; Draper, S. M.; Davis, A. P., *J. Chem. Soc., Dalton Trans.* **2000**, 173-179; (b) Christensen, C. A.; Bryce, M. R.; Batsanov, A. S.; Becher, J., *Chem. Commun.* **2000**, 331-332; (c) D'Aleo,; Williams,; Osswald,; Edamana,; Hahn,; van

Heyst,; Tichelaar,; Vogtle, F.; De Cola, L., *Adv. Funct. Mater.* **2004**, *14*, 1167-1177; (d) Hardy, A. D. U.; Macnicol, D. D.; Swanson, S.; Wilson, D. R., *J. Chem. Soc., Perkin Trans. 2* **1980**, 999-1005; e) Kumar, N.; Milton, M. D.; Singh, J. D., *Tetrahedron Lett.* **2004**, *45*, 6611-6613; (f) Macnicol, D. D.; Wilson, D. R., *J. Chem. Soc., Chem. Commun.* **1976**, 494-495; (g) McMorran, D. A.; Steel, P. J., *Tetrahedron* **2003**, *59*, 3701-3707; (h) Singh, J. D.; Maheshwari, M.; Khan, S.; Butcher, R. J., *Tetrahedron Lett.* **2008**, *49*, 117-121.

[65] Pauling, L., *The nature of the chemical bond and the structure of molecules and crystals; an introduction to modern structural chemistry*, Cornell University Press, Ithaca, N.Y., **1960**, p. 644.

[66] (a) Ahamed, B. N.; Arunachalam, M.; Ghosh, P., *Inorg. Chem.* **2011**, *50*, 4772-4780; (b) Arroyo, M.; Bernes, S.; Calixto, N.; Gomez, C., *J. Fluorine Chem.* **2006**, *127*, 22-28.

[67] (a) Evans, D. A.; Burgey, C. S.; Kozlowski, M. C.; Tregay, S. W., *J. Am. Chem. Soc.* **1999**, *121*, 686-699; (b) Imrie, C.; Cook, L.; Levendis, D. C., *J. Organomet. Chem.* **2001**, *637*, 266-275; (c) Kageyama, H.; Tani, K.; Kato, S.; Kanda, T., *Heteroat. Chem* **2001**, *12*, 250-258.

[68] (a) Koketsu, M.; Mizutani, K.; Ogawa, T.; Takahashi. A.; Ishihara, H., *J. Org. Chem.* **2004**, *69*, 8938-8941; (b) Kumar, S.; Tripathi, S. K.; Singh, H. B.; Wolmershauser, G., *J. Organomet. Chem.* **2004**, *689*, 3046-3055; (c) Shefter, E.; Kennard, O., *Science* **1966**, *153*, 1389-1390; (d) Sieler, J.; Olk, R. M.; Dietzsch, W.; Hoyer, E.; Olk, B., *J. Prak. Chem.-Chem. Ztg.* **1992**, *334*, 72-75.

[69] Sahami, S.; Weaver, M. J., *J. Electroanal. Chem.* **1981**, *122*, 155-170.

[70] Burgess, M. R.; Jing, S.; Morley, C. P., *J. Organomet. Chem.* **2006**, *691*, 3484-3489.

[71] (a) Aguilar-Aguilar, A.; Allen, A. D.; Cabrera, E. P.; Fedorov, A.; Fu, N. Y.; Henry-Riyad, H.; Leuninger, J.; Schmid, U.; Tidwell, T. T.; Verma, R., *J. Org. Chem.* **2005**, *70*, 9556-9561; (b) Breit, B.; Breuninger, D., *Synthesis* **2005**, 2782-2786.

[72] Zavada, J.; Pankova, M.; Holy, P.; Tichy, M., *Synthesis* **1994**, 1132-1132.

[73] Kawai, H.; Umehara, T.; Fujiwara, K.; Tsuji, T.; Suzuki, T., *Angew. Chem. Int. Edit.* **2006**, *45*, 4281-4286.

[74] (a) Sheldrick, G. M., in *SHELXTL PC Version 6.1 An Integrated System for Solving, Refining, and Displaying Crystal Structures from Diffraction Data, Bruker Analytical X-ray Systems, 2000;, Vol*; (b) Sheldrick, G. M.; *Acta Crystallogr., Sect. A* **2008**, *64*, 112-122.

Chapter 3

Polydentate Chalcogen Reagents for the Facile Preparation of Pd_2 and Pd_4 Complexes

(Mahmood Azizpoor Fard, Mathew J. Willans, Bahareh Khalili Najafabadi, Tetyana I. Levchenkoa and John. F. Corrigan, *Dalton Trans.,* **2015**, *44*, 8267–8277)

3.1 Introduction

There has been considerable interest in the chemistry of the platinum group metal chalcogenide and chalcogenolate complexes due in part to their interesting photophysical properties[1] and their potential utility in organic syntheses.[2] Due to the high affinity of platinum-group metals for chalcogen based ligands, a variety of platinum and palladium-chalcogen complexes have been reported:[3,4] The ligand chemistry of thiolates and selenolates has mainly focused on the preparation of mononuclear complexes of monodentate chalcogenolates.[5,6,7]

More than seventy years ago Chatt and Mann reported the thiolate-bridged dinuclear palladium complex from the reaction of $[Pd_2Cl_2(\mu\text{-}Cl)_2(PBu_3)_2]$ and 4-chlorobenzene-1,2-dithiol.[8] The synthesis of binuclear palladium complexes is typically carried out by the reaction of various types of alkylchalcogenols (R-EH) and alkali chalcogenides (ME-R) with a mono- or dinuclear palladium complex; this yields different types of binuclear palladium complexes depending on the reaction conditions.[9] Oxidative addition reactions of diorgano-disulfides and -diselenides with palladium(0) precursors, $[Pd(PPh_3)_4]$ or $[Pd(PPh_3)_2(olefin)]$, in general, can also yield binuclear derivatives, $[Pd_2(\mu\text{-}ER)_2(ER)_2(PR'_3)_2]$ (E = S or Se).[10]

Dinuclear chalcogenolate-bridged group 10 metal complexes are generally more stable than the analogous complexes with chalcogenide (E^{2-}) bridges. With the

latter, the chalcogen sites are known to react with various organic nucleophiles, including chlorinated solvents.[11] The chalcogen lone pairs of the M_2E_2 (M = Pt, Pd; E = S, Se) fragment are sufficiently basic to act as a donor ligand.[12] Using organo chalcogenolate ligands as a bridging ligand suppresses the reactivity of these binuclear complexes by closing a free coordination site of the chalcogen.[13] Recently Henderson and co-workers have applied ferrocenylalkyl compounds $Fc(CH_2)_nX$ (n = 1, 6, 11; X = Cl, Br) to alkylate a chalcogenide-bridged dinuclear platinum(II) complex $[Pt_2(\mu\text{-}S)_2(PPh_3)_4]$ to its corresponding cationic alkylchalcogenelate complex $[Pt_2(\mu\text{-}S)(\mu\text{-}S(CH_2)_nFc)(PPh_3)_4]^+$.[14] Hor and co-workers have previously shown the high nucleophilicity of a bridging chalcogenide in $[Pt_2(\mu\text{-}E)_2(PPh_3)_4]$ (E = S, Se) and $[Pt_2(\mu\text{-}E)_2(P\cap P)_2]$ towards various dihaloalkanes.[13a,15]

Bidentate chalcogen ligands can also be employed for the construction of dinuclear palladium(II) complexes. These bidentate ligands mostly adopt a combination of terminal and bridging coordination modes[16] as displayed in the complex $[Pd_2(\mu\text{-}\kappa^1S\text{-}(S_2Fc)_2)_2(P^nBu_3)_2]$ (Fc = $Fe(C_5H_4)_2$) (Figure 3.1a).[17] There are also reports in which the bridging ligand is coordinated to Pd atoms in a chelate fashion (Figure 3.1b). For example, Rawson and co-workers showed that the oxidative addition reaction of $(Ph\overline{CNSSN})_2$ with $[Pd(dppe)_2]$ gives a mixture of mononuclear [(dppe)Pd{SNC(Ph)NS}] and bimetallic $[(dppe)_2Pd_2\text{-}\mu\text{-}\kappa^2S\text{-}\{SNC(Ph)N(H)S\}]^{2+}$ palladium dithiadiazolyl complex, which two Pd centres bridged by the two sulfur atoms of a protonated dithiadiazolyl ligand.[18] Cao and Hong later reported the condensation reactions of mononuclear palladium(II) complexes with diphosphine and dithiolate ligands, $[(dppp)Pd(S(CH_2)_nS)]$ (n = 2, 3) through oxidation of the ligands with elemental Se in the presence of Me_4NCl. This affords the products $[(dppp)_2Pd_2\text{-}\mu\text{-}\kappa^2S\text{-}(S(CH_2)_nS)]Cl_2$ (n = 2, 3, respectively). Due to the flexibility of $\text{-}S(CH_2)_nS\text{-}$ ligands, these complexes can be viewed as two $[Pd(P\cap P)]_2$ fragments sharing a common dithiolate ligand. A single resonance peak in their $^{31}P\{^1H\}$ NMR shows the magnetically equivalent spin systems of phosphorus atoms in such structures.[19]

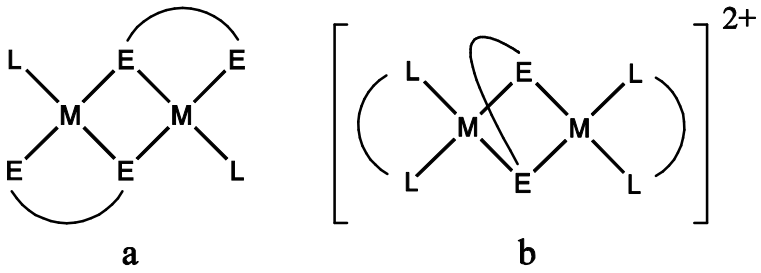

Figure 3.1. Structures observed for bidentate organochalcogenolate-bridged dinuclear platinum(II) and palladium(II) complexes (M = Pt, Pd; E = S, Se).

As part of our development of the use of silylated–chalcogen precursors for assembling new polydentate chalcogen-bridged metal complexes, we report herein the synthesis of new disubstituted thio- and selenotrimethylsilane reagents 1,2-$(Me_3SiECH_2)_2C_6H_4$ (E = S, **13**; E = Se, **14**) which provide a simple method for the preparation of the cationic dinuclear palladium complexes; $\{(dppp)_2Pd_2\text{-}\mu\text{-}\kappa^2S\text{-}[1,2\text{-}(SCH_2)_2C_6H_4]\}^{2+}$, $[\mathbf{15}]^{2+}$ and $\{(dppp)_2Pd_2\text{-}\mu\text{-}\kappa^2Se\text{-}[1,2\text{-}(SeCH_2)_2C_6H_4]\}^{2+}$, $[\mathbf{16}]^{2+}$. They show very interesting NMR spectroscopic behaviour which comes from the rigidity and special orientation of the bridging ligands in these structures. Taking advantage of the silylated organochalcogen to develop the chemistry of butterfly metal-chalcogen clusters, we also detail a unique tetranuclear palladium complex $[(dppp)_4Pd_4\text{-}\mu\text{-}\kappa^4S\text{-}\{1,2,4,5\text{-}(SCH_2)_4C_6H_2\}]^{4+}$, $[\mathbf{17}]^{4+}$ which is prepared from the reaction of $1,2,4,5\text{-}(Me_3SiSCH_2)_4C_6H_2$ and $[PdCl_2(dppp)]$ in the presence of lithium bromide. Complete structural characterization and spectroscopic data are presented.

3.2 Results and discussion

The reactivity of silylated chalcogen reagents (-$ESiMe_3$) for the formation of metal–chalcogen bonds, which has been demonstrated in simple coordination chemistry and polynuclear clusters,[20] offers a convenient route for the construction of chalcogen-palladium complexes. These silylated reagents react with metal salts through the thermodynamically favourable formation of $XSiMe_3$ (X = Cl, OAc) to yield metal–chalcogenolate (M–ER) bonds (E = S, Se). The solubility of $RESiMe_3$ reagents in common organic solvent can offer an advantage over using related alkali metal chalcogenolates. Previously we have shown that the reaction of 1,1´-bis(trimethylsilylseleno)ferrocene with trans-[$MCl_2(P^nBu_3)_2$] (M = Pt, Pd) yields dimeric complexes with two edge-sharing, square–planar platinum/palladium coordination centres. These are held together by two μ_2-bridging selenolate ligands, one from each of the bis(seleno)ferrocenyl moieties forming a planar Pd_2–Se_2 ring (as in Figure 3.1a).[17]

1,2-bis((trimethylsilylchalcogeno)methyl)benzene **13** and **14** are readily prepared in good yield from the reaction of 1,2-bis(bromomethyl)benzene with lithio(trimethylsilyl)-chalcogenolate (Scheme 3.1), further expanding on the reported synthesis of 1,4-, 1,3,5- and 1,2,4,5-polychalcogenosilanes $Ar(CH_2ESiMe_3)_n$ (n = 2, 3, 4) from the corresponding polybromomethylbenzene and alkali metal (trimethylsilyl) chalcogenolate M[$ESiMe_3$] (M = Na, Li) under mild conditions.[21] The portion-wise addition of organobromine reagent to the solution of Li[$ESiMe_3$] in Et_2O at room temperature, followed by stirring for twelve hours, yielded 1,2-$(Me_3SiSCH_2)_2(C_6H_4)$ (84%) **13** and 1,2-$(Me_3SiSeCH_2)_2(C_6H_4)$ (71%) **14** as a colourless and pale yellow oily solids, respectively, upon extraction with pentane. They decompose readily in the presence of air; however, they are stable for several days at room temperature under an inert atmosphere.

E = S, 84%; E = Se, 71%

Scheme 3.1. Synthesis of reagents **13**, E = S, and **14**, E = Se.

The chemical shifts of the -Si(CH_3)$_3$ moieties of the diselenodisilane **14** resonate at lower field in both ^{1}H (0.44 ppm) and ^{13}C{^{1}H} (1.7 ppm) NMR spectra versus the corresponding sulfur compound **13** (0.33 ppm and 1.1 ppm, respectively). The methylene (-CH_2-) groups in both ligands show close chemical shift values in their ^{1}H NMR spectra (**13** = 3.86 ppm; **14** = 3.90 ppm) but the corresponding resonance in the ^{13}C{^{1}H} NMR spectrum of the selenide has lower chemical shift values (**13** = 28.3 ppm; **14** = 19.0 ppm). The ^{77}Se{^{1}H} chemical shift for **14** showed a singlet at -18.4 ppm. These results match well with previously reported data for 1,2,4,5-(Me_3SiECH_2)$_4$(C_6H_2) (E = S, Se).[21]

Treatment of *cis*-[MCl_2L_2] (M = Ni, Pt, Pd; L = mono- or $^1/_2$-bidendate phosphine ligand) with organochalcogenides RE^- readily gives mononuclear *cis*-[$M(ER)_2L_2$] (E = S, Se, Te), and the complexes have proven to be important precursors for the stepwise synthesis of dinuclear complexes. Thus, the reaction of another *cis*-[MCl_2L_2], activated in the presence of a cation, with *cis*-[$M(ER)_2L_2$] gives a homo-binuclear complex [$M_2(ER)_2L_2$]X_2.[22] Introducing ionic salts as the source of cation, used to abstract chloride from [MCl_2L_2] in the presence of organochalcogenides, yields chalcogen-bridged cationic binuclear complexes.[22a-c] The reaction of **13** and **14** with

bis(diphenylphosphino)propane)palladium(II) represents a new route to dinuclear palladium complexes with a chalcogen-bearing bridging/chelate ligand.

In a one-step reaction, a freshly prepared solution of 1,2-$(Me_3SiECH_2)_2(C_6H_4)$ (E = S; **13** or E = Se; **14**) is reacted with $[PdCl_2(dppp)]$ in chloroform at room temperature to yield the dinuclear organochalcogenido-bridged palladium metal complexes $[Pd_2(dppp)_2\text{-}\mu\text{-}\kappa^2E\text{-}\{1,2\text{-}(ECH)_2C_6H_4\}]^{2+}$ (E = S, $[\mathbf{15}]^{2+}$; Se, $[\mathbf{16}]^{2+}$). Reactions proceed via the generation of a pale orange suspension for $[\mathbf{15}]^{2+}$ and dark red solutions for $[\mathbf{16}]^{2+}$ (Scheme 3.2). Filtration followed by layering the solutions with pentane results in the formation of colourless plate and light yellow block crystals for $[\mathbf{15}]X_2$ and $[\mathbf{16}]X_2$ (X = Cl, Br), respectively, suitable for analysis by single crystal X-ray crystallography.

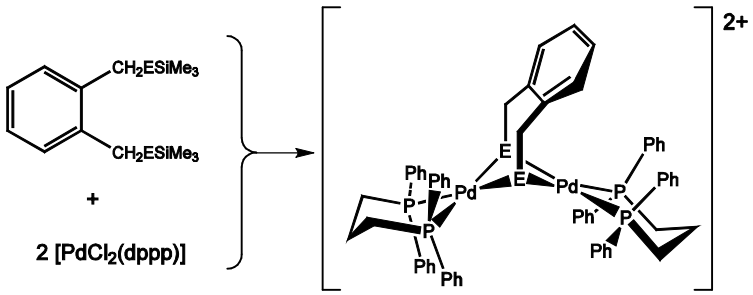

E = S, 45%; E = Se, 40%

Scheme 3.2. Synthesis of complexes $[\mathbf{15}]^{2+}$ (E = S) and $[\mathbf{16}]^{2+}$ (E = Se).

The molecular structure of complexes $[\mathbf{15}]^{2+}$ and $[\mathbf{16}]^{2+}$ established by X-ray diffraction analyses are depicted in Figures 3.3 and 3.4, respectively. Crystallographic parameters are reported in Table 3.1. The isostructural complexes

of [**15**]$^{2+}$ and [**16**]$^{2+}$ may be considered as two palladium-phosphine fragments sharing a common dichalcogenolate ligand to yield a butterfly Pd_2E_2 ring. Each chalcogen atom acts as μ-bridging donor between two palladium centres. The bridging ligand is hinged at methylene groups (E = S, 115.7(5)°, 116.0(5)°; E = Se, 113.7(4)°, 114.9(4)°), which causes the phenyl group to be closer to one side of the Pd_2E_2 ring (Pd1). The structures contain a non-crystallographic mirror plane which bisects the two Pd(II) and the bridging ligand. Such dinuclear square-planar complexes with M_2E_2 or $M_2(ER)_2$ rings can present either a planar (θ = 180°) or bent (θ < 180°) M_2E_2 core (Figure 3.2). The flexibility of these systems can result in long E···E and M···M interactions in Pd_2E_2/Pt_2E_2 rings and gain extra stabilization.[23] In pursuit of nucleophilic addition of a bridging chalcogenide, Hor's group has shown reaction of nucleophilic platinum complex, $[Pt_2(\mu\text{-}S)_2(dppp)_2]$ with 1,2-bis(chloromethyl)benzene at high-pressure terminates as a dithiolato bridged cation $[(dppp)_2Pt_2\text{-}\mu\text{-}\kappa^2S\text{-}\{1,2\text{-}(SCH_2)_2C_6H_4\}]^{2+}$.[15a] They also illustrated that the reaction of $1,2\text{-}(ClCH_2)_2C_6H_4$ with the platinum-selenide complex $[Pt_2(\mu\text{-}Se)_2(PPh_3)_4]$ in the presence of excess NH_4PF_6 generates the structurally related butterfly dinuclear organochalcogenolate-bridged structure $[Pt_2\text{-}\mu\text{-}\kappa^2Se\text{-}\{1,2\text{-}(SeCH_2)_2C_6H_4\}(PPh_3)_4]^{2+}$.[15b]

Table 3.1. Crystallographic data and parameters for compounds [**15**]X_2, [**16**]X_2 and [**17**]X_4

	[**15**]X_2·4$CHCl_3$	[**16**]X_2·6$CHCl_3$	[**17**]X_4·6$CHCl_3$
Formula	$C_{62}H_{60}BrClP_4Pd_2S_2$·4$CHCl_3$	$C_{62}H_{60}Cl_2P_4Pd_2Se_2$·6$CHCl_3$	$C_{118}H_{114}Br_3ClP_8Pd_4S_4$·6C
Formula weight	1798.73	2086.81	3325.08
Crystal system	Monoclinic	Monoclinic	Orthorhombic
Space group	$P2_1/n$	$P2_1/c$	*Pbca*
a (Å)	17.4473(8)	18.668(4)	17.875(7)
b (Å)	23.7638(11)	17.724(4)	26.862(10)
c (Å)	18.3345(9)	24.914(5)	26.933(11)
α (º)	90.00	90.00	90.00
β (º)	103.015(2)	93.11(3)	90.00
γ (º)	90.00	90.00	90.00
V (Å^3)	7406.5(6)	8231(3)	12932(8)
Z	4	4	4
ρ_{cal} (g cm^{-3})	1.613	1.684	1.708
μ (Mo Kα) (mm^{-1})	1.676	2.088	2.080
F(000)	3600	4136	6640
Temperature (K)	150(2)	150(2)	110(2)
θ_{min}, θ_{max} (º)	2.25, 24.75	2.20, 27.48	1.5, 25.1
h, *k*, *l* (min; max)	-21, -28, -22; 21, 29, 22	-24, -22, -32; 24, 22, 32	-21, -31, -32; 21, 31, 32
Total reflns	154031	35017	213930
Unique reflns	15167	18760	11459
R(int)	0.1083	0.0404	0.0698
Data/restraints/param	8972/0/ 806	13101/0/ 920	8783/45/793
*R*1, w*R*2 [$I \geq 2\sigma$ (*I*)]	0.0538, 0.1194	0.0585, 0.1524	0.0670, 0.1846
*R*1, w*R*2 (all data)	0.1167, 0.1493	0.0934, 0.1868	0.0952, 0.2191
GOF on F^2	1.029	1.040	1.119

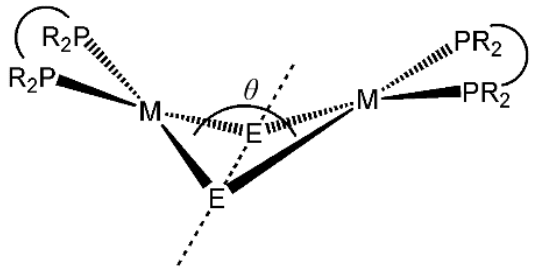

Figure 3.2. M_2E_2 core; coplanar arrangement (θ = 180°) or hinged arrangement (θ < 180°).

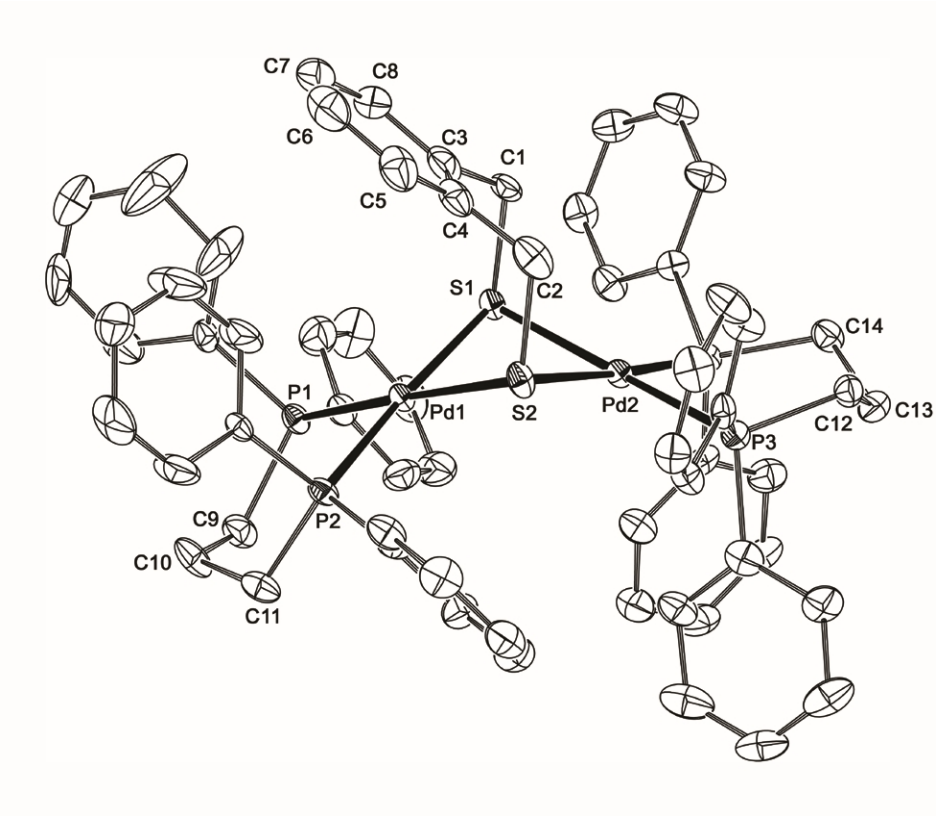

Figure 3.3. The molecular structure of complex [**15**]$^{2+}$. The thermal ellipsoids have been drawn at 40% probability. Hydrogen atoms, solvent molecules and counter ions have been omitted for clarity.

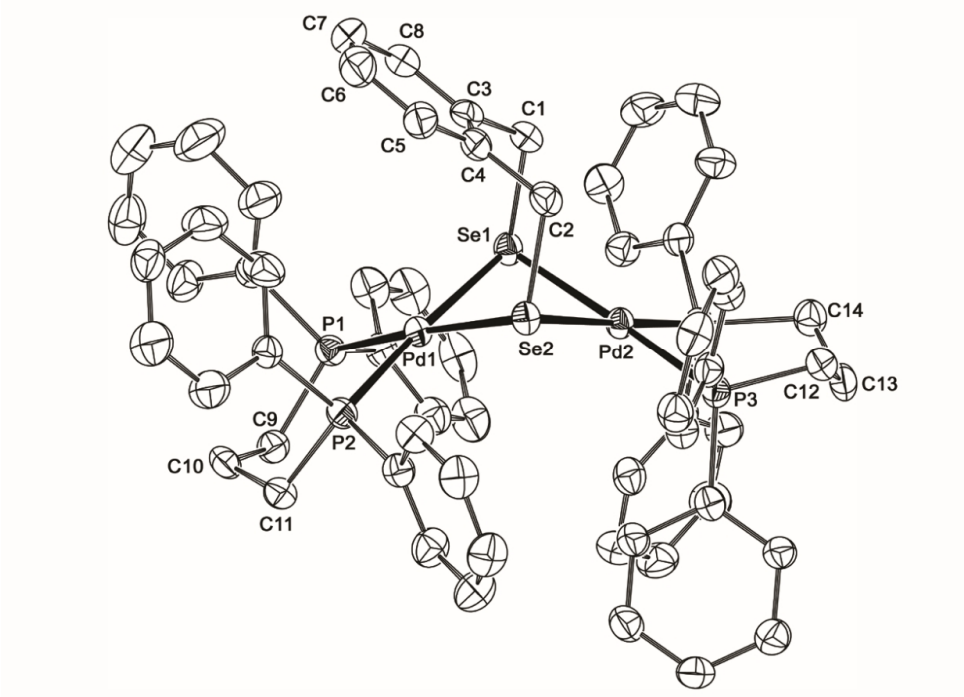

Figure 3.4. The molecular structure of complex $[\mathbf{16}]^{2+}$. The thermal ellipsoids have been drawn at 40% probability. Hydrogen atoms, solvent molecules and counter ions have been omitted for clarity.

With the Pd(II) complexes, each of the two chalcogen atoms of the ligands bridges two metal atoms, and the Pd_2E_2 moiety is folded along its E···E vector (E = S, 134.21°; E = Se, 130.77°), as observed in $[Pd_2(dppp)_2(S(CH_2)_3S)]^{2+}$ (129.7°)[24] and platinum $[(dppp)_2Pt_2\text{-}\mu\text{-}\kappa^2S\text{-}\{1,2\text{-}(SCH_2)_2C_6H_4\}]^{2+}$ (132.4°).[15a] In $[\mathbf{15}]^{2+}$ and $[\mathbf{16}]^{2+}$, the Pd···Pd (E = S, 3.2370(6) Å; E = Se, 3.3073(8) Å) and E···E lengths (E = S, 3.192(2) Å; E = Se, 3.363(1) Å) are too long to be assigned any direct intramolecular interaction. Both palladium atoms in each complex show, expectedly, slightly distorted square-planar coordination geometry. The bite angles P-Pd-P around two palladium atoms are slightly different (E = S, 91.55(6)° for Pd1 and 93.47(6)° for Pd2; E = Se, 93.53(5)° for Pd1 and 93.23(5)° for Pd2). The length of bridging Pd-E bonds (E = S, 2.361(2) - 2.384(2) Å; E = Se, 2.4631(8)-2.4950(8) Å) are in good agreement with the reported values for palladium-thiolate or palladium-selenolate bonds.[25] The average bond length of E-Pd1 (E = S, 2.364(1)

Å; E = Se, 2.4646(6) Å) bonds is slightly shorter than E-Pd2 (E = S, 2.382(1) Å; E = Se, 2.490(4) Å). These data reveal the asymmetrical geometry of $[\mathbf{15}]^{2+}$ and $[\mathbf{16}]^{2+}$ which dramatically influences the spectroscopic behaviour of these complexes in solution.

Electronic spectral data of complexes $[\mathbf{15}]X_2$ and $[\mathbf{16}]X_2$ in dichloromethane (2.0×10^{-5} M) are provided in Table 3.2. The absorption spectra are dominated by strong charge-transfer bands[26] between 200 and 400 nm trailing out into regions of higher wavelength. The spectrum of $[\mathbf{15}]X_2$ shows two peaks at 300 and 354 nm while the $[\mathbf{16}]X_2$ reveals two absorption maxima at 306 and 366 nm (Figure 3.5).

Table 3.2. Principal electronic transitions in $[\mathbf{15}]X_2$, $[\mathbf{16}]X_2$ and $[PdCl_2(dppp)]$.

Compounds	λ_{max} /nm (ε /10^3 dm^3 mol^{-1} cm^{-1})	
$[\mathbf{15}]X_2$	300 (33500)	354 (19200)
$[\mathbf{16}]X_2$	306 (32500)	366 (17900)
$[PdCl_2(dppp)]$	269 (46900)	327 (11400)

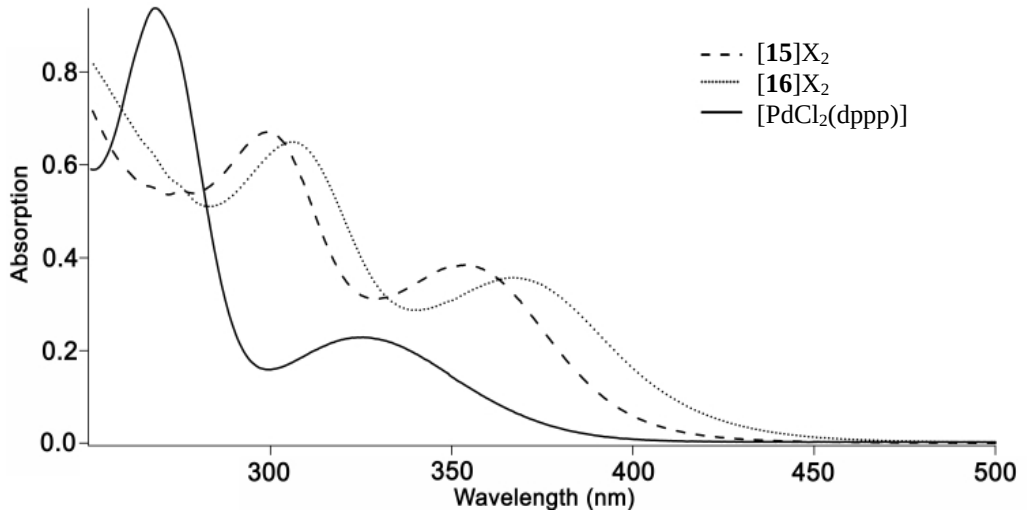

Figure 3.5. UV–Vis absorption spectra of $[\mathbf{15}]X_2$, $[\mathbf{16}]X_2$ (X = Cl/Br) and $[PdCl_2(dppp)]$.

Oganochalcogenolate-bridged palladium complexes have been characterized extensively by multinuclear NMR (^{1}H, ^{13}C, ^{31}P, ^{77}Se, ^{125}Te,) data.[27] The ^{31}P{^{1}H} NMR spectra of [(μ-ER)$_2$M$_2$L$_2$] and [μ-κ^2E-(E∩E)M$_2$L$_2$] (M = Pd; E = S, Se; L = $^1/_2$-bidendate phosphine) complexes usually exhibit one signal which arises from their symmetrical structures and the flexibility of bridging ligand.[18,24,27] However, in the ^{31}P{^{1}H} NMR spectra of [**15**]X$_2$ and [**16**]X$_2$, two sets of multiplet resonances are observed (Figures 3.6 and 3.7, respectively) implying two different sets of phosphorus atoms in these complexes. This suggests that the bridging ligands are stereochemically rigid on the NMR timescale and not fluxional in solution (in the temperature range +25 to +50 °C) and that the configurations of [**15**]$^{2+}$ and [**16**]$^{2+}$ in solution are consistent with their solid-state structures. Such rigidity has also been described for Pt(II) complexes by Hor.[15a,15b] Each multiplet signal in the ^{31}P{^{1}H} NMR spectra can be attributed to two phosphorus atoms on each side of the bridging ligand and the coupling between the phosphorus atoms on two sides of the bridging ligand, in spite of four-bond separation. The resonances occur in the expected range of chelating phosphine complexes of palladium(II),[5a] with a gradual downfield shift in the thiolate complex relative to the selenolate complex ([**15**]X$_2$, 9.6 and 8.2 ppm; [**16**]X$_2$, 3.8 and 2.6 ppm).

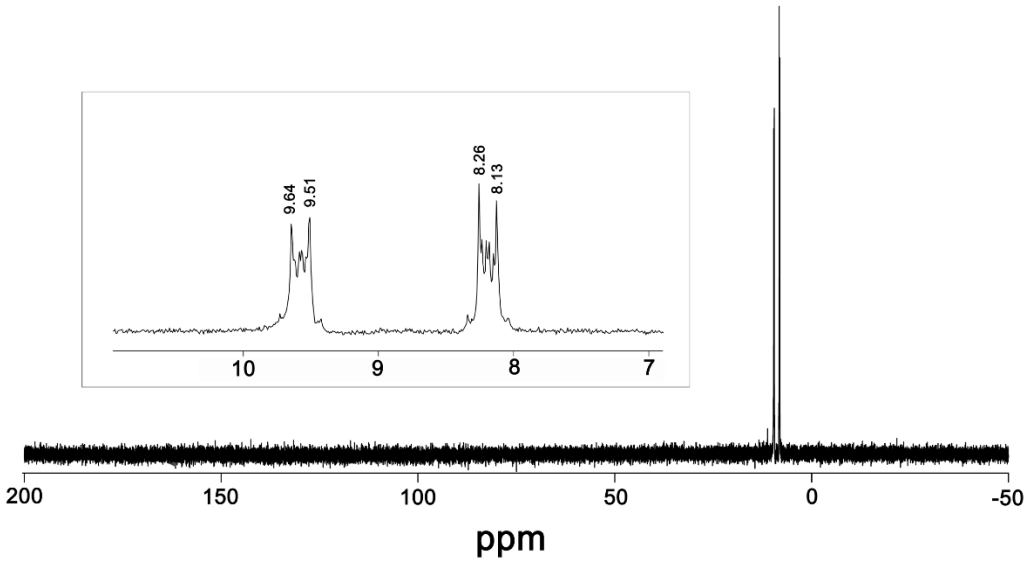

Figure 3.6. ^{31}P{^{1}H} NMR spectrum of [**15**]X$_2$ (CDCl$_3$, 25 °C, 161.97 MHz).

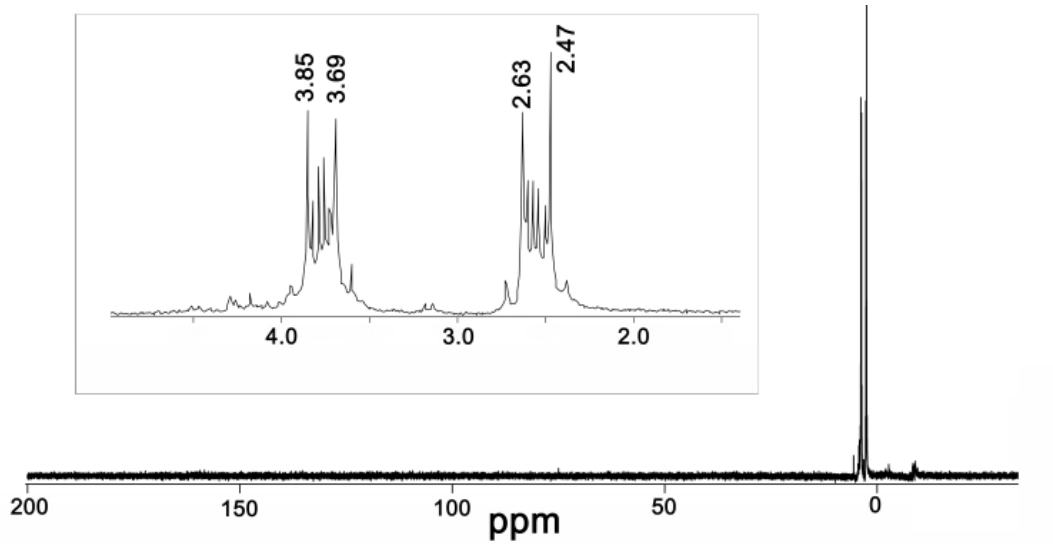

Figure 3.7 $^{31}P\{^{1}H\}$ NMR spectrum of [**16**]X_2 ($CDCl_3$, 25 °C, 161.97 MHz).

While the direct assignment of the ^{1}H NMR spectrum of solutions of [**15**]X_2 and [**16**]X_2 was not possible, they clearly indicate the presence of several magnetically non-equivalent protons on the structure, the overall pattern of the two spectra is similar (Figures 3.8a and 3.9a). $^{1}H\{^{31}P\}$ NMR was used to simplify and clarify the *J*-coupling of the peaks in the aliphatic region (Figures 3.8b and 3.9b). $^{1}H\{^{31}P\}$ NMR spectra show eight sets of peaks between ~1.1 and 5.2 ppm ([**15**]X_2, 1.19, 1.32, 2.38, 2.43, 2.53, 4.00, 4.61, 5.05 ppm at CD_2Cl_2, 25 °C; [**16**]X_2, 1.11, 1.42, 2.34, 2.47, 2.84, 4.04, 4.67, 5.16 ppm in $CDCl_3$, 25 °C). The largest difference between the two sets (2.43 ppm for [**15**]X_2 in CD_2Cl_2 and 2.84 ppm for [**16**]X_2 in $CDCl_3$) is for resonances assigned to the protons close to chalcogen atoms (see below).

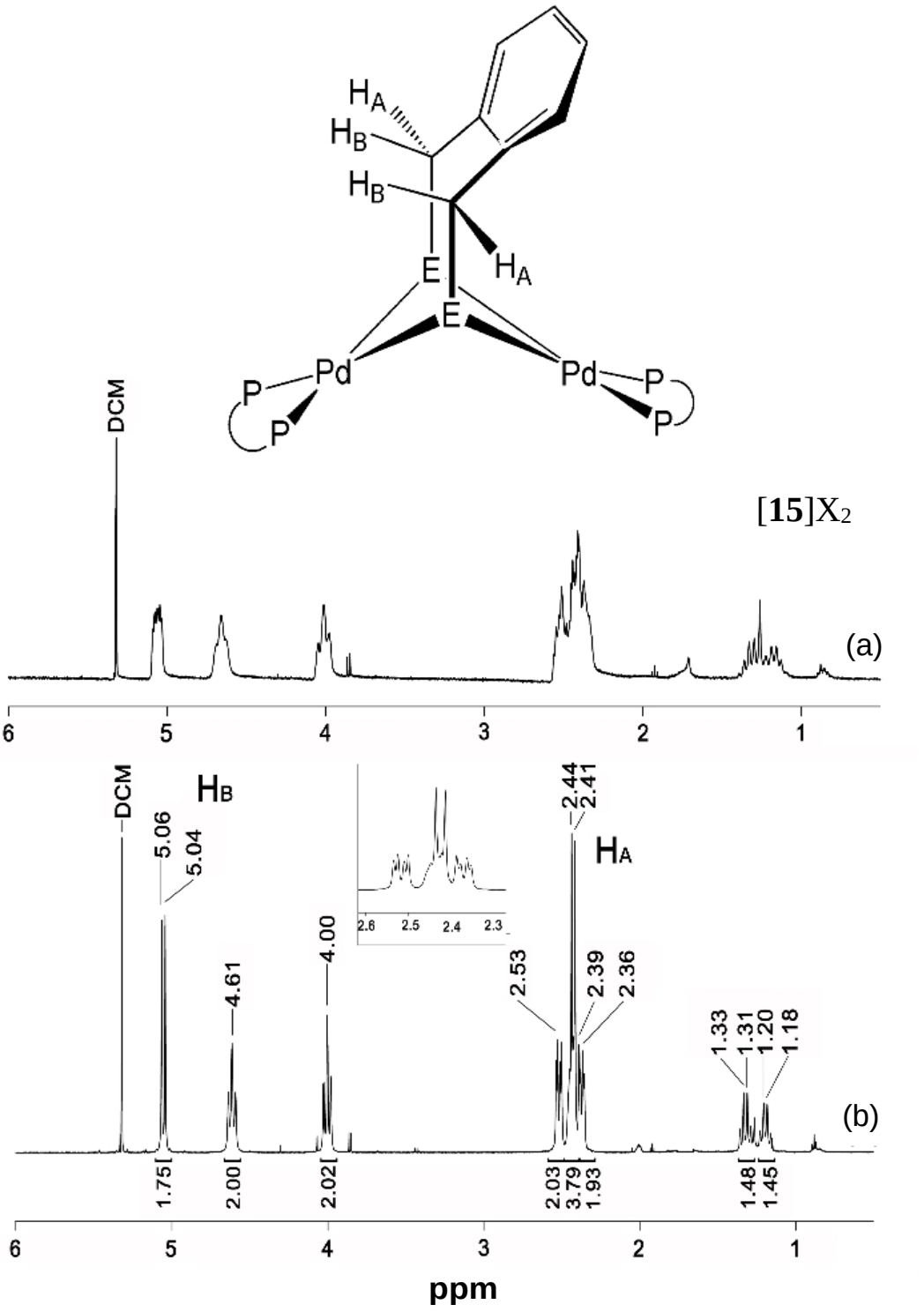

Figure 3.8. Selected regions of (a) ^{1}H NMR spectrum of [**15**]X_2, (b) $^{1}H\{^{31}P\}$ NMR spectrum of [**15**]X_2 (CD_2Cl_2, 25 °C, 599.48 MHz) (E = S)

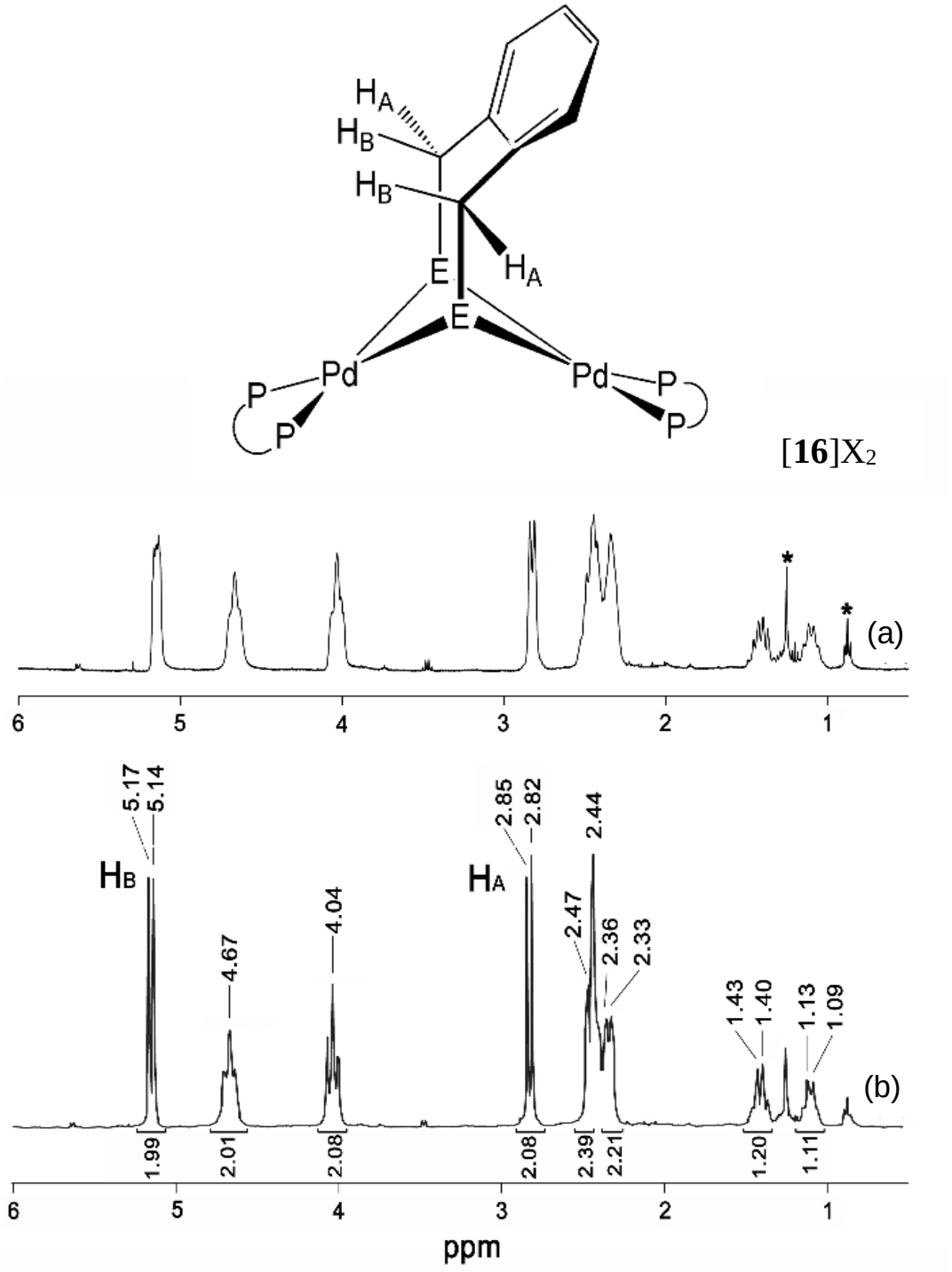

Figure 3.9. (a) ^{1}H NMR spectrum of [**16**]X_2 and (b) $^{1}H\{^{31}P\}$ NMR spectrum of [**16**]X_2 ($CDCl_3$, 25 °C, 399.76 MHz), (* = solvent) (E = Se).

The $^{13}C\{^{1}H\}$ NMR spectrum ($CDCl_3$, 25°C) of [**16**]X_2 in the aliphatic region (Figure 3.10) exhibits two singlets at 18.2 and 18.4 ppm due to the central -CH_2- of the ligand dppp. Two pseudo-triplets at 23.3 and 23.9 ppm arise from the coupling of the side -CαH_2- groups of dppp with the phosphorus nuclei. The singlet at 30.0 ppm arises from the methylene groups of the bridging ligand. The same pattern was observed for [**15**]X_2 ($CDCl_3$, 25°C) two singlets at 18.1, 18.3; two pseudo-triplets at 23.6 and 24.1 and a singlet at 36.9 ppm (Figure 3.11).

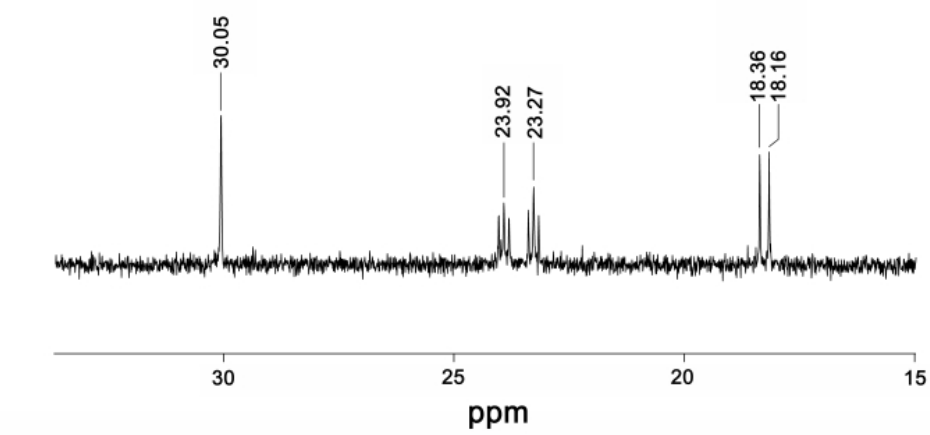

Figure 3.10. Selected region of the $^{13}C\{^{1}H\}$ NMR spectrum of [**16**]X_2 ($CDCl_3$, 25 °C, 150.74 MHz).

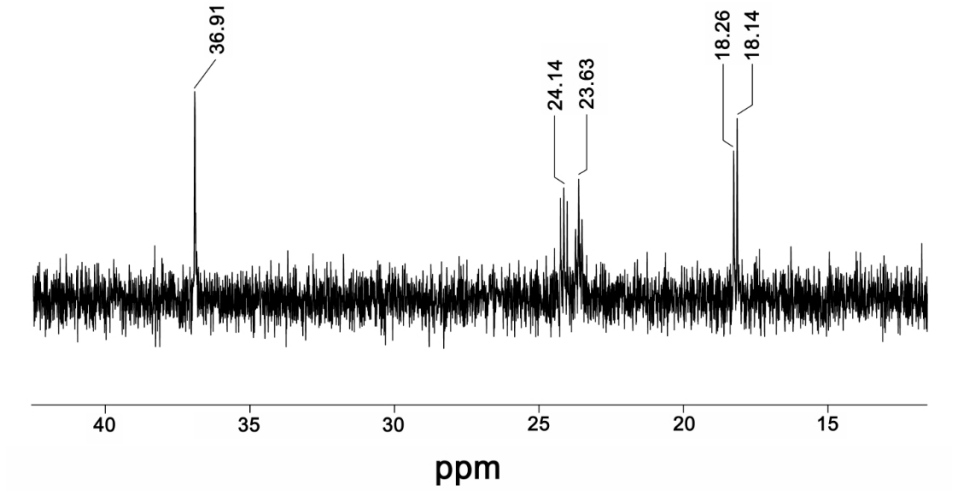

Figure 3.11. Selected region of the $^{13}C\{^{1}H\}$ NMR spectrum of [**15**]X_2 ($CDCl_3$, 25 °C, 150.74 MHz).

Further analysis of the aliphatic area by a 2D ^{1}H-^{1}H COSY (Correlated Spectroscopy) experiment shows a correlation between the two doublets at 2.84 and 5.16 ppm (J = 12.5 Hz) for [**16**]X_2 (Figure 3.12). The same correlation is revealed for two doublet at 2.43 and 5.05 ppm for [**15**]X_2 (Figure 3.13; J = 13.2 Hz). In agreement with these observations, ^{1}H-^{13}C HSQC (Heteronuclear Single Quantum Correlation) spectrum shows that these two sets of peaks correlate with one type of carbon centre (30.0 ppm for [**16**]X_2 and 36.9 ppm for [**15**]X_2), assigned to the -CH_2- groups of the bridging ligand (Figures 3.14 and 3.15, respectively). As the two carbon atoms of these methylene groups are magnetically equivalent, the observed difference between the chemical shifts of two doublets in the ^{1}H NMR spectra are assigned to the magnetically inequivalent hydrogen atoms (Figure 3.16) ([**15**]X_2, J = 13.2 Hz; [**16**]X_2, J = 12.5 Hz). Two hydrogen atoms that are positioned over the phenyl rings (H_A) (see Figure 3.16) are likely considerably shielded and are assigned to the signals at lower frequency. Other correlated peaks in the 2D ^{1}H-^{1}H COSY spectrum of [**16**]X_2 are at 4.04/4.67, 2.34/2.46 and 1.11/1.42 ppm. A correlation between the signals at 4.61, 2.38 and 1.19 ppm and the peaks at 4.00, 2.54 and 1.32 ppm, respectively, for [**15**]X_2 are also revealed from the 2D ^{1}H-^{1}H COSY spectrum.

The ^{1}H-^{13}C HSQC of [**16**]X_2 reveals the correlation between signals at 4.67 and 2.34 ppm in the ^{1}H NMR spectrum with the carbon signal at 23.3 ppm in the ^{13}C{^{1}H}. The signals at 4.04 and 2.46 ppm (^{1}H NMR) correlate with the other set of carbon signals at 23.9 ppm (Figure 3.11b). It also reveals that each of these pairs of peaks arises from the side -CH_2- groups of different propyl chains on the two sides of the bridging ligand dppp. A complete description for these units is provided in Supporting Information. Noteworthy, in the ^{1}H-^{31}P HMBC (Heteronuclear Multiple Bond Correlation) spectra, the doublets at higher field (2.43 ppm, J_{HH} = 13.2 Hz for [**15**]X_2; 2.84 ppm, J_{HH} = 12.5 Hz for [**16**]X_2) couple with both sets of phosphorus nuclei, but the signals with a larger chemical shift (5.05 ppm for [**15**]X_2 and at 5.15 ppm for [**16**]X_2) only couple with the phosphorus resonance at lower frequency (Figures 3.11c and 3.12c).

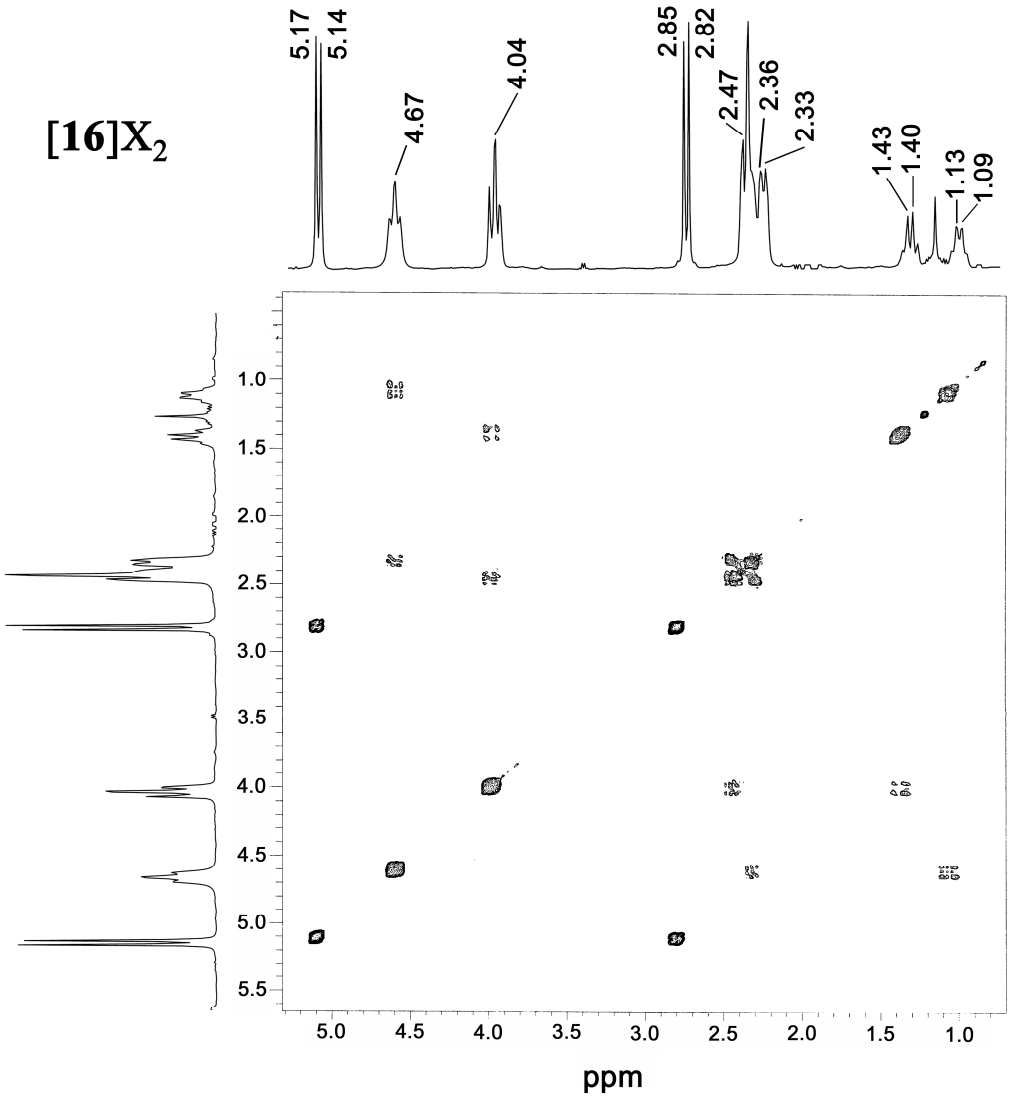

Figure 3.12. Selected region of 2D NMR spectra of [**16**]X_2; ^1H–^1H COSY (CD_2Cl_2, 25 °C, ^1H; 400.08 MHz).

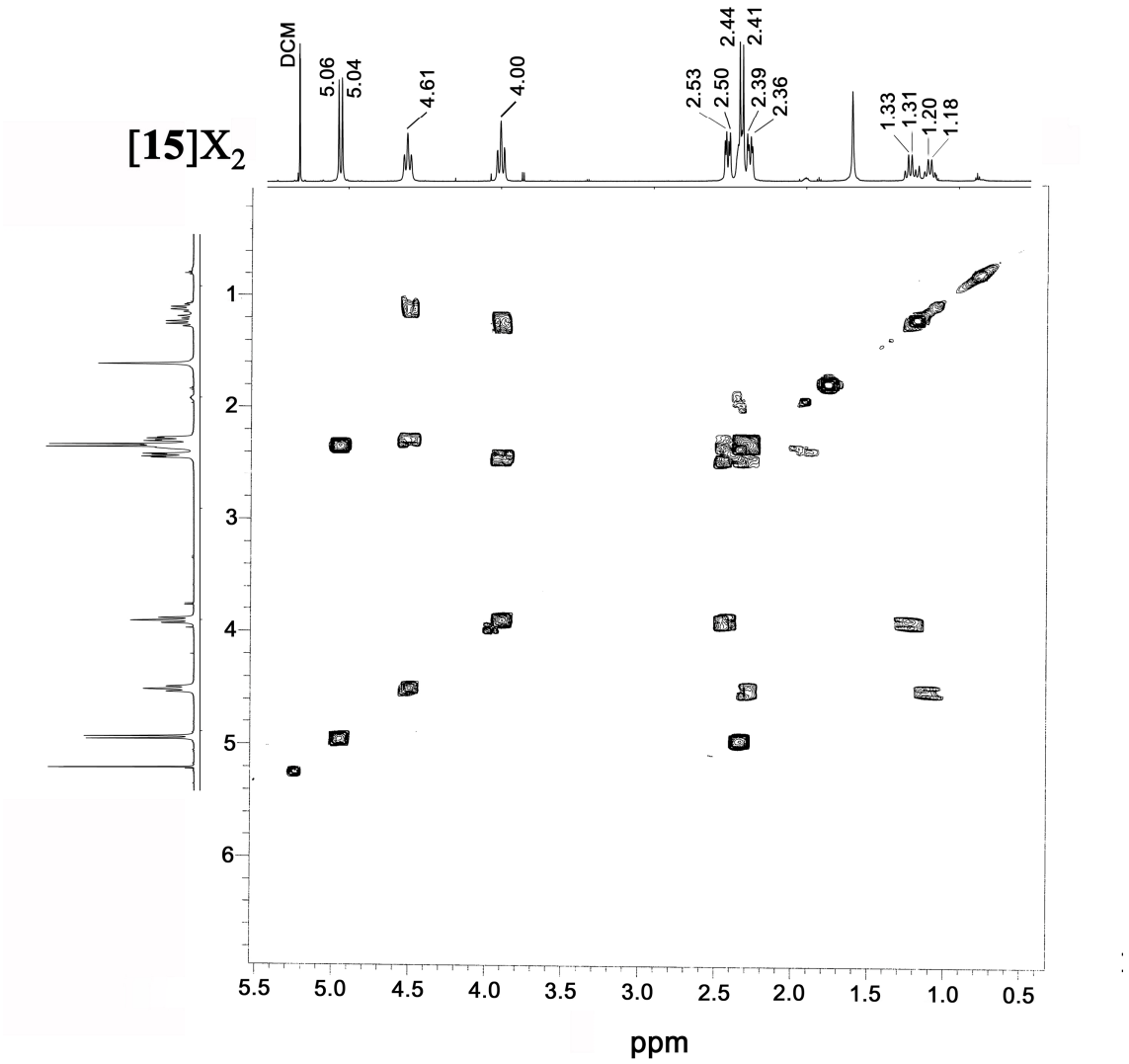

Figure 3.13. Selected region of 2D NMR spectra of [**15**]X_2; ^1H–^1H COSY (CD_2Cl_2, 25 °C, ^1H; 400.08 MHz).

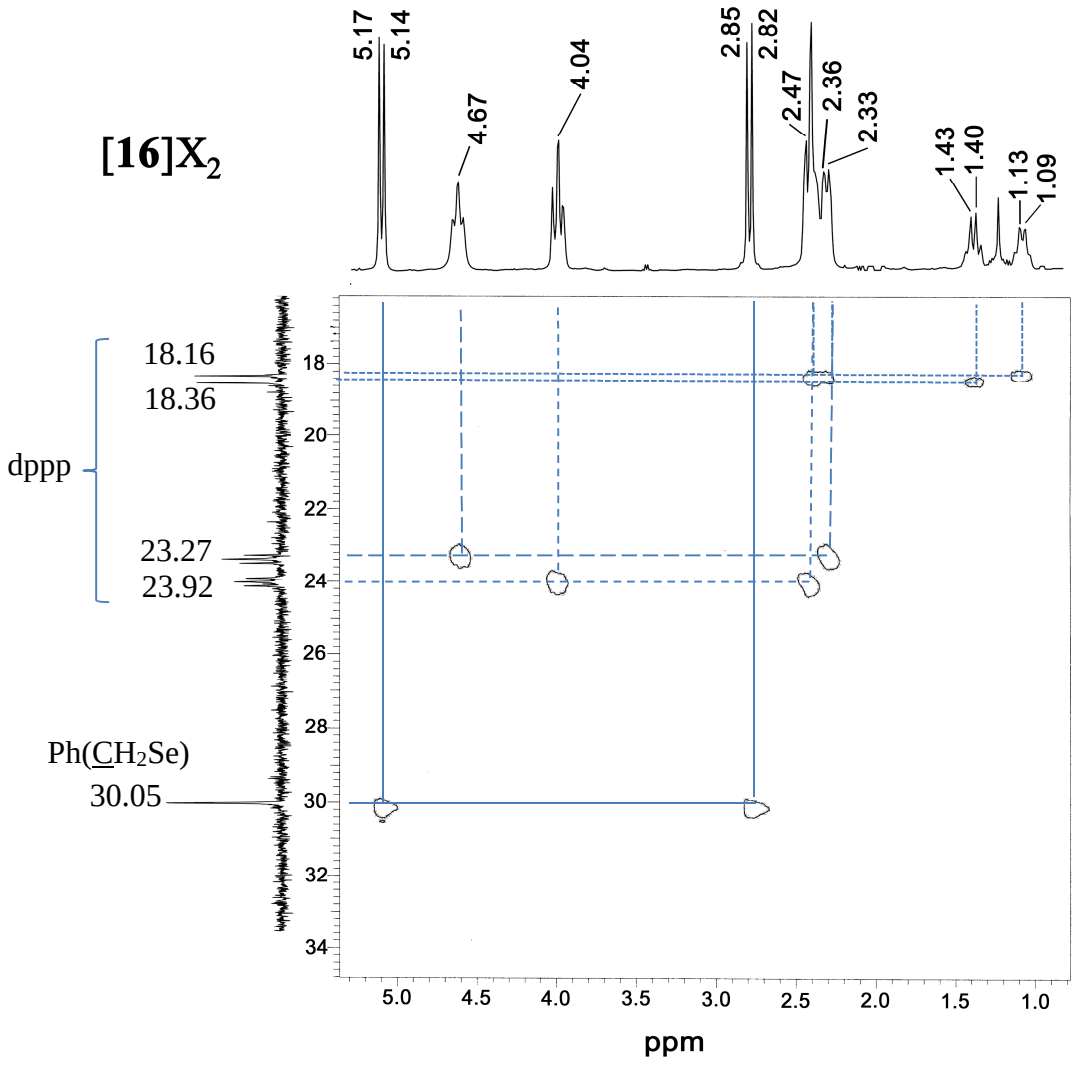

Figure 3.14. Selected region of 2D NMR spectra of [**16**]X_2; ^{1}H–^{13}C HSQC (CD_2Cl_2, 25 °C, ^{1}H; 399.76 MHz, ^{13}C; 100.52 MHz).

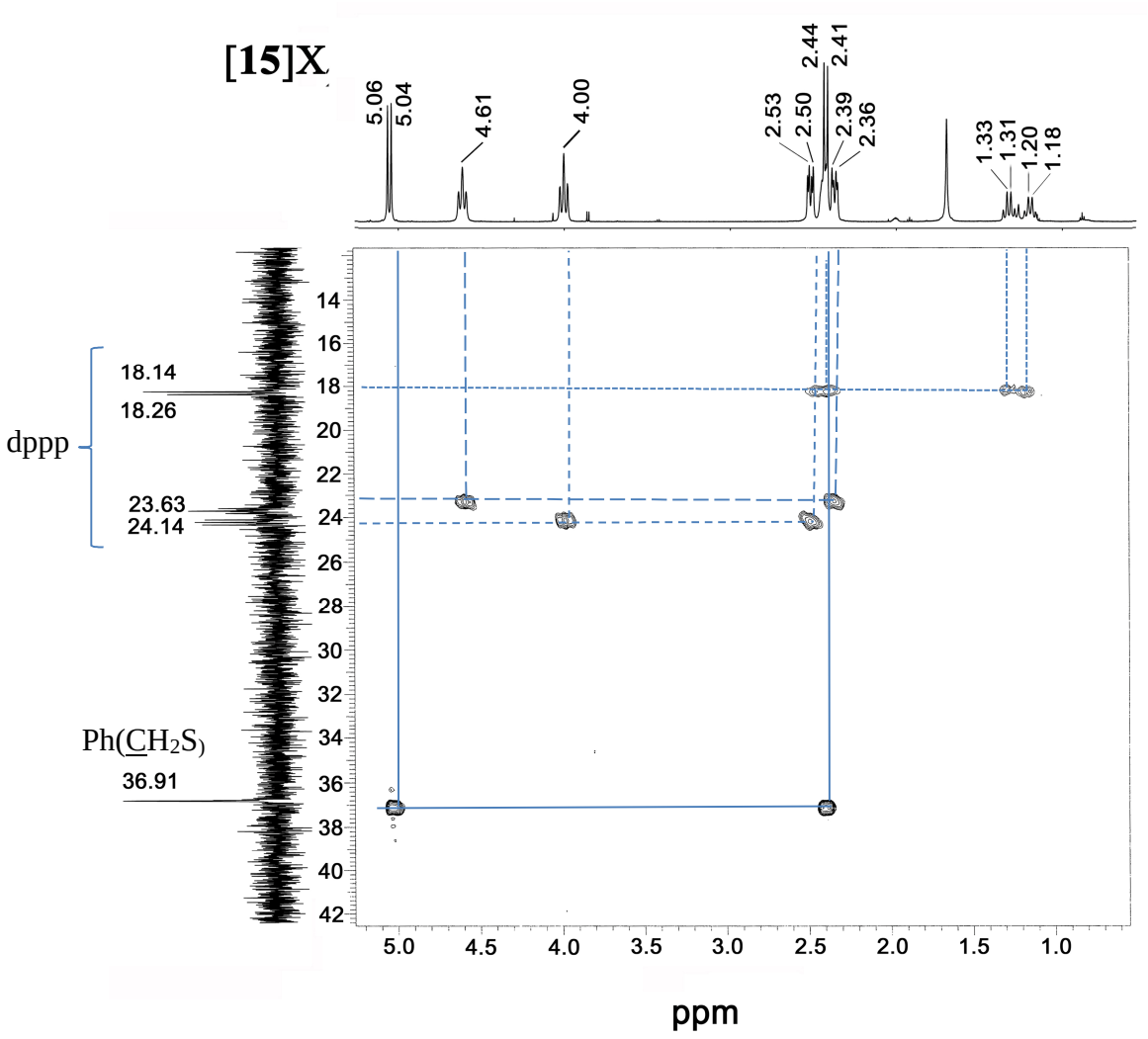

Figure 3.15. Selected region of 2D NMR spectra of [**15**]X_2; ^{1}H–^{13}C HSQC (CD_2Cl_2, 25 °C, ^{1}H; 399.76 MHz, ^{13}C; 100.52 MHz).

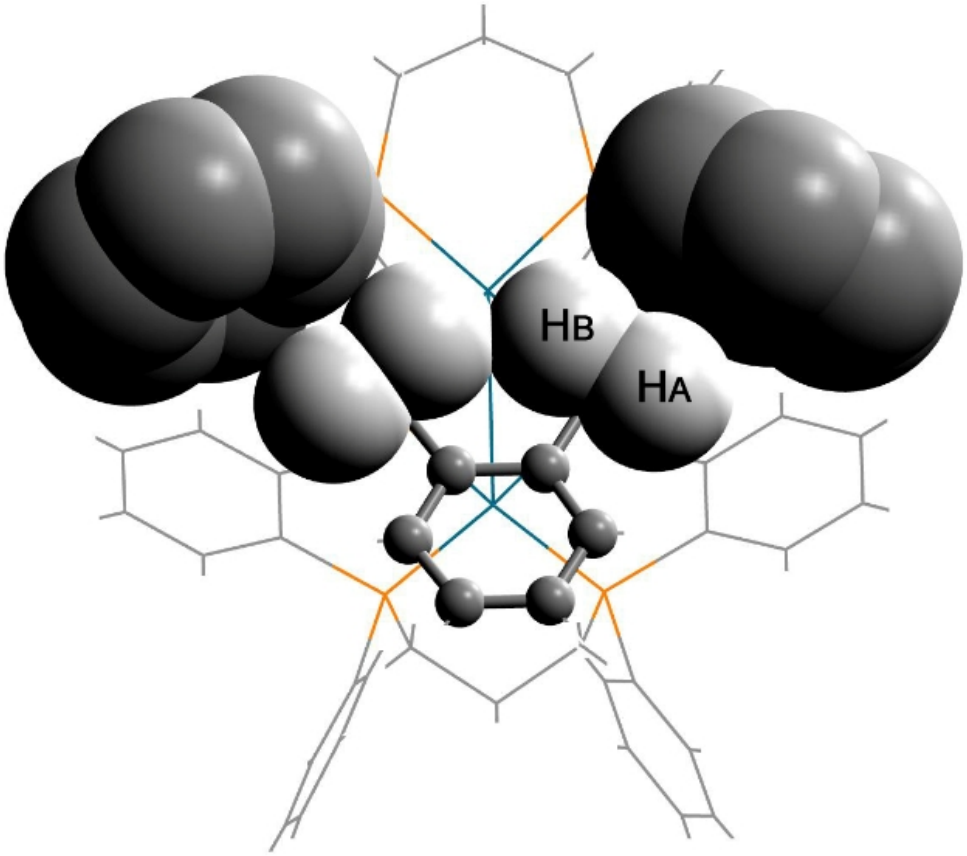

Figure 3.16. A view of molecular structure of [**16**]X_2 showing different environment around protons of the metylene groups on the bridging ligand. Other hydrogen atoms, solvent molecules and counter ions have been omitted for clarity.

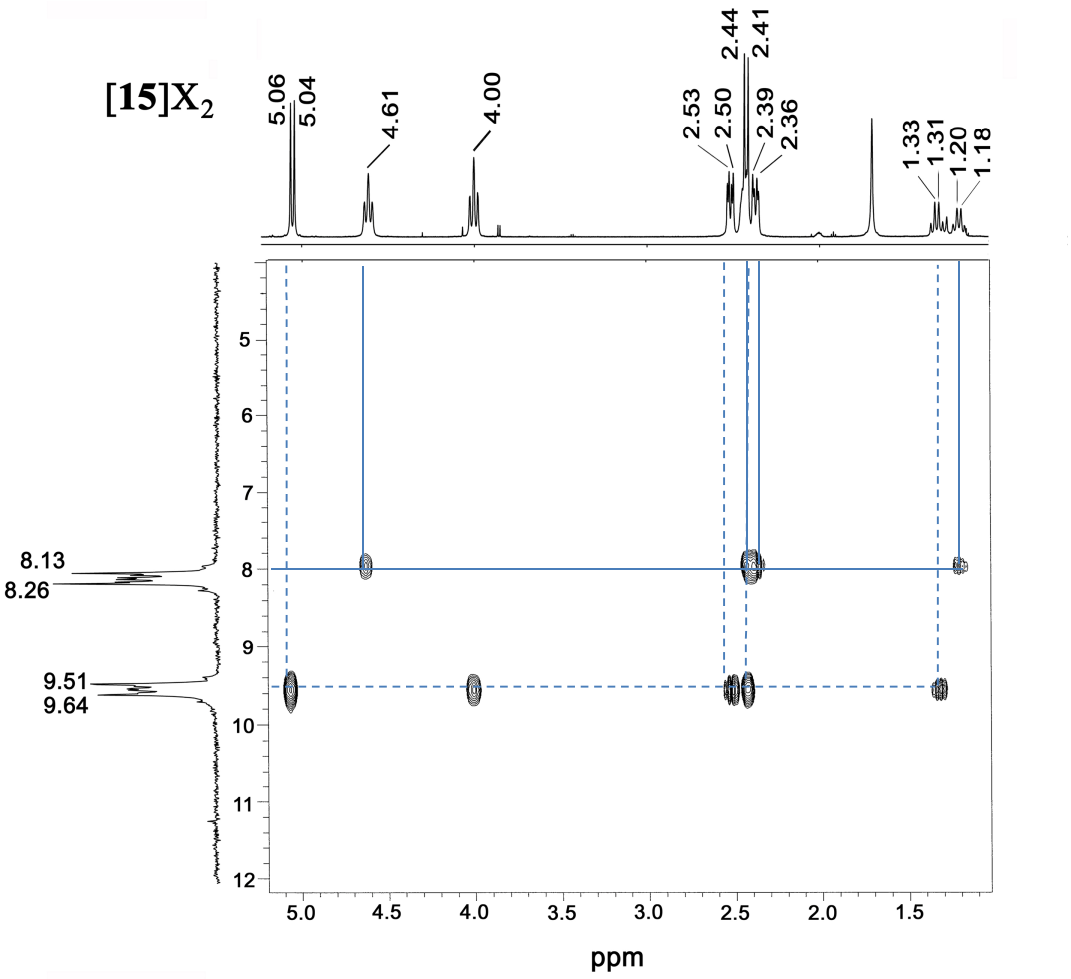

Figure 3.17. Selected region of 2D NMR spectra of [**15**]X_2; ^{1}H–^{31}P HMBC (CD_2Cl_2, 25 °C, ^{1}H; 599.47 MHz, J = 16 Hz).

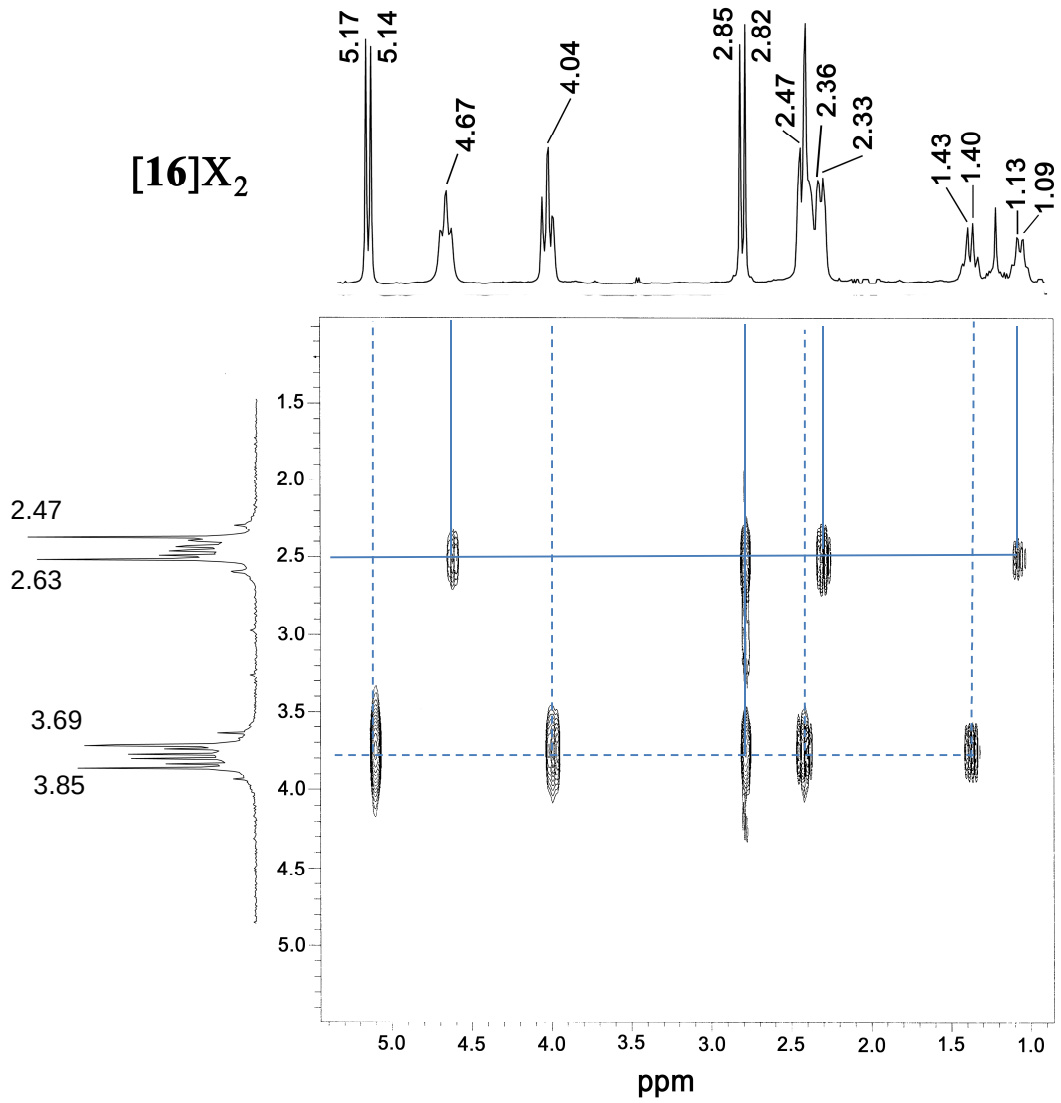

Figure 3.18. Selected region of 2D NMR spectra of [**16**]X_2; ^{1}H–^{31}P HMBC (CD_2Cl_2, 25 °C, ^{1}H; 599.47 MHz, J = 16 Hz).

Recently, the direct reaction of the tetrathiol 1,2,4,5-$(HSCH_2)_4C_6H_2$ with two equivalents of $Fe_3(CO)_{12}$ was shown to generate a double-butterfly complex.[28] The symmetrical distribution of sulfur centres in 1,2,4,5-$(Me_3SiSCH_2)_4(C_6H_2)$ thus suggested an entry into Pd_4 complexes. The direct reaction between $[PdCl_2(dppp)]$ and 1,2,4,5-$(Me_3SiSCH_2)_4(C_6H_2)$ (4:1) did not yield any crystalline material, with no selectivity, as determination by $^{31}P\{^1H\}$ NMR spectroscopy. However, repeating the reaction in the presence of LiBr yielded the Pd_4 complex, $[(dppp)_4Pd_4$-μ-κ^4S-{1,2,4,5-$(SCH_2)_4C_6H_2$}$]X_4$, [**17**]X_4 in fair yield (Scheme 3.3).

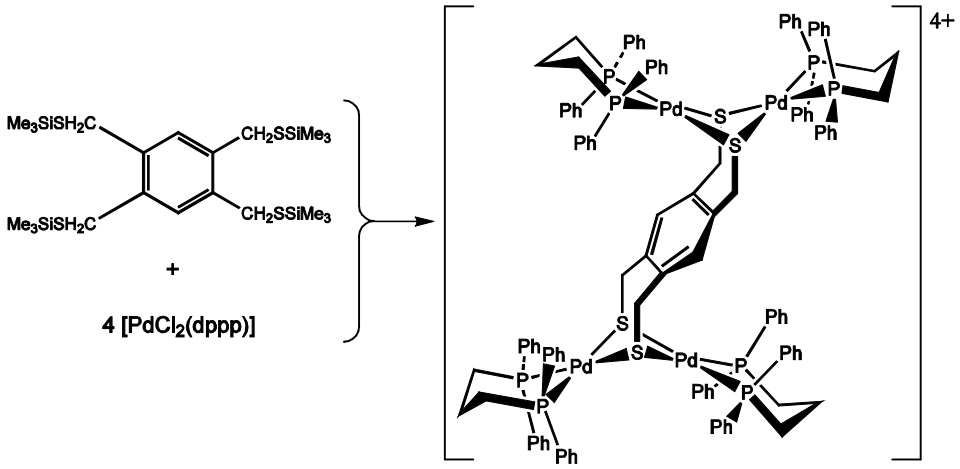

Yield = 25%

Scheme 3.3. Synthesis of complex [**17**]$^{4+}$.

Complex [**17**]$^{4+}$ crystallizes in the orthorhombic space group *Pbca* and possesses a centre of symmetry, located in the middle of the central aromatic ring. As can be seen in Figure 3.19, complex [**17**]$^{4+}$ contains two identical Pd_2S_2 butterfly subclusters which are connected through their μ-S atoms to two neighbouring -CH_2- groups of the central benzene ring. In other words, this can be described as a dimeric

structure of complex [**15**]$^{2+}$. The Pd_2S_2 moieties are folded along the S···S vector with the angle of 131.50° and the intracluster Pd···Pd distance is 3.184(1) Å and thus no meaningful intra molecular interaction between metal centres. Similar to [**15**]$^{2+}$, the S-Pd1 bond length on the side on which the ligands are hinged (2.358(2) and 2.370(2) Å) is shorter than those on the opposite side (S-Pd2 (2.387(2) and 2.388(2) Å). The non co-planar nature of the 2 × Pd_2 units contrasts with planar, conjugated structures prepared from group 10 metals and arenetetrathiolate ligands.[29] The NMR data for [**17**]X_4 are not reported due to its poor solubility in common organic solvents. Attempts at improving the yield of [**17**]$^{4+}$ by repeating the synthesis with the more soluble [nBu_4N]Br did not result in the formation of pure material as shown by ESI-MS and elemental analysis.

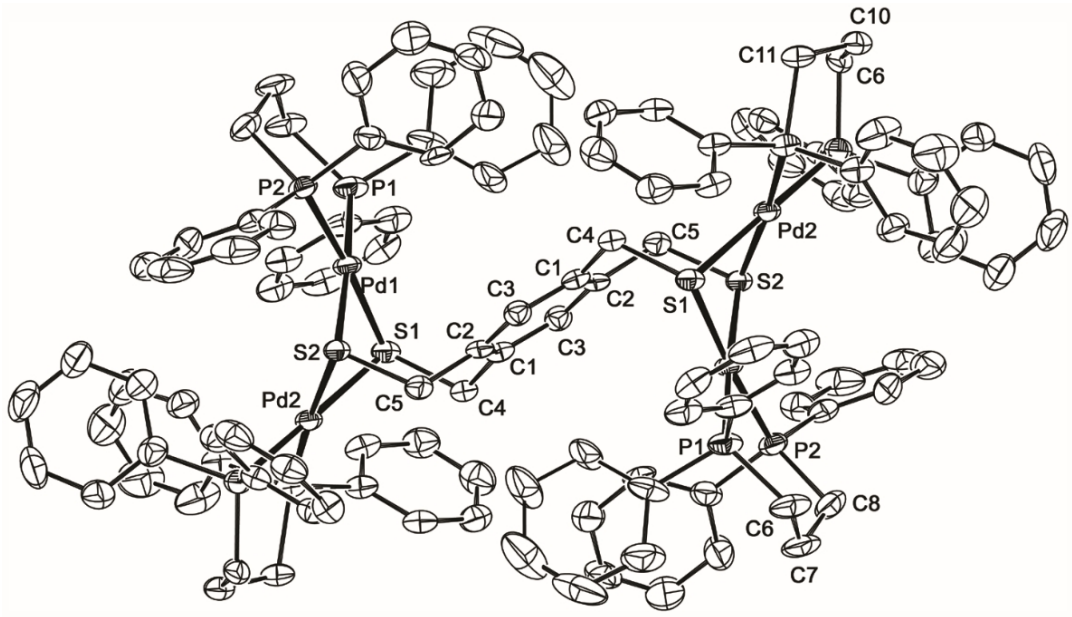

Figure 3.19. The molecular structure of complex [**17**]$^{4+}$. The thermal ellipsoids have been drawn at 40% probability. Hydrogen atoms, solvent molecules, disordered phenyl group and counter ions have been omitted for clarity.

In the case of {[**17**]X_4}, the dominant peak at m/z = 2714 is assigned to {[**17**]I_3}$^+$ (Figure 3.20), that is arising from the sodium iodide used as the instrument calibrant. Both X-ray diffraction analyses and the mass spectra of [**15**]X_2 and [**16**]X_2 complexes indicate the trace amounts of bromide as counter ion for [**15**]$^{2+}$ and [**16**]$^{2+}$, which likely arises from the impurity of lithium bromide as the side product in preparation of the ligands **13** and **14**. In the mass spectrum of complex [**15**]X_2, three peaks, at m/z = 1241, 1285 and 1333, are observed (Figure 3.21). The most intense peak at m/z = 1241 can be assigned to {[**15**]Cl}$^+$. The weak signal at m/z = 1285 arises from {[**15**]Br}$^+$. Finally the peak with m/z = 1333, which corresponds to {[**15**]I}$^+$. The mass spectrum of complex [**16**]X_2 showed three peaks as well, at m/z = 1335, 1381 and 1427 due to {[**16**]Cl}$^+$, {[**16**]Br}$^+$ and {[**16**]I}$^+$, respectively (Figure 3.22). The presence of the mixed halide counter ions does not manifest itself in the solution state NMR spectra (vide supra)

Thus the mass spectrometric investigation on these complexes reveal the formation of mono cationic particles {[**15**]X}$^+$, {[**16**]X}$^+$ and {[**17**]X_3}$^+$ with the correct isotopic pattern for the proposed formulas (Figure 3.23); there is no evidence for dicationic species.

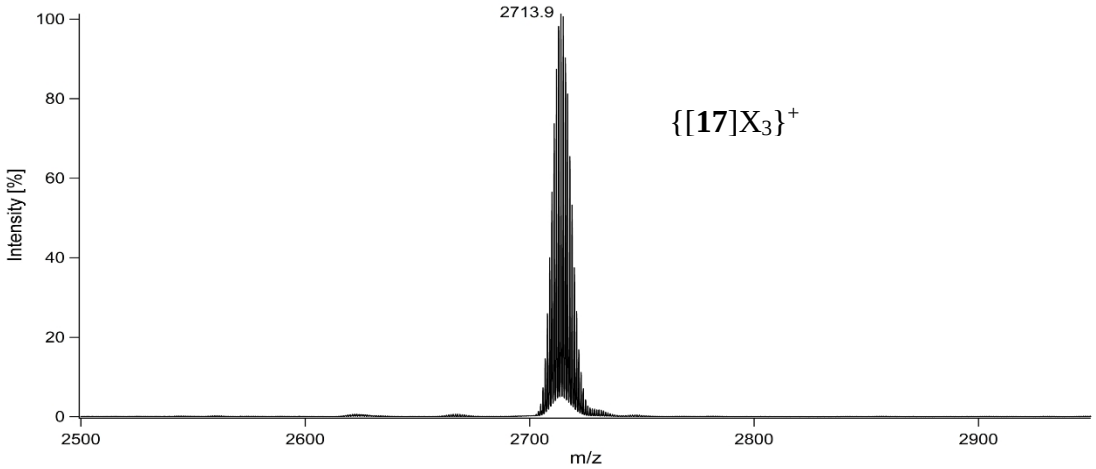

Figure 3.20. Mass spectrum obtained by electrospraying [**17**]X_4 suspended in toluene at an ESI capillary voltage of 4.5 kV. Charge states are indicated as 1+ for [**17**]I_3^+.

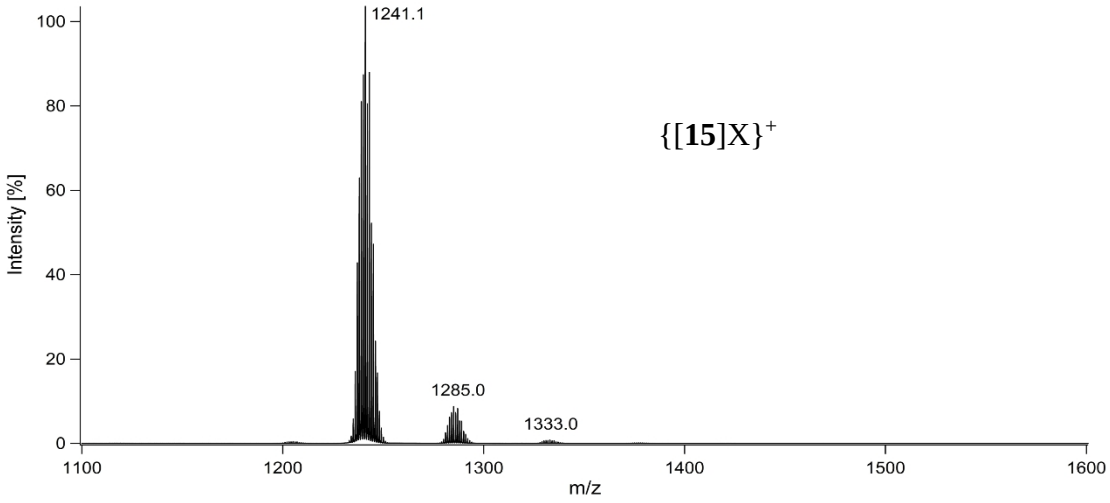

Figure 3.21. Mass spectrum obtained by electrospraying [**15**]X_2 in dichloromethane at an ESI capillary voltage of 4.5 kV. Charge states are indicated as 1+ for different counter ions.

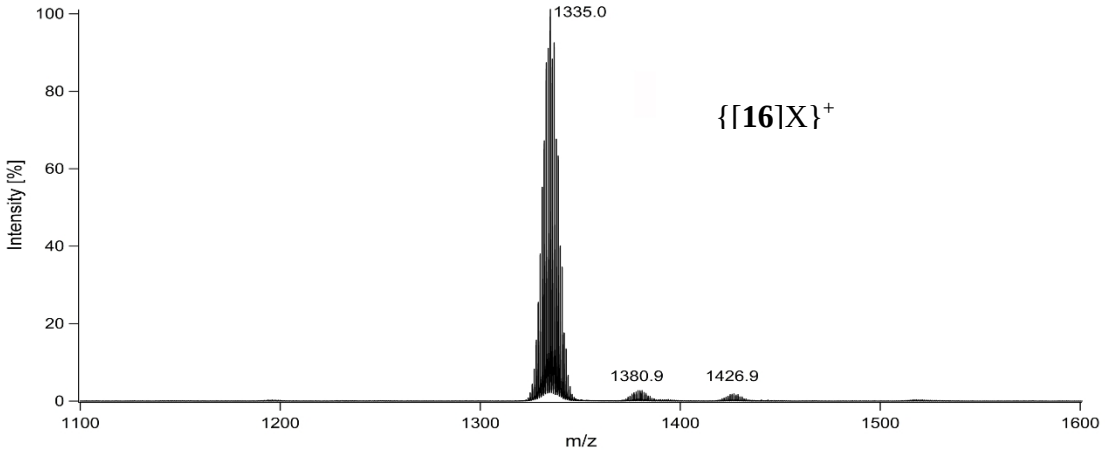

Figure 3.22. Mass spectrum obtained by electrospraying [**16**]X_2 in tetrahydrofuran at an ESI capillary voltage of 4.5 kV. Charge states are indicated as 1+ for different counter ions.

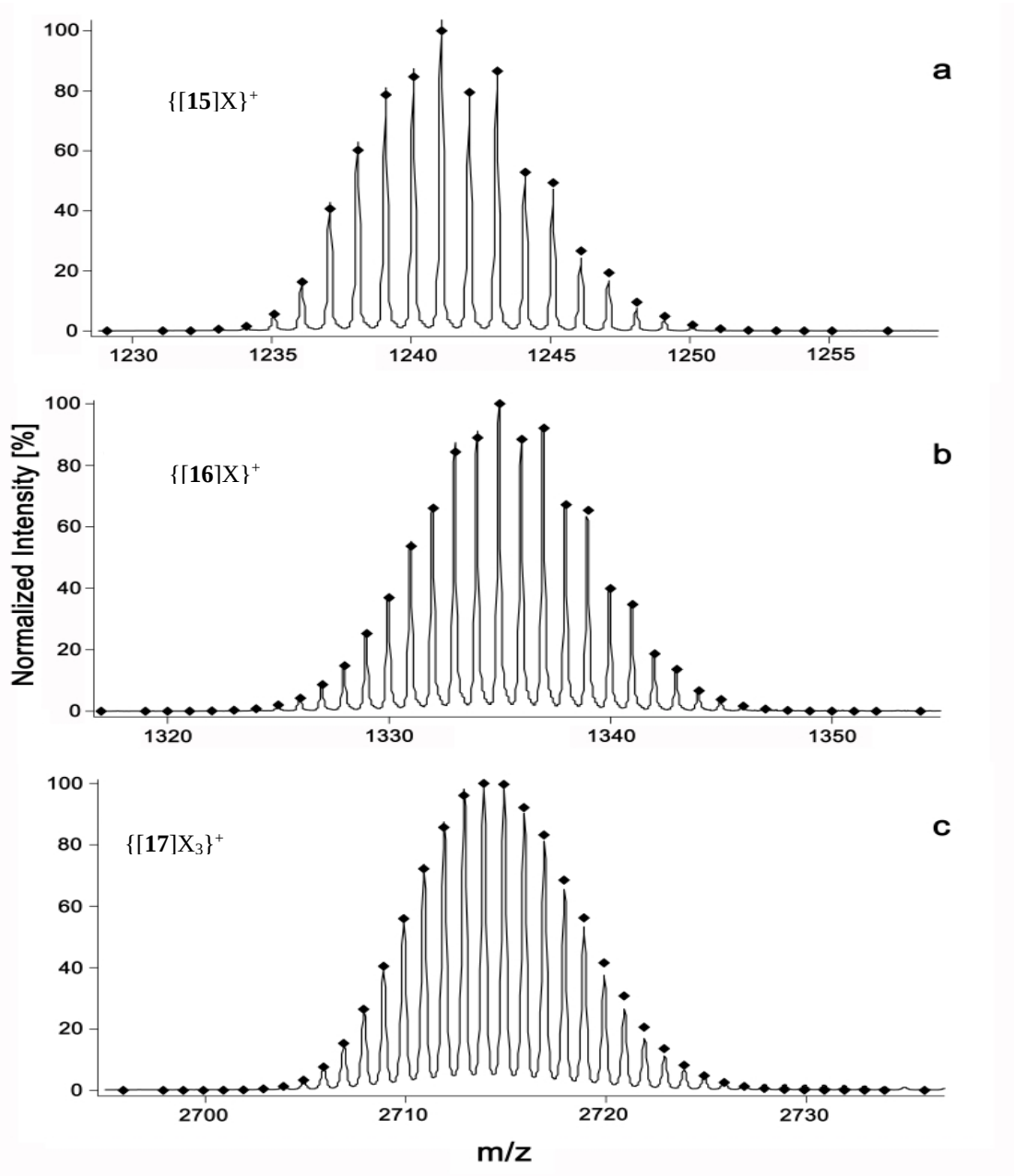

Figure 3.23. Close-up view of the most intense isotope peak region for (a) {[**15**]X}$^+$; (X = Cl), (b) {[**16**]X}$^+$; (X = Cl) and (c) {[**17**]X_3}$^+$; (X = I). Squares in each panel indicate the expected isotope pattern.

3.3 Experimental

All syntheses were carried out under an atmosphere of high-purity dried nitrogen using standard double-manifold Schlenk line techniques and nitrogen-filled glove boxes unless otherwise stated. Solvents were dried and collected using an MBraun MB-SP Series solvent purification system with tandem activated alumina (tetrahydrofuran) and an activated alumina/copper redox catalyst (pentane). Chlorinated solvent (chloroform-d) was dried and distilled over P_2O_5. Dichloromethane-d2 was purchased from CIL. Chemicals were used as received from Sigma-Aldrich. [$PdCl_2$(dppp)],[30] 1,2-bis(bromomethyl)benzene,[31] 1,2,4,5-$(Me_3SiSCH_2)_4C_6H_2$[21] and Li[$ESiMe_3$][32] (E = S, Se) were synthesized according to literature procedures.

High-resolution mass spectral measurments (**13** and **14**) were performed on Finningan MAT 8400 using electron impact (EI) ionization. Mass spectra and exact mass determinations of the samples [**15**]X_2 and [**16**]X_2 in THF and [**17**]X_4 in DCM were performed on a Bruker micrOTOF II instrument or Finningan MAT 8400 using positive electron spray ionization: m/z values have been rounded to the nearest integer or half-integer; sodium iodide was used as a calibrant. Expected isotope distribution patterns were simulated by the Bruker Compass DataAnalysis program. UV−vis absorption spectra were measured with a Varian Cary 100 spectrophotometer.

Infrared spectra ([**15**]X_2 and [**16**]X_2) were collected using a Bruker Vector33 spectrometer. The samples (~0.05 mg) was dispersed in dry KBr and packed into a pellet using a press. ATR spectrum of [**17**]X_4 was collected using a Perkin Elmer Spectrum Two ATR-FTIR spectrometer. The wave number range scanned was 4000–400 nm (Figures 3.24, 3.25 and 3.26). Elemental analysis was performed by Laboratoire d′Analyze Élementaire de l′Université de Montréal, Montreal, Canada. Samples were dried for twelve hours prior to send for analysis.

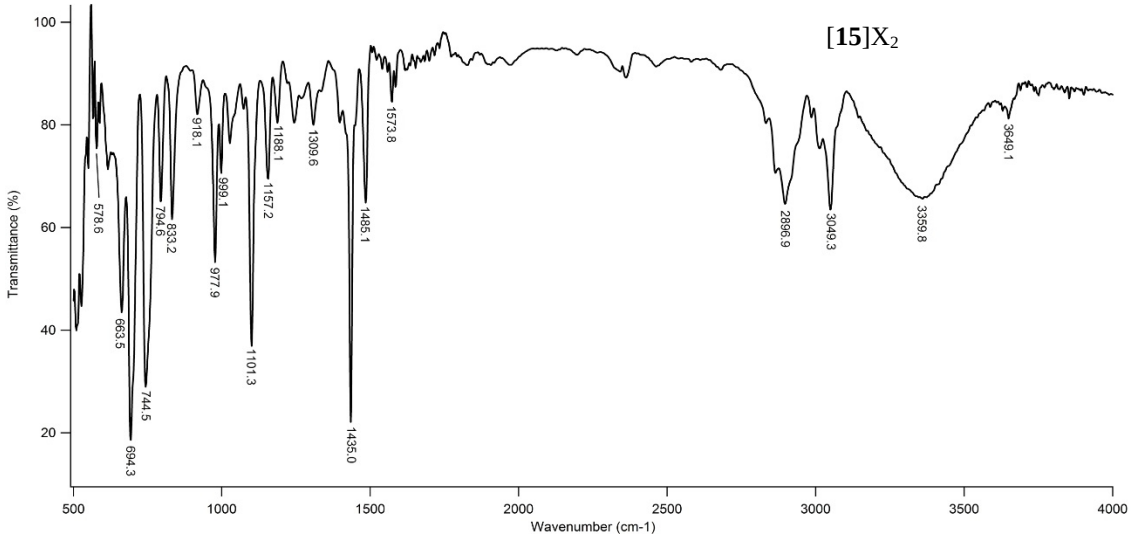

Figure 3.24. FT-IR spectrum of [**15**]X_2 in KBr.

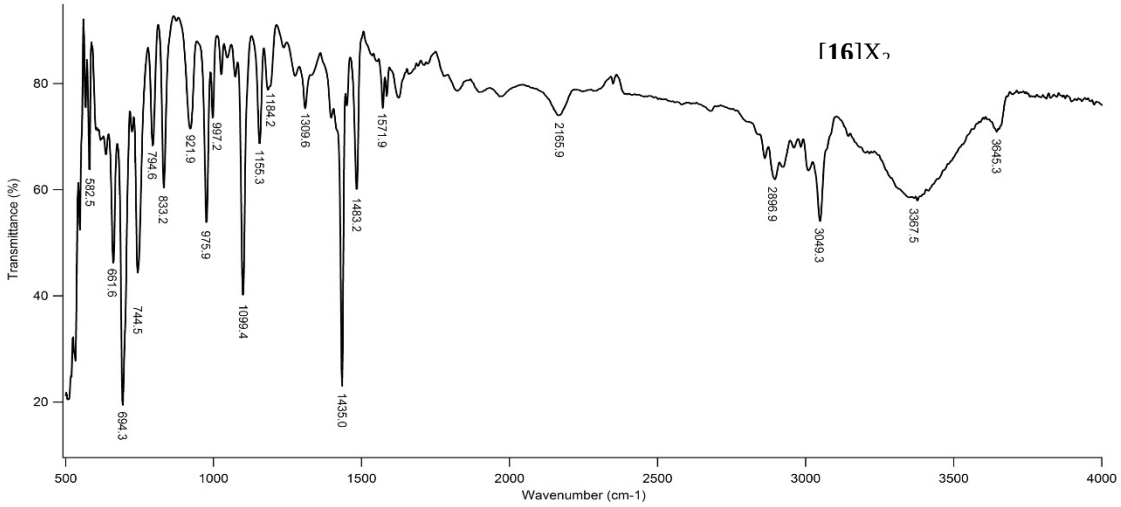

Figure 3.25. FT-IR spectrum of [**16**]X_2 in KBr.

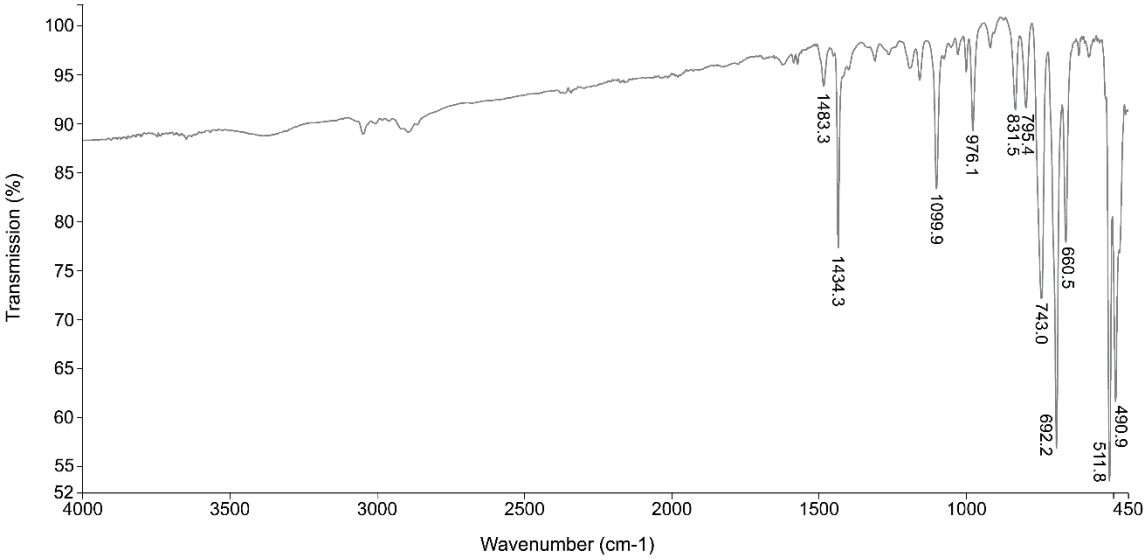

Figure 3.26. ATR spectrum of [**17**]X_4.

Experimentally obtained values suggests some residual lattice solvent remained. In order to quantify this, thermogravimetric analysis (TGA) was carried out on samples [**15**]X_2 and [**16**]X_2, and **[17]X_4** using a Q600 SDT thermal analyses instrument at a heating rate of 2 °C/min, under nitrogen flow. Results for [**15**]X_2 indicated ~3 % weight loss at 150 °C corresponding to 0.3 equivalents of residual $CHCl_3$ in the lattice. For [**16**]X_2 a ~4% weight loss was observed (0.5 $CHCl_3$). For **[17]X_4**, 6.5 % mass loss was observed (1.6 $CHCl_3$). Calculated molecular formulae (below) include these residual lattice solvents.

NMR spectra were recorded on Varian Mercury 400, Inova 400 and Inova 600 NMR spectrometers. ^{1}H and ^{13}C chemical shifts are referenced to $SiMe_4$, using solvent peak as a secondary reference, ^{31}P chemical shifts are referenced to 85% H_3PO_4.

Single-crystal X-ray diffraction measurements were completed on a Bruker APEX-II CCD ([**15**]X_2, [**17**]X_4) and Enraf-Nonius KappaCCD ([**16**]X_2)

diffractometers equipped with graphite-monochromated Mo Kα (λ = 0.71073 Å) radiation. Single crystals of the complexes were carefully selected, immersed in paraffin oil and mounted on MiteGen micromounts. The structures were solved using direct methods and refined by the full-matrix least-squares procedure of SHELXTL.[33] All non-hydrogen atoms were refined with anisotropic thermal parameters. Hydrogen atoms were included as riding on their respective carbon atoms.

Solvent molecules are present in the lattice of all three crystals. Some disordered solvent was refined with isotropic displacement parameters using partial occupancy at some positions. In [**17**]$^{4+}$, one of the phenyl groups of dppp was modelled as being disordered over two positions, with refined complementary site occupancy factors. The experimental composition of counter ions was determined by the variable site occupancy of Cl and Br atoms. In [**15**]X_2, two counter ions are refined with displacement parameters to an occupancy of 70:30% chloride to bromide for one position and 30:70% for the other site. Both counter-ions in [**16**]X_2 were refined as chloride, but the electrospray ionization (ESI) mass study showed a small amount of bromide in this compound as well. In [**17**]X_4 bromide occupies 75% of the counter ions positions.

3.3.1 Synthesis of 1,2-$(Me_3SiSCH_2)_2C_6H_4$, **13**

1,2-bis(bromomethyl)benzene (0.500 g, 1.56 mmol) and freshly prepared Li[$SSiMe_3$] (3.12 mmol) were each dissolved in anhydrous diethyl ether (30 mL and 15 mL respectively). The solutions were mixed at room temperature and stirred overnight resulting in an opaque suspension. The solvent was removed under vacuum and 30 mL of dry pentane were added to solubilize the product **13**. The reaction mixture was filtered by passing the suspension through a sintered glass frit packed with dried Celite. The solvent was removed in vacuo yielding a colourless, oily solid (84% yield).

- ^{1}H NMR (400.08 MHz, $CDCl_3$, 23 °C): δ 7.28 (m, 2H, Ar-*H*), 7.18 (m, 2H, Ar-*H*), 3.88 (s, 4H, C*H*$_2$), 0.33 (s, 18H, Si-C*H*$_3$) ppm.
- ^{13}C{^{1}H} NMR (100.61 MHz, $CDCl_3$, 23 °C): δ 138.5, 130.0, 127.4 (*C*$_6$), 28.0 (*C*H$_2$), 0.9 (Si-*C*H$_3$).
- [M$^+$] $C_{14}H_{26}S_2Si_2$: found (calculated) at *m/z* = 314.1006 (314.1014).

3.3.2 Synthesis of 1,2-$(Me_3SiSeCH_2)_2C_6H_4$, **14**

1,2-bis(bromomethyl)benzene (0.500 g, 1.56 mmol) was reacted with Li[$SeSiMe_3$] (3.12 mmol) as described for the preparation of **13** yielding a pale yellow, oily solid (71% yield).

- ^{1}H NMR (400.08 MHz, $CDCl_3$, 23 °C): δ 7.22 (m, 2H, Ar-*H*), 7.14 (m, 2H, Ar-*H*), 3.90 (s, 4H, C*H*$_2$), 0.44 (s, 18H, Si-C*H*$_3$) ppm.
- ^{13}C{^{1}H} NMR (100.61 MHz, $CDCl_3$, 23 °C): δ 138.8, 130.2, 127.2 (*C*$_6$), 19.0 (*C*H$_2$), 1.7 (Si-*C*H$_3$) ppm.
- ^{77}Se{^{1}H} NMR (76.20 MHz, $CDCl_3$, 23 °C): δ -18.4 ppm.
- [M$^+$] $C_{14}H_{26}S_2Si_2$: found (calculated) at *m/z* = 407.9907 (407.9911)

3.3.3 Synthesis of $[(dppp)_2Pd_2$-μ-κ_2S-{1,2-$(SCH_2)_2C_6H_4$}]X_2, [**15**]X_2

0.357 g (0.605 mmol) of [$PdCl_2$(dppp)] was suspended in 10 mL chloroform. A solution of 1,2-$(CH_2SSiMe_3)_2C_6H_4$ **13** (0.303 mmol, 0.0925 g) in chloroform (5 mL) was added drop-wise at room temperature and the solution was stirred at this temperature for 2 hours by which time a pale orange suspension had formed. The reaction solution was filtered over dried Celite to yield a yellow solution and to ensure removal of precipitated side-products. The solvent was reduced to ~10 mL under vacuum, at which point it was layered with 20 mL of pentane. Colourless plates crystalized after a few days. The mother liquor

was removed via pipette and the crystals were washed with 2×10 mL of pentane and dried under vacuum. Yield 45 %; m.p. 230-234 °C.

- ü $^{1}H\{^{31}P\}$ NMR (599.48 MHz, CD_2Cl_2, 25 °C): δ 7.96 (br, 8H) 7.78-6.93 (multiplets, 36H), 5.05 (d, 2H, J = 13.2 Hz), 4.62 (d, 1H, J = 13.2 Hz), 4.60 (d, 1H, J = 13.2 Hz), 4.02 (d, 1H, J = 13.2 Hz), 4.00 (d, 1H, J = 13.2 Hz), 2.53 (m, 2H), 2.44 (m,2H) 2.43 (d, 2H, J = 13.2 Hz), 2.38 (m, 2H), 1.32 (m, 1H), 1.19 (m, 1H) ppm.
- ü $^{13}C\{^{1}H\}$ NMR (150.74 MHz, $CDCl_3$, 25 °C): δ 141.0 (s), 135.0 (m), 132.8 (m), 132.6 (m), 132.0 (s), 131.5 (s), 130.6 (s), 130.3 (m), 130.1 (m), 129.9 (s), 129.3 (s), 128.5 (m), 127.6 (m), 127.0 (s), 36.9 (s), 24.1 (t, J = 17.3 Hz), 23.6 (t, J = 17.3 Hz), 18.3 (s), 18.1 (s) ppm.
- ü $^{31}P\{^{1}H\}$ NMR (161.97 MHz, $CDCl_3$, 25 °C): δ 9.6 (m) 8.2 (m) ppm.
- ü Anal. Calcd for $C_{62}H_{60}BrClP_4Pd_2S_2 \cdot 0.3CHCl_3$: C 55.13, H 4.48, S, 4.73; found C 55.09, H 4.69; S 4.73.

3.3.4 Synthesis of $[(dppp)_2Pd_2\text{-}\mu\text{-}\kappa^2Se\text{-}\{1,2\text{-}(SeCH_2)_2C_6H_4\}]X_2$, [**16**]$X_2$

0.830 g (1.408 mmol) of $[PdCl_2(dppp)]$ was suspended in 20 mL chloroform. A solution of 1,2-$(CH_2SeSiMe_3)_2C_6H_4$ **14** (0.704 mmol, 0.288 g) in chloroform (10 mL) was added drop-wise at room temperature and the solution was stirred at this temperature for 1 hour by which time a clear dark red solution had formed. The reaction solution was filtered over a filter paper. The solvent was reduced to ~15 mL under vacuum, at which point it was layered with 20 mL of pentane. Yellow block crystals deposited after 12 hours. The mother liquor was removed via pipette and the crystals were washed with 2×10 mL of pentane and dried under vacuum. Yield 40 %; m.p. 220-223 °C.

- ü $^{1}H\{^{31}P\}$ NMR (399.76 MHz, $CDCl_3$, 25 °C): δ 7.99-6.95 (multiplets, 44H), 5.16 (d, 2H, J = 12.5 Hz), 4.69 (d, 1H, J = 12.5 Hz), 4.66 (d, 1H, J = 12.5 Hz), 4.06 (d, 1H, J = 12.5 Hz), 4.03 (d, 1H, J = 12.5 Hz), 2.84 (d, 2H, J = 12.5 Hz), 2.47 (m, 2H), 2.44 (m, 2H), 2.34 (m, 2), 1.42 (m, 1H), 1.11 (m, 1H) ppm.

- ü $^{13}C\{^{1}H\}$ NMR (150.74 MHz, $CDCl_3$, 25 °C): δ 140.5 (s), 134.9 (m), 133.3 (s), 133.0 (s), 132.4 (m), 132.2 (m), 131.9 (s), 131.4 (s), 130.6 (m), 129.9 (s), 129.7 (s), 129.3 (s), 128.5 (m), 128.3 (m), 127.5 (m), 127.4 (s), 127.2 (s), 126.7 (s), 125.5 (m), 30.0 (s), 23.9 (t, J = 16.7 Hz), 23.3 (t, J = 16.7 Hz), 18.4 (s), 18.2 (s) ppm.
- ü $^{31}P\{^{1}H\}$ NMR (161.97 MHz, $CDCl_3$, 25 °C): δ 3.8 (m) 2.6 (m) ppm.
- ü Anal. Calcd for $C_{62}H_{60}Cl_2P_4Pd_2Se_2 \cdot 0.5CHCl_3$: C 52.48, H 4.18; found C 50.81, H 4.17;

3.3.5 Synthesis of $[(dppp)_4Pd_4\text{-}\mu\text{-}\kappa^4S\text{-}\{1,2,4,5\text{-}(SCH_2)_4C_6H_2\}]X_4$, [**17**]$X_4$

0.360 g (0.610 mmol) of $[PdCl_2(dppp)]$ was suspended in 15 mL chloroform. A solution of 1,2,4,5-$(CH_2SSiMe_3)_4C_6H_2$ (0.153 mmol, 0.0841 g) in chloroform (5 mL) was added drop-wise at room temperature, followed by adding 0.610 mmol LiBr (0.0530 g) portion-wise. The suspension was stirred at this temperature for two hours by which time an orange suspension had formed. The reaction solution was filtered over dried Celite to ensure removal of precipitated side-products and remaining LiBr. The resulting yellow solution was layered with 20 mL of pentane. Colourless prisms crystalized after a few days. The mother liquor was removed via pipette and the crystals were washed with 2×10 mL of pentane and dried under vacuum. Yield 25 %; m.p. > 260 °C.

- ü Anal. Calcd for $C_{118}H_{114}Br_3ClP_8Pd_4S_4 \cdot 1.6CHCl_3$ C 51.30, H 4.16, S 4.58; found 49.23, H 4.13, S4.12.

3.4 Conclusions

The work presented here illustrates the single step, straightforward synthesis of the dinuclear organochalcogenide-bridged palladium complexes [**15**]X_2 and [**16**]X_2 using the easily handled reagents **13** and **14**, respectively, and (1,3-bis(diphenylphosphino)propane)palladium(II) chloride. The structural rigidity of the chalcogenolate ligands in the bridging coordination mode induces interesting spectroscopic characteristics in the Pd_2E_2 complexes, specifically asymmetry in the bimetallic complex. Various types of nuclear magnetic resonance spectroscopic techniques were used to interpret corresponding NMR behaviour. Taking advantage of silylated–chalcogen reagents for the facile preparation of butterfly shaped Pd_2E_2 complexes, the use of tetrasulfur reagent promotes the formation of the novel tetranuclear palladium complex [**17**]X_4 consisting of a double-butterfly metal-thiolate framework.

3.5 References

[1] (a) Yam, V. W.-W.; Yu, K.-L.; Cheng, E. C.-C.; Yeung, P. K.-Y.; Cheung, K.-K.; Zhu, N., *Chem. Eur. J.* 2002, **8**, 4121-4128; (b) Yam, V. W.-W.; Yeung, P. K.-Y.; Cheung, K.-K., *J. Chem. Soc., Chem. Commun.* 1995, 267-269; (c) Cheon, J. W.; Talaga, D. S.; Zink, J. I., *Chem. Mater.* 1997, **9**, 1208-1212; (d) Folmer, J. C. W.; Turner, J. A.; Parkinson, B. A., *J. Solid State Chem.* 1987, **68**, 28-37; (e) Yam, V. W.-W.; Yeung, P. K.-Y.; Cheung, K.-K., *J. Chem. Soc., Dalton Trans.* 1994, 2587-2588; (f) Yam, V. W.-W., *C. R. Chimie* 2005, **8**, 1194-1203; (g) Poon, S.-Y.; Wong, W.-Y.; Cheah, K.-W.; Shi, J.-X., *Chem. Eur. J.* 2006, **12**, 2550-2563; (h) Saito, K.; Nakao, Y.; Umakoshi, K.; Sakaki, S., *Inorg. Chem.* 2010, **49**, 8977-8985; (i) Schneider, J.; Du, P.; Wang, X.; Brennessel, W. W.; Eisenberg, R., *Inorg. Chem.* 2009, **48**, 1498-1506; (j) Tzeng, B.-C.; Chiu, T.-H.; Lin, S.-Y.; Yang, C.-M.; Chang, T.-Y.; Huang, C.-H.; Chang, A. H.-H.; Lee, G.-H., *Cryst. Growth Des.* 2009, **9**, 5356-5362.

[2] (a) Kumar, A.; Rao, G. K.; Kumar, S.; Singh, A. K., *Organometallics* 2014, **33**, 2921-2943; (b) Kumar, S.; Rao, G. K.; Kumar, A.; Singh, M. P.; Singh, A. K., *Dalton Trans.* 2013, **42**, 16939-16948; (c) Sharma, K. N.; Joshi, H.; Sharma, A. K.; Prakash, O.; Singh, A. K., *Organometallics* 2013, **32**, 2443-2451; (d) Aleksanyan, D. V.; Kozlov, V. A.; Nelyubina, Y. V.; Lyssenko, K. A.; Puntus, L. N.; Gutsul, E. I.; Shepel, N. E.; Vasil'ev, A. A.; Petrovskii, P. V.; Odinets, I. L., *Dalton Trans.* 2011, **40**, 1535-1546; (e) Kozlov, V. A.; Aleksanyan, D. V.; Nelyubina, Y. V.; Lyssenko, K. A.; Gutsul, E. I.; Vasil'ev, A. A.; Petrovskii, P. V.; Odinets, I. L., *Dalton Trans.* 2009, 8657-8666.

[3] (a) Ishii, A.; Nakata, N.; Uchiumi, R.; Murakami, K., *Angew. Chem.-Int. Ed.* 2008, **47**, 2661-2664; (b) Albano, V. G.; Monari, M.; Orabona, I.; Panunzi, A.; Ruffo, F., *J. Am. Chem. Soc.* 2001, **123**, 4352-4353; (c) Albano, V. G.; Monari, M.; Orabona, I.; Panunzi, A.; Roviello, G.; Ruffo, F., *Organometallics* 2003, **22**, 1223-1230; (d) Nakata, N.; Ikeda, T.; Ishii, A., *Inorg. Chem.* 2010, **49**, 8112-8116; (e) Wrackmeyer, B.; Hernandez, Z. G.; Kempe, R.; Herberhold, M., *Eur. J. Inorg. Chem.* 2007, 239-246.

[4] (a) Chauhan, R. S.; Kedarnath, G.; Wadawale, A.; Slawin, A. M. Z.; Jain, V. K., *Dalton Trans.* 2013, **42**, 259-269; (b) Ji, W.; Jing, S.; Liu, Z. Y.; Shen, J.; Ma, J.; Zhu, D. R.; Cao, D. K.; Zheng, L. M.; Yao, M. X., *Inorg. Chem.* 2013, **52**, 5786-5793; (c) Saleem, F.; Rao, G. K.; Singh, P.; Singh, A. K., *Organometallics* 2013, **32**, 387-395; (d) Niebel, T.; MacDonald, D. G.; Khadka, C. B.; Corrigan, J. F., *Z. Anorg. Allg. Chem.* 2010, **636**, 1095-1099; (e) Aucott, S. M.; Milton, H. L.; Robertson, S. D.; Slawin, A. M. Z.; Walker, G. D.; Woollins, J. D., *Chem.-Eur. J.* 2004, **10**, 1666-1676.

[5] (a) Jain, V. K.; Jain, L., *Coord. Chem. Rev.* 2005, **249**, 3075-3197; (b) Kedarnath, G.; Jain, V. K., *Coord. Chem. Rev.* 2013, **257**, 1409-1435.

[6] (a) Chauhan, R. S.; Sharma, R. K.; Kedarnath, G.; Cordes, D. B.; Slawin, A. M. Z.; Jain, V. K., *J. Organomet. Chem.* 2012, **717**, 180-186; (b) Hirano, M.; Tatesawa, S.-y.; Yabukami, M.; Ishihara, Y.; Hara, Y.; Komine, N.; Komiya, S., *Organometallics* 2011, **30**, 5110-5122; (c) Tsuji, T.; Kuwamura, N.; Yoshinari, N.; Konno, T., *Inorg.*

Chem. 2013, **52**, 5350-5358; (d) Vetter, C.; Kaluđerović, G. N.; Paschke, R.; Gómez-Ruiz, S.; Steinborn, D., *Polyhedron* 2009, **28**, 3699-3706.

[7] (a) Hannu-Kuure, M. S.; Komulainen, J.; Oilunkaniemi, R.; Laitinen, R. S.; Suontamo, R.; Ahlgren, M., *J. Organomet. Chem.* 2003, **666**, 111-120; (b) Kirij, N. V.; Tyrra, W.; Pantenburg, I.; Naumann, D.; Scherer, H.; Naumann, D.; Yagupolskii, Y. L., *J. Organomet. Chem.* 2006, **691**, 2679-2685; (c) Panunzi, A.; Roviello, G.; Ruffo, F., *Inorg. Chem. Commun.* 2003, **6**, 1282-1286; (d) Risto, M.; Jahr, E. M.; Hannu-Kuure, M. S.; Oilunkaniemi, R.; Laitinen, R. S., *J. Organomet. Chem.* 2007, **692**, 2193-2204.

[8] Chatt, J.; Mann, F. J., *J. Chem. Soc.* 1938, 1949-1954.

[9] (a) Jain, V. K., *Inorg. Chim. Acta* 1987, **133**, 261-266; (b) Jain, V. K.; Patel, R. P.; Muralidharan, K. V.; Bohra, R., *Polyhedron* 1989, **8**, 2151-2155; (c) Padilla, E. M.; Jensen, C. M., *Polyhedron* 1991, **10**, 89-93; (d) Padilla, E. M.; Golen, J. A.; Richmann, P. N.; Jensen, C. M., *Polyhedron* 1991, **10**, 1343-1352; (e) Jain, V. K.; Kannan, S., *J. Organomet. Chem.* 1992, **439**, 231-235; (f) Kumbhare, L. B.; Wadawale, A. P.; Jain, V. K.; Kolay, S.; Nethaji, M., *J. Organomet. Chem.* 2009, **694**, 3892-3901; (g) Nakata, N.; Uchiumi, R.; Yoshino, T.; Ikeda, T.; Kamon, H.; Ishii, A., *Organometallics* 2009, **28**, 1981-1984.

[10] (a) Oilunkaniemi, R.; Laitinen, R. S.; Ahlgren, M., *J. Organomet. Chem.* 2001, **623**, 168-175; (b) Morley, C. P.; Webster, C. A.; Di Vaira, M., *J. Organomet. Chem.* 2006, **691**, 4244-4249; (c) Ananikov, V. P.; Malyshev, D. A.; Beletskaya, I. P.; Aleksandrov, G. G.; Eremenko, I. L., *J. Organomet. Chem.* 2003, **679**, 162-172; (d) Beletskaya, I. P.; Ananikov, V. P., *Eur. J. Org. Chem.* 2007, 3431-3444; (e) Ananikov, V. P.; Beletskaya, I. P., *Dokl. Chem.* 2003, **389**, 81-86.

[11] (a) Mas-Balleste, R.; Capdevila, M.; Champkin, P. A.; Clegg, W.; Coxall, R. A.; Lledos, A.; Megret, C.; Gonzalez-Duarte, P., *Inorg. Chem.* 2002, **41**, 3218-3229; (b) Gukathasan, R. R.; Morris, R. H.; Walker, A., *Can. J. Chem.-Rev. Can. Chim.* 1983, 61, 2490-2492; (c) Yam, V. W. W.; Yeung, P. K. Y.; Cheung, K. K., *J. Chem. Soc.-Chem. Commun.* 1995, 267-269; (d) Briant, C. E.; Gardner, C. J.; Hor, T. S. A.; Howells, N. D.; Mingos, D. M. P., *J. Chem. Soc., Dalton Trans.* 1984, 2645-2651.

[12] (a) Yeo, J. S. L.; Vittal, J. J.; Henderson, W.; Hor, T. S. A, *J. Chem. Soc., Dalton Trans*. 2002, 328-336; (b) Matsumoto, K.; Kotoku, N.; Shizuka, T.; Tanaka, R.; Okeya, S., *Inorg. Chim. Acta* 2001, **321**, 167-170; (c) Liu, H.; Tan, A. L.; Mok, K. F.; Mak, T. C. W.; Batsanov, A. S.; Howard, J. A. K.; Hor, T. S. A., *J. Am. Chem. Soc.* 1997, **119**, 11006-11011; (d) Capdevila, M.; Carrasco, Y.; Clegg, W.; Coxall, R. A.; Gonzalez-Duarte, P.; Lledos, A.; Sola, J.; Ujaque, G., *Chem. Commun.* 1998, 597-598; (e) Zhou, M.; Xu, Y.; Tan, A.-M.; Leung, P.-H.; Mok, K. F.; Koh, L. L.; Hor, T. S. A., *Inorg. Chem.* 1995, **34**, 6425-6429.

[13] (a) Ujam, O. T.; Devoy, S. M.; Henderson, W.; Nicholson, B. K.; Hor, T. S. A., *Dalton Trans.* 2012, **41**, 12773-12780; (b) Chong, S. H.; Henderson, W.; Hor, T. S. A., *Dalton Trans.* 2007, 4008-4016; (c) Ujam, O. T.; Henderson, W.; Nicholson, B. K.; Andy Hor, T. S., *Inorg. Chim. Acta* 2011, **376**, 255-263.

[14] Devoy, S. M.; Henderson, W.; Nicholson, B. K., *Inorg. Chim. Acta* 2013, **406**, 81-86.

[15] (a) Chong, S. H.; Young, D. J.; Hor, T. S. A., *J. Organomet. Chem.* 2006, **691**, 349-355; (b) Yeo, J. S. L.; Vittal, J. J.; Henderson, W.; Hor, T. S. A., *Organometallics* 2002, **21**, 2944-2949; (c) Yeo, J. S. L.; Vittal, J. J.; Hor, T. S. A., Eur. *J. Inorg. Chem.* 2003, 277-280.

[16] (a) Cao, R.; Hong, M.; Jiang, F.; Kang, B.; Xie, X.; Liu, H., *Polyhedron* 1996, **15**, 2661-2670; (b) Ford, S.; Morley, C. P.; Di Vaira, M., *Inorg. Chem.* 2004, **43**, 7101-7110; (c) Gibson, V. C.; Long, N. J.; White, A. J. P.; Williams, C. K.; Williams, D. J., *Chem. Commun.* 2000, 2359-2360; (d) Gibson, V. C.; Long, N. J.; Williams, C. K.; Fontani, M.; Zanello, P., *Dalton Trans.* 2003, 3599-3605; (e) Kudoh, K.; Okamoto, T.; Yamaguchi, S., *Organometallics* 2006, **25**, 2374-2377; (f) Sato, O.; Sakai, A.; Aoki, M.; Kuramochi, T.; Nakayama, J., *Heterocycles* 2012, **86**, 1253-1260; (g) Pop, F.; Branzea, D. G.; Cauchy, T.; Avarvari, N., *C. R. Chimie* 2012, **15**, 904-910.

[17] Brown, M. J.; Corrigan, J. F., *J. Organomet. Chem.* 2004, **689**, 2872-2879.

[18] Banister, A. J.; Howard, J. A. K.; May, I.; Rawson, J. M., *Chem. Commun.* 1997, 1763-1764.

[19] Su, W. P.; Cao, R.; Hong, M. C.; Wu, D. X.; Lu, J. X., *J. Chem. Soc.-Dalton Trans.* 2000, 1527-1532.

[20] (a) Fuhr, O.; Dehnen, S.; Fenske, D., *Chem. Soc. Rev.* **2013,** *42*, 1871-1906; (b) MacDonald, D. G.; Corrigan, J. F., *Philos. Trans. R. Soc. A-Math. Phys. Eng. Sci.* **2010,** *368*, 1455-1472; (c) DeGroot, M. W.; Corrigan, J. F., *Z. Anorg. Allg. Chem.* **2006,** *632*, 19-29.

[21] Fard, M. A.; Khalili Najafabadi, B.; Hesari, M.; Workentin, M. S.; Corrigan, J. F., *Chem. Eur. J.* 2014, **20**, 7037-7047.

[22] (a) Mitchell, K. A.; Streveler, K. C.; Jensen, C. M., *Inorg. Chem.* 1993, **32**, 2608-2609; (b) Garcia, J. J.; Arevalo, A.; Montiel, V.; Del Rio, F.; Quiroz, B.; Adams, H.; Maitlis, P. M., *Organometallics* 1997, **16**, 3216-3220; (c) Capdevila, M.; Clegg, W.; Gonzalez-Duarte, P.; Harris, B.; Mira, I.; Sola, J.; Taylor, I. C., *J. Chem. Soc., Dalton Trans.* 1992, 2817-2826; (d) Redin, K.; Wilson, A. D.; Newell, R.; DuBois, M. R.; DuBois, D. L., *Inorg. Chem.* 2007, **46**, 1268-1276.

[23] Aullón, G.; Hamidi, M.; Lledós, A.; Alvarez, S., *Inorg. Chem.* 2004, **43**, 3702-3714.

24 Su, W.; Cao, R.; Hong, M.; Wu, D.; Lu, J., *J. Chem. Soc., Dalton Trans.* 2000, 1527-1532.

[25] (a) Oilunkaniemi, R.; Laitinen, R. S.; Ahlgren, M., *J. Organomet. Chem.* 1999, **587**, 200-206; (b) Forniés-Cámer, J.; Aaliti, A.; Ruiz, N.; Masdeu-Bultó, A. M.; Claver, C.; Cardin, C. J., *J. Organomet. Chem.* 1997, **530**, 199-209.

[26] Zheng, A. X.; Ren, Z. G.; Wang, H. F.; Li, H. X.; Lang, J. P., *Inorg. Chim. Acta* 2012, **382**, 43-51.

[27] (a) Dey, S.; Jain, V. K.; Varghese, B., *J. Organomet. Chem.* 2001, **623**, 48-55; (b) Goggin, P. L.; Goodfellew, R. J; Reed, F. J. S., *J. Chem. Soc. A* 1971, 2031-2038; (c) Henderson, W.; McCaffrey, L. J.; Nicholson, B. K., *J. Chem. Soc., Dalton Trans.* 2000, 2753-2760; (d) Romerosa, A.; López-Magaña, C.; Saoud, M.; Mañas, S., *Eur. J. Inorg. Chem.* 2003, 2003, 348-355; (e) Singhal, A.; Jain, V. K., *J. Organomet. Chem.* 1995, **494**, 75-80.

[28] Song, L. C.; Qi, C. H.; Bao, H. L.; Fang, X. N.; Song, H. B., *Organometallics* 2012, **31**, 5358-5370.

[29] Arumugam, K.; Shaw, M. C.; Chandrasekaran, P.; Villagran, D.; Gray, T. G.; Mague, J. T.; Donahue, J. P., *Inorg. Chem.* 2009, **48**, 10591-10607.

[30] Sanger, A. R., *J. Chem. Soc., Dalton Trans.* 1977, 1971-1976.

[31] Wenner, W., *J. Org. Chem.* 1952, **17**, 523-528.

[32] Taher, D.; Wallbank, A. I.; Turner, E. A.; Cuthbert, H. L.; Corrigan, J. F., *Eur. J. Inorg. Chem.* 2006, 4616-4620.

[33] (a) Sheldrick, G. M., *Acta Crystallogr. Sect. A* 2008, **64**, 112-122; (b) Sheldrick, G. M., SHELXTL PC Version 6.1 An Integrated System for Solving, Refining, and Displaying Crystal Structures from Diffraction Data, Bruker Analytical X-ray Systems, 2000.

Chapter 4

Tethered Poly-Copper-Chalcogenolate Assemblies Enabled via NHC Ligation

4.1 Introduction

Silylated chalcogen reagents of the type $RESiMe_3$ (R = an organic group, E = S, Se) have been shown to be a convenient source of organo-chalcogenolate (RE^-) as easily formed synthons in the synthesis of chalcogenoesters,[1] and are well developed for the preparation of metal chalcogen bonds.[2] With the latter, their utility in coordination chemistry has been confirmed for both the preparation of polynuclear metal-chalcogen (cluster) architectures[3] as well as single metal coordination complexes.[4] The tunability of the substituent R has been shown to be very effective at incorporating a tailored surface onto metal-chalcogen clusters and has the benefit of stabilizing the surface of the cluster at the same time allowing the incorporation of specific chemical functionalities.

With continued interest in the assembly of the molecules containing $–ESiMe_3$ groups, we reported recently the synthesis and the characterization of a series of poly-chalcogenotrimethylsilanes $Ar(CH_2ESiMe_3)_n$, (Ar = aryl; E = S, Se; n = 2 (ortho, para), 3 and 4).[5] These complexes represent the first examples of the incorporation of such a large number of reactive $–ESiMe_3$ moieties onto an organic molecular scaffold. We also demonstrated the reactivity of $–ESiMe_3$ moieties towards ferrocenoyl chloride as a simple route for the formation of poly-ferrocenylchalcogenoesters.[5]

Also demonstrated was the simple preparation of butterfly shaped Pd_2E_2 (E = S, Se) complexes via the reaction of $[(dppp)PdCl_2]$ (1,3-

bis(diphenylphosphino)propane)palladium(II) and the disubstituted thio- and selenotrimethylsilane reagents, 1,2-$(Me_3SiECH_2)_2(C_6H_4)$.[6] Taking advantage of the symmetrical distribution of chalcogen centers in 1,2,4,5-$(Me_3SiSCH_2)_4(C_6H_2)$ offers an entry into "double-butterfly" Pd_2S_2 complexes, therefore demonstrating the use of such polysilylated chalcogen reagents with defined spacers between the formed metal-chalcogenolate units.[6]

Herein we use these reagents to develop the chemistry of novel polynuclear copper(I)-chalcogenolate complexes. These compounds are of significant interest because of their biological relevance to the cysteine-rich copper(I) proteins and other copper based thioneins[7] together with their potential as catalysts.[8] The development in these areas cannot be driven without careful examination of supporting ligands, which can permit one to fine-tune the stability and reactivity in the coordination sphere of the metal center. Given that N-heterocyclic carbenes (NHCs) show powerful coordination ability toward a wide range of metal ions to form strong M–C bonds, significant advances can be expected in the synthetic and structural chemistry of transition metal complexes bearing NHCs and (poly)chalcogenolate ligands.

As the only example of polydentate organochalcogen spacers for the assembly of poly-(NHC)copper chalcogenolates, Zhang and Warren emulated the role of histidine and cysteine ligands at trigonal copper sites by employing large N-heterocyclic carbene ligands along with C_3 and C_4 alkyldithiolate linkers. The addition of either 1,3-propanedithiol or 1,4-butanedithiol to 2 equiv. [$(Cl_2IPr)CuO^tBu$] (Cl_2IPr = 1,3-bis-(2,6-diisopropylphenyl)-4,5-dichloroimidazol-2-ylidene) led to the formation of the corresponding dinuclear copper(I) thiolate complexes [$\{(Cl_2IPr)Cu\}_2(\mu$-$S(CH_2)_nS)$] (n = 3 or 4). Crystallization of these two complexes showed two different dicopper-dithiolate motifs dependent on the length of the linkers.[7a]

We have previously shown that the reaction of $[(^iPr_2$-bimy$)CuCl]_2$ ($^iPr_2$-bimy = 1,3-di-isopropylbenzimidazole-2-ylidene) with one equivalent of Ph-$ESiMe_3$ (E = S, Se) yielded a six-membered E_3Cu_3 cluster with three $^iPr_2$-bimy on the Cu atoms.[9] The formation of bridging μ-ER in these complexes reflects the smaller size of the carbene ligands. In order

to develop the coordination chemistry and structural properties of carbene-copper chalcogenolates with multidentate organic spacers, the poly-chalcogenotrimethylsilane complexes 1,4-$(Me_3SiECH_2)_2(C_6Me_4)$, 1,3,5-$(Me_3SiECH_2)_3(C_6Me_3)$ (E = S, Se), 1,2,4,5-$(Me_3SiSeCH_2)_4(C_6H_2)$ and 1,1´-fc$(CH_2ESiMe_3)_2$ (E = S, Se) are used in this study. The reactivity of such complexes has been demonstrated with copper(I) salts. For this purpose, we selected [(IPr)CuOAc] (IPr = 1,3-bis(2,6-diisopropylphenyl)imidazol-2-ylidene): this carbene ligand has already been well established in the chemistry of monomeric copper(I) thiolate complexes, [(IPr)CuS$(CH_2)_n$Ph] (n = 0, 1).[8]

The silylated reagents Ar$(CH_2ESiMe_3)_n$ and 1,1´-fc$(CH_2ESiMe_3)_2$, via reaction with [(IPr)CuOAc] and the formation of Me_3SiOAc, facilitate a one-step synthetic procedure for the formation of the polynuclear NHC-copper chalcogenolates 1,4-[{(IPr)CuECH_2}$_2(C_6Me_4)$] (E = S **18**, E = Se **19**), 1,1´-[fc$(CH_2ECuIPr)_2$] (E = S **20**, E = Se **21**), 1,3,5-[{(IPr)CuECH_2}$_3(C_6Me_3)$] (E = S **22**, E = Se **23**) and 1,2,4,5-[{(IPr)CuECH_2}$_4(C_6H_2)$] (E = Se **24**). These are the first examples of such NHC ligated Cu-chalcogen assemblies and represent a new route into polynuclear copper-chalcogenolate chemistry.

NHCs have gained increasing interest over the last years and now play a central role in organometallic chemistry[10,11] There strong bonding characteristics have also been used to stabilize a typical oxidation states and bonding motifs of the main group elements, which are otherwise unstable.[12] In a similar context, coinage metal-NHCs are widely studied for their interesting structural properties[13] and their potential applications in medicine,[14] nanomaterials, liquid crystals,[15] and catalysis.[16] Despite being the least stable among the coinage metal-NHC complexes, investigations on Cu(I)-NHCs have increased substantially. Compared with their phosphine counterparts, Cu(I)-NHCs with bulky and robust substituents present many advantages such as thermal stability and ease of preparation of differing ligand types.[13b]

4.2 Results and discussion

As outlined in Scheme 4.1, a series of polynuclear NHC ligated copper chalcogenolate complexes can be synthesized through the reactions of [(IPr)CuOAc] and polychalcogenotrimethylsilane reagents in good yields. Reactions of di- and tri-substituted 1,4-$(Me_3SiECH_2)_2(C_6Me_4)$, 1,3,5-$(Me_3SiECH_2)_3(C_6Me_3)$ and 1,1´-fc$(CH_2ESiMe_3)_2$ (E = S, Se) and 1,1'-fc$(CH_2ESiMe_3)_2$ (E = S, Se) with [(IPr)CuOAc] proceed at room temperature. However, because of the instability of **24** at ambient temperatures, 1,2,4,5-$(Me_3SiECH_2)_4(C_6H_2)$, was reacted with four equivalents of [(IPr)CuOAc] at -40 °C in THF. After warming to -25 °C and layering with cold pentane, **24** was obtained as colorless crystals.

At present there are but a few examples of solid-state structures of NHC-copper chalcogenolate complexes.[7a, 8, 17] In this study, single crystals of 1,4-[{(IPr)CuECH_2}$_2$(C_6Me_4)] (E = S **18**, E = Se **19**), 1,1´-[fc$(CH_2ECuIPr)_2$] (E = S **20**, E = Se **21**) and 1,2,4,5-[{(IPr)CuSeCH_2}$_4$(C_6H_2)] (**24**) suitable for X-ray diffraction study were obtained through solvent diffusion (pentane) to the reaction solutions (Table 4.1). Molecules of **18** and **19** crystallize in monoclinic space group $P2_1/c$. The molecular structures of **18** and **19**, which reside about a crystallographic inversion center, confirm that the two (IPr)Cu-E moieties lie on opposite sides of the aromatic spacer (Figures 4.1 and 4.2, respectively). The C-E-Cu angles in **18** and **19** (100.61(9)° and 97.48(2)°, respectively) are close to the C-E-Si angles in their corresponding trimethylsilylchalcogenide reagents 1,4-$(Me_3SiECH_2)_2(C_6Me_4)$ (E = S, 99.84(7) °; E = Se, 97.47(1) °). The S-Cu (**18** 2.1363(8) Å) and Se-Cu (**19** 2.241(1) Å) distances are similar to those previously reported for chalcogenolate-copper(NHC) single bonds.[7a, 17b] These two molecular structures also illustrate the expected, near-linear coordination geometry of the copper(I) center (**18** 174.35(8) and **19** 174.4(2)°). The central arene C_6 in **18** and **19** is not parallel with either of the NHC C_3N_2, which are rotated relative to the central aromatic (29.55° for **18** and 29.64° for **19**, respectively). The ferrocenyl complexes **20** and **21** also reside about a crystallographic inversion center in the monoclinic space group

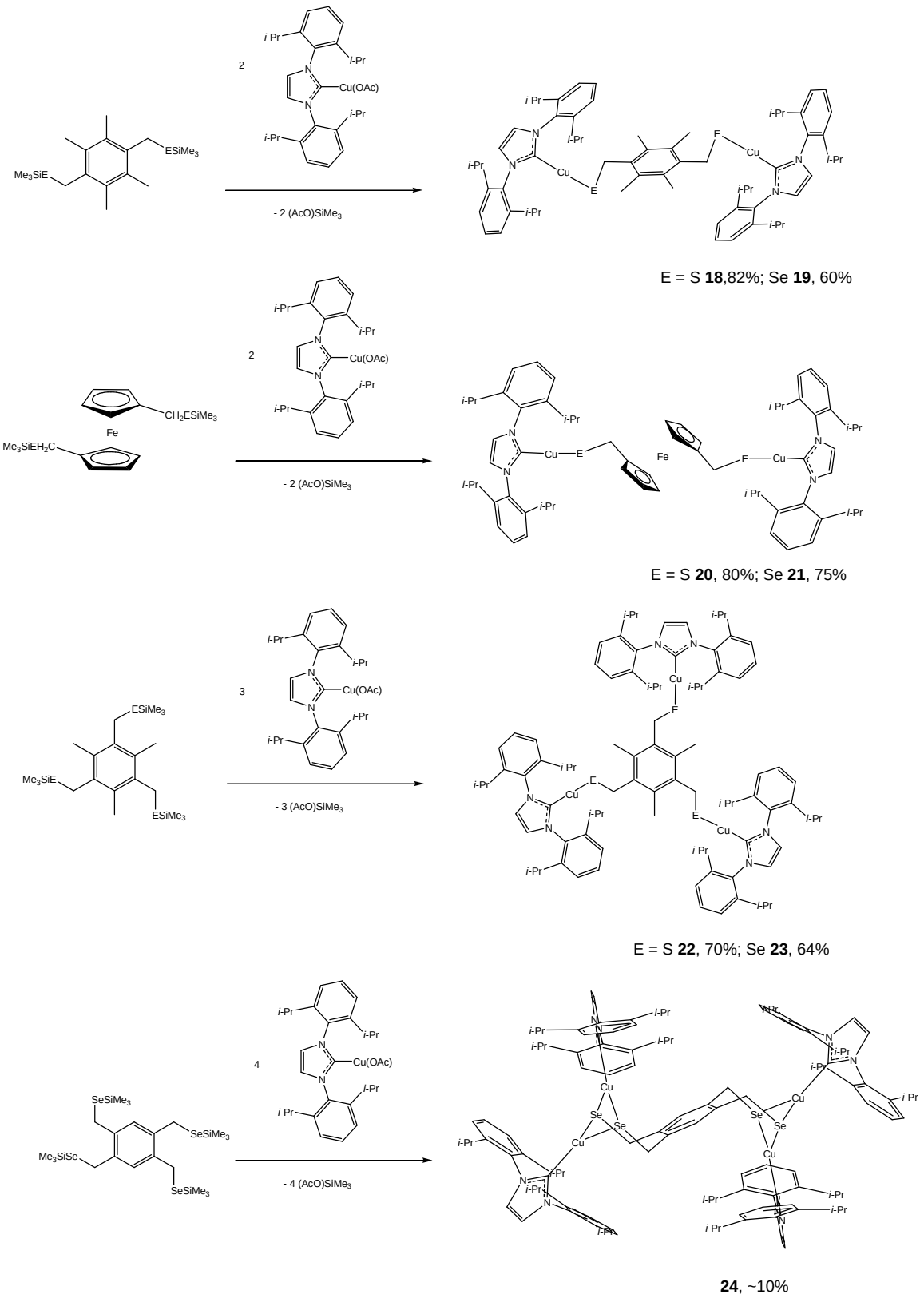

Scheme 4.1. Synthesis of **18-24**

$P2_1/c$. The two carbene-copper chalcogenolate groups are held in a *trans* configuration in the solid state with the two Cp rings adopting a staggered conformation (Figures 4.3 and 4.4). The Fe atom sits on the crystallographic inversion center with the planes of the cyclopentadienyl rings parallel and the CH_2 groups lying in the plane of their respectiveCp rings. Similar to **18** and **19**, these two molecular structures reveal the near-linear coordination geometry for copper(I) centres (**20** 178.3(2) and **21** 179.1(1)°). The imidazol-2-ylidene and Cp rings are, however, not coplanar (rotated 54.92° for **20** and 55.09° for **21**). Due to the obtuse angles of Cp-CH_2-E (113.7(4)° for both **20** and **21**) and CH_2-E-Cu (**20** E = S, 105.6(2); **21** E = Se, 101.8(2)°) and the dihedral angles of Cp-CH_2-E-Cu (**20** E = S, 85.6(4)°; **21** E = Se, 87.3(4)°) the (IPr)Cu-E^- groups are located away from each other. The angles of CH_2-E-Cu in **20** and **21** are larger than those observed for **18** and **19**.

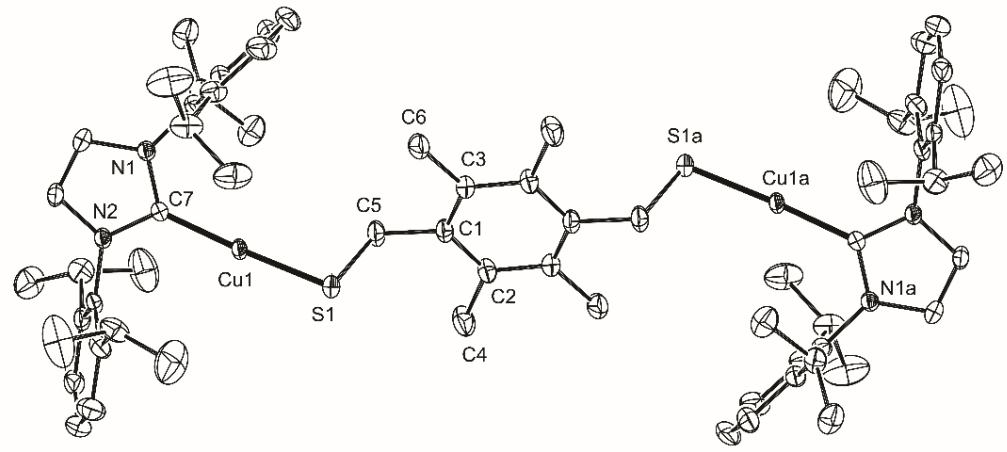

Figure 4.1. Thermal ellipsoid plot (40% probability level) of **18** with the selected atom numbering scheme. Hydrogen atoms and solvent molecule are omitted for clarity. Selected bond distances (Å) and angles (º): S1-Cu1 2.1363(8), Cu1-C7 1.893 (2), C5-S1 1.843(3), C5-S1-Cu1 100.61(9), S1-Cu1-C7 174.35(8).

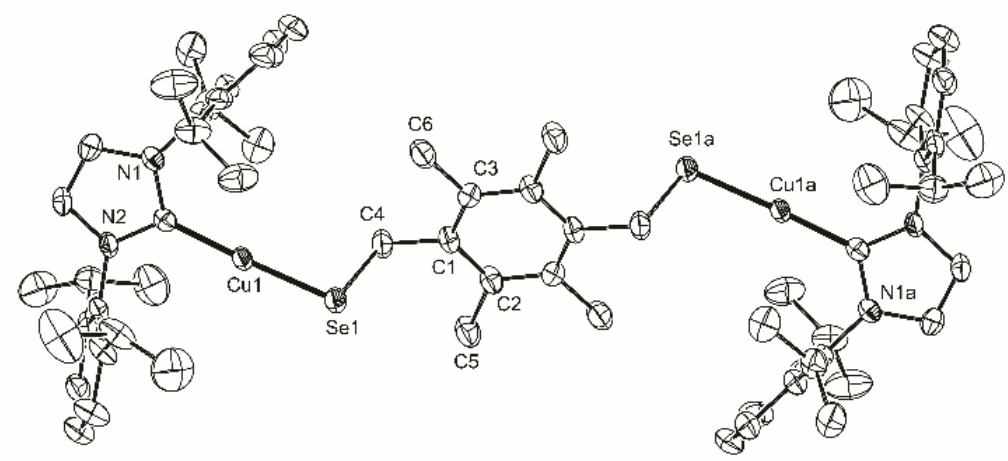

Figure 4.2. Thermal ellipsoid plot (40% probability level) of **19** with the selected atom numbering scheme. Hydrogen atoms and solvent molecule are omitted for clarity. Selected bond distances (Å) and angles (º): Se1-Cu1 2.241(1), Cu1-C7 1.883 (6), C4-Se1 1.995(7), C4-Se1-Cu1 97.5(2), Se1-Cu1-C7 174.4(2).

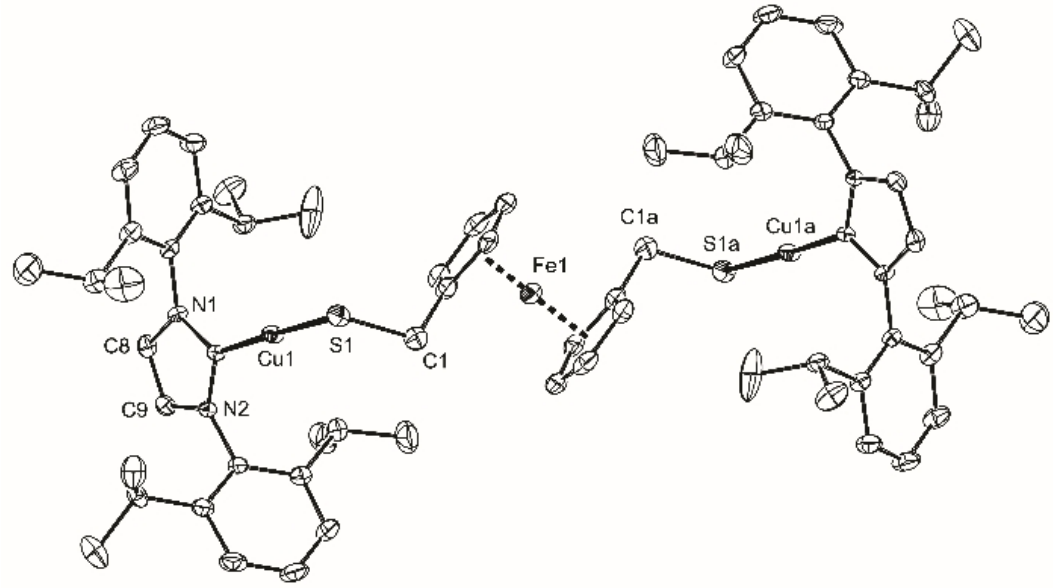

Figure 4.3. Thermal ellipsoid plot (40% probability level) of **20** with the selected atom numbering scheme. Hydrogen atoms and solvent molecules are omitted for clarity. Selected bond distances (Å) and angles (º): S1-Cu1 2.137(2), Cu1-C7 1.888 (5), C1-S1 1.871(6), C1-S1-Cu1 105.6(2), S1-Cu1-C7 178.3(2), C2-C1-S1 113.7(4).

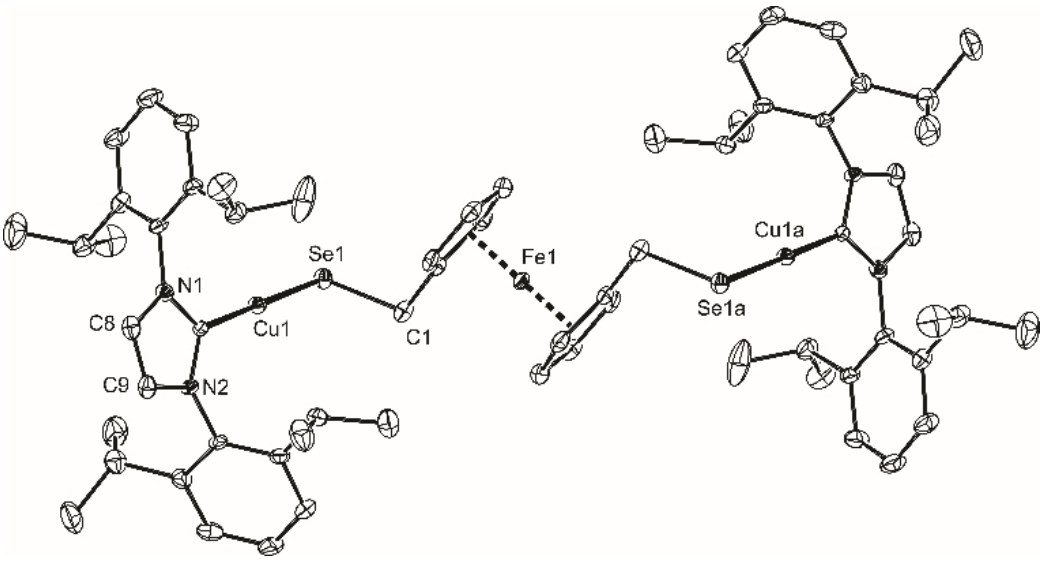

Figure 4.4. Thermal ellipsoid plot (40% probability level) of **21** with the selected atom numbering scheme. Hydrogen atoms and solvent molecules are omitted for clarity. Selected bond distances (Å) and angles (º): Se1-Cu1 2.248(1), Cu1-C7 1.900(5), C1-Se1 1.991(6), C1-Se1-Cu1 101.8(2), Se1-Cu1-C7 179.1(1), C2-C1-Se1 113.7(4).

Table 4.1. Crystallographic data and parameters for compounds **18**, **19**, **20**, **21** and **24**.[a]

	18	**19**	**20**	**21**	**24**
formula	$C_{66}H_{88}Cu_2N_4Se_2 \cdot C_7H_8$	$C_{66}H_{88}Cu_2N_4Se_2 \cdot C_6H_6$	$C_{66}H_{84}Cu_2FeN_4S_2 \cdot CH_2Cl_2$	$C_{66}H_{84}Cu_2FeN_4Se_2 \cdot C_5H_{12}$	$C_{118}H_{154}Cu_4N_8Se_4 \cdot 3THF$
formula weight	1220.73	1300.51	1265.34	1346.36	2470.79
crystal system	monoclinic	monoclinic	monoclinic	monoclinic	triclinic
space group	$P\,2_1/c$	$P\,2_1/c$	$P\,2_1/c$	$P\,2_1/c$	$P\bar{1}$
a [Å]	12.333(3)	12.295(6)	20.836(8)	20.825(9)	13.006(4)
b [Å]	18.948(4)	19.047(9)	9.596(4)	9.791(4)	14.080(5)
c [Å]	15.858(3)	15.877(7)	16.941(5)	17.063(5)	19.173(7)
α [°]	90	90	90	90	71.160(15)
β [°]	112.28(3)	111.530(12)	101.905(8)	102.294(8)	89.187(15)
γ [°]	90	90	90	90	65.456(10)
V [Å^3]	3429.1(14)	3459(3)	3314(2)	3399(2)	2993.2(17)
Z	2	2	2	2	1
ρ_{cal} [g cm^{-3}]	1.182	1.249	1.268	1.315	1.692
M ($Mo_{K\alpha}$) [mm^{-1}]	0.723	1.708	1.036	1.943	1.972
F(000)	1304	1360	1332	1404	1290
temperature [K]	110	110	110	110	110
θ_{min}, θ_{max} [°]	2.80, 30.37	2.54, 23.64	2.74, 29.00	2.71, 30.09	2.35, 31.61
total reflns	65891	53528	47566	75915	71877
unique reflns	10494	5315	5323	5473	20161
R(int)	0.0440	0.0306	0.0653	0.0600	0.0240
$R1$	0.0538	0.0509	0.0680	0.0549	0.0459
w$R2$ [$I \geq 2\sigma(I)$]	0.1546	0.1433	0.2016	0.1589	0.1284
$R1$ (all data)	0.0882	0.0973	0.0818	0.0669	0.0843
w$R2$ (all data)	0.1883	0.1916	0.2128	0.1728	0.1610
GOF	1.093	1.076	1.142	1.366	1.121

[a] $R_1 = \sum(|F_o| - |F_c|)/\sum F_o$, $wR_2 = [\sum(w(F_o^2 - F_c^2)^2)/\sum(wF_o^2)]^{1/2}$, GOF $= [\sum(w(F_o^2 - F_c^2)^2)/(N_{observns} - N_{params})]^{1/2}$

The ^{1}H NMR spectra for **20** and **21** display the expected peaks for the equivalent carbene ligands, one singlet assigned to CH_2 groups (**20** 2.94; **21** 2.86 ppm) and two singlets assigned to the CH groups of the Cp ring (**20** 3.57, 3.40; **21** 3.62, 3.43 ppm). In the $^{13}C\{^1H\}$ NMR spectra of **20** and **21** the peaks of CH_2 groups are observed at 23.7 and 23.8 ppm, respectively. Three peaks corresponding to the central ferrocene are detected in $^{13}C\{^1H\}$ spectra, at 93.2 (C_{ipso}), 68.3 and 67.5 for **20** and at 92.8 (C_{ipso}), 68.2 and 67.6 ppm for **21**.

The facile assembly of these dicopper complexes suggested an expansion of the number of metal sites around the C_6 tether via reagents with increasing number of $ESiMe_3$. Although single crystals of 1,3,5-[{(IPr)CuECH_2}$_2$(C_6Me_3)] (E = S, **22**, E = Se, **23**) proved elusive, formation of these tri-chalcogenolate complexes could be confirmed via spectral and elemental analysis. The ^{1}H NMR ($CDCl_3$, 25 °C) spectra of **18**, **19**, **22** and **23** show the expected carbene peaks and two singlets assigned to CH_2 and CH_3 of the central spacer. The chemical shift values of the methylene groups are shifted significantly upfield (**18** 2.61, **19** 2.63, **22** 2.94 and **23** 2.98 ppm) compared to the corresponding polysilyl–chalcogen precursors (3.72, 3.75, 3.72, 3.72 ppm, respectively). The chemical shift values of methyl groups bonded to the central arene ring (**18** 1.91, **19** 1.91, **22** 1.83, **23** 1.80 ppm) slightly differ versus the corresponding precursors (2.32, 2.32, 2.46, 2.42 ppm, respectively). The ^{13}C{^{1}H} NMR spectra of **18**, **19**, **22** and **23**, in addition to the expected peaks of the carbine ligand, reveal two extra signals in the aliphatic region for these CH_2 and CH_3 groups (**18** 23.5, 16.0; **19** 10.6, 16.0; **22** 23.1, 15.4 and **23** 10.2, 15.3 ppm, respectively) together with two extra signals in the aromatic region (**18** 138.8, 131.0; **19** 138.3, 130.9; **22** 138.2, 131.3 and **23** 137.8, 1309 ppm) from the corresponding spacers. ^{77}Se{^{1}H} NMR spectra of **19** and **23** display sharp signals at -101.9 and -108.8 ppm respectively.

The tetrasubstituted 1,2,4,5-($Me_3SiSeCH_2$)$_4$(C_6H_2) can be similarly used for the preparation of 1,2,4,5-[{(IPr)CuSeCH_2}$_4$(C_6H_2)] **24**. Single crystal X-ray analysis illustrates that compound **24** forms two lateral four-membered butterfly shaped Cu_2Se_2 rings on a central $C_6H_2(CH_2Se)_4$ spacer, involving a crystallographic inversion centre (Figure 4.5). In this structure, which crystallizes in the triclinic space group $P\bar{1}$ with one molecule per unit cell, all copper atoms adopt distorted trigonal planar coordination environments and all are coordinated by two (bridging) selenolates and the carbon atom of the NHC ligand. As shown in Figure 4.5 the two adjacent carbene ligands on Cu_2Se_2 rings rotate by an angle of 66.80° with respect to one each other. In **24** the Cu···Cu distance (2.6705(8) Å) is significantly smaller than the sum of the van der Waals radii (2.80Å) while the Se···Se length (3.792(1) Å) is far too long to be assigned any direct intramolecular interaction. In the reported structural analyses of dinuclear copper(I)-chalcogenolates only

a few cases are known with a central four membered (Cu_2E_2) unit.[18] Recently Fuhr and co-workers reported a series of binuclear copper(I) thiolate and selenolate complexes $[Cu_2(ER)_2(dpppt)_2]$ (E = S, Se; R = alkyl or aryl group, dpppt = 1,5-bis(diphenylposphino)pentane) through the reaction of solution of copper(I) acetate, and phosphine ligand (dpppt) in toluene with the addition of different monodentate chalcogenolate ($RESiMe_3$) sources.[19] The dinuclear Cu_2E_2 motif with a diamond-like structure is very well-known in biological systems and revealed the first metal-metal bond observed in nature.[7d, 20] The short Cu···Cu distance enables the unit to act as a very efficient electron transfer agent, cycling between the oxidation states Cu(1.5)Cu(1.5) and Cu(I)Cu(I). It has motivated considerable efforts to understand the structure–function relationship in this highly unusual bimetallic center.[7d, 20]

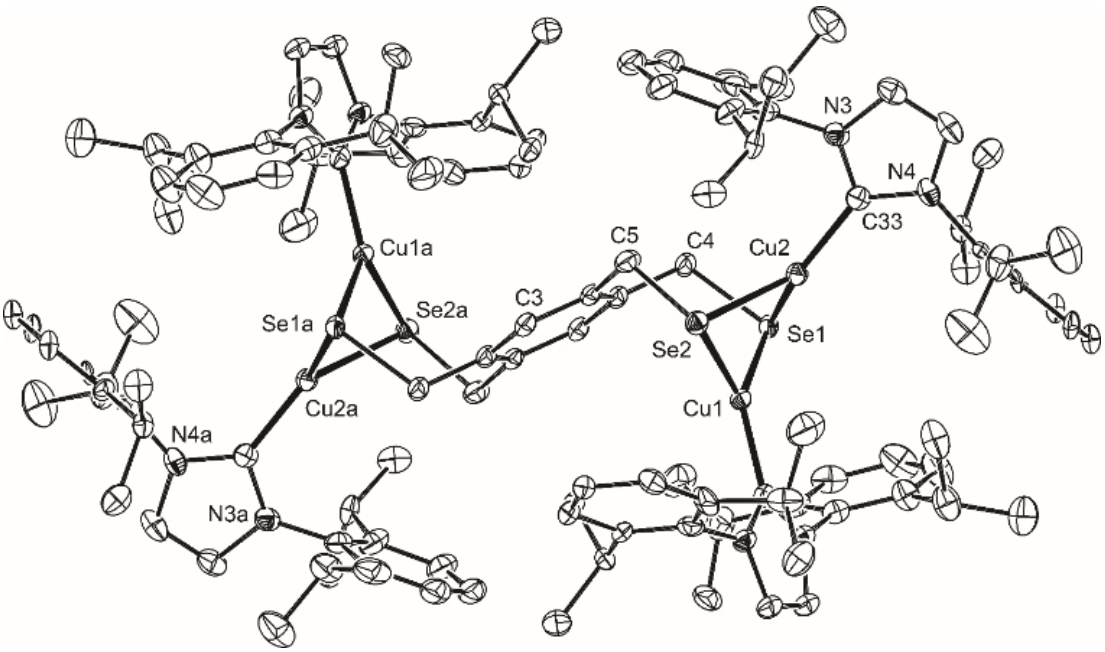

Figure 4.5. Thermal ellipsoid plot (40% probability level) of **24** with the selected atom numbering scheme. Hydrogen atoms, solvent molecules and disorders are omitted for clarity. Selected bond distances (Å) and angles (º): Cu1-Cu2 2.6705(8), Cu1-Se1 2.399(1), Cu1 Se2 2.3793(9), Cu2-Se1 2.4791(9), Cu2-Se2 2.5282(9), Cu2-C33 1.936(3), Cu1-C6 1.928(2), Cu1-Se1-Cu2 66.36(2), Cu1-Se2-Cu2 65.85(2), Se1-Cu1-Se2 105.04(2), Se2-Cu2-Se1 98.44(2), Se1-C4-C1 115.5(2), Se2-C5-C2 114.1(2), C4-Se1-Cu1 103.96(9), C4-Se1-Cu2 90.97(9), C5-Se2-Cu1 106.68(8), C5-Se2-Cu2 92.79(8), C6-Cu1-Se1 126.8(1), C6-Cu1-Se2 127.4(1), C33-Cu2-Se1 130.39(9), C33-Cu2-Se2 128.83(9).

The presence of two redox-active metal centers (Cu and Fe) in **20** and **21** make these complexes ideal candidates for investigating their redox properties. The reversibility and relative oxidation potentials of the redox processes in these compounds were investigated by cyclic voltammetry (CV) of 1mM solutions of each complex in dichloromethane, containing 0.1 M $[(^{n}Bu)_4N]PF_6$ as the supporting electrolyte. The cyclic voltammograms of **20** and **21** show two irreversible oxidations (E_{ox}: **20** 0.30, 0.50V; **21** 0.20, 0.42V) and one chemically reversible oxidation processes (**20** E_{ox}: 0.70, ΔE: 0.13; **21** E_{ox}: 0.73, ΔE: 0.17 V) at scan rate of 100 mV s^{-1} (Figure 4.6).

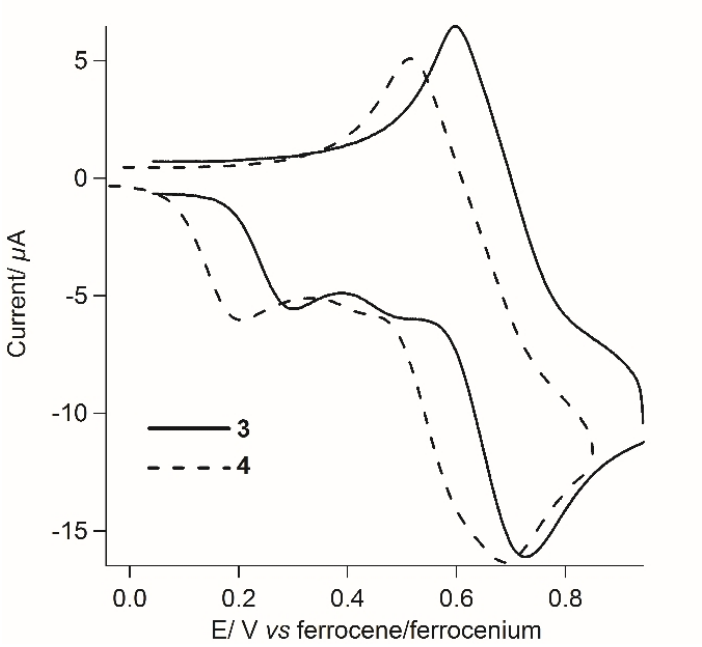

Figure 4.6. Cyclic voltammograms (CVs) of 1 mM solutions of **20** (solid) and **21** (dashed), in dichloromethane with 0.1m $TBAPF_6$ as supporting electrolyte (Recorded at 100 mVs^{-1} scan rate and are referenced to ferrocene at 0.475 V *vs* SCE).

The two small irreversible oxidation peaks might be correspondence to copper(I/II) oxidation. Lowering the intensity of these two irreversible oxidation peaks, in the second and third cycles, indicates the decomposition of **20** and **21** through the oxidation process (Figures 4.7 and 4.8). The dominant reversible peak is assigned to the reversible oxidation of Fe(II/III) in the ferrocene containing moieties that are formed after decomposition of these complexes.

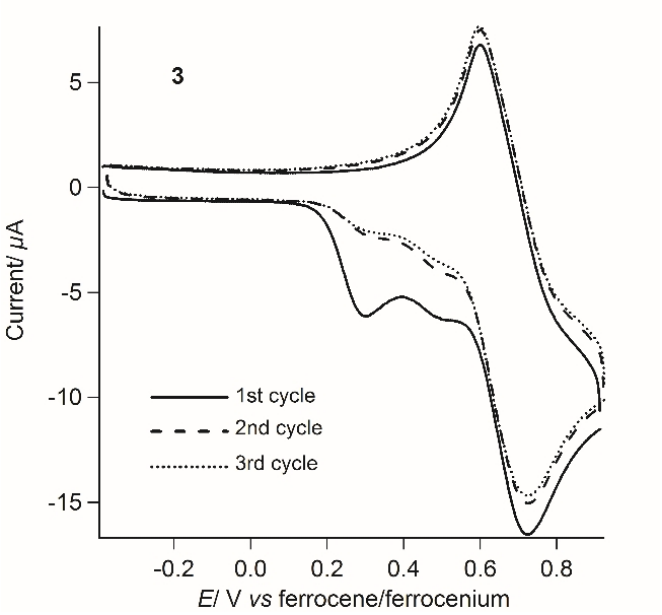

Figure 4.7. Multicyclic voltammogram (CV) of 1 mm solutions of **20**, in dichloromethane with 0.1m $TBAPF_6$ as supporting electrolyte (Recorded at 100 mVs^{-1} scan rate and are referenced to ferrocene at 0.475 V *vs* SCE).

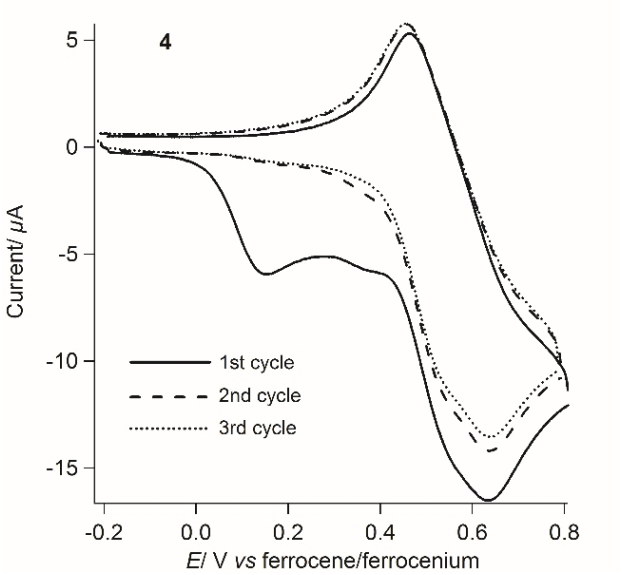

Figure 4.8. Multicyclic voltammogram (CV) of 1 mm solutions of **21**, in dichloromethane with 0.1m $TBAPF_6$ as supporting electrolyte (Recorded at 100 mVs^{-1} scan rate and are referenced to ferrocene at 0.475 V *vs* SCE).

4.3 Experimental Section

All syntheses were carried out under an atmosphere of high-purity dried nitrogen using standard double-manifold Schlenk line techniques and nitrogen-filled glove boxes unless otherwise stated. Solvents were dried and collected using an MBraun MB-SP Series solvent purification system with tandem activated alumina (tetrahydrofuran) and an activated alumina/copper redox catalyst (pentane). Chlorinated solvents (dichloromethane, chloroform, chloroform-d, dichloromethane-d2) were dried and distilled over P_2O_5.

Other chemicals were used as received from commercial sources (Alfa Aesar and Aldrich). 1,4-$(Me_3SiECH_2)_2(C_6Me_4)$,[5] 1,3,5-$(Me_3SiECH_2)_3(C_6Me_3)$ (E = S, Se),[5] 1,2,4,5-$(Me_3SiSeCH_2)_4(C_6H_2)$,[5] 1,1´-fc$(CH_2ESiMe_3)_2$ (E = S, Se)[21] and [(IPr)CuOAc][22] were synthesized according to literature procedures.

NMR spectra were recorded on Varian Mercury 400, Inova 400 and Inova 600 NMR spectrometers. ^1H and $^{13}C\{^1H\}$ chemical shifts are referenced to $SiMe_4$, using solvent peak as a secondary reference; ^{77}Se chemical shifts are referenced to Me_2Se. HSQC (Heteronuclear Single Quantum Correlation) and HMBC (Heteronuclear Multiple Bond Correlation) spectroscopic techniques were used to assign the peaks for $^{13}C\{^1H\}$ NMR spectra.

Elemental analysis was performed by Laboratoire d′Analyze Élementaire de l′Université de Montréal, Montréal, Canada. Samples were dried for twelve hours prior to sending for analysis. Experimentally obtained values of elemental analysis and NMR spectra suggests some residual lattice solvent remained. NMR spectra of the dried samples showed ~1 and 0.75 toluene molecule in the molecular formulas of **18** and **19** respectively.

A Bas 100B\W Electrochemical Analyzer was used for cyclic voltammetry (CV) experiments. A homemade glassy carbon (GC, Tokai GC-20) working-electrode 3 mm in diameter was prepared by polishing over silicon carbide papers (500, 1200, 2400 and 4000) followed by diamond paste (Struers, 1 and 0.25 mm). The GC electrodes were stored in ethanol and polished before each set of experiments with the 0.25 mm diamond paste (Struers), rinsed with dry ethanol (Commercial Alcohols) and sonicated in dry ethanol for

5 minutes. Platinum wires served as the reference and counter electrodes. Electrochemical experiments were carried out in dry dichloromethane solutions of the analyte (~1 mM), containing 0.1 M tetrabutylammonium hexafluorophosphate ($TBAPF_6$) as the supporting electrolyte. Potentials are referenced internally to ferrocene (~1 mM, 0.475 V *vs.* SCE)[23] added at the end of the experiments.

Single-crystal X-ray diffraction measurements were completed on Bruker APEX-II CCD diffractometer equipped with graphite-monochromated Mo Kα (λ = 0.71073 Å) radiation. Single crystals of the complexes were carefully selected, immersed in paraffin oil and mounted on MiteGen micromounts. The structures were solved using direct methods and refined by the full-matrix least-squares procedure of SHELXTL.[24] All non-hydrogen atoms, with the exception of disordered carbon centers, were refined with anisotropic thermal parameters.

4.3.1 Synthesis of 1,4-[{(IPr)CuSCH$_2$}$_2$(C$_6$Me$_4$)] **18**

To a solution of 67 mg [(IPr)CuOAc] (0.13 mmol) in 5 mL toluene was added to 24 mg 1,4-(Me_3SiSCH_2)$_2$(C_6Me_4) (0.065 mmol) in 5mL toluene at -40 °C. The mixture was stirred for 30 minutes and warmed up to the room temperature resulting a clear colourless solution. This solution was layered with 20-25 mL of pentane. Colourless block crystals suitable for X-ray diffraction were obtained after 4-5 days. The crystals were washed with 3×10 ml of pentane and dried under dynamic vacuum for further analyses (82 % yield); m.p. above 260 °C.

- ^{1}H NMR ($CDCl_3$, 599.36 MHz, 25 °C): δ 7.43 (t, *J* = 7.81 Hz, 4H, *para*-C*H*), 7.26 (d, *J* = 7.81 Hz, 8H, *meta*-C*H*), 7.08 (s, 4H, NC*H*), 3.11 (s, 4H, CH_2), 2.59 (sept., *J* = 6.64 Hz, 8H, C*H*(CH_3)$_2$), 1.88 (s, 12H, Ar-CH_3) 1.30 (d, *J* = 6.64 Hz, 24H, CH(CH_3)$_2$), 1.20 (d, *J* = 6.64 Hz, 24H, CH(CH_3)$_2$), ppm.
- ^{13}C{^{1}H} NMR ($CDCl_3$, 100.53 MHz, 25 °C): 182.4 (N*C*Cu), 145.6 (*ortho-C*), 138.8 (*central ring*), 134.7 (*ipso-C*), 131.0 (*central ring*), 130.3 (*para-C*), 124.1 (*meta-C*),

122.6 (N*C*H), 28.8 (*C*H(CH$_3$)$_2$), 24.7 (CH(*C*H$_3$)$_2$), 23.9 (CH(*C*H$_3$)$_2$), 23.5 (*C*H$_2$) 16.0 (Ar-*C*H$_3$) ppm.

- Anal. Calcd for $C_{66}H_{90}Cu_2N_4S_2 \cdot 0.75C_7H_8$: C, 71.33; H, 8.06; N, 4.67; S, 5.34. Found: C, 72.06; H, 8.12; N, 4.47; S, 5.58.

4.3.2 Synthesis of 1,4-[{(IPr)CuSeCH$_2$}$_2$(C$_6$Me$_4$)] **19**

To a solution of 160 mg [(IPr)CuOAc] (0.312 mmol) in 5 mL toluene was reacted to 72 mg 1,4-(Me$_3$SiSeCH$_2$)$_2$(C$_6$Me$_4$) (0.156 mmol) in 5mL toluene as described for the preparation of **18**. The resulting clear pale yellow solution was layered with 20-25 mL of pentane. Colourless crystals were obtained after 4-5 days. The crystals were washed with 3×10 ml of pentane and dried under dynamic vacuum for further analyses. Repeating the reaction in benzene at room temperature followed by pentane diffusion in the gas phase to the mother liquor yielded colourless plate crystals suitable for X-ray diffraction (60 % yield); m.p. decomposed at ~240-245 °C.

- ^{1}H NMR (CDCl$_3$, 599.40 MHz, 25 °C): δ 7.45 (t, J = 6.63 Hz, 4H, *para*-C*H*), 7.28 (d, J = 6.63 Hz, 8H, *meta*-C*H*), 7.11 (s, 4H, NC*H*), 3.05 (s, 4H, C*H*$_2$), 2.63 (sept., J = 6.45 Hz, 8H, C*H*(CH$_3$)$_2$), 1.91 (s, 12H, Ar-C*H*$_3$) 1.34 (d, J = 6.45 Hz, 24H, CH(C*H*$_3$)$_2$), 1.22 (d, J = 6.45 Hz, 24H, CH(C*H*$_3$)$_2$) ppm.
- ^{13}C{^{1}H} NMR (CDCl$_3$, 100.61 MHz, 25 °C): 182.6 (NCCu), 145.6 (*ortho-C*), 138.3 (*central ring*), 134.6 (*ipso-C*), 130.9 (*central ring*), 130.3 (*para-C*), 124.0 (*meta-C*), 122.6 (N*C*H), 28.7 (*C*H(CH$_3$)$_2$), 24.7 (CH(*C*H$_3$)$_2$), 23.9 (CH(*C*H$_3$)$_2$), 15.9 (Ar-*C*H$_3$), 10.6 (CH$_2$) ppm.
- ^{77}Se{^{1}H} NMR (CDCl$_3$, 76.24 MHz, 25 °C) -101.9 ppm.
- Anal. Calcd for $C_{66}H_{90}Cu_2N_4Se \cdot C_7H_8$: C, 66.59; H, 7.50; N, 4.26. Found: C, 66.87; H, 7.43; N, 4.08.

4.3.3 Synthesis of 1,1´-[fc($CH_2SCuIPr)_2$] **20**

To a solution of 124 mg of [(IPr)CuOAc] (0.242 mmol) in 5 mL chloroform was mixed with 51 mg 1,1´-fc($CH_2SSiMe_3)_2$ (0.121 mmol) in 5mL chloroform at -40 °C. The mixture was stirred for 30 minutes and warmed to room temperature resulting in a clear, pale orange coloured solution; this was layered with 30-35 mL of pentane. Yellow block crystals suitable for X-ray diffraction were obtained after two days. The crystals were washed with 2×10 ml of diethyl ether and 2×10 ml of pentane and dried under dynamic vacuum for further analyses (80 % yield); m.p. 211-214 °C.

- ^{1}H NMR ($CDCl_3$, 400.08 MHz, 25 °C): δ 7.50 (t, J = 7.63 Hz, 4H, *para*-C*H*), 7.30 (d, J = 7.63 Hz, 8H, *meta*-C*H*), 7.08 (s, 4H, NC*H*), 3.57 (s, 4H, Cp-*H*), 3.40 (s, 4H, Cp-*H*) 2.94 (s, 4H, CH_2), 2.58 (sept., J = 7.04 Hz, 8H, C*H*($CH_3)_2$), 1.32 (d, J = 7.04 Hz, 24H, CH(C$H_3)_2$), 1.22 (d, J = 7.04 Hz, 24H, CH(C$H_3)_2$) ppm.
- ^{13}C{^{1}H} NMR ($CDCl_3$, 150.73 MHz, 25 °C): 182.1 (N*C*Cu), 145.7 (*ortho*-*C*), 134.7 (*ipso*-*C*), 130.4 (*para*-*C*), 124.1 (*meta*-*C*), 122.7 (N*C*H), 93.2 (*ipso*-C_5), 68.3 (Cp), 67.5 (Cp), 28.8 (*C*H($CH_3)_2$), 24.9 (CH(*C*$H_3)_2$), 23.9 (CH(*C*$H_3)_2$), 23.7 (*C*H_2) ppm.
- Anal. Calcd for $C_{66}H_{84}Cu_2FeN_4S_2$: C, 67.15; H, 7.17; N, 4.75; S, 5.43. Found: C, 66.34; H, 7.23; N, 4.69; S, 5.22.

4.3.4 Synthesis of 1,1´-[fc($CH_2SeCuIPr)_2$] **21**

92 mg of [(IPr)CuOAc] (0.18 mmol) was reacted with 46.5 mg 1,1´-fc($CH_2SeSiMe_3)_2$ (0.090 mmol) as described for the preparation of **20**. The resulting clear orange solution was layered with 30-35 mL of pentane. Orange block crystals suitable for X-ray diffraction were obtained after two days. The crystals were washed with 2×10 ml of diethyl ether and 2×10 ml of pentane and dried under dynamic vacuum for further analyses. (75 % yield); m.p. 186-189 °C.

- ^{1}H NMR ($CDCl_3$, 599.36 MHz, 25 °C): δ 7.51 (t, J = 7.04 Hz, 4H, *para*-C*H*), 7.32 (d, J = 7.63 Hz, 8H, *meta*-C*H*), 7.10 (s, 4H, NC*H*), 3.62 (s, 4H, Cp-*H*), 3.43 (s, 4H, Cp-*H*) 2.86 (s, 4H, CH_2), 2.60 (sept., J = 7.04 Hz, 8H, C*H*($CH_3)_2$), 1.32 (d, J = 7.04 Hz, 24H, CH(C$H_3)_2$), 1.22 (d, J = 7.04 Hz, 24H, CH(C$H_3)_2$) ppm.

- ü $^{13}C\{^{1}H\}$ NMR ($CDCl_3$, 100.53 MHz, 25 °C): 145.6 (*ortho-C*), 134.5 (*ipso-C*), 130.4 (*para-C*), 124.1 (*meta-C*), 122.8 (N*C*H), 92.8 (*ipso-*C_5), 68.2 (Cp), 67.6 (Cp), 28.7 ($CH(CH_3)_2$), 24.9 ($CH(CH_3)_2$), 23.8 ($CH(CH_3)_2$), 9.4 (CH_2) ppm.
- ü $^{77}Se\{^{1}H\}$ NMR ($CDCl_3$, 76.24 MHz, 25 °C) -12.0 ppm.
- ü Anal. Calcd for $C_{66}H_{90}Cu_2N_4Se$: C, 62.21; H, 6.64; N, 4.40. Found: C, 61.43; H, 6.88; N, 4.30.

4.3.5 Synthesis of 1,3,5-[{(IPr)CuSCH$_2$}$_3$(C$_6$Me$_3$)] **22**

To a solution of 129 mg of [(IPr)CuOAc] (0.252 mmol) in 5 mL chloroform was added to 40 mg 1,3,5-($Me_3SiSeCH_2$)$_3$(C_6Me_3) (0.084 mmol) in 5mL chloroform at -40 °C. The mixture was stirred and warmed to room temperature, resulting in a colourless solution. The solvent and volatile (OAc)$SiMe_3$ were removed under vacuum. The off-white residue was washed with 2×10 ml of diethyl ether and 2×10 ml pentane followed by drying under vacuum (70 % yield); m.p. 221-224 °C.

- ü ^{1}H NMR ($CDCl_3$, 599.36 MHz, 25 °C): δ 7.42 (t, J = 7.63 Hz, 6H, *para*-C*H*), 7.26 (d, J = 7.63 Hz, 12H, *meta*-C*H*), 7.08 (s, 6H, NC*H*), 2.98 (s, 6H, CH_2), 2.60 (sept., J = 6.45 Hz, 12H, C*H*(CH_3)$_2$), 1.83 (s, 9H, Ar-CH_3) 1.32 (d, J = 6.45 Hz, 36H, CH(CH_3)$_2$), 1.20 (d, J = 6.45 Hz, 36H, CH(CH_3)$_2$), ppm.
- ü $^{13}C\{^{1}H\}$ NMR ($CDCl_3$, 150.73 MHz, 25 °C): 182.6 (N*C*Cu), 145.6 (*ortho-C*), 138.2 (*central ring*), 134.7 (*ipso-C*), 131.3 (*central ring*), 130.4 (*para-C*), 124.0 (*meta-C*), 122.5 (N*C*H), 28.7 (*C*H(CH_3)$_2$), 24.8 (CH(*C*H_3)$_2$), 23.9 (CH(*C*H_3)$_2$), 23.1 (Ar*C*H_2), 15.4 (Ar*C*H_3) ppm.

4.3.6 Synthesis of 1,3,5-[{(IPr)CuSeCH$_2$}$_3$(C$_6$Me$_3$)] **23**

To a solution of 92 mg of [(IPr)CuOAc] (0.18 mmol) in 5 mL chloroform was reacted to 37 mg 1,3,5-($Me_3SiSeCH_2$)$_3$(C_6Me_3) (0.060 mmol) in 5mL chloroform as described for the preparation of **22**, resulting in a pale yellow solution. The solvent and volatile (OAc)$SiMe_3$ were removed under vacuum. The pale yellow residue was washed with 2×10

ml of diethyl ether and 2×10 ml pentane followed by drying under vacuum (63.9 yield); m.p. 212-214 °C.

- ü ^{1}H NMR ($CDCl_3$, 599.36 MHz, 25 °C): δ 7.43 (t, J = 7.63 Hz, 6H, *para*-C*H*), 7.26 (d, J = 7.63 Hz, 12H, *meta*-C*H*), 7.09 (s, 6H, NC*H*), 2.94 (s, 6H, CH_2), 2.61 (sept., J = 6.45 Hz, 12H, C*H*(CH_3)$_2$), 1.80 (s, 9H, Ar-CH_3) 1.34 (d, J = 6.45 Hz, 36H, CH(CH_3)$_2$), 1.22 (d, J = 6.45 Hz, 36H, CH(CH_3)$_2$), ppm.
- ü ^{13}C{^{1}H} NMR ($CDCl_3$, 100.61 MHz, 25 °C): 182.7 (N*C*Cu), 145.5 (*ortho-C*), 137.8 (*central ring*), 134.5 (*ipso-C*), 130.9 (*central ring*), 130.3 (*para-C*), 124.0 (*meta-C*), 122.4 (N*C*H), 28.6 (*C*H(CH_3)$_2$), 24.7 (CH(*C*H_3)$_2$), 23.8 (CH(*C*H_3)$_2$), 15.3 (*central ring*-Ar*C*H_3), 10.2 (*C*H_2); ^{77}Se{^{1}H} NMR ($CDCl_3$, 76.24 MHz, 25 °C) -108.8 ppm.

4.3.7 Synthesis of 1,2,4,5-[{(IPr)CuSeCH$_2$}$_4$(C_6H_2)] **24**

To a solution of 145 mg [(IPr)CuOAc] (0.283 mmol) in 5 mL tetrahydrofuran was reacted to 52 mg 1,2,4,5-($Me_3SiSeCH_2$)$_4$(C_6H_2) (0.071 mmol) in 5mL tetrahydrofuran at -40 °C, resulting in a pale yellow solution. The reaction solution was warmed up to -25 °C followed by layering with 40 ml pentane. Yellow block crystals suitable for X-ray diffraction were obtained after ten days.

Repeating the same reaction in $CDCl_3$ at -40 °C and maintaining the solution at -25 °C for 12 hours showed the concomitant formation of 1,2,4,5-[{(IPr)CuSeCH$_2$}$_4$(C_6H_2)] **24** and the side product (AcO)$SiMe_3$ via ^{1}H NMR spectroscopy.

- ü ^{1}H NMR ($CDCl_3$, 599.36 MHz, 25 °C): δ 7.54 (t, J = 7.6 Hz, 8H, *para*-C*H*), 7.34 (d, J = 7.6 Hz, 48H, *meta*-C*H*), 7.19 (s, 8H, NC*H*), 2.57 (sept., J = 7.0 Hz, 16H, C*H*(CH_3)$_2$), 1.72 (s, 12H, Ar-CH_2) 1.30 (d, J = 7.0 Hz, 48H, CH(CH_3)$_2$), 1.24 (d, J = 7.0 Hz, 48H, CH(CH_3)$_2$), ppm.

4.4 Conclusion

The results show that the polydentate trimethylsilyl chalcogenolate reagents provide a convenient route to prepare poly (NHC)carbene-copper-chalcogenolate complexes. The structure of **24** reveals that the pair of adjacent -$CH_2SeSiMe_3$ groups on 1,2,4,5-$(Me_3SiSCH_2)_4(C_6H_2)$ precursor induces interesting butterfly shaped bimetallic Cu_2Se_2 structures on two sides of the C_6 ring, while complexes 1,4-[{(IPr)$CuECH_2$}$_2$(C_6Me_4)] (E = S **18**, E = Se **19**) and 1,1´-[fc($CH_2ECuIPr)_2$] (E = S **20**, E = Se **21**) exhibit near linear geometry on the Cu centers. The CVs of **20** and **21** show what appears to be two chemically irreversible oxidation processes and one single reversible oxidation peak. These might be due to the irreversible oxidation of Cu(I) centres and the reversible oxidation of ferrocene moiety incorporated on these complexes and reveal the electrochemical instability of these two copper-chalcogenolate complexes.

4.5 References

[1] (a) Taher, D.; Awwadi, F. F.; Pfaff, U.; Speck, J. M.; Rüffer, T.; Lang, H., *J. Organomet. Chem.* **2013,** *736*, 9-18; (b) Capperucci, A.; Degl'Innocenti, A.; Tiberi, C., *Synlett* **2011**, 2248-2252; (c) Taher, D.; Corrigan, J. F., *Organometallics* **2011,** *30*, 5943-5952.

[2] MacDonald, D. G.; Corrigan, J. F., *Phil. Trans. R. Soc. A* **2010,** *368*, 1455-1472.

[3] Fuhr, O.; Dehnen, S.; Fenske, D., *Chem. Soc. Rev.* **2013,** *42*, 1871-1906.

[4] (a) Postigo, L.; Maestre, M. a. d. C.; Mosquera, M. E. G.; Cuenca, T.; Jiménez, G., *Organometallics* **2013,** *32*, 2618-2624; (b) Kluge, O.; Gerber, S.; Krautscheid, H., *Z. Anorg. Allg. Chem.* **2011,** *637*, 1909-1921; (c) Thomson, R.; Graves, C.; Scott, B.; Kiplinger, J., *J. Chem. Crystallogr.* **2011,** *41*, 1241-1244.

[5] Fard, M. A.; Khalili Najafabadi, B.; Hesari, M.; Workentin, M. S.; Corrigan, J. F., *Chem. -Eur. J.* **2014,** *20*, 7037-7047.

[6] Azizpoor Fard, M.; Willans, M. J.; Khalili Najafabadi, B.; Levchenko, T. I.; Corrigan, J. F., *Dalton Trans.* **2015,** *44*, 8267-8277.

[7] (a) Zhang, S.; Warren, T. H., *Chem. Sci.* **2013,** *4*, 1786-1792; (b) Solomon, E. I.; Randall, D. W.; Glaser, T., *Coord. Chem. Rev.* **2000,** *200–202*, 595-632; (c) Henkel, G.; Krebs, B., *Chem. Rev.* **2004,** *104*, 801-824; (d) Gennari, M.; Pécaut, J.; DeBeer, S.; Neese, F.; Collomb, M.-N.; Duboc, C., *Angew. Chem., Int. Ed.* **2011,** *50*, 5662-5666.

[8] Delp, S. A.; Munro-Leighton, C.; Goj, L. A.; Ramírez, M. A.; Gunnoe, T. B.; Petersen, J. L.; Boyle, P. D., *Inorg. Chem.* **2007,** *46*, 2365-2367.

[9] Humenny, W. J.; Mitzinger, S.; Khadka, C. B.; Najafabadi, B. K.; Vieira, I.; Corrigan, J. F., *Dalton Trans.* **2012,** *41*, 4413-4422.

[10] (a) Nolan, S. P., Ed. N-Heterocyclic Carbenes in Synthesis; Wiley-VCH: Weinheim, Germany. **2006**; (b) Kuhl, O., *Chem. Soc. Rev.* **2007,** *36*, 592-607; (c) Bourissou, D.; Guerret, O.; Gabbaï, F. P.; Bertrand, G., *Chem. Rev.* **1999,** *100*, 39-92; (d) Crabtree, R. H., *J. Organomet. Chem.* **2005,** *690*, 5451-5457.

[11] Tonner, R.; Heydenrych, G.; Frenking, G., *Chem. Asian J.* **2007,** *2*, 1555-1567.

[12] (a) Crudden, C. M.; Allen, D. P., *Coord. Chem. Rev.* **2004,** *248*, 2247-2273; (b) Jacobsen, H.; Correa, A.; Poater, A.; Costabile, C.; Cavallo, L., *Coord. Chem. Rev.* **2009,** *253*, 687-703.

[13] (a) Hahn, F. E.; Jahnke, M. C., *Angew. Chem., Int. Ed.* **2008,** *47*, 3122-3172; (b) Lin, J. C. Y.; Huang, R. T. W.; Lee, C. S.; Bhattacharyya, A.; Hwang, W. S.; Lin, I. J. B., *Chem. Rev.* **2009,** *109*, 3561-3598; (c) Garrison, J. C.; Youngs, W. J., *Chem. Rev.* **2005,** *105*, 3978-4008.

[14] (a) Kascatan-Nebioglu, A.; Panzner, M. J.; Tessier, C. A.; Cannon, C. L.; Youngs, W. J., *Coord. Chem. Rev.* **2007,** *251*, 884-895; (b) Hindi, K. M.; Siciliano, T. J.; Durmus, S.; Panzner, M. J.; Medvetz, D. A.; Reddy, D. V.; Hogue, L. A.; Hovis, C. E.; Hilliard, J. K.; Mallet, R. J.; Tessier, C. A.; Cannon, C. L.; Youngs, W. J., *J. Med. Chem.* **2008,** *51*, 1577-1583.

[15] Lee, C. K.; Vasam, C. S.; Huang, T. W.; Wang, H. M. J.; Yang, R. Y.; Lee, C. S.; Lin, I. J. B., *Organometallics* **2006,** *25*, 3768-3775.

[16] (a) Marion, N.; Díez-González, S.; Nolan, S. P., *Angew. Chem., Int. Ed.* **2007,** *46*, 2988-3000; (b) Fraser, P. K.; Woodward, S., *Tetrahedron Lett.* **2001,** *42*, 2747-2749; (c) Diez-Gonzalez, S.; Nolan, S. P., *Synlett* **2007**, 2158-2167.

[17] (a) Ferrara, S. J.; Mague, J. T.; Donahue, J. P., *Inorg. Chem.* **2012,** *51*, 6567-6576; (b) Melzer, M. M.; Li, E.; Warren, T. H., *Chem. Commun.* **2009**, 5847-5849.

[18] (a) Raper, E. S.; Creighton, J. R.; Robson, D.; Wilson, J. D.; Clegg, W.; Milne, A., *Inorg. Chim. Acta* **1988,** *143*, 95-100; (b) Constable, E. C.; Raithby, P. R., *J. Chem. Soc., Dalton Trans.* **1987**, 2281-2283; (c) Chadha, R. K.; Kumar, R.; Tuck, D. G., *Can. J. Chem.* **1987,** *65*, 1336-1342.

[19] Hu, B.; Su, C.-Y.; Fenske, D.; Fuhr, O., *Inorg. Chim. Acta* **2014,** *419*, 118-123.

[20] (a) Savelieff, M.; Lu, Y., *J. Biol. Inorg. Chem.* **2010,** *15*, 461-483; (b) Randall, D. W.; Gamelin, D. R.; LaCroix, L. B.; Solomon, E. I., *J. Biol. Inorg. Chem.* **2000,** *5*, 16-29.

[21] Ahmar, S.; Nitschke, C.; Vijayaratnam, N.; MacDonald, D. G.; Fenske, D.; Corrigan, J. F., *New J. Chem.* **2011,** *35*, 2013-2017.

[22] Mankad, N. P.; Gray, T. G.; Laitar, D. S.; Sadighi, J. P., *Organometallics* **2004,** *23*, 1191-1193.

[23] Gunderson, V. L.; Smeigh, A. L.; Kim, C. H.; Co, D. T.; Wasielewski, M. R., *J. Am. Chem. Soc.* **2012,** *134*, 4363-4372.

[24] (a) Sheldrick, G. M., SHELXTL PC Version 6.1 An Integrated System for Solving, Refining, and Displaying Crystal Structures from Diffraction Data, Bruker Analytical X-ray Systems, 2000;; (b) Sheldrick, G. M., *Acta Crystallogr. Sect. A* **2008,** *64*, 112-122.

Chapter 5

Simple but effective: thermally stable Cu–$ESiMe_3$ via NHC ligation

(Mahmood Azizpoor Fard, Florian Weigend and John F. Corrigan, *Chem. Commun.,* **2015**, *51*, 8361—8364)

5.1 Introduction

The chemistry of ligand stabilized copper(I) silyl chalcogenolates [L_nCu-E-$SiMe_3$] (L = trialkyl-, dialkylaryl- or alkyldiarylphosphine; *n* = 2, 3) and related complexes as a soluble source of "cuprachalcogenolate", CuE^-, has resulted in the formation of several interesting ternary metal-copper-chalcogenide clusters when these coordination complexes are reacted with a second metal salt.[1,2] The high reactivity of copper bonded trimethylsilylchalcogen groups has led to a facile formation of mixed metal-copper-chalcogenide framework, through replacement of the chalcogen-silicon bond with a chalcogen-M´ interaction (M´ = In, Ga, Ag, Hg).[1a,2] Larger $–SiR_3$ substituents about the chalcogen can adversely affect these selective E-Si bond cleavage reactions.[3] The approach of using a trimethylsilyl functionality on the chalcogen for a ternary M´ME cluster evolved from the extensive reaction chemistry of $E(SiMe_3)_2$ with Cu(I) which yields both molecular and nanoscopic copper(I) chalcogenide complexes that display rich and diverse structural features due to various coordination modes of both the copper(I) and chalcogen centres.[4] There are now several copper(I)-chalcogenide based heterometallic clusters accessed by utilizing the reactivity of the copper trimethylsilylchalcogenolate and the ultimate ability of the chalcogenide ligands to adopt bridging coordination modes between different metal centres

including $[Cu_6In_8S_{13}Cl_4(PEt_3)_{12}]$,[2b] $[Hg_{15}Cu_{20}S_{25}(PPr_3)_{18}]$[2b] and $[(Et_3PCu)_6(MeGa)_4Ga_4S_{13}]$.[2c]

To date, however, the low melting points and thermal instability of these $[L_nCu\text{-}ESiMe_3]$ have made them relatively difficult to handle and store for longer periods of time with the adverse effect on being able to control their reactivity for ternary cluster formation. In part, this can be attributed to the rather labile nature of the coordinated tertiary phosphines. Using an alternate ancillary ligand such as IPr (IPr = 1,3-bis(2,6-diisopropylphenyl)imidazolin-2-ylidene), we set out to increase the thermal stability of Cu-$ESiMe_3$, at the same time promoting an oriented coordination on copper centre. We also reasoned that the strong bonding of IPr with Cu(I) would enhance the kinetic stability first formed Cu-S-M´ complexes. Here, as the first example, we introduced the N-heterocyclic carbene 1,3-bis(2,6-diisopropylphenyl)imidazolin-2-ylidene (IPr) as the ancillary ligand in the synthesis of copper(I)-trimethylsilylchalcogenolates, $[(IPr)Cu\text{-}ESiMe_3]$ (E = S, **25**; Se, **26**; Te, **27**). We demonstrate the reactivity of the thiolate precursor in the synthesis of a mixed metal chalcogenide complexes (Hg-S-Cu), a rare example of a Cu(I)-Hg(II)-chalcogenide polynuclear complex.

N-heterocyclic carbenes (NHCs) now rival phosphines as ligands in organometallic chemistry and the extensive range of accessible NHC-based complexes continues to grow at a rapid rate.[5] The strong σ-donor and relatively weak π-acceptor properties of NHCs bear similarities to the coordination characteristics of phosphines, although NHCs are generally better electron-donors.[6] This provides thermodynamically stronger metal–ligand bonds, reflected in the typically greater bond dissociation energies and shorter metal–ligand bond lengths when compared to their phosphine counterparts, although notable exceptions to this trend arise when steric constraints interfere with metal–ligand binding.

5.2 Results and Discussion

The NHC 1,3-bis(2,6-diisopropylphenyl)imidazolin-2-ylidene (IPr) has recently been shown to ligate with CuCl and, when treated with a source of PhS^-, to promote terminal

coordination of the arylthiolate in [(IPr)Cu-SPh].[7] When [(IPr)CuOAc] is treated with one equivalent of bis(trimethylsilyl)chalcogenide $E(SiMe_3)_2$ at -70 °C and stored at -25 °C, complexes [(IPr)Cu-$ESiMe_3$] (**25** E = S; **26** E = Se; **27** E = Te) are isolated via the addition of a hydrocarbon counter solvent and isolated in 50-62% yields as off-white solids (Scheme 5.1a). Each can be stored under an inert atmosphere at room temperature. In all cases, only one -$ESiMe_3$ is activated in $E(SiMe_3)_2$ to form **25-27**, with no evidence of any other competitive side reactions. Indeed, monitoring the reactions via ^{1}H NMR spectroscopy indicates the quantitative replacement of ligated OAc^- with Me_3SiE^- and the concomitant formation of $(AcO)SiMe_3$. ^{1}H NMR spectra of isolated samples of [(IPr)Cu-$SSiMe_3$] **25** in $CDCl_3$ show, in addition to a set of resonances assigned to one IPr ligand, a high field resonance at -0.17 ppm from the coordinated -$SSiMe_3$ which satisfactorily integrates as nine hydrogen atoms versus IPr (Figure 5.1). This chemical shift is at slightly higher field compared to those reported for this resonance in tetrahedral [L_3Cu-$SSiMe_3$].[1a] The selenium complex **26** (δ = -0.04 ppm) and the tellurium containing **27** (δ = 0.15 ppm) also display resonances at higher field for the –$SiMe_3$ moieties (Figures 5.2 and 5.3) compared to [L_3Cu-$ESiMe_3$] but the trends in the differences ($\delta\Delta$) on going from S→Se→Te within a series is similar in both cases.

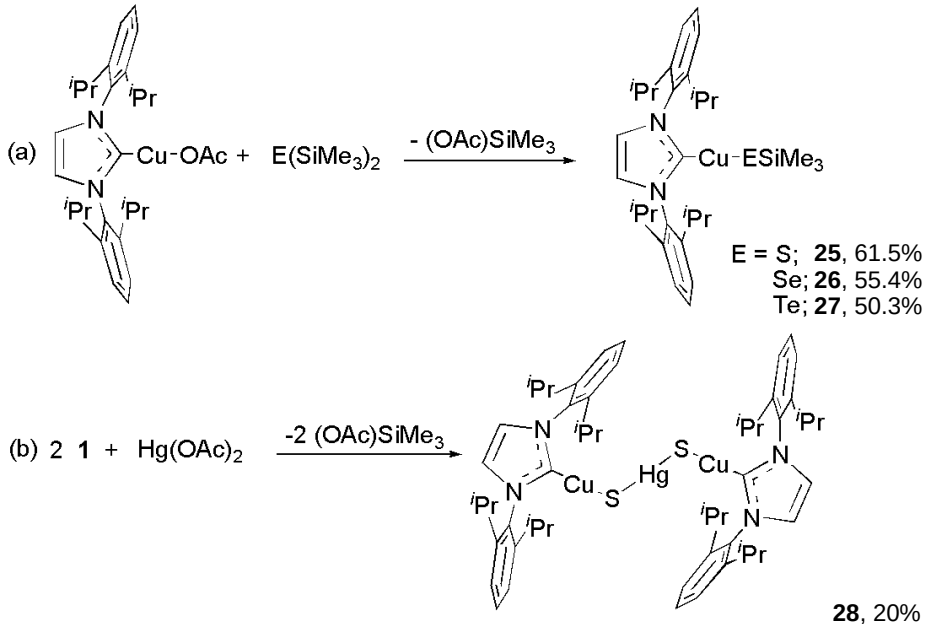

Scheme 5.1. Synthesis of **25-28**

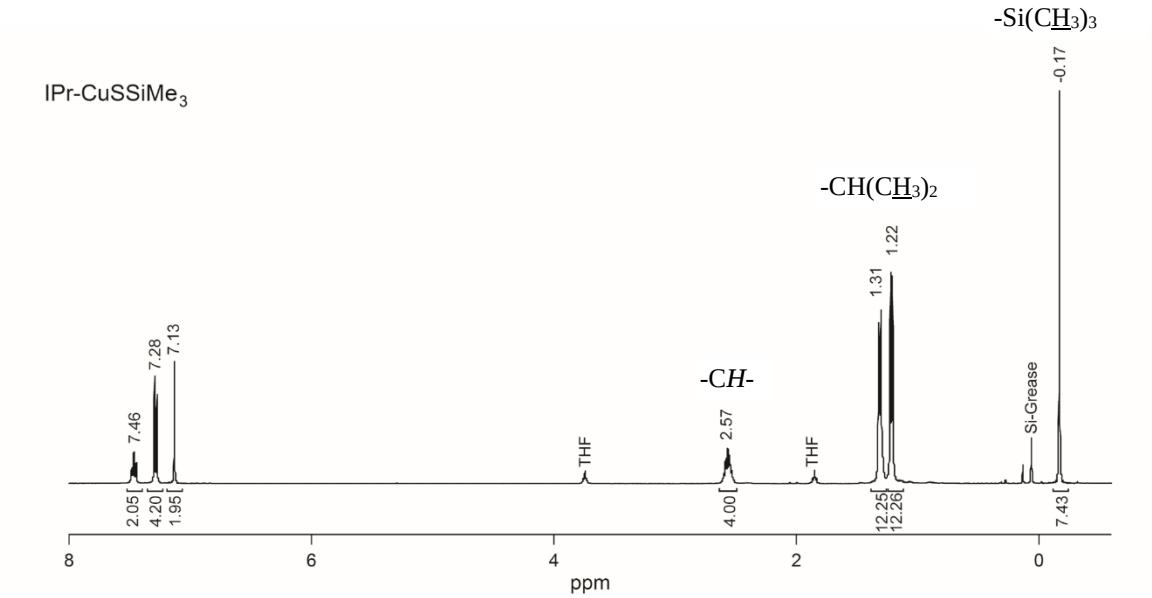

Figure 5.1. ^{1}H NMR spectrum of **25** ($CDCl_3$, -10 °C, 399.76 MHz).

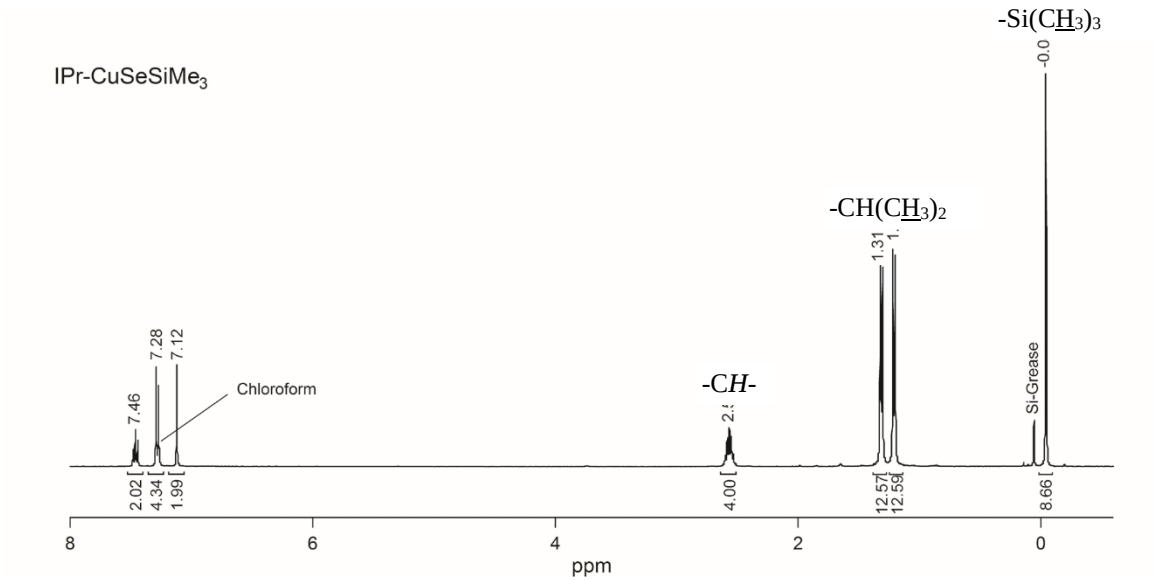

Figure 5.2. ^{1}H NMR spectrum of **26** (CDCl3, -10 °C, 399.76 MHz).

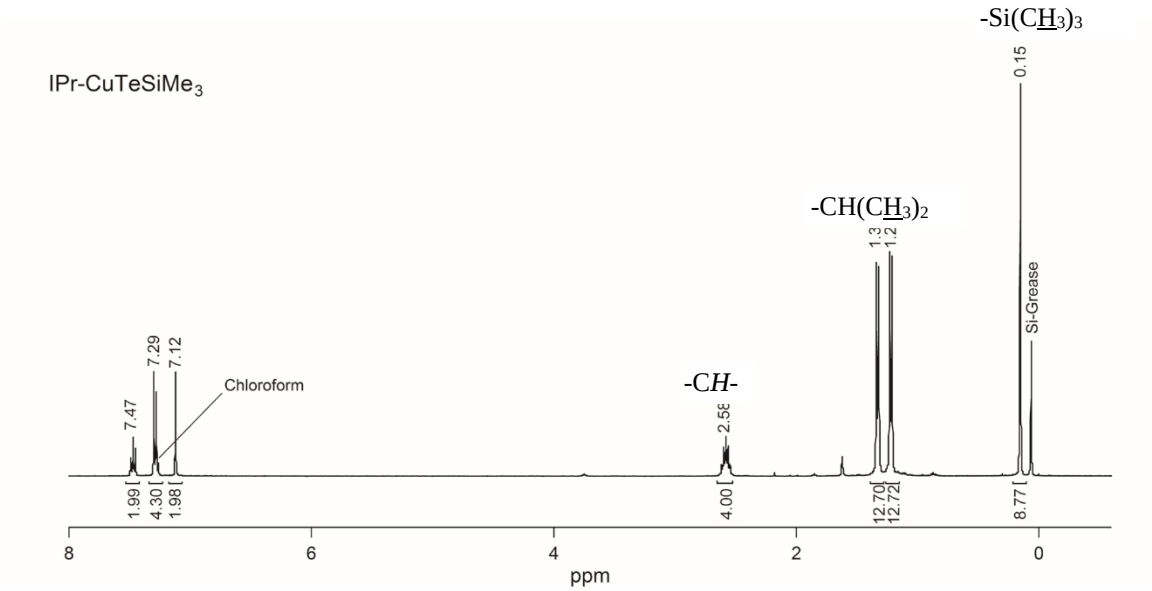

Figure 5.3. ^{1}H NMR spectrum of **27** (CDCl3, -15 °C, 399.76 MHz).

Notably, the high melting points of the [(IPr)Cu-ESiMe$_3$] (**25**; 171-172, **26**; 166-168, **27**; 178-180 °C) are in stark contrast to those of the phosphine ligated [L$_3$Cu-ESiMe$_3$], the most thermally stable of which could only be handled below ~10°C and for which the tellurium analogues are prone to decomposition at the melting point.[1b] The relative stabilities of **25-27** in solution also facilitate their crystallization and multinuclear NMR analyses.

The molecular structures **25-27**, as determined via single crystal X-ray diffraction (Figures 5.4, 5.5, and 5.6, respectively) illustrate the expected, near-linear coordination geometry of the copper(I) centre (∠IPr-Cu-E = ~170-176°), and the orientation of the pendant -SiMe$_3$ moiety bonded to the chalcogen atom. The nearly orthogonal angles for Cu-E-Si (1; 104.64(5)°, 2; 100.42(2)°, 3; 94.52(2)°) contrast with those for [L$_3$Cu-ESiMe$_3$] which range from ~120-130°.[1a,1b,8] The copper-chalcogen and chalcogen-silicon bond lengths display the expected increase from sulfur to selenium to tellurium (Cu-E: 1; 2.133(1), 2; 2.2431(7), 3; 2.424(1) Å, E-Si: 1; 2.105(2), 2; 2.2502(7), 3; 2.424(1) Å). Notable, however, is the markedly shorter Cu-E (Δ ~ 0.25-0.3 Å) in the two-coordinate NHC complexes versus tetrahedral [L$_3$Cu-ESiMe$_3$]. The shorter copper-chalcogen bond

lengths in **25**, **26** and **27** may be attributed to increase in the s orbital character at the Cu ("sp" vs "sp^3"). The Cu-C distances of **25-27** do not show any dependence on the nature of the chalcogen *trans* to the NHC ligand. Overall, the differences in Cu-E lengths and Cu-E-Si angles are consistent with the different coordination numbers of the Cu atoms and related steric effects.

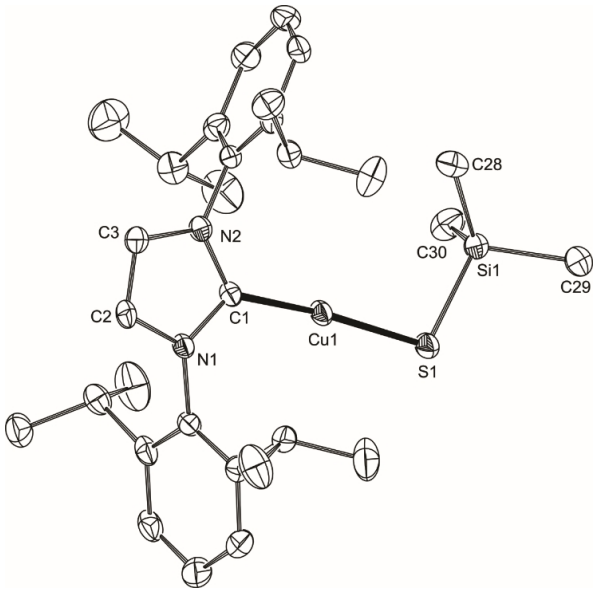

Figure 5.4. The molecular structure of [IPrCu-SSiMe_3] **25** (40% probability); Selected bond lengths (Å) and angles (°): C1-Cu1 1.885(3), Cu1-S1 2.133(1), S1-Si1 2.105(2), C1-Cu1-S1 171.6(1), Cu1-S1-Si1 104.65(5). Hydrogen atoms are omitted.

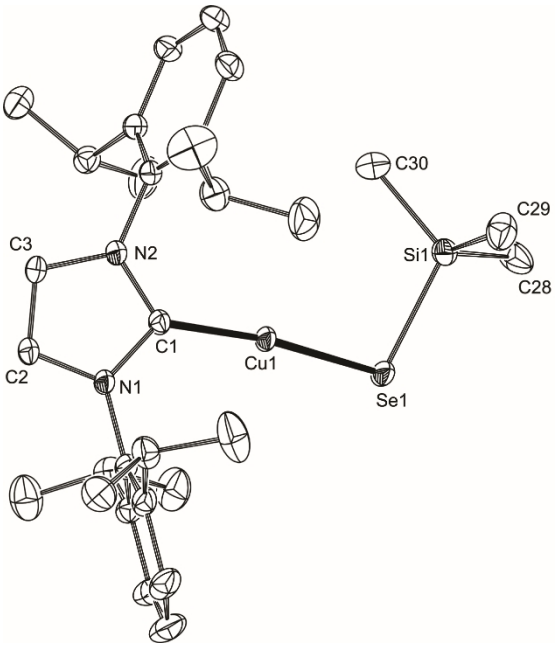

Figure 5.5. The molecular structure of [IPrCu-SeSiMe$_3$] **26** (40% probability); Selected bond lengths (Å) and angles (°): C1-Cu1 1.884(1), Cu1-Se1 2.2431(7), Se1-Si1 2.2502(7), C1-Cu1-Se1 170.68(5), Cu1-Se1-Si1 100.42(2). Hydrogen atoms are omitted.

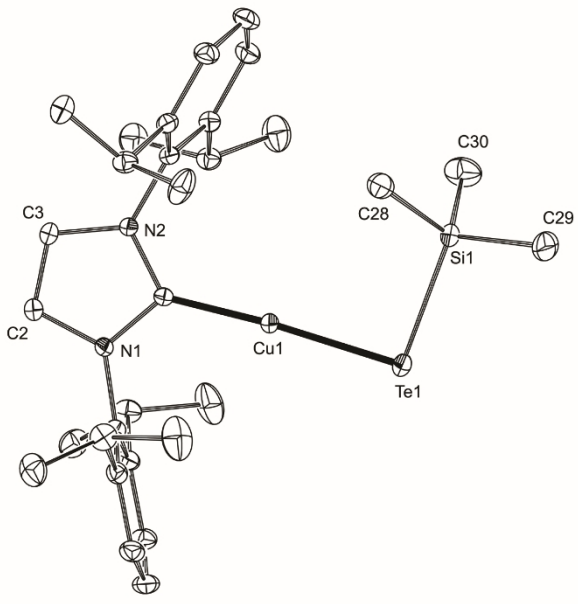

Figure 5.6. The molecular structure of [IPrCu-SeSiMe$_3$] **27** (40% probability); Selected bond lengths (Å) and angles (°): C1-Cu1 1.902(2), Cu1-Te1 2.424(1), Te1-Si1 2.487(1), C1-Cu1-Te1 176.00(5), Cu1-Te1-Si1 94.52(2). Hydrogen atoms are omitted.

Table 5.1. Crystallographic data and parameters for compounds **25-28**

	25·THF	**26**·THF	**27**	**28**·4CH_2Cl_2
formula	$C_{30}H_{45}CuN_2SSi$·THF	$C_{30}H_{45}CuN_2SeSi$·THF	$C_{30}H_{45}CuN_2SiTe$	$C_{54}H_{72}Cu_2HgN_4S_2$·4CH_2Cl_2
formula weight	629.47	676.37	652.91	1508.64
crystal system	monoclinic	monoclinic	Monoclinic	monoclinic
space group	*C*2/*c*	*C*2/*c*	$P2_1/n$	$P2_1/n$
a [Å]	28.986(15)	29.597(6)	9.789(3)	13.026(3)
b [Å]	12.887(7)	12.842(3)	21.443(11)	16.803(3)
c [Å]	19.067(9)	19.184(4)	15.580(6)	16.264(4)
α [°]	90.00	90.00	90.00	90.00
β [°]	92.619(12)	93.196(5)	100.673(19)	106.93(3)
γ [°]	90.00	90.00	90.00	90.00
V [Å^3]	7115(6)	7280(3)	3214(2)	3405.6(14)
Z	8	8	4	2
ρ_{cal} [g cm^{-3}]	1.175	1.234	1.349	1.471
μ (MoK_α) [mm^{-1}]	0.733	1.659	1.626	3.279
F(000)	2704	2848	1336	1524
temperature [K]	110	110	110	110
θ_{min}, θ_{max} [°]	2.51, 27.46	2.47, 36.21	2.83, 36.00	2.66, 29.58
total reflns	60384	150833	109050	18008
unique reflns	8905	17704	11631	5492
R(int)	0.0771	0.0306	0.0305	0.0380
*R*1	0.0573	0.0365	0.0249	0.0518
w*R*2 [$I \geq 2\sigma(I)$]	0.1633	0.1025	0.0836	0.1454
*R*1 (all data)	0.1080	0.0625	0.0328	0.0658
w*R*2 (all data)	0.2016	0.1284	0.0984	0.1676
GOF	1.195	1.081	1.313	1.216

The pendent –$SiMe_3$ in M-S$SiMe_3$ have been shown to react with M´-X (X = halide; carboxylate) to yield M-E-M´[9] and the reaction of [$(Pr_3P)_3CuSSiMe_3$] with $Hg(OAc)_2$ has been shown to lead to the ternary cluster [$Hg_{15}Cu_{20}S_{25}(PPr_3)_{18}$] via activation of the S-Si bond, and ligand stabilized assembly of the forming Cu-S-Hg units.[2a] Krautscheid and co-workers recently reported the isolation the Lewis acid:base adduct [($^iPr_3P)_2Cu(\mu$-$SSiMe_3)(InMe_3)$], which can be described as the first formed interaction en route to activation of the S-Si bond.[10] The use of the NHC stabilized Cu-E$SiMe_3$ reagents in **25**-**27** offers a complementary entry into the formation of ternary complexes where, because of the size of the NHC coupled with the inherent stability of the NHC-Cu bond, controlled M-E bond forming reactions and the isolation of low nuclearity fragments en route to larger architectures can be anticipated. When **25** is treated with 0.5 equivalent of $Hg(OAc)_2$ at lower temperatures [{(IPr)CuS}$_2$Hg] **28** forms (Scheme 5.1b). This is achieved via the

controlled cleavage of the S-Si bonds, the formation of mercuric sulfide bonds and generation of $(AcO)SiMe_3$. Complex **28** (Figure 5.7) consists of a linear S-Hg-S arrangement with Hg-S distances of 2.309(2) Å, the Hg atom residing on a crystallographic inversion centre. The Cu-S-Hg angle (86.61(8)°) is significantly smaller than ∠Cu-S-Si in **25** (104.64(5)°). Although the Cu-S (2.125(2) Å) and Hg-S distances are typical for Cu-SR[11] and Hg-SR[11] interactions, the Cu-S-Hg angle (86.61(8)°) is markedly less than the Hg-S-C angles observed in $[Hg(SAr)_2]$.[13] Despite the acute nature of ∠Cu-S-Hg (and Hg···Cu = 3.044(1) Å), calculations at the DFT level (TPSS/dhf-TZVP)[14a-c] do not suggest any significant Hg···Cu interactions. For instance, the shared electron numbers[15] for Cu-Hg amount to 0.04, for Hg-S, Cu-S and Cu-C they are about ten times larger, 0.39 to 0.48. The structural arrangement emphasizes the description of the (IPr)Cu-S$^-$ as a "cuprathiolate" moiety, two of which bond to Hg(II) to yield **28**. The two IPr ligands in **28** kinetically stabilize the structure from subsequent condensation reactions, en route to larger Cu(I)-Hg(II)-sulfide polynuclear complexes.[2a,2b]

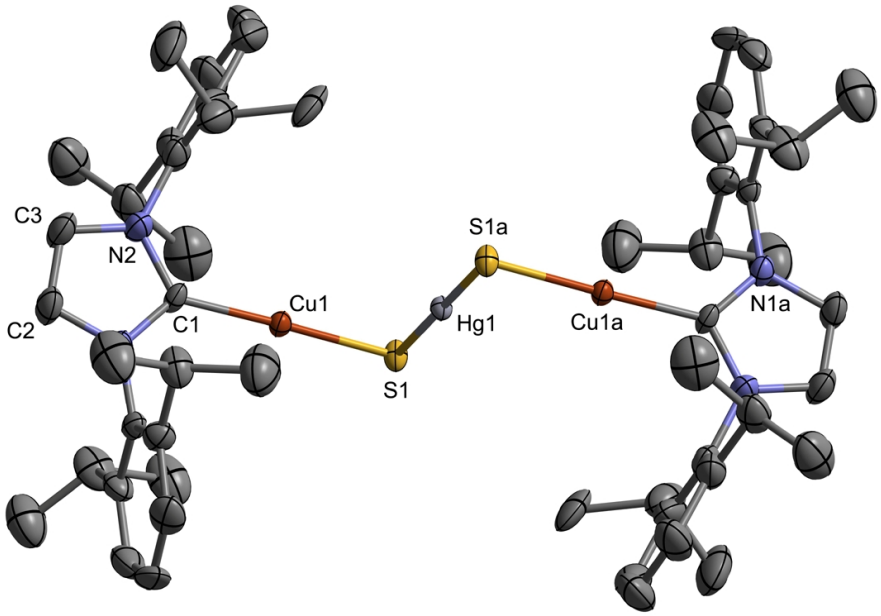

Figure 5.7. Molecular structure of $[\{(IPr)CuS\}_2Hg]$ **28** in the crystal (40 % probability; hydrogen atoms omitted). The cluster resides on a crystallographic inversion centre relating the two halves of the molecule. Selected bond lengths (Å) and angles (°): C1-Cu1 1.891(8), Cu1-S1 2.125(2), S1-Hg1 2.309(2), C1-Cu1-S1 177.4(3), Cu1-S1-Hg1 86.61(8). Hg1···Cu1: 3.044(1) Å.

5.3 Experimental

All synthetic and handling procedures were carried out under an inert atmosphere of high purity dried nitrogen using Schlenk line techniques and inert atmosphere glove boxes. Non-chlorinated solvents were dried using an MBraun MB-SP Series Solvent Purification system with tandem activated alumina (THF) or activated alumina-activated copper redox catalyst (pentane). Chloroform-d and dichloromethane were dried and distilled over P_2O_5. Dichloromethane-d was purchased from CIL. Mercuric(II) acetate was used as received from commercial source (Aldrich). The corresponding carbene copper(I) acetate IPrCu(OAc),[16] $S(SiMe_3)_2$,[17] $Se(SiMe_3)_2$[9c] and $Te(SiMe_3)_2$[9c] were prepared according to literature procedures.

NMR spectra were recorded on Varian Mercury 400, Inova 400 and Inova 600 NMR spectrometers. ^1H and ^{13}C chemical shifts are referenced to $SiMe_4$, using residual solvent as a secondary peak (^1H chemical shifts of compound **25** reference to trace amount of thf because of overlapping and low intensity of the $CDCl_3$ solvent peak). ^{77}Se chemical shift is referenced to Me_2Se and ^{125}Te chemical shift is referenced to Me_2Te. The peak from CO_2 in the ^{13}C NMR spectra arises from dry ice, used for making NMR samples at low temperature. Elemental analysis was performed by Laboratoire d'Analyse Élementaire de l'Université de Montréal, Canada.

Single-crystal X-ray diffraction measurements were completed on a Bruker APEX-II CCD diffractometer equipped with graphite-monochromated Mo Kα (λ = 0.71073 Å) radiation. Single crystals of the complexes were carefully selected, immersed in paraffin oil and mounted on MiteGen micromounts. The structures were solved using direct methods and refined by the full-matrix least-squares procedure of SHELXTL. All non-hydrogen atoms, with the exception of disordered carbon atoms of the solvent, were refined with anisotropic thermal parameters. Hydrogen atoms were included as riding on their respective carbon atoms. In compound **28**, one of the iso-propyl groups of the carbene was modelled as being disordered over two positions, with refined complementary site occupancy factors. Files CCDC 1045224-1045227 contain the supplementary

crystallographic data for this paper. These data can be obtained free of charge from the Cambridge Crystallographic Data Centre via www.ccdc.cam.ac.uk/data_request/cif.

5.3.1 Synthesis of [IPrCuSSiMe$_3$] **25**

46 μL of S(SiMe$_3$)$_2$ (0.218 mmol) was added to a cold (-70 °C) solution of one equivalent of IPrCu(OAc) (111 mg, 0.217 mmol) in 10 mL tetrahydrofuran, followed by storing the solution at -25 °C overnight. The reaction was layered with 30 mL of pentane at low temperature. Five to six days later colourless plate-like single crystals were obtained and identified by X-ray crystallography to be [IPrCuSSiMe$_3$]. The crystals were washed with 3×10 mL cold pentane (-70°C) and dried under dynamic vacuum at 0°C.

25 can be precipitated in higher yields by adding 40 mL of cold pentane to reaction solutions; storing at -25°C overnight forms an off-white suspension. Washing and drying the precipitated solid with 5×10 mL cold pentane, followed by drying under vacuum at 0 °C, gives **25** as an analytically pure product as small crystals (62% yield); m.p. 171-172 °C.

- ^{1}H NMR (CDCl$_3$, 399.76 MHz, -10 °C): δ 7.46 (t, J = 7.8 Hz, 2H, *para*-C*H*), 7.28 (d, J = 7.8 Hz, 4H, *meta*-C*H*), 7.13 (s, 2H, NC*H*), 2.57 (sept., J = 7.0 Hz, 4H, C*H*(CH$_3$)$_2$), 1.31 (d, J = 7.0 Hz, 12H, CH(C*H*$_3$)$_2$), 1.22 (d, J = 7.0 Hz, 12H, CH(C*H*$_3$)$_2$), -0.17 (s, 9H, -Si(C*H*$_3$)$_3$) ppm.
- ^{13}C{^{1}H} NMR (CDCl$_3$, 100.53 MHz, -10 °C): 181.1 (N*C*Cu), 145.4 (*ortho-C*), 134.4 (*ipso-C*), 130.2 (*para-C*), 124.0 (*meta-C*), 122.6 (N*C*H), 28.6 (*C*H(CH$_3$)$_2$), 24.9 (CH(*C*H$_3$)$_2$), 23.9 (CH(*C*H$_3$)$_2$), 6.7 (-Si(*C*H$_3$)$_3$) ppm.
- Anal. Calcd for C$_{30}$H$_{45}$CuN$_2$SSi: C, 64.64; H, 8.14; N, 5.03; S, 5.75. Found: C, 64.24; H, 8.28; N, 4.97; S, 5.49.

5.3.2 Synthesis of [IPrCuSeSiMe$_3$] **26**

53 μL of Se(SiMe$_3$)$_2$ (0.211 mmol) was reacted with one equivalent of of IPrCu(OAc) (108 mg, 0.211 mmol) in 10 mL tetrahydrofuran as described for the preparation of **25**. Colourless single crystals suitable for X-ray diffraction were obtained after five to six days by layering the mother liquor with 30 mL of pentane at -25°C.

The product can be isolated as an off-white powder by adding 40-50 mL of cold pentane to reaction solutions at -25°C, as described for **25**. Washing and drying the precipitated solid with 5×10 mL cold pentane, followed by drying under vacuum at 0 °C, gives **26** as small crystals (55% yield); m.p. 166-168 °C.

- ^{1}H NMR (CDCl$_3$, 399.76 MHz, -10 °C): δ 7.46 (t, *J* = 7.8 Hz, 2H, *para*-C*H*), 7.28 (d, *J* = 7.8 Hz, 4H, *meta*-C*H*), 7.12 (s, 2H, NC*H*), 2.58 (sept., *J* = 7.0 Hz, 4H, C*H*(CH$_3$)$_2$), 1.31 (d, *J* = 7.0 Hz, 12H, CH(C*H*$_3$)$_2$), 1.21 (d, *J* = 7.0 Hz, 12H, CH(C*H*$_3$)$_2$), -0.04 (s, 9H, -Si(C*H*$_3$)$_3$) ppm.
- ^{13}C{^{1}H} NMR (CDCl$_3$, 100.53 MHz, -10 °C): 181.6 (N*C*Cu), 145.4 (*ortho-C*), 134.4 (*ipso-C*), 130.2 (*para-C*), 124.0 (*meta-C*), 122.6 (N*C*H), 28.6 (*C*H(CH$_3$)$_2$), 25.0 (CH(*C*H$_3$)$_2$), 23.9 (CH(*C*H$_3$)$_2$), 7.3 (-Si(*C*H$_3$)$_3$) ppm.
- ^{77}Se NMR (CDCl$_3$, 76.20 MHz, -10°C): -481 ppm.
- Anal. Calcd for C$_{30}$H$_{45}$CuN$_2$SeSi: C, 59.63; H, 7.51; N, 4.64. Found: C, 58.43; H, 7.89; N, 4.47.

5.3.3 Synthesis of [IPrCuTeSiMe$_3$] **27**

67 μL of Te(SiMe$_3$)$_2$ (0.237 mmol) was reacted with one equivalent of IPrCu(OAc) (121 mg, 0.237 mmol) in 10 mL tetrahydrofuran as described for the preparation of **25**. Colourless single crystals suitable for X-ray diffraction were obtained after five to six days by layering the mother liquor with 35 mL of pentane at -25°C.

Compound **27** was isolated as an off-white powder according to the procedure for **25** and **26**; (50.3% yield); m.p. 178-180 °C.

- ^{1}H NMR ($CDCl_3$, 399.76 MHz, -15 °C): δ 7.47 (t, J = 7.8 Hz, 2 H, *para*-C*H*), 7.29 (d, J = 7.8 Hz, 4 H, *meta*-C*H*), 7.12 (s, 2H, NCH), 2.58 (sept., J = 7.0 Hz, 4 H, C*H*$(CH_3)_2$), 1.33 (d, J = 7.0 Hz, 12 H, CH(C*H*$_3)_2$), 1.22 (d, J = 7.0 Hz, 12H, CH(C*H*$_3)_2$), 0.15 (s, 9H, -Si(C*H*$_3)_3$) ppm.
- ^{13}C{^{1}H} NMR ($CDCl_3$, 100.53 MHz, -15 °C): 145.5 (*ortho-C*), 134.4 (*ipso-C*), 130.3 (*para-C*), 124.0 (*meta-C*), 122.6 (N*C*H), 28.7 (*C*H$(CH_3)_2$), 25.1 (CH(*C*H$_3)_2$), 23.8 (CH(*C*H$_3)_2$), 8.3 (-Si(*C*H$_3)_3$) ppm.
- ^{125}Te NMR ($CDCl_3$, 126.12 MHz, -15 °C): -1179 ppm.

5.3.4 Synthesis of [(IPrCuS)$_2$Hg] **28**

41 μL of S(SiMe$_3)_2$ (0.194 mmol) was added to a cold (-70 °C) solution of one equivalent of IPrCu(OAc) (99 mg, 0.194 mmol) in 10 mL tetrahydrofuran, followed by storage at -25 °C overnight. The reaction solution was cooled to -70 °C to mix with 0.097 mmol Hg$(OAc)_2$ (31 mg in 5 mL of thf) at this temperature. After warming to -25 °C and keeping the solution at this temperature for 2 hrs, the solvent was removed under vacuum at 0 °C. The off-white solid was redissolved in a minimum amount of cold dichloromethane and the solution layered with 30 mL cold pentane (-70 °C). Colourless blocks as single crystals suitable for X-ray diffraction were obtained after six to seven days (~20 % yield); m.p. 139-141 °C.

- ^{1}H NMR (CD_2Cl_2, 599.38 MHz, 25 °C): δ 7.48 (t, J = 7.6 Hz, 4H, *para*-C*H*), 7.28 (d, J = 7.6 Hz, 8H, *meta*-C*H*), 7.08 (s, 4H, NC*H*), 2.54 (sept., J = 7.0 Hz, 8H, C*H*$(CH_3)_2$), 1.27 (d, J = 7.0 Hz, 24H, CH(C*H*$_3)_2$), 1.18 (d, J = 7.0 Hz, 24H, CH(C*H*$_3)_2$) ppm.
- ^{13}C{^{1}H} NMR (CD_2Cl_2, 150.73 MHz, 25 °C): δ 146.2 (*ortho-C*), 135.3 (*ipso-C*), 130.9 (*para-C*), 124.7 (*meta-C*), 123.3 (N*C*H), 29.2 (*C*H$(CH_3)_2$), 25.4 (CH(*C*H$_3)_2$), 24.2 (CH(*C*H$_3)_2$) ppm.
- Anal. Calcd for $C_{54}H_{72}Cu_2HgN_4S_2$: C, 55.48; H, 6.21; N, 4.79; S, 5.49. Found: C, 56.74; H, 6.38; N, 4.78; S, 5.40.

5.4 Conclusions

The strategy outlined above for the synthesis of NHC-stabilized Cu-ESiMe$_3$ and the demonstrated reactivity in the formation of the copper-mercury sulfide cluster **28** suggest a powerful route into a variety of ternary complexes. In this approach a thermally stable silylated chalcogenolate precursor of copper has allowed terminal coordination of two copper-sulfide units onto Hg(II) centre yielding the cluster **28**, stable in both solution and the solid state. This suggests that complexes **25-27** may prove to be even superior synthons for the formation of stabilized heterometallic complexes compared to their phosphine analogues, including for the formation of the photovoltaic nanomaterials $CuInS_2$ and related systems. We are actively developing these opportunities.

5.5 References

[1] (a) A. Borecki, J. F. Corrigan, *Inorg. Chem.* 2007, **46**, 2478-2484; (b) D. T. T. Tran, J. F. Corrigan, *Organometallics* 2000, **19**, 5202-5208; (c) M. W. DeGroot, J. F. Corrigan, *Z. Anorg. Allg. Chem.* 2006, **632**, 19-29; (d) T. Komuro, T. Matsuo, H. Kawaguchi, K. Tatsumi, *Angew. Chem., Int. Ed.* 2003, **42**, 465-468.

[2] (a) D. T. T. Tran, N. J. Taylor, J. F. Corrigan, *Angew. Chem., Int. Ed.* 2000, **39**, 935-937; (b) D. T. T. Tran, L. M. C. Beltran, C. M. Kowalchuk, N. R. Trefiak, N. J. Taylor, J. F. Corrigan, *Inorg. Chem.* 2002, **41**, 5693-5698; (c) O. Kluge, R. Biedermann, J. Holldorf, H. Krautscheid, *Chem. Eur. J.* 2014, **20**, 1318-1331.

[3] F. Komuro, T. Matsuo, H. Kawaguchi, K. Tatsumi, *Dalton Trans.*, 2004, 1618–1625.

[4] O. Fuhr, S. Dehnen, D. Fenske, *Chem. Soc. Rev.* 2013, **42**, 1871-1906.

[5] M. N. Hopkinson, C. Richter, M. Schedler, F. Glorius, *Nature* 2014, **510**, 485-496.

[6] (a) D. Bourissou, O. Guerret, F. P. Gabbai, G. Bertrand, *Chem. Rev.* 2000, **100**, 39-91; (b) C. M. Crudden, D. P. Allen, *Coord. Chem. Rev.* 2004, **248**, 2247-2273; (c) F. E. Hahn, M. C. Jahnke, *Angew. Chem., Int. Ed.* 2008, **47**, 3122-3172; (d) H. Jacobsen, A. Correa, A. Poater, C. Costabile, L. Cavallo, *Coord. Chem. Rev.* 2009, **253**, 687-703; (e) J. C. Y.Lin, R. T. W.Huang, C. S. Lee, A. Bhattacharyya, W. S. Hwang, I. J. B. Lin, *Chem. Rev.* 2009, **109**, 3561-3598.

[7] (a) S. A. Delp, C. Munro-Leighton, L. A. Goj, M. A. Ramírez, T. B. Gunnoe, J. L. Petersen, P. D. Boyle, *Inorg. Chem.* 2007, **46**, 2365-2367; (b) M. M. Melzer, E. Li, T. H. Warren, *Chem. Commun.* 2009, 5847-5849.

[8] A. I. Wallbank, J. F. Corrigan, *Can. J. Chem.* 2002, **80**, 1592-1599.

[9] (a) M. W. DeGroot, N. J. Taylor, J. F. Corrigan, , *J. Am. Chem. Soc.* 2003, **125**, 864-865; (b) M. W. DeGroot, J. F. Corrigan, *Angew. Chem., Int. Ed.* 2004, **43**, 5355-5357; (c) M. W. DeGroot, N. J. Taylor, J. F. Corrigan, *J. Mater. Chem.* 2004, **14**, 654-660; (d) J. L. Kuiper, P. A. Shapley, C. M. Rayner, *Organometallics* 2004, **23**, 3814-3818; (e) M. W. DeGroot, N. J. Taylor, J. F. Corrigan, *Inorg. Chem.* 2005, **44**, 5447-5458; (f) C. B. Khadka, A. Eichhöfer, F. Weigend, J. F. Corrigan, *Inorg. Chem.* 2012, **51**, 2747-2756.

[10] R. Biedermann, O. Kluge, D. Fuhrmann, H. Krautscheid, *Eur. J. Inorg. Chem.* 2013, **2013**, 4727-4731.

[11] (a) A. Kohner-Kerten, E. Y. Tshuva, *J. Organomet. Chem.* 2008, **693**, 2065-2068; (b) S. Groysman, R. H. Holm, *Inorg. Chem.* 2009, **48**, 621-627.

[12] (a) G. G. Hoffmann, I. Steinfatt, W. Brockner, V. Kaiser, , *Z. Naturforsch., B: Chem. Sci.* 1999, **54**, 887-894; (b) H. Strasdeit, A. von Dollon, W. Saak, M. Wilhelm, *Angew. Chem., Int. Ed.* 2000, **39**, 784-786.

[13] (a) J. X. Chen, W. H. Zhang, X. Y. Tang, Z. G. Ren, H. X. Li, Y. Zhang, J. P. Lang, *Inorg. Chem.* 2006, **45**, 7671-7680; (b) J. G. Melnick, K. Yurkerwich, G. Parkin, *Inorg. Chem.* 2009, **48**, 6763-6772.

[14] (a)TURBOMOLE Version 6.5, TURBOMOLE GmbH 2014. TURBOMOLE is a development of University of Karlsruhe and Forschungszentrum Karlsruhe 1989–2007, TURBOMOLE GmbH since 2007; (b) Tao, J., Perdew, J.P., Staroverov, V.N., Scuseria, G.E, *Phys. Rev. Lett.* 2003, **91**, 146401. (c) F. Weigend, A. Baldes; *J. Chem. Phys*. 2010, **133**, 174102.

[15] C. Ehrhardt, R. Ahlrichs, *Theor. Chim. Acta* 1985, **68**, 231-245.

[16] N. P. Mankad, T. G. Gray, D. S. Laitar, J. P. Sadighi, *Organometallics* 2004, **23**, 1191-1193.

[17] So, J. H.; Boudjouk, P., *Synthesis* 1989, 306-307.

Chapter 6

Stable –$ESiMe_3$ Complexes of Cu(I) and Ag(I) (E = S, Se): New Synthons for Ternary Nanocluster Assembly

6.1. Introduction

To date the exploration of binary, late d-block metal-chalcogenide nanoclusters has been much more extensive[1] than that of ternary (MM´E) (E = S, Se, Te) systems. This may be attributed, in part, to a lack of suitable "binary" reagents that can be employed to yield ternary chalcogenide clusters in a controlled manner. A general molecular synthetic route to access ternary nanoclusters is desirable since the incorporation of different metals in ternary clusters can markedly affect, for example, the photophysical properties,[2] mirroring the tailoring of optical and electronic properties in extended solid materials.[3] In this regard, metal-chalcogenolate complexes of the d-block containing trimethylsilyl moieties (M-$ESiMe_3$; E = S, Se, Te), continue to draw considerable attention[4] due to their optimized reactivity which can be used for the controlled assembly of ternary cluster and nanocluster complexes.[5] This is achieved via the selective cleavage of the E-Si bond when the "binary" silyl reagent, M-$ESiMe_3$ is reacted with a second metal salt, M´-X, to yield M-E-M´ units along with $XSiMe_3$ and form, ultimately, a ternary polynuclear complex. This strategy has been demonstrated with the formation of phosphine stabilized ternary clusters from the reaction between [$(R_3P)_nCu$-$ESiMe_3$] (E = S, Se) with In, Ga, Ag and Hg salts.[6]

Not only do the steric and electronic properties of the ancillary phosphine play a role in the final size and shape of ternary metal chalcogenide nanocluster cores but they are key

components in the formation of the metal chalcogenolate precursors as well.[1a] Despite their utility, the coordination complexes of Cu and, especially, Ag are thermally sensitive even when isolated from solvent. Although enhanced thermal stability can be achieved with larger substituents about the silicon centre, this ultimately prohibits selective-Si bond cleavage with other metal salts. As part of the continued interest in developing the chemistry of metal chalcogenolate precursors,[7] we communicated recently the use of an alternate ancillary ligand such as the N-heterocyclic carbene IPr (IPr = 1,3-bis(2,6-diisopropylphenyl)imidazolin-2-ylidene) to increase the thermal stability of Cu-ESiMe$_3$, at the same time promoting an oriented coordination on the copper centre with the preparation of [(IPr)Cu-ESiMe$_3$] (Chapter 5). We also demonstrated that the strong bonding of IPr with Cu(I) enhances the kinetic stability first formed [{(IPr)CuS$_2$}Hg].[8]

In this vein access to a range of [(NHC)M-ESiMe$_3$] (NHC = N-heterocyclic carbene; M = Cu, Ag; E = S, Se) is of fundamental importance for the formation of new ternary metal chalcogenide nanocluster architectures. For a comparison with the recently reported [(IPr)Cu-ESiMe$_3$][8] and to evaluate the influence of metal or ancillary ligand change on the structural features and thermal stability, here we report the synthesis, crystal structures and spectroscopic characterization of the new silver(I)- and copper(I)-(trimethylsilyl)chalcogenolates stabilized with IPr and (^{i}Pr$_2$-bimy) respectively: [(IPr)Ag-ESiMe$_3$] (E = S, **29**; E = Se, **30**) and [(^{i}Pr$_2$-bimy)Cu-ESiMe$_3$] (E = S, **32**; E = Se, **33**). We also describe details of the reactivity of **29** and **32** via the reaction with mercuric(II) acetate and the formation of the ternary mixed-metal clusters [{(IPr)AgS}$_2$Hg], **31** and [{(^{i}Pr-bimy)$_6$Cu$_{10}$S$_8$Hg$_3$}] **34**.

6.2 Results and Discussion

The facile synthetic route to **29** and **30** involves dissolving [(IPr)AgOAc] with one equivalent of bis(trimethylsilyl)chalcogenide in tetrahydrofuran at low temperature (-70 °C) (Scheme 6.1). We have already shown that the large N-heterocyclic carbene ligand is critical for the stabilisation of [(IPr)Cu-ESiMe$_3$], as it is essential to occupy/block the

coordination sites around the metal centre and to force terminal coordination of the formed silylchalcogenolate, thus avoiding the generation of polynuclear copper-chalcogenide complexes. Unlike the phosphine ligated metal silylchalcogenolates where an excess amount of phosphine is required to force terminal coordination of the chalcogenolate ligand, applying a large volume NHC such as the ligand IPr ensures such a terminal coordination on the metal centre. Thus when a solution of the N-heterocyclic carbene silver acetate adduct [(IPr)AgOAc] is cooled to -70 °C and one equivalent of bis(trimethylsilyl)chalcogenide is added, [(IPr)Ag-ESiMe$_3$] forms selectively in good yields. Under these conditions, there is selective displacement of one of the two E–SiMe$_3$ bonds to yield **29** (S) and **30** (Se). Solutions are warmed to -25 °C and kept at that temperature for 10-12 hours, followed by layering with cold pentane to crystallize the coordination complexes.

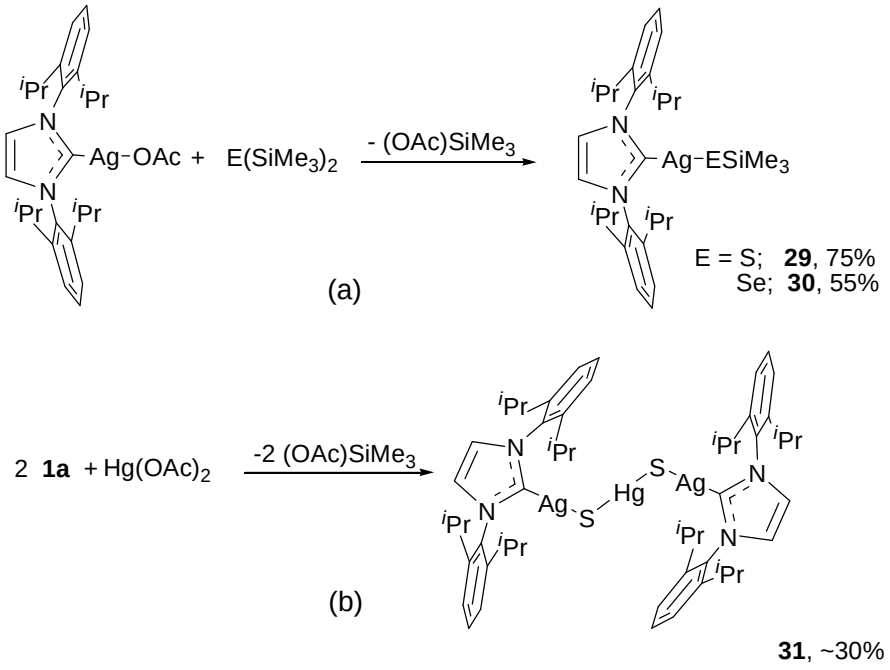

Scheme 6.1. Synthesis of (a) [(IPr)Ag-ESiMe$_3$] (E = S, **29**; E = Se, **30**); (b) [{(IPr)Ag-E}$_2$Hg] **31**.

Complexes **29** and **30** crystallize as colourless blocks with relatively high melting points (**29**, 175-179; **30**, 170-175 °C). The high thermal stability of **29** and **30** contrasts with those for $[(R_3P)_nAg\text{-}ESiMe_3]$ (T < 10 °C) and arises from the use of the ancillary ligand IPr. Such an improvement in the thermal stability, which also has already been shown for [(IPr)Cu-$ESiMe_3$], facilitates their crystal growth, purification and their "bottleability" for use in subsequent cluster forming reaction steps.

Complete structural information was obtained for **29** and **30** from single-crystal X-ray crystallographic analyses (Table 6.1). The molecular structures of [(IPr)Ag-$SSiMe_3$] **29** and [(IPr)Ag-$SeSiMe_3$] **30** are illustrated in Figures 6.1 and 6.2, respectively. The complexes **29** and **30** are the first examples of structurally characterized silver-chalcogenolates containing the -$ESiMe_3$ moiety.

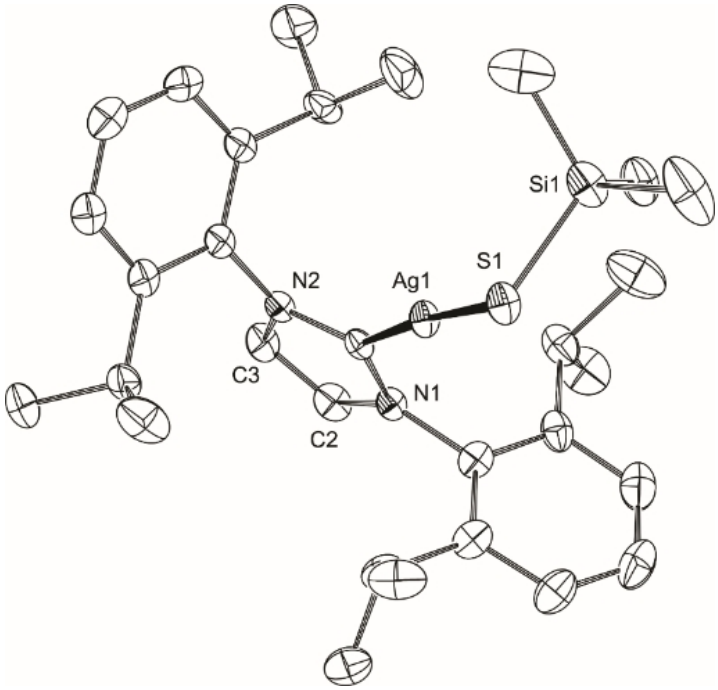

Figure 6.1. The molecular structure of [(IPr)Ag-$SSiMe_3$], **29** (40% probability; hydrogen atoms are omitted); Selected bond lengths (Å) and angles (°): C1-Ag1 2.089(6), Ag1-S1 2.341(2), S1-Si1 2.093(3), C1-Ag1-S1 175.2(2), Ag1-S1-Si1 101.6(1).

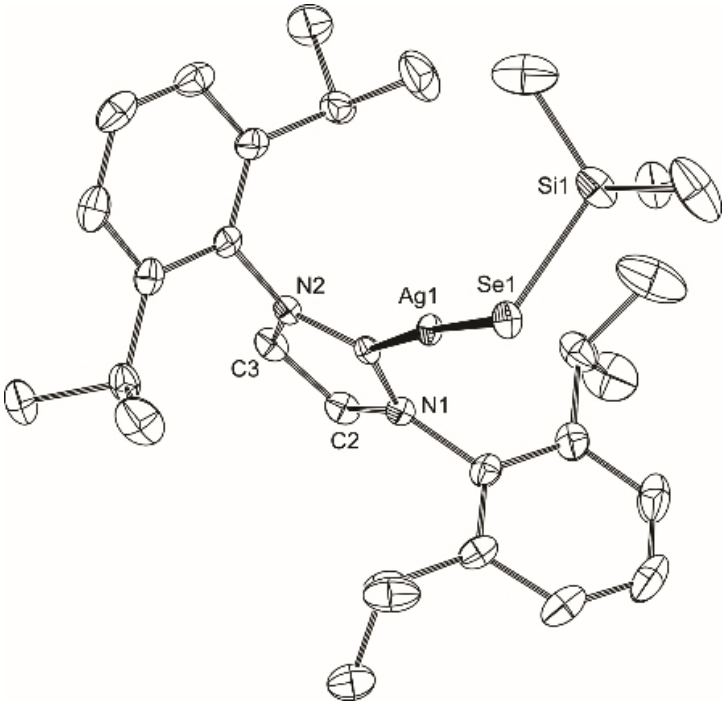

Figure 6.2. The molecular structure of [IPrAg-SeSiMe$_3$], **30** (40% probability; hydrogen atoms are omitted); Selected bond lengths (Å) and angles (°): C1-Ag1 2.093(3), Ag1-Se1 2.4334(9), Se1-Si1 2.238(2), C1-Ag1-Se1 175.18(9), Ag1-Se1-Si1 98.53(9).

Table 6.1. Crystallographic data and parameters for compounds **29**, **30**, **31**, **32**, **33** and **34**.[a]

	29	**30**	**31**	**32**	**33**	**34**
Formula	$C_{30}H_{45}AgN_2SSi$ ·1THF	$C_{30}H_{45}AgN_2SeSi$ ·1THF	$C_{54}H_{72}Ag_2HgN_4S_2$ ·4THF	$C_{32}H_{54}Cu_2N_4S_2$ ·1THF	$C_{32}H_{54}Cu_2N_4Se_2$ ·2THF	$C_{78}H_{108}Cu_{10}Hg_3N_{12}S_8$ ·5.49THF
formula weight	673.80	720.70	1546.02	814.27	980.18	3103.44
crystal system	triclinic	triclinic	triclinic	monoclinic	monoclinic	monoclinic
space group	$P\bar{1}$	$P\bar{1}$	$P\bar{1}$	$C2/c$	$P2_1/c$	$P2_1/n$
a [Å]	10.196(2)	10.309(3)	14.614(3)	10.379(3)	20.371(5)	17.820(4)
b [Å]	12.625(3)	12.604(5)	16.118(3)	16.442(4)	21.812(5)	34.856(4)
c [Å]	16.038(5)	16.151(5)	16.572(3)	24.602(7)	21.819(6)	21.289(4)
α [°]	67.516(13)	68.375(15)	88.030(8)	90	90	90
β [°]	79.534(12)	78.886(13)	66.251(8)	94.930(13)	101.334(10)	100.093(10)
γ [°]	71.104(9)	71.154(11)	87.115(9)	90	90	90
V [Å^3]	1800.8(9)	1839.9(10)	3567.8(11)	4182.7(19)	9506(4)	13018(4)
Z	2	2	2	4	8	4
ρ_{cal} [g cm^{-3}]	1.243	1.301	1.439	1.293	1.370	1.583
M ($Mo_{K\alpha}$) [mm^{-1}]	0.677	1.595	2.795	1.206	2.512	5.295
F(000)	712	748	1580	1728	4064	6151
temperature [K]	110	110	110	110	110	110
θ_{min}, θ_{max} [°]	2.64, 30.00	2.60, 34.22	2.95, 28.17	2.48, 34.85	2.51, 29.25	2.61, 28.66
total reflns	20047	25554	31783	69222	209634	561862
unique reflns	5584	5942	21890	9133	29090	63135
R(int)	0.0507	0.0377	0.0562	0.0422	0.0306	0.1237
$R1$	0.0610	0.0333	0.0534	0.0277	0.0494	0.0686
w$R2$ [$I \geq 2\sigma$ (I)]	0.1740	0.1028	0.1399	0.0904	0.1433	0.1879
$R1$ (all data)	0.0735	0.0382	0.0967	0.0422	0.1237	0.1875
w$R2$ (all data)	0.1945	0.1180	0.1954	0.1205	0.1713	0.2464
GOF	1.141	1.125	1.075	1.175	1.033	1.038

[a] $R_1 = \sum(|F_o| - |F_c|)/\sum F_o$, $wR_2 = [\sum(w(F_o^2 - F_c^2)^2)/\sum(wF_o^2)]^{1/2}$, GOF = $[\sum(w(F_o^2 - F_c^2)^2)/(N_{observns} - N_{params})]^{1/2}$

Compounds **29** and **30** crystallize in space group $P\bar{1}$. Selected bond angles and distances, as well as those for the related [(IPr)Cu-ESiMe$_3$] for comparison are summarized in Table 6.2. **29** and **30** display a slightly less distorted linear coordination geometry (C-Ag-E ≈ 175°) compared to their copper analogues (C-Cu-E ≈ 171°).[8] Expectedly, **29** and **30** display longer metal-chalcogen and metal-carbon bonds versus [(IPr)Cu-ESiMe$_3$]. These longer metal-chalcogen and metal-carbon distances are accompanied by a larger torsion angle between the pendent trimethylsilyl group and the plane defined by the imidazolin-2-ylidene ring of the carbene ligand. The M-E-Si angles in **29** and **30** are slightly larger than those for [(IPr)Cu-SSiMe$_3$][8] and [(IPr)Cu-SeSiMe$_3$].[8] The silver-chalcogen and chalcogen-silicon bond lengths display the expected increase from sulfur to selenium.

Table 6.2. Selected bond lengths (Å), bond angles (°) and torsion angle (°) between the plane defined by the central ring of the IPr ligand and the E-Si vector of **29**, **30** and the isostructural copper complexes.[8]

	C-M-E (°)	M-C (Å)	M-E (Å)	C_3N_2···E-Si (°)	M-E-Si (°)	E-Si (Å)
[(IPr)Ag-SSiMe$_3$] **29**	175.2(2)	2.089(6)	2.431(2)	15.3(3)	104.65(5)	2.093(3)
[(IPr)Ag-SeSiMe$_3$] **30**	175.18(9)	2.093(3)	2.4334(9)	2.70(2)	100.42(2)	2.238(2)
[(IPr)Cu-SSiMe$_3$]	171.6(1)	2.133(1)	2.133(1)	85.1(5)	101.6(1)	2.105(2)
[(IPr)Cu-SeSiMe$_3$]	170.68(5)	1.884(1)	2.2431(7)	85.2(3)	98.53(4)	2.2502(7)

Although **29** and **30** are unstable in solution above 0 °C, they remain stable in solvent for extended periods at lower temperatures. Monitoring the reactions for the formation of **29** and **30** via ^{1}H NMR spectroscopy at low temperatures indicates the quantitative replacement of the acetate group with -ESiMe$_3$ to form [(IPr)Ag-ESiMe$_3$] and (AcO)SiMe$_3$. In addition to a set of resonances assigned to one molecule of (AcO)SiMe$_3$ and the coordinated IPr ligand, a high field signal is observed at -0.13 and -0.02 ppm from the coordinated -SSiMe$_3$ and –SeSiMe$_3$, respectively, which satisfactorily integrates as nine hydrogen atoms versus IPr. The chemical shifts of –ESiMe$_3$ are at slightly lower field compared to those reported for their copper analogous (δ [IPrCuSSiMe$_3$], -0.17; [IPrCuSeSiMe$_3$], -0.04 ppm) and at considerably higher field compared to those reported in tetrahedral [L$_3$Ag-ESiMe$_3$] (L = R$_3$P, δ 0.10-0.34 ppm). ^{13}C{^{1}H} NMR can also be used

confirm coordination of -$ESiMe_3$ ligands, with a peak observed at 7.0 and 7.6 ppm for -$ESiMe_3$ in **29** and **30**, respectively.

The pendent –$SSiMe_3$ in [(IPr)Cu-$SSiMe_3$] have been shown to react with $Hg(OAc)_2$ to yield the heterometallic complex [{(IPr)CuS}$_2$Hg], which contains two (IPr)Cu-S^- fragments bonded to a central Hg(II).[8] This builds upon the reaction of [$(Pr_3P)_3$Cu-$SSiMe_3$] with $Hg(OAc)_2$ which has been shown to lead to the ternary cluster [$Hg_{15}Cu_{20}S_{25}(PPr_3)_{18}$] via activation of S-Si bonds and the ligand stabilized assembly of the forming Cu-S-Hg units.[6a]

The known reactivity of silver salts toward -$ESiMe_3$ reagents in the assembly of Ag_2S megaclusters[9] makes Ag-$ESiMe_3$ extremely attractive targets for the assembly of polynuclear Ag-E-M. Efforts to use [$(L)_n$AgS$SiMe_3$] (L= tertiary phosphine) for reactions with Hg(II) metal salts for ternary Ag-S-Hg cluster formation have proven more difficult than those for Cu vis à vis formation of monosdisperse clusters. However, the more stable chalcogenolates **29** offer an entry point for the formation of the first mercury-silver-sulfide ternary cluster. When **29** is treated with 0.5 equivalents of $Hg(OAc)_2$ at low temperatures the trimetallic complex [{(IPr)AgS}$_2$Hg] **31** forms (Scheme 6.1b). This is achieved via the controlled cleavage of the S-Si and the formation of mercury-sulfur bonds via the generation of (AcO)$SiMe_3$. Layering reaction solutions with pentane at -25 °C leads to the formation of colourless, crystal blocks suitable for single-crystal X-ray analysis after 4-5 days. The structure of **31** in the crystal consists of two independent [{(IPr)AgS}$_2$Hg] molecules in the asymmetric unit (Figure 6.3) and each reside about a crystallographic inversion center. Data in the text refer to independent molecule 1. Molecules of **31** show near-linear S-Hg-S arrangements with Hg-S distances of 2.326(2) Å. The Ag-S-Hg angle (91.46(8)°) is significantly smaller than ∠Hg-S-Si in **29** (104.65(5)°) resulting in a short Ag···Hg distance (3.3211(8) Å). While such an acute ∠M-S-M´ (and Hg···Cu = 3.044(1) Å) was observed in [{(IPr)CuS}$_2$Hg], calculations at the DFT level did not suggest any significant Hg···Cu interactions.[8] The structural arrangement emphasizes the description of the (IPr)Ag-S^- as an “argentathiolate” moiety, two of which bond to Hg(II) to yield the cluster **31**.

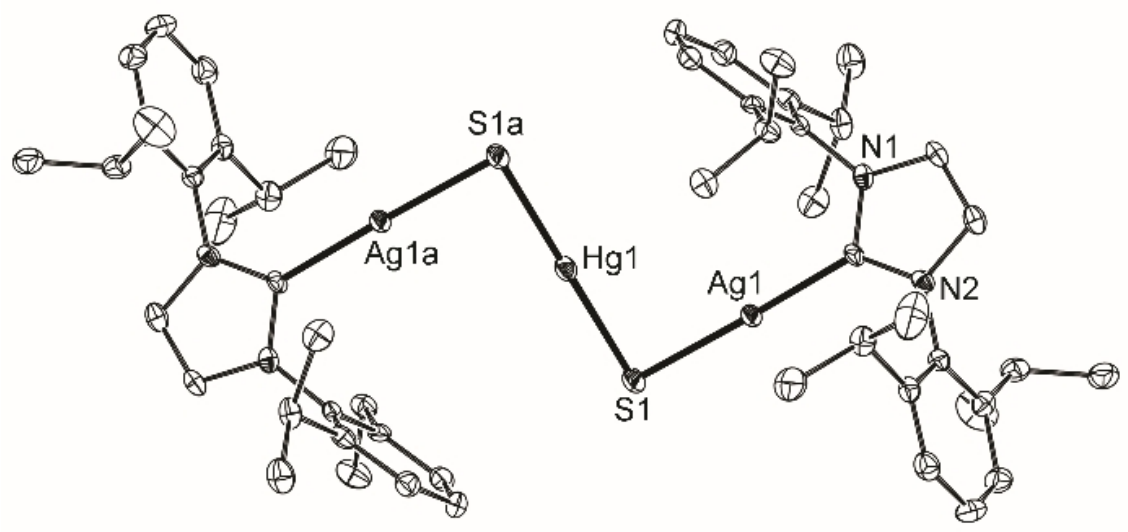

Figure 6.3. Molecular structure of [{(IPr)AgS}$_2$Hg] **31** in the crystal (40% probability; hydrogen atoms omitted). Selected bond lengths (Å) and angles (°): C-Ag 2.088(6), Ag-S 2.326(2), S-Hg 2.313(2), Hg-Ag 3.3211(8), C-Ag-S 175.9(2)-, Ag-S-Hg 91.46(8).

The demonstrated, straightforward preparative chemistry for the formation of [(IPr)M-ESiMe$_3$] suggested that other NHC ligated M-ESiMe$_3$ could also be targeted, which would provide flexibility in the assembly of different ternary frameworks (*vide infra*). In analogy with the work developed for PR$_3$ ligands on metal-chalcogenide frameworks,[1] this would open an interesting opportunity to begin the development of NHC/cluster relationships. In this vein the smaller NHC ^{i}Pr$_2$-bimy (^{i}Pr$_2$-bimy = 1,3-diisopropylbenzimidazolin-2-ylidene) was selected. The %V$_{bur}$ at 2.00 Å for ^{i}Pr$_2$-bimy = 27.9, versus 44.5 for the larger IPr.[10] The approach for the synthesis of [(^{i}Pr$_2$-bimy)Cu-ESiMe$_3$)] complexes **32** and **33** parallels the procedure developed for the formation of the silver complexes **29** and **30** and reported [(IPr)Cu-ESiMe$_3$]. Thus [(^{i}Pr$_2$-bimy)Cu-OAc] was reacted with E(SiMe$_3$)$_2$ at -70 °C (Scheme 6.2a) and complexes **32** and **33** crystallize as colorless block and needle crystals, respectively. Complex **32** shows relatively high thermal stability with the melting point of 91-93 °C, while **33**, unexpectedly, is much more thermally sensitive, decomposing at temperatures above -25°C in the solid state. Indeed due to this sensitivity, complex **33** can ultimately only be isolated as a pure product a few single crystals at a time, although monitoring reaction solutions via NMR spectroscopy indicate selective formation of **33**.

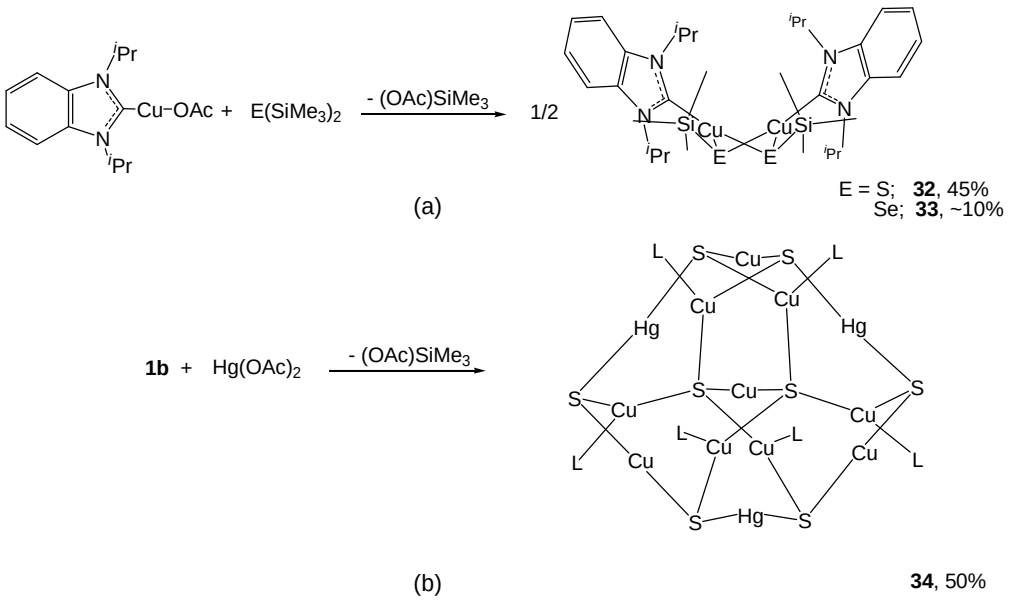

Scheme 6.2. Synthesis of (a) [(^{i}Pr$_2$-bimy)Cu-ESiMe$_3$] (E = S, **32**; E = Se, **33**); (b) [{(^{i}Pr$_2$-bimy)$_6$Cu$_{10}$S$_8$Hg$_3$] **34**.

Complexes **32** and **33** were satisfactorily solved and refined in the space groups *C*2/*c* and *P*2$_1$/*c*, respectively (Figures 6.4 and 6.5). Crystals of **33** contain two virtually identical but independent molecules in the asymmetric unit; details in the text refer to molecule 1. Both **32** and **33** exist as [(^{i}Pr$_2$-bimy)$_2$Cu$_2$(μ-ESiMe$_3$)$_2$] dimers in the solid state, with a hinged butterfly shaped E$_2$Cu$_2$ central ring (hinge angle: E = S **32**, 119°; E = Se **33**, 138°). Obviously the smaller size of the ancillary carbene (^{i}Pr$_2$-bimy) compared to IPr provides access to the additional coordination spaces around the Cu metal and enables such a dimerization of two Cu-ESiMe$_3$. All copper centers in **32** and **33** assume distorted, trigonal planar coordination geometry at the wingtip positions of the butterfly structure, ligated by one NHC and two μ_2-ESiMe$_3$ moieties.

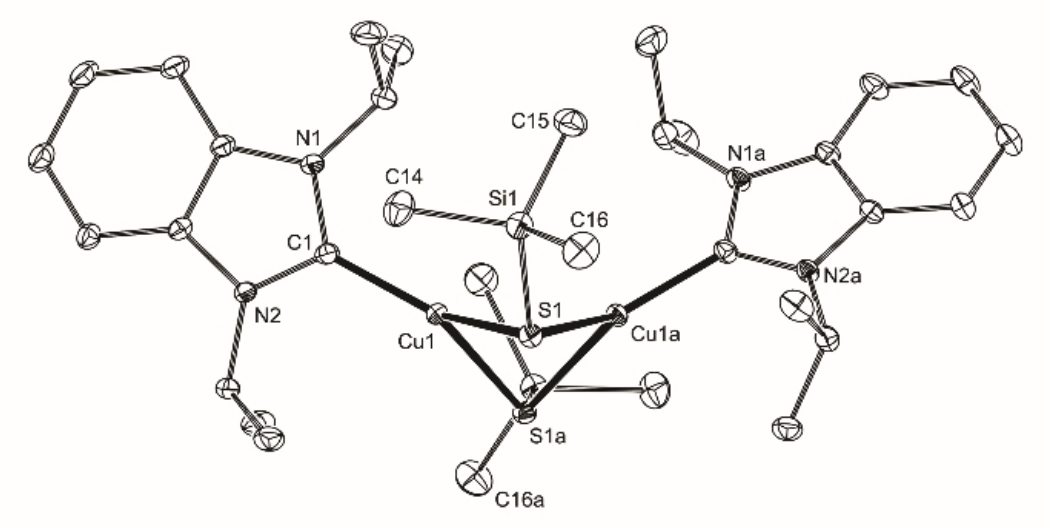

Figure 6.4. The molecular structure of [(^{i}Pr$_2$-bimy)Cu-SSiMe$_3$], **32** (40% probability; hydrogen atoms omitted); Selected bond lengths (Å) and angles (°): C1-Cu1 1.918(1), Cu1-S1 2.3105(9), S1-Si1 2.1133(7), C1-Cu1-S1 138.04(4), Cu1-S1-Si1 109.04(2).

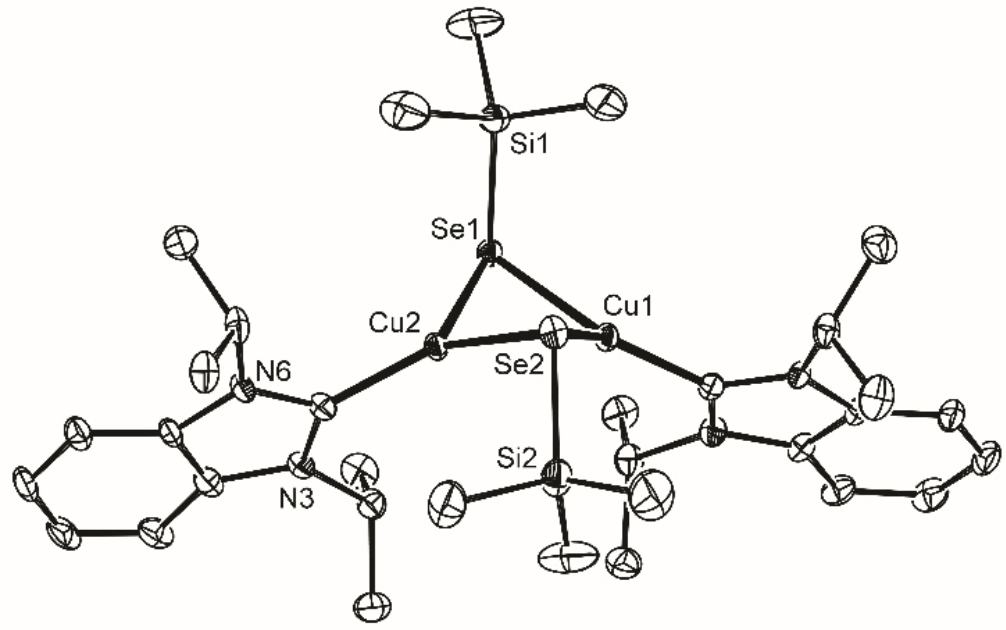

Figure 6.5. The molecular structure of [(^{i}Pr$_2$-bimy)Cu-SeSiMe$_3$], **33** (40% probability; hydrogen atoms omitted); Selected bond lengths (Å) and angles (°): C-Cu 1.916(4)-1.924(4), Cu-Se 2.3853(7)- 2.5149(8), Se-Si1 2.257(1)-2.259(2), C-Cu-Se 115.3(1)-140.3(1), Se-Cu-Se 104.23(2)-104.44(2), Cu-Se-Cu 63.00(2)-65.82(2), Cu-Se-Si 96.79(4)-104.96(4).

In **32** the dimeric molecule resides about a two-fold axis. Interestingly both –$SiMe_3$ groups in **32** are found on the same side (*cis*) of the hinged central ring and oriented towards the wingtip positions. In this molecule the Cu-S bond lengths range from 2.3105(9) to 2.3408(7) Å, the Cu-C bonds are 1.918(1) Å and the Cu···Cu separation (2.7047(8) Å) is slightly shorter than the sum of the van der Waals radii for 2 x Cu(I) (2.80 Å). In the dimeric molecules of **33**, the –$SiMe_3$ moieties adopt a *trans* orientation. The Cu-Se-Cu angles of **33** are smaller (63.00(2)°) compared to the related angles in **32** (71.19(2)°). On the other hand the Se-Cu-Se angle in **33** (103.86(2)°) is considerably larger than the related angle in **32** (89.01(2)°). Consequently molecules of **33** show shorter Cu···Cu separation (2.6125(9) Å) than is observed in **32**.

^1H and $^{13}C\{^1H\}$ NMR spectra of **32** were obtained at low temperature via dissolving crystalline samples in $CDCl_3$. Due to the lower stability of **33** in solution, spectral analysis was completed by monitoring reaction solutions. A clear, colorless reaction solution of [($^iPr_2$-bimy)CuOAc] in deuterated chloroform was cooled to -40 °C and treated with 1 equivalent of $Se(SiMe_3)_2$. The ^1H and $^{13}C\{^1H\}$ NMR spectra of the reaction solution display, in addition to the peaks of ligated carbene, those arising from the formed $(AcO)SiMe_3$ and the appearance of an additional signal in the high-field region assigned to the -$SeSiMe_3$. There is an evident downfield shift observed in the ^1H NMR spectra for the $SiMe_3$ signals on going from S (0.25 ppm) to Se (0.45 ppm) (Figure 6.6). These chemical shifts are themselves well downfield from those of [(IPr)Cu-$ESiMe_3$] (δ = -0.17 S; -0.04, Se)[8] and this may suggest that the bridging interaction of the E-$SiMe_3$ is retained in solution. Monitoring the ^1H NMR spectra of **33** over a period of one hour at -35 °C revealed that the intensity of the peaks corresponding to **33** decreases accompanied via the growth of a new set of resonances for a $^iPr_2$-bimy containing species (Figure 6.7) together with an overall darkening of the color of the reaction solution to dark brown.

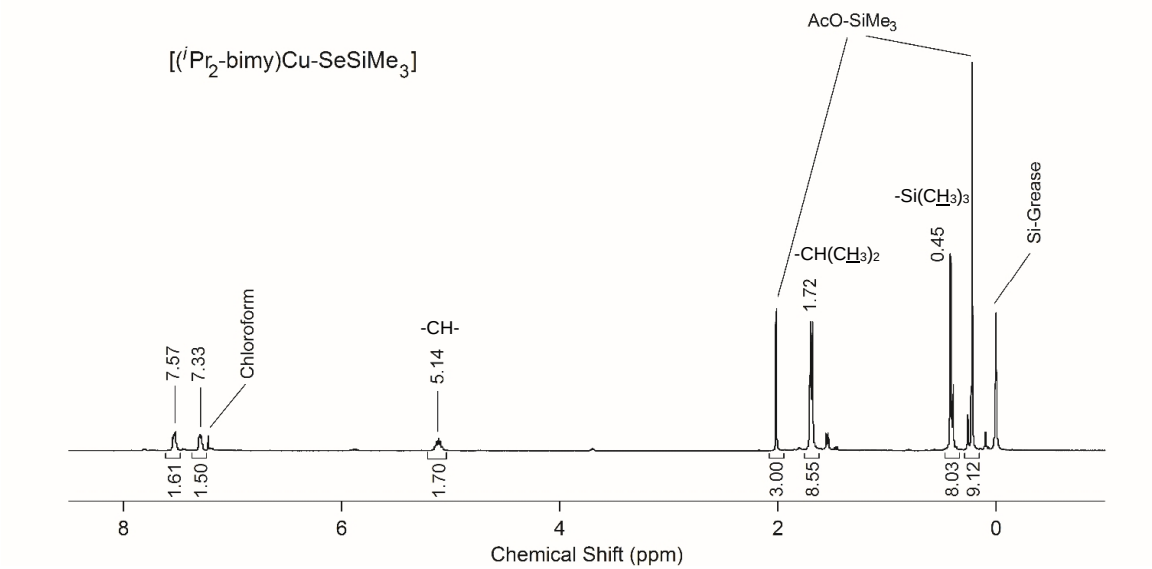

Figure 6.6. ^{1}H NMR of [(^{i}Pr$_2$-bimy)Cu-SeSiMe$_3$], **33** ($CDCl_3$, -35 °C, 399.76 MHz), ~20-30 min after the reaction.

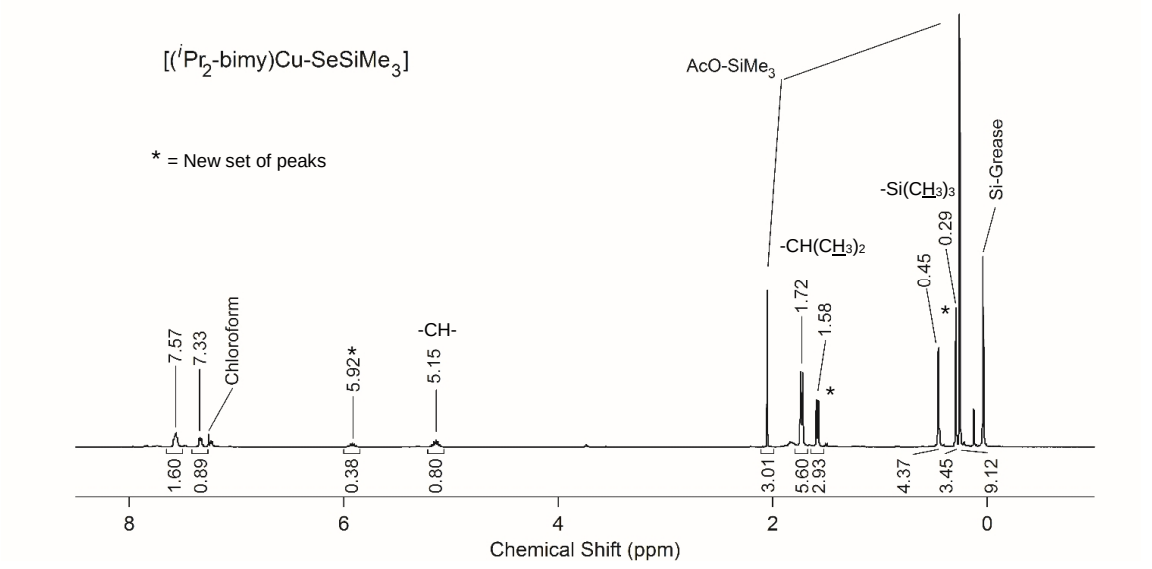

Figure 6.7. ^{1}H NMR of [(^{i}Pr$_2$-bimy)Cu-SeSiMe$_3$], **33** ($CDCl_3$, -35 °C, 399.76 MHz), ~ 60-80 min after the reaction.

The reactivity of the E-Si bond and the effect of the smaller NHC ligand in [(^{i}Pr$_2$-bimy)Cu-SSiMe$_3$] are both demonstrated with the formation of the nanocluster [(^{i}Pr$_2$-bimy)$_6$Cu$_{10}$S$_8$Hg$_3$] **34**, when a solution of **32** is treated with 0.5 equivalents of Hg(OAc)$_2$ (Scheme 6.2b). Storage of the reaction solution at -25 °C leads to the selective formation of yellow crystals of **34**. X-ray analysis indicates that **34** is composed of 10 copper and 3 mercury atoms and 8 sulfide bridging ligands, and this core is stabilized with six surface ^{i}Pr$_2$-bimy. This framework can be contrasted with that of [{(IPr)CuS}$_2$Hg], which forms with the larger NHC under similar reaction conditions.[8] In cluster **34** there are four, two-coordinate near-linear Cu(I) in **34** bonded to two adjacent bridging sulfide atoms, one in the center (∠S-Cu-S = 176.32°) and three on the edges of the cluster (∠S-Cu-S = 175.08(9)-177.14(9)°; Figure 6.8). The other six Cu(I) assume distorted trigonal planar geometry, bonded to two μ_3-bridging sulfide ligands and each terminally bonded to a ^{i}Pr$_2$-bimy. There is little variation observed in the Cu-C bond lengths (1.910(1)-1.959(9) Å) which are themselves similar to those in the precursor **32**. The three Hg(II) are each bonded to two sulfide ligands, leading to a distorted linear S-Hg-S arrangement (∠S-Hg-S = 172.42(8)-173.29(7)°). The Hg-S bond lengths range from 2.322(2) to 2.336(3) Å. Six sulfide ligands adopt μ_3 face-capping coordination modes with one Hg and two Cu atoms. The other two sulfide ligands are μ_4-bonded to the central Cu and three outer Cu. The closest Cu···Cu and Cu···Hg contacts are 2.762(1) and 2.971(1) Å, respectively, consistent with the d^{10} electron configurations on the metal.[11] Structurally, cluster **34** can be viewed as being intermediate in size between the trinuclear [{(IPr)CuS}$_2$Hg] and the phosphine ligated [Hg$_{15}$Cu$_{20}$S$_{25}$(PPr$_3$)$_{18}$][6a] although, clearly, the varying Cu:Hg ratio prevents a more in depth comparison. Each of these represents a rare example of a Cu(I)/Hg(II)-sulfide cluster.

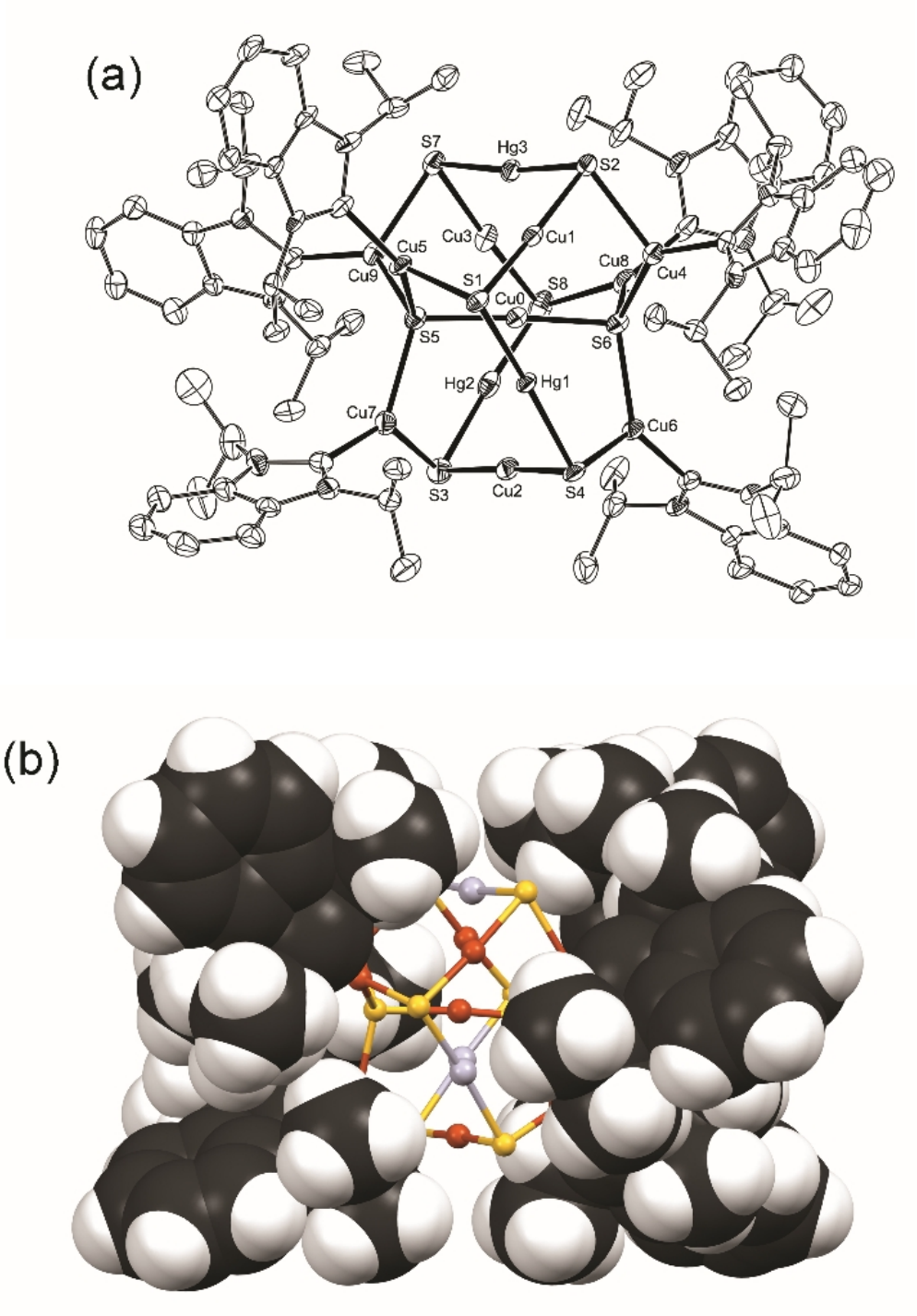

Figure 6.8. Molecular structure of [(^{i}Pr$_2$-bimy)$_6$Cu$_{10}$S$_8$Hg$_3$] **34** in the crystal (a) Thermal ellipsoid diagram (40 % probability; hydrogen atoms omitted), (b) Space-filling diagram of the (^{i}Pr$_2$-bimy) surface ligands together with ball-and-stick diagram of the Cu$_{10}$S$_8$Hg$_3$ core: Cu=orange, S=yellow, Hg=grey, C=black, H=white.

Crystals of [(^{i}Pr$_2$-bimy)$_6$Cu$_{10}$S$_8$Hg$_3$] **34** display a broad emission at ~800 nm (Figure 6.9); this can be contrasted with the recent reports by Eichhöfer and co-workers on the luminescent properties of similarly sized [Cu$_{12}$S$_6$(L∩L)] clusters (L∩L = bidentate phosphine ligand), with strong, sharp emissions being observed ~ 700 nm.[12] Crystals of **34** are stable under an inert atmosphere at room temperature; however, in solution the clusters decompose quickly, as evidenced by the formation of a black-colored suspension in the reaction solution. Although crystals of **34** are unstable in solution, ^{1}H and ^{13}C{^{1}H} NMR spectra can be obtained by dissolving the crystals in cold CDCl$_3$ (-30 °C; NMR spectra of **34** display only one set of resonances for the ligated carbenes.

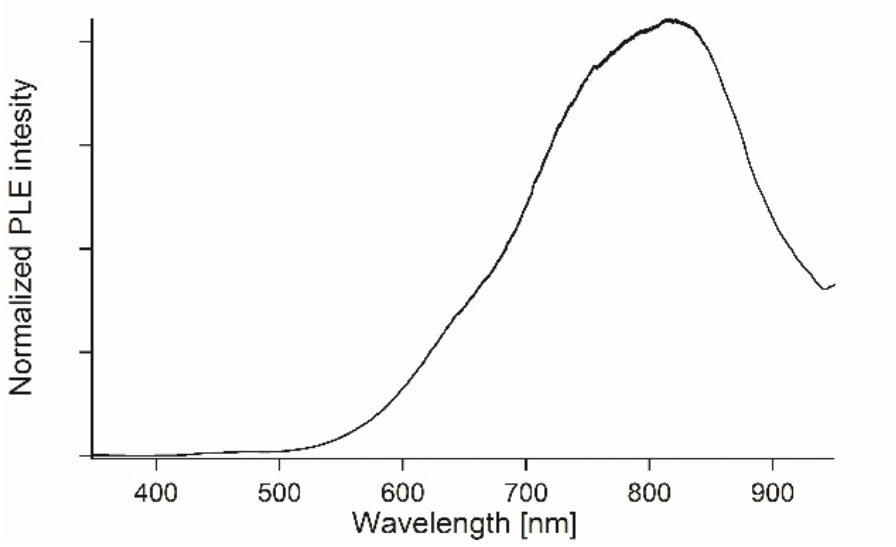

Figure 6.9. Photoluminescence emission spectra for **34** as dried crystalline powder measured at ambient temperature.

6.3 Experimental Section

All syntheses were carried out under an atmosphere of high-purity dried nitrogen using standard double-manifold Schlenk line techniques and nitrogen-filled glove boxes unless otherwise stated. Solvents were dried and collected using an MBraun MB-SP Series solvent purification system with tandem activated alumina (tetrahydrofuran) and an activated alumina/copper redox catalyst (pentane). Chlorinated solvents (chloroform-d, dichloromethane-d2) were dried and distilled over P_2O_5.

Other chemicals were used as received from commercial sources (Alfa Aesar and Aldrich). [(IPr)AgOAc],[13] (^{i}Pr$_2$-bimy).HI[14] and E(SiMe$_3$)$_2$ (E = S, Se)[5d, 15] were synthesized according to literature procedures.

NMR spectra were recorded on Varian Mercury 400, Inova 400 and Inova 600 NMR spectrometers. ^{1}H and ^{13}C{^{1}H} chemical shifts are referenced to SiMe$_4$, using solvent peaks as a secondary reference.

Elemental analysis was performed by Laboratoire d′Analyze Élementaire de l′Université de Montréal, Montréal, Canada. Samples were dried for ~twelve hours prior to send for analysis. Experimentally obtained values of elemental analysis and NMR spectra suggests some residual lattice solvent remained for **32** (~0.75 THF molecule per molecular formula).

Single-crystal X-ray diffraction measurements were completed on a Bruker APEX-II CCD diffractometer equipped with graphite-monochromated Mo Kα (λ = 0.71073 Å) radiation. Single crystals of the complexes were carefully selected, immersed in paraffin oil and mounted on MiteGen micromounts. The structures were solved using direct methods and refined by the full-matrix least-squares procedure of SHELXTL.[16] All non-hydrogen atoms, with the exception of disordered carbon centers, were refined with anisotropic thermal parameters. For **31**, the TWIN command in SHELXTL was used to refine the structure. In **34** some of the disordered THF solvents in the crystal packing were removed by the SQUEEZE program. Solid state PL spectra were obtained at room temperature using the experimental setup shown in Figure 6.10. An excitation beam from

laser diode (US-Lasers, Inc.) with wavelength 405 ± 10 nm and power output of 120 mW was filtered using a low pass (405 nm) filter. The emitted fluorescence was filtered using a long pass filter and analyzed using a HRS-BD1 Mightex Spectrometer equipped with CCD multichannel detector with entrance slit size 10 μm and wavelength range 300-1050 nm. Calibration and data processing were performed with custom-made code using Matlab (version 2014) software.

To prepare samples for solid state PL measurements, a small amount of solid material was suspended in 1-2 ml of pentane. One drop of such a suspension was placed on a cleaned Si wafer and allowed to evaporate; procedure was repeated until desired density of coverage was achieved, then the substrate with a thin film of a sample was thoroughly dried, finally under vacuum.

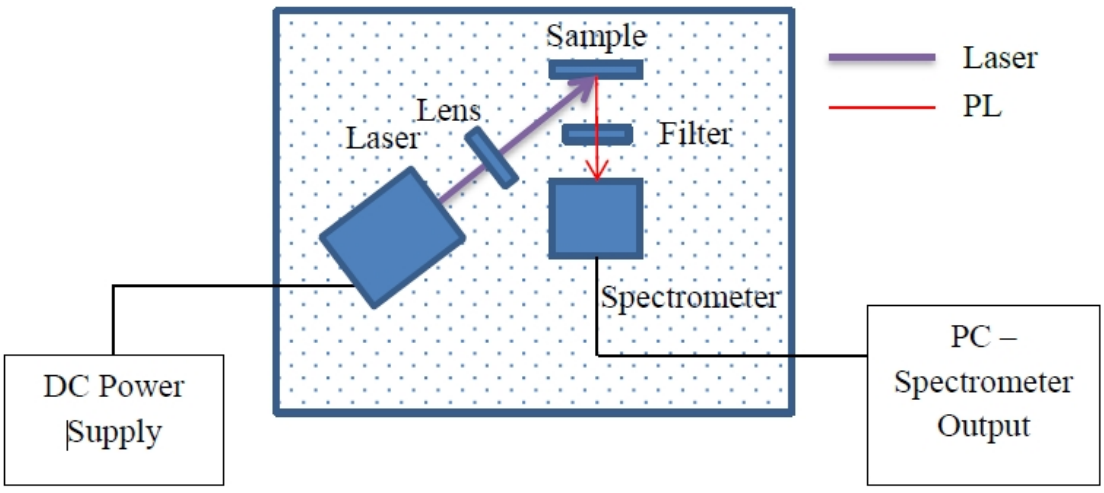

Figure 6.10. Schematic of the experimental setup used for PL measurements in solid state.

6.3.1 Synthesis of [(IPr)Ag-SSiMe$_3$] **29**

38 μL of S(SiMe$_3$)$_2$ (0.18 mmol) was added to the cold (-70 °C) solution of one equivalent of [(IPr)AgOAc] (100 mg, 0.18 mmol) in 10 mL tetrahydrofuran, followed by storing the solution at -25 °C overnight. The reaction was layered with 30 mL of pentane at this temperature. Colorless, block-like single crystals formed after 3-4 days. The crystals were washed with 3×10 mL cold pentane (-70°C) and dried under dynamic vacuum (75 % yield); m.p. 175-179 °C.

Performing the reaction in $CDCl_3$ at -40 °C and maintaining the solution at -25 °C confirmed the concomitant formation of [(IPr)Ag-SSiMe$_3$] and the side product (AcO)SiMe$_3$ via ^{1}H NMR spectroscopy.

- ^{1}H NMR for **29** ($CDCl_3$, 599.36 MHz, 25 °C): δ 7.46 (t, J = 7.6 Hz, 2H, *para*-C*H*), 7.28 (d, J = 7.6 Hz, 4H, *meta*-C*H*), 7.18 (s, 2H, NC*H*), 2.56 (sept., J = 7.0 Hz, 4H, C*H*(CH$_3$)$_2$), 1.29 (d, J = 7.0 Hz, 12H, CH(C*H*$_3$)$_2$), 1.20 (d, J = 7.0 Hz, 12H, CH(C*H*$_3$)$_2$), -0.13 (s, 9H, -Si(C*H*$_3$)$_3$) ppm.
- ^{13}C{^{1}H} NMR ($CDCl_3$, 100.53 MHz, -30 °C): 145.3 (*ortho-C*), 134.5 (*ipso-C*), 130.3 (*para-C*), 124.0 (*meta-C*), 123.1 (N*C*H), 28.5 (*C*H(CH$_3$)$_2$), 24.9 (CH(*C*H$_3$)$_2$), 23.9 (CH(*C*H$_3$)$_2$), 7.0 (-Si(*C*H$_3$)$_3$) ppm.
- Anal. Calcd for $C_{30}H_{45}AgN_2SSi$: C, 59.88; H, 7.45; N, 4.66; S, 5.33. Found: C, 60.02; H, 7.56; N, 4.63; S, 4.32.

6.3.2 Synthesis of [(IPr)AgSeSiMe$_3$] **30**

35 μL of Se(SiMe$_3$)$_2$ (0.14 mmol) was reacted with one equivalent of [(IPr)AgOAc] (78 mg, 0.14 mmol) in 10 mL tetrahydrofuran as described for the preparation of **29**. Colourless block single crystals suitable for X-ray diffraction were obtained after five to six days by layering the mother liquor with 30 mL of pentane at -25 °C (55 % yield); m.p. 170-175 °C.

Monitoring this reaction via ^{1}H NMR spectroscopy in $CDCl_3$ showed the formation of **30** and trimethylsilylacetate.

- ^{1}H NMR ($CDCl_3$, 399.76 MHz, -30 °C): δ 7.47 (t, J = 7.8 Hz, 2H, *para*-C*H*), 7.28 (d, J = 7.8 Hz, 4H, *meta*-C*H*), 7.21 (s, 2H, NC*H*), 2.51 (sept., J = 7.0 Hz, 4H, C*H*(CH_3)$_2$), 1.30 (d, J = 7.0 Hz, 12H, CH(C*H*$_3$)$_2$), 1.20 (d, J = 7.0 Hz, 12H, CH(C*H*$_3$)$_2$), -0.02 (s, 9H, -Si(C*H*$_3$)$_3$) ppm.
- $^{13}C\{^{1}H\}$ NMR ($CDCl_3$, 100.53 MHz, -30 °C): 145.3 (*ortho-C*), 134.5 (*ipso-C*), 130.3 (*para-C*), 124.0 (*meta-C*), 123.1 (N*C*H), 28.5 (*C*H(CH_3)$_2$), 25.0 (CH(*C*H$_3$)$_2$), 23.8 (CH(*C*H$_3$)$_2$), 7.6 (-Si(*C*H$_3$)$_3$) ppm.
- Anal. Calcd for $C_{30}H_{45}AgN_2SeSi$: C, 55.55; H, 6.99; N, 4.32. Found: C, 55.59; H, 7.10; N, 4.25.

6.3.3 Synthesis of [{(IPr)AgS}$_2$Hg] **31**

53 μL of S(SiMe$_3$)$_2$ (0.251 mmol) was added to the cold (-70 °C) solution of one equivalent of [(IPr)AgOAc] (140 mg, 0.251 mmol) in 10 mL tetrahydrofuran, followed by storage at -25 °C overnight. The reaction solution was cooled down to -70 °C again to mix with 5 mL solution of 125 mmol Hg(OAc)$_2$ (40 mg) at this temperature. After warming and keeping the solution to -25 °C for 6 hrs, the solvent was layered with cold pentane (-70 °C). Colourless block single crystals suitable for X-ray diffraction were obtained after five to six days (~30 % yield); m.p. 190 -195 °C (decom.).

- ^{1}H NMR ($CDCl_3$, 399.76 MHz, -30 °C): δ 7.44 (t, J = 7.8 Hz, 4H, *para*-C*H*), 7.23 (d, J = 7.8 Hz, 8H, *meta*-C*H*), 7.14 (s, 4H, NC*H*), 2.45 (sept., J = 7.0 Hz, 8H, C*H*(CH_3)$_2$), 1.24 (d, J = 7.0 Hz, 24H, CH(C*H*$_3$)$_2$), 1.14 (d, J = 7.0 Hz, 24H, CH(C*H*$_3$)$_2$) ppm.
- $^{13}C\{^{1}H\}$ NMR ($CDCl_3$, 100.53 MHz, -30 °C): δ 145.2 (*ortho-C*), 134.4 (*ipso-C*), 130.4 (*para-C*), 124.0 (*meta-C*), 122.9 (N*C*H), 28.5 (*C*H(CH_3)$_2$), 25.2 (CH(*C*H$_3$)$_2$), 23.7 (CH(*C*H$_3$)$_2$) ppm.
- Anal. Calcd for $C_{30}H_{45}AgN_2SeSi$: C, 51.57; H, 5.77; N, 4.45; S, 5.10. Found: C, 51.77; H, 5.89; N, 4.45; S, 5.05.

6.3.4 Synthesis of [(^{i}Pr$_2$-bimy)CuOAc]

A 100-mL Schlenk flask was charged with copper(I) acetate (0.67 g, 5.49 mmol) and ^{i}Pr$_2$-bimy. THF (25 mL) was added via syringe. The resulting cloudy yellow solution was stirred for 12 hours, and then filtered through Celite. The clear, gold-colored filtrate was dried *in vacuo* affording [(^{i}Pr$_2$-bimy)CuOAc] as an off-white powder, 1.62 g (90.8 %); m.p. 145-148 °C.

- ^{1}H NMR ($CDCl_3$, 399.76 MHz, 25 °C): δ 7.55 (m, 2H), 7.33 (m, 2H), 5.09 (sept., J = 7.0 Hz, 2H, C*H*$(CH_3)_2$), 2.15 (br, 3H, C*H*$_3$C$(O)_2$) 1.77 (d, J = 7.0 Hz, 12H, CH(C*H*$_3)_2$) ppm.
- ^{13}C{^{1}H} NMR (CD_2Cl_2, 100.53 MHz, 25 °C): 133.2, 123.3,112.0 (Ar-*C*), 52.6 (*C*H$(CH_3)_2$), 22.9 (CH(*C*H$_3)_2$) ppm.
- Anal. Calcd for $C_{15}H_{21}CuN_2O_2$: C, 55.45; H, 6.52; N, 8.62. Found: C, 55.25; H, 6.56; N, 8.56.

6.3.5 Synthesis of [(^{i}Pr$_2$-bimy)CuSSiMe$_3$] **32**

83 μL of S$(SiMe_3)_2$ (0.33 mmol) was added to a cold (-70 °C) solution of [(^{i}Pr$_2$-bimy)CuOAc] (108 mg, 0.33 mmol) in 10 mL tetrahydrofuran, followed by storing the solution at -25 °C overnight. The reaction was layered with 30 mL of pentane at low temperature. Three to four days later colorless block-like single crystals were obtained. The crystals were washed with 3×10 mL cold pentane (-70°C) and dried under dynamic vacuum for further analysis (45 % yield); m.p. 91-93 °C.

- ^{1}H NMR (CD_2Cl_2, 399.76 MHz, -60 °C): δ 7.58 (m, 2H), 7.32 (m, 2H), 5.08 (sept., J = 7.0 Hz, 2H, C*H*$(CH_3)_2$), 1.69 (d, J = 7.0 Hz, 12H, CH(C*H*$_3)_2$), 0.25 (s, 9H, -Si(C*H*$_3)_3$) ppm.
- ^{13}C{^{1}H} NMR (CD_2Cl_2, 100.53 MHz, -60 °C): 132.7, 122.9,112.2 (Ar-*C*), 52.7 (*C*H$(CH_3)_2$), 22.5 (CH(*C*H$_3)_2$), 6.9 (-Si(*C*H$_3)_3$) ppm.
- Anal. Calcd for $C_{16}H_{27}CuN_2SSi$·0.75THF: C, 53.67; H, 7.82; N, 6.59; S, 7.54. Found: C, 53.15; H, 8.06; N, 6.93; S, 7.38.

6.3.6 Synthesis of [(^{i}Pr$_2$-bimy)CuSeSiMe$_3$] **33**

74 μL of Se(SiMe$_3$)$_2$ (0.296 mmol) was added to the cold (-70 °C) solution of one equivalent of [(^{i}Pr$_2$-bimy)CuOAc] (96 mg, 0.296 mmol) in 10 mL tetrahydrofuran, followed by storing the solution at -40 °C overnight. The reaction was layered with 30 mL of pentane at low temperature. Three to four days later colourless needle-like single crystals formed. The crystals were washed with 3×10 mL cold pentane (-70°C) and dried under dynamic vacuum for further analysis (~ 10 % yield).

- ^{1}H NMR (CDCl$_3$, 399.76 MHz, -35 °C): δ 7.57 (m, 2H), 7.33 (m, 2H), 5.14 (sept., J = 7.0 Hz, 2H, C*H*(CH$_3$)$_2$), 1.72 (d, J = 7.0 Hz, 12H, CH(C*H*$_3$)$_2$), 0.45 (s, 9H, -Si(C*H*$_3$)$_3$) ppm;
- ^{13}C{^{1}H} NMR (CDCl$_3$, 100.53 MHz, -35 °C): 132.6, 123.1,112.2 (Ar-*C*), 52.6 (*C*H(CH$_3$)$_2$), 22.7 (CH(*C*H$_3$)$_2$), 7.6 (-Si(*C*H$_3$)$_3$) ppm.

6.3.7 Synthesis of [(^{i}Pr$_2$-bimy)$_6$Cu$_{10}$S$_8$Hg$_3$] **34**

A solution of [(^{i}Pr$_2$-bimy)Cu-SSiMe$_3$] (0.37 mmol) in 10 mL THF, prepared as described above and cooled to -70 °C, was added to a 5 mL solution of 0.18 mmol of Hg(OAc)$_2$ (57 mg) in THF at this temperature. The yellow solution was warmed to -25 °C. and maintained at this temperature Yellow, block-like single crystals suitable for X-ray diffraction were obtained after six days (50 % yield); m.p. (decomp.) ~100 °C.

- ^{1}H NMR (CDCl$_3$, 399.76 MHz, -30 °C): δ 7.78 (m, 2H), 7.52 (m, 2H), 5.33 (sept., J = 7.0 Hz, 2H, C*H*(CH$_3$)$_2$), 1.74 (d, J = 7.0 Hz, 12H, CH(C*H*$_3$)$_2$) ppm.
- ^{13}C{^{1}H} NMR (CDCl$_3$, 100.53 MHz, -30 °C): 129.2, 125.6,114.8 (Ar-*C*), 52.1 (*C*H(CH$_3$)$_2$), 21.0 (CH(*C*H$_3$)$_2$) ppm.
- Anal. Calcd for C$_{78}$H$_{108}$Cu$_{10}$Hg$_3$S$_8$N$_{12}$: C, 34.60; H, 4.02; N, 6.21; S, 9.47. Found: C, 35.07; H, 4.29; N, 5.89; S, 9.54.

6.4 Conclusion

Exploiting the stabilizing effect of ligated N-heterocyclic carbenes to metal-chalcogenolate M-ESiMe$_3$ moieties, here we have isolated [(IPr)Ag-ESiMe$_3$] and [(^{i}Pr$_2$-bimy)Cu-ESiMe$_3$] (E = S, Se) complexes. The reaction of [(IPr)Ag-SSiMe$_3$] with mercuric(II) acetate afforded the heterometallic complex [{(IPr)AgS}$_2$Hg], representing the first example of a mixed silver-mercury-sulfide cluster complex. The smaller NHC ^{i}Pr$_2$-bimy provides decent stability for –Cu-SSiMe$_3$, although [(^{i}Pr$_2$-bimy)Cu-SeSiMe$_3$] was dramatically less thermally stable. Using [(^{i}Pr$_2$-bimy)Cu-SSiMe$_3$] as a precursor for ternary cluster formation led to the high nuclearity [(^{i}Pr$_2$-bimy)$_6$Cu$_{10}$S$_8$Hg$_3$] demonstrating the dramatic effect of changing surface ligands in this system. The strategy outlined above for the synthesis of NHC stabilized metal chalcogenolate complexes offers a powerful new route into a variety of binary and ternary metal-chalcogen clusters.

6.5 References

[1] (a) Fuhr, O.; Dehnen, S.; Fenske, D., *Chem. Soc. Rev.* **2013,** *42*, 1871-1906; (b) DeGroot, M. W.; Corrigan, J. F., In *Comprehensive Coordination Chemistry II,*, M. Fujita; Powell, A.; C. Creutz, Eds. 2004; Vol. 7, pp 57–113; (c) Corrigan, J. F.; Fuhr, O.; Fenske, D., *Adv. Mater.* **2009,** *21*, 1867-1871.

[2] (a) Stieler, R.; Burrow, R. A.; Piquini, P.; Lang, E. S., *J. Organomet. Chem.* **2012,** *703*, 9-15; (b) Singh, N.; Gupta, S., *Int. J. Inorg. Mater.* **2000,** *2*, 427-435.

[3] (a) Singh, N.; Gupta, S.; Sinha, R. K., *Inorg. Chem. Commun.* **2003,** *6*, 416-422; (b) Singh, N.; Singh, V., *Transition Met. Chem.* **2001,** *26*, 435-439.

[4] (a) DeGroot, M. W.; Corrigan, J. F., *Organometallics* **2005,** *24*, 3378-3385; (b) Shapley, P. A.; Liang, H.-C.; Dopke, N. C., *Organometallics* **2001,** *20*, 4700-4704; (c) Khadka, C. B.; Macdonald, D. G.; Lan, Y. H.; Powell, A. K.; Fenske, D.; Corrigan, J. F., *Inorg. Chem.* **2010,** *49*, 7289-7297; (d) Niebel, T.; MacDonald, D. G.; Khadka, C. B.; Corrigan, J. F., *Z. Anorg. Allg. Chem.* **2010,** *636*, 1095-1099; (e) Bonasia, P. J.; Gindelberger, D. E.; Arnold, J., *Inorg. Chem.* **1993,** *32*, 5126-5131.

[5] (a) Howarth, A.; Liu, J.; Konermann, L.; Corrigan, John F., *Z. Anorg. Allg. Chem.* **2011,** *637*, 1203-1206; (b) DeGroot, M. W.; Taylor, N. J.; Corrigan, J. F., *J. Am. Chem. Soc.* **2003,** *125*, 864-865; (c) DeGroot, M. W.; Taylor, N. J.; Corrigan, J. F., *Inorg. Chem.* **2005,** *44*, 5447-5458; (d) DeGroot, M. W.; Taylor, N. J.; Corrigan, J. F., *J. Mater. Chem.* **2004,** *14*, 654-660.

[6] (a) Tran, D. T. T.; Taylor, N. J.; Corrigan, J. F., *Angew. Chem., Int. Ed.* **2000,** *39*, 935-937; (b) Borecki, A.; Corrigan, J. F., *Inorg. Chem.* **2007,** *46*, 2478-2484; (c) Tran, D. T. T.; Beltran, L. M. C.; Kowalchuk, C. M.; Trefiak, N. R.; Taylor, N. J.; Corrigan, J. F., *Inorg. Chem.* **2002,** *41*, 5693-5698; (d) Kluge, O.; Biedermann, R.; Holldorf, J.; Krautscheid, H., *Chem. -Eur. J.* **2014,** *20*, 1318-1331.

[7] (a) Tran, D. T. T.; Corrigan, J. F., *Organometallics* **2000,** *19*, 5202-5208; (b) DeGroot, M. W.; Corrigan, J. F., *Z. Anorg. Allg. Chem.* **2006,** *632*, 19-29; (c) Wallbank, A. I.; Corrigan, J. F., *Can. J. Chem.-Rev. Can. Chim.* **2002,** *80*, 1592-1599; (d) DeGroot, M. W.; Corrigan, J. F., *Angew. Chem.-Int. Edit.* **2004,** *43*, 5355-5357.

[8] Fard, M. A.; Weigend, F.; Corrigan, J. F., *Chem. Commun.* **2015,** *51*, 8361-8364.

[9] Fenske, D.; Anson, C. E.; Eichhöfer, A.; Fuhr, O.; Ingendoh, A.; Persau, C.; Richert, C., *Angew. Chem., Int. Ed.* **2005,** *44*, 5242-5246.

[10] Clavier, H.; Nolan, S. P., *Chem. Commun.* **2010,** *46*, 841-861.

[11] (a) Sculfort, S.; Braunstein, P., *Chem. Soc. Rev.* **2011,** *40*, 2741-2760; (b) Merz, K. M.; Hoffmann, R., *Inorg. Chem.* **1988,** *27*, 2120-2127.

[12] Yang, X.-X.; Issac, I.; Lebedkin, S.; Kuhn, M.; Weigend, F.; Fenske, D.; Fuhr, O.; Eichhofer, A., *Chem. Commun.* **2014,** *50*, 11043-11045.

[13] Yamashita, K.; Hase, S.; Kayaki, Y.; Ikariya, T., *Org. Lett.* **2015,** *17*, 2334-2337.

[14] Chen, W.-C.; Lai, Y.-C.; Shih, W.-C.; Yu, M.-S.; Yap, G. P. A.; Ong, T.-G., *Chem. - Eur. J.* **2014,** *20*, 8099-8105.

[15] So, J. H.; Boudjouk, P., *Synthesis* **1989**, 306-307.

[16] (a) Sheldrick, G. M., SHELXTL PC Version 6.1 An Integrated System for Solving, Refining, and Displaying Crystal Structures from Diffraction Data, Bruker Analytical X-ray Systems, 2000;; (b) Sheldrick, G. M., *Acta Crystallogr. Sect. A* **2008,** *64*, 112-122.

Chapter 7

Functional -$ESiMe_3$ Containing Reagents: From Organo-polychalcogenolates to NHC Ligated M-E-$SiMe_3$

7.1 Conclusion and Future Work

The research described in this thesis focused around two main aspects of chalcogen chemistry. First, the preparation of a new series of polychalcogenolate complexes and their potential in the synthesis of polychalcogenoesters was developed (Chapter 2). Furthermore, their coordination behavior was explored in different systems (Chapter 3 and 4). In the second area, a new methodology to prepare thermally stable "metallachalcogenolate" precursors via the ligation of ancillary N-heterocyclic carbene ligands was probed. Also developed was the behavior of these complexes in reactions with a second metal salt as a route to ternary MM´E clusters.

7.1.1 Polychalcogenolates

In Chapter 2 a straightforward synthesis of a novel series of di-, tri-, and tetra-chalcogenotrimethylsilanes ($Ar(CH_2ESiMe_3)_n$, E = S, Se, n = 2 , 3 and 4) was described. These complexes are prepared by the reaction of lithium/sodium (trimethylsilyl)chalcogenolate Li/Na[$ESiMe_3$] with the corresponding polyorganobromide.

As was already highlighted, these complexes are the first examples of molecules containing such a large number of reactive –$ESiMe_3$ groups onto an organic spacer.

These reagents represent a new class of reactive poly-functionalized precursors for the facile preparation of poly chalcogenoesters; the latter have attracted considerable attention due to in part the importance of these systems in organic synthesis. In this context the reaction between these poly chalcogenolate precursors and ferrocenyl acid chloride led to the formation of a new series of polyferrocenylseleno- and thioester assemblies. This methodology can be applied in the synthesis of other polychalcogenoesters via reactions with various acyl chlorides.

It has been demonstrated previously that silylated chalcogen reagents of the type $RESiMe_3$ (R = an organic group, E = S, Se) are a convenient source of organo-chalcogenide (RE^-) in metal chalcogen bond formation reactions.[1] As part of the continued interest in developing this methodology in the synthesis of polymetallic chalcogenolates via organochalcogenotrimethylsilane reagents, the coordination chemistry of $Ar(CH_2ESiMe_3)_n$ in two different systems was developed. In the first system, which was discussed in Chapter 3, the reaction of [(dppp)$PdCl_2$], (1,3-bis(diphenylphosphino)propane)palladium(II), with $Ar(CH_2ESiMe_3)_n$ (E = S, Se) when n = 2 (ortho) or 4 (1,2,4,5) provided a single- or double-butterfly shaped Pd_2E_2 cluster on the aromatic spacer, respectively. In the second system (Chapter 4) the silylated reagents $Ar(CH_2ESiMe_3)_n$ (n = 2 (para), 3 (1,3,5)) were used to form a series of multinuclear carbene-copper chalcogenolates complexes, $Ar(CH_2ECuIPr)_n$ via reaction with [(IPr)CuOAc]. These results represent a new route to prepare suitable polydentate chalcogen based spacers in the synthesis of organic-inorganic frameworks. Future work could involve further expansion of this methodology by using various carbene metal salts and exploring their structural features.

7.1.2 [(NHC)M-$ESiMe_3$]

The molecular precursor approach to ternary nanocluster MEM´ (M = coinage metal, E = S, Se, Te; M´ = second metal) was investigated and is described in Chapter 5 and 6. Prior

work in this area centred on precursors that are stabilized via the coordination of tertiary phosphines (trialkyl-, dialkylaryl- or alkyldiarylphosphine) to copper(I)- and silver(I)-trimethylsilylchalcogenolates. While these sources of "metallachalcogenolate", ME^- resulted in the formation of several interesting ternary M-E-M´ clusters, their low melting points and thermal instability render them relatively difficult to handle. In this context using the alternate ancillary ligand N-heterocyclic carbene (NHC), the stability of M-$ESiMe_3$ was increased at the same time promoting an oriented coordination on the metal centre.

In Chapter 5, the preparation of a series of thermally stable NHC ligated copper chalcogenolate complexes of the general formula [(IPr)Cu-$ESiMe_3$] (IPr = 1,3-bis(2,6-diisopropylphenyl)imidazolin-2-ylidene; E = S, Se, Te) was described. These complexes can be prepared selectively in high yield and are useful precursors for ternary M-E-M´. The reaction of [(IPr)Cu-$SSiMe_3$] with mercuric(II) acetate affords the heterometallic complex [{(IPr)CuS}$_2$Hg] containing two (IPr)Cu-S^- fragments bonded to a central Hg(II). In Chapter 6 it was confirmed that the synthesis of the isostructure silver complexes, [(IPr)Ag-$ESiMe_3$] (E = S, Se) and their reactivity toward metal salts was presented. Similar to the copper analogues, the reaction of [(IPr)Ag-$SSiMe_3$] with mercuric(II) acetate afforded the heterometallic complex [{(IPr)AgS}$_2$Hg], representing the first example of a mixed silver-mercury-sulfide cluster complex. Furthermore, the influence of the ancillary ligand on the structural features and thermal stability of –Cu$ESiMe_3$ was evaluated. The smaller NHC ^{i}Pr$_2$-bimy provides decent stability for –Cu$SSiMe_3$, although [(^{i}Pr$_2$-bimy)Cu-$SeSiMe_3$] was dramatically less thermally stable. Using [(^{i}Pr$_2$-bimy)Cu-$SSiMe_3$] as a precursor for ternary cluster led to the high nuclearity [(^{i}Pr$_2$-bimy)$_6$Cu$_{10}$S$_8$Hg$_3$] demonstrating the dramatic effect of changing surface ligands in this system.

With the ability to enhance thermal stability via (NHC)M-$ESiMe_3$ future work should involve further expansion of this methodology to probe the general applicability of various type of N-heterocyclic carbenes; furthermore, a development of this ligand class for other d-block metal-$ESiMe_3$ beyond Group 11 warrants investigation (Figure 7.1). The use of a series of carbene ligands with different structural/chemical features may give a trend between the size of the NHC as the ancillary ligand and the stability of M-$ESiMe_3$ precursor

together with the nuclearity (size/shape) of the formed ternary cluster using such reagents. Indeed, such NHC libraries should also be developed for the formation of *binary* metal-chalcogenide nanocluster frameworks for which PR_3 ligation has been well developed but whose materials chemistry has been limited by the facile ligand dissociation of such species when redissolved in common solvents. The simple approach to metal chalcogen cluster complexes involves the self-assembly of metal and chalcogen in the presence of stabilizing ancillary ligands. Chalcogenolate anions RE^- can also be used in conjunction with chalcogenide to produce mixed chalcogenolate/chalcogenide clusters together with surface NHC ligation.

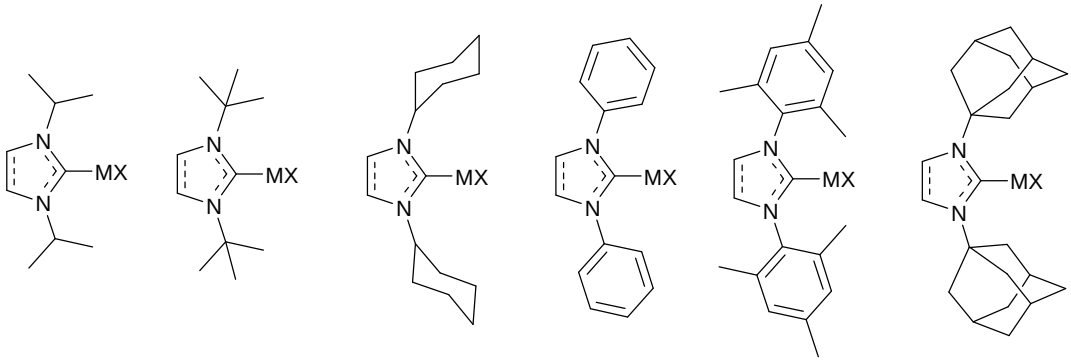

Figure 7.1. Various type of NHC-MX for future work

7.2 References

[1] (a) MacDonald, D. G.; Corrigan, J. F., *Phil. Trans. R. Soc. A* **2010,** *368*, 1455-1472; (b) Fuhr, O.; Dehnen, S.; Fenske, D., *Chem. Soc. Rev.* **2013,** *42*, 1871-1906.

Appendices

Appendix 1 Permission to Reuse Copyrighted Material

JOHN WILEY AND SONS LICENSE TERMS AND CONDITIONS

Jul 16, 2015

This Agreement between Mahmood Azizpoor Fard ("You") and John Wiley and Sons ("John Wiley and Sons") consists of your license details and the terms and conditions provided by John Wiley and Sons and Copyright Clearance Center.

License Number	3671130585795
License date	Jul 16, 2015
Licensed Content Publisher	John Wiley and Sons
Licensed Content Publication	Angewandte Chemie International Edition
Licensed Content Title	Copper Chalcogenolate Complexes as Precursors to Ternary Nanoclusters: Synthesis and Characterization of [Hg15Cu20S25(nPr3P)18]
Licensed Content Author	Diem T. T. Tran,Nicholas J. Taylor,John F. Corrigan
Licensed Content Date	Mar 3, 2000
Pages	3
Type of use	Dissertation/Thesis
Requestor type	University/Academic
Format	Print and electronic
Portion	Figure/table
Number of figures/tables	1
Original Wiley figure/table number(s)	Figure 2
Will you be translating?	No
Title of your thesis / dissertation	synthesis of polychalcogenolate reagents, their structures and coordination chemistry and stabilized M-E-SiMe3 (M = Ag, Cu; E = S, Se, Te) via NHC ligation as a source of "metallachalcogenolate" in ternary complexes
Expected completion date	Aug 2015
Expected size (number of pages)	300

Total 0.00 USD

Terms and Conditions

TERMS AND CONDITIONS

This copyrighted material is owned by or exclusively licensed to John Wiley & Sons, Inc. or one of its group companies (each a"Wiley Company") or handled on behalf of a society with which a Wiley Company has exclusive publishing rights in relation to a particular work (collectively "WILEY"). By clicking accept in connection with completing this licensing transaction, you agree that the following terms and conditions apply to this transaction (along with the billing and payment terms and conditions established by the Copyright Clearance Center Inc., ("CCC's Billing and Payment terms and conditions"), at the time that you opened your Rightslink account (these are available at any time at http://myaccount.copyright.com).

Terms and Conditions

- The materials you have requested permission to reproduce or reuse (the "Wiley Materials") are protected by copyright.
- You are hereby granted a personal, non-exclusive, non-sub licensable (on a stand-alone basis), non-transferable, worldwide, limited license to reproduce the Wiley Materials for the purpose specified in the licensing process. This license is for a one-time use only and limited to any maximum distribution number specified in the license. The first instance of republication or reuse granted by this licence must be completed within two years of the date of the grant of this licence (although copies prepared before the end date may be distributed thereafter). The Wiley Materials shall not be used in any other manner or for any other purpose, beyond what is granted in the license. Permission is granted subject to an appropriate acknowledgement given to the author, title of the material/book/journal and the publisher. You shall also duplicate the copyright notice that appears in the Wiley publication in your use of the Wiley Material. Permission is also granted on the understanding that nowhere in the text is a previously published source acknowledged for all or part of this Wiley Material. Any third party content is expressly excluded from this permission.
- With respect to the Wiley Materials, all rights are reserved. Except as expressly granted by the terms of the license, no part of the Wiley Materials may be copied, modified, adapted (except for minor reformatting required by the new Publication), translated, reproduced, transferred or distributed, in any form or by any means, and no derivative works may be made based on the Wiley Materials without the prior permission of the respective copyright owner. You may not alter, remove or suppress in any manner any copyright, trademark or other notices displayed by the Wiley Materials. You may not license, rent, sell, loan, lease, pledge, offer as security, transfer or assign the Wiley Materials on a stand-alone basis, or any of the rights granted to you hereunder to any other person.

ROYAL SOCIETY OF CHEMISTRY LICENSE TERMS AND CONDITIONS

Jul 16, 2015

This is a License Agreement between Mahmood Azizpoor Fard ("You") and Royal Society of Chemistry ("Royal Society of Chemistry") provided by Copyright Clearance Center ("CCC"). The license consists of your order details, the terms and conditions provided by Royal Society of Chemistry, and the payment terms and conditions.

All payments must be made in full to CCC. For payment instructions, please see information listed at the bottom of this form.

License Number	3671130081675
License date	Jul 16, 2015
Licensed content publisher	Royal Society of Chemistry
Licensed content publication	Chemical Communications (Cambridge)
Licensed content title	N-Heterocyclic carbene stabilized Ag–P nanoclusters
Licensed content author	Bahareh Khalili Najafabadi,John F. Corrigan
Licensed content date	Nov 21, 2014
Volume number	51
Issue number	4
Type of Use	Thesis/Dissertation
Requestor type	academic/educational
Portion	figures/tables/images
Number of figures/tables/images	2
Format	print and electronic
Distribution quantity	6
Will you be translating?	no
Order reference number	None
Title of the thesis/dissertation	synthesis of polychalcogenolate reagents, their structures and coordination chemistry and stabilized M-E-SiMe3 (M = Ag, Cu; E = S, Se, Te) via NHC ligation as a source of "metallachalcogenolate" in ternary complexes
Expected completion date	Aug 2015
Estimated size	300
Total	0.00 CAD

Terms and Conditions

This License Agreement is between {Requestor Name} ("You") and The Royal Society of Chemistry ("RSC") provided by the Copyright Clearance Center ("CCC"). The license consists of your order details, the terms and conditions provided by the Royal Society of Chemistry, and the payment

ROYAL SOCIETY OF CHEMISTRY LICENSE TERMS AND CONDITIONS

Jul 16, 2015

This is a License Agreement between Mahmood Azizpoor Fard ("You") and Royal Society of Chemistry ("Royal Society of Chemistry") provided by Copyright Clearance Center ("CCC"). The license consists of your order details, the terms and conditions provided by Royal Society of Chemistry, and the payment terms and conditions.

All payments must be made in full to CCC. For payment instructions, please see information listed at the bottom of this form.

License Number	3671130887609
License date	Jul 16, 2015
Licensed content publisher	Royal Society of Chemistry
Licensed content publication	Dalton Transactions
Licensed content title	N-heterocyclic carbene stabilized copper- and silver-phenylchalcogenolate ring complexes
Licensed content author	Will J. Humenny,Stefan Mitzinger,Chhatra B. Khadka,Bahareh Khalili Najafabadi,Isabelle Vieira,John F. Corrigan
Licensed content date	Feb 22, 2012
Volume number	41
Issue number	15
Type of Use	Thesis/Dissertation
Requestor type	academic/educational
Portion	figures/tables/images
Number of figures/tables/images	1
Format	print and electronic
Distribution quantity	6
Will you be translating?	no
Order reference number	None
Title of the thesis/dissertation	synthesis of polychalcogenolate reagents, their structures and coordination chemistry and stabilized M-E-SiMe3 (M = Ag, Cu; E = S, Se, Te) via NHC ligation as a source of "metallachalcogenolate" in ternary complexes
Expected completion date	Aug 2015
Estimated size	300
Total	0.00 CAD

Terms and Conditions

This License Agreement is between {Requestor Name} ("You") and The Royal Society of Chemistry

JOHN WILEY AND SONS LICENSE TERMS AND CONDITIONS

Jul 03, 2015

This Agreement between Mahmood Azizpoor Fard ("You") and John Wiley and Sons ("John Wiley and Sons") consists of your license details and the terms and conditions provided by John Wiley and Sons and Copyright Clearance Center.

License Number	3661440099812
License date	Jul 03, 2015
Licensed Content Publisher	John Wiley and Sons
Licensed Content Publication	Chemistry - A European Journal
Licensed Content Title	New Polydentate Trimethylsilyl Chalcogenide Reagents for the Assembly of Polyferrocenyl Architectures
Licensed Content Author	Mahmood Azizpoor Fard,Bahareh Khalili Najafabadi,Mahdi Hesari,Mark S. Workentin,John F. Corrigan
Licensed Content Date	May 7, 2014
Pages	11
Type of use	Dissertation/Thesis
Requestor type	Author of this Wiley article
Format	Print and electronic
Portion	Full article
Will you be translating?	No
Title of your thesis / dissertation	synthesis of polychalcogenolate reagents, their structures and coordination chemistry and stabilized M-E-SiMe3 (M = Ag, Cu; E = S, Se, Te) via NHC ligation as a source of "metallachalcogenolate" in ternary complexes
Expected completion date	Aug 2015
Expected size (number of pages)	300

Royal Society of Chemistry (RSC)

Re-use permission requests

Material published by the Royal Society of Chemistry and other publishers is subject to all applicable copyright, database protection, and other rights. Therefore, for any publication, whether printed or electronic, permission must be obtained to use material for which the author(s) does not already own the copyright. This material may be, for example, a figure, diagram, table, photo or some other image.

Author reusing their own work published by the Royal Society of Chemistry

You do not need to request permission to reuse your own figures, diagrams, etc, that were originally published in a Royal Society of Chemistry publication. However, permission should be requested for use of the whole article or chapter except if reusing it in a thesis. If you are including an article or book chapter published by us in your thesis please ensure that your co-authors are aware of this.

Reuse of material that was published originally by the Royal Society of Chemistry must be accompanied by the appropriate acknowledgement of the publication. The form of the acknowledgement is dependent on the journal in which it was published originally, as detailed in ‘Acknowledgements’.

Appendix 2 Crystallographic Tables

Table A.1. Summary of Crystal Data and Details of the Structure Determination for **1-4**

	1	**2**	**3**	**4**
Formula	$C_{18}H_{34}S_2Si_2$	$C_{18}H_{34}Se_2Si_2$	$C_{21}H_{42}S_3Si_3$	$C_{21}H_{42}Se_3Si_3$
formula Weight	370.75	464.55	475.00	615.70
crystal System	Triclinic	Triclinic	Triclinic	Triclinic
space group	$P\bar{1}$	$P\bar{1}$	$P\bar{1}$	$P\bar{1}$
a (Å)	6.4020(5)	6.2310(3)	10.0634(1)	10.125(2)
b (Å)	7.3238(4)	7.5548(4)	11.5851(2)	11.630(2)
c (Å)	11.9751(9)	12.1830(7)	13.0520(2)	13.257(3)
α (º)	103.313(4)	103.265(2)	86.4372(9)	87.81(3)
β (º)	97.665(3)	97.939(3)	68.2215(9)	67.71(3)
γ (º)	92.821(5)	93.901(3)	79.5821(9)	82.00(3)
V (Å^3)	539.64(7)	549.88(5)	1389.75(4)	1430.2(6)
Z	1	1	2	2
ρ_{cal} (g cm^{-3})	1.141	1.403	1.135	1.430
μ (Mo Kα) (mm^{-1})	0.354	3.468	0.402	3.990
F(000)	202	238	516	624
temperature (K)	150	150	150	150
θ_{min}, θ_{max} (º)	3.0, 27.8	2.8, 27.7	1.7, 39.8	2.2, 27.6
total reflns	4614	4460	90834	11696
unique reflns	2492	2510	16840	6548
R(int)	0.025	0.024	0.071	0.034
R1	0.0405,	0.0397,	0.0543,	0.0496,
wR2 [$I \geq 2\sigma$ (I)]	0.0932	0.1021	0.1269	0.1198
R1 (all data)	0.0551	0.0470	0.1550	0.0816
wR2 (all data)	0.1007	0.1051	0.1736	0.1360
GOF	1.046	1.173	0.992	1.042
min peak	-0.298	-0.596	-0.626	-0.687
max peak	0.284	0.546	1.012	1.494

Table A.2. Atomic Coordinates for **1**

Atom	x	y	z	$U_{iso/equiv}$
S1	0.27134(9)	0.59048(7)	0.22156(4)	0.0366(2)
Si1	0.31362(8)	0.30456(7)	0.13632(4)	0.0258(2)
C1	0.4760(3)	0.8167(2)	0.42992(15)	0.0273(5)
C2	0.6315(3)	0.9462(3)	0.41463(15)	0.0280(5)
C3	0.6589(3)	1.1298(3)	0.48691(15)	0.0287(6)
C4	0.4569(3)	0.6160(3)	0.35784(16)	0.0344(6)
C5	0.7634(4)	0.8939(3)	0.31760(18)	0.0419(7)
C6	0.8346(4)	1.2655(3)	0.47374(18)	0.0403(7)
C7	0.5919(3)	0.2831(3)	0.1081(2)	0.0449(7)
C8	0.2454(4)	0.1449(3)	0.22831(19)	0.0417(7)
C9	0.1311(3)	0.2542(3)	-0.00374(16)	0.0336(6)

Table A.3. Atomic Coordinates for **2**

Atom	x	y	z	$U_{iso/equiv}$
Se1	0.22561(7)	0.40241(5)	0.28535(4)	0.0351(1)
Si1	0.16747(16)	0.69606(13)	0.36564(9)	0.0234(3)
C1	0.0134(6)	0.1775(5)	0.0688(3)	0.0234(10)
C2	-0.1407(6)	0.0420(5)	0.0807(3)	0.0248(10)
C3	0.1580(6)	0.1341(5)	-0.0104(3)	0.0246(10)
C4	0.0223(7)	0.3704(5)	0.1390(3)	0.0298(11)
C5	-0.2845(7)	0.0827(6)	0.1721(4)	0.0385(12)
C6	0.3330(7)	0.2777(6)	-0.0201(4)	0.0346(12)
C7	-0.1224(7)	0.7075(7)	0.3836(5)	0.0458(16)
C8	0.2441(8)	0.8482(6)	0.2736(4)	0.0409(16)
C9	0.3429(7)	0.7585(6)	0.5080(3)	0.0343(12)

Table A.4. Atomic Coordinates for **3**

Atom	x	y	z	$U_{iso/equiv}$
S1	0.08346(5)	0.29167(4)	0.10327(4)	0.0344(1)
S2	0.26831(6)	-0.21428(4)	0.26784(4)	0.0372(1)
S3	0.52153(5)	-0.13240(5)	-0.29411(4)	0.0377(1)
Si1	-0.12673(5)	0.39440(4)	0.18402(4)	0.0301(1)
Si2	0.30151(6)	-0.38914(4)	0.32751(4)	0.0313(1)
Si3	0.71311(5)	-0.10880(4)	-0.43218(4)	0.0287(1)
C1	0.15418(17)	0.06851(14)	0.01865(13)	0.0239(4)
C2	0.12889(17)	-0.02242(14)	0.09619(12)	0.0238(4)
C3	0.23272(18)	-0.12507(14)	0.07912(12)	0.0240(4)
C4	0.36661(17)	-0.13308(14)	-0.00997(13)	0.0243(4)
C5	0.39272(17)	-0.04070(14)	-0.08577(13)	0.0244(4)
C6	0.28541(18)	0.05946(14)	-0.07286(13)	0.0254(4)
C7	0.03961(19)	0.17640(15)	0.03560(15)	0.0288(5)
C8	-0.00911(19)	-0.00732(16)	0.19831(14)	0.0313(5)
C9	0.20057(19)	-0.22706(14)	0.15696(13)	0.0277(4)
C10	0.4825(2)	-0.24054(16)	-0.02434(16)	0.0340(5)
C11	0.53493(18)	-0.05038(15)	-0.18221(13)	0.0281(4)
C12	0.3122(2)	0.15609(17)	-0.15786(16)	0.0365(5)
C13	-0.2368(2)	0.3101(2)	0.30067(19)	0.0489(7)
C14	-0.2206(2)	0.4333(2)	0.08538(19)	0.0496(7)
C15	-0.0899(2)	0.52719(19)	0.2347(2)	0.0469(7)
C16	0.1361(3)	-0.4151(2)	0.4443(2)	0.0578(8)
C17	0.4539(3)	-0.3930(2)	0.3769(2)	0.0539(8)
C18	0.3460(3)	-0.49945(19)	0.2176(2)	0.0523(8)
C19	0.8729(2)	-0.1330(2)	-0.3899(2)	0.0518(8)
C20	0.7294(3)	-0.2195(2)	-0.53558(18)	0.0474(7)

Table A.5. Atomic Coordinates for **4**

Atom	x	y	z	$U_{iso/equiv}$
Se1	0.10389(5)	0.80145(4)	0.09815(4)	0.0463(2)
Se2	0.24296(6)	0.29030(4)	0.28154(4)	0.0469(2)
Se3	0.51429(5)	0.35162(5)	-0.29522(4)	0.0482(2)
Si1	-0.12132(14)	0.89818(12)	0.18823(11)	0.0438(4)
Si2	0.30470(17)	0.10102(13)	0.31461(13)	0.0549(5)
Si3	0.71684(14)	0.38453(12)	-0.44052(9)	0.0408(4)
C1	0.1594(4)	0.5674(4)	0.0164(3)	0.0333(12)
C2	0.1275(4)	0.4797(4)	0.0955(3)	0.0349(12)
C3	0.2265(5)	0.3783(4)	0.0797(3)	0.0334(12)
C4	0.3609(4)	0.3679(4)	-0.0071(3)	0.0335(12)
C5	0.3919(4)	0.4572(4)	-0.0832(3)	0.0338(14)
C6	0.2905(5)	0.5547(4)	-0.0734(3)	0.0350(12)
C7	0.0500(5)	0.6737(4)	0.0311(4)	0.0388(12)
C8	-0.0104(5)	0.4971(4)	0.1960(4)	0.0429(14)
C9	0.1845(5)	0.2774(4)	0.1561(3)	0.0391(12)
C10	0.4710(5)	0.2632(4)	-0.0167(4)	0.0417(14)
C11	0.5341(5)	0.4443(4)	-0.1795(3)	0.0367(12)
C12	0.3238(5)	0.6477(4)	-0.1608(4)	0.0481(17)
C13	-0.2143(6)	0.8196(6)	0.3147(5)	0.069(2)
C14	-0.2269(6)	0.9063(5)	0.0998(5)	0.060(2)
C15	-0.0929(6)	1.0451(5)	0.2189(5)	0.0657(19)
C16	0.1484(9)	0.0489(7)	0.4239(6)	0.100(3)
C17	0.3544(8)	0.0068(5)	0.1937(6)	0.081(3)
C18	0.4567(7)	0.1020(6)	0.3607(6)	0.084(3)
C19	0.8753(6)	0.3597(6)	-0.4002(5)	0.065(2)
C20	0.7323(7)	0.2786(5)	-0.5473(4)	0.0620(19)

Table A.6. Summary of Crystal Data and Details of the Structure Determination for **6**-**8** and **11**

	6	**7**	**8**	**11**
Formula	$C_{22}H_{46}Se_4Si_4$	$C_{34}H_{34}Fe_2O_2S_2$	$C_{34}H_{34}Fe_2O_2Se_2$	$C_{54}H_{46}Fe_4O_4S_4$
formula Weight	738.79	650.43	744.23	1110.55
crystal System	Monoclinic	Triclinic	Monoclinic	Triclinic
space group	$P2_1/c$	$P\bar{1}$	$P2_1/c$	$P\bar{1}$
a (Å)	11.5701(11)	8.0896(16)	5.748(2)	5.7476(5)
b (Å)	6.5046(5)	10.354(2)	23.046(10)	13.3324(12)
c (Å)	21.8713(18)	18.010(4)	21.718(8)	14.9342(13)
α (º)	90	94.803(15)	90	91.675(4)
β (º)	95.733(5)	100.219(10)	95.791(10)	100.183(4)
γ (º)	90	98.517(14)	90	93.298(4)
V (Å^3)	1637.8(2)	1458.8(5)	2862.3(19)	1123.60(17)
Z	2	2	4	1
ρ_{cal} (g cm^{-3})	1.498	1.481	1.727	1.641
μ (Mo Kα) (mm^{-1})	4.636	1.168	3.588	1.501
F(000)	740	676	1496	570
temperature (K)	150	110	110	110
θ_{min}, θ_{max} (º)	1.8, 25.0	1.2, 28.0	2.8, 26.4	1.4, 27.5
total reflns	47682	20483	47265	21808
unique reflns	2880	20483	5860	5171
R(int)	0.252	0.000	0.094	0.061
R1	0.0438,	0.0525,	0.0415,	0.0639
wR2 [$I \geq 2\sigma$ (I)]	0.0714	0.0952	0.0838	0.1683
R1 (all data)	0.1195	0.1081	0.0754	0.0904
wR2 (all data)	0.0856	0.1138	0.0955	0.1935
GOF	0.913	1.008	1.016	1.079
min peak	-0.601	-0.534	-0.562	-0.699
max peak	0.134	0.529	0.855	2.064

Table A.7. Atomic Coordinates for **6**

Atom	x	y	z	$U_{iso/equiv}$
Se1	0.27701(5)	0.16959(11)	0.09063(3)	0.0268(2)
Se2	0.69898(5)	0.17510(11)	0.13549(3)	0.0285(2)
Si1	0.28769(15)	0.0032(3)	0.18316(8)	0.0268(6)
Si2	0.85035(16)	0.3468(3)	0.09917(8)	0.0301(6)
C1	0.4568(5)	0.4337(8)	0.0545(3)	0.0181(19)
C2	0.5425(5)	0.3186(9)	0.0297(2)	0.0199(17)
C3	0.5834(5)	0.3870(8)	-0.0242(3)	0.021(2)
C4	0.4045(5)	0.3692(9)	0.1115(2)	0.025(2)
C5	0.5924(5)	0.1267(8)	0.0600(2)	0.023(2)
C6	0.2615(5)	0.1855(10)	0.2454(2)	0.034(2)
C7	0.1767(5)	-0.2016(10)	0.1728(3)	0.038(2)
C8	0.4336(5)	-0.1099(9)	0.2002(3)	0.037(3)
C9	0.9016(6)	0.2099(10)	0.0322(3)	0.051(3)
C10	0.8142(6)	0.6173(9)	0.0784(3)	0.043(3)
C11	0.9635(5)	0.3375(11)	0.1660(3)	0.045(3)

Table A.8. Atomic Coordinates for **7**

Atom	x	y	z	$U_{iso/equiv}$
Fe1	0.32966(4)	1.16884(3)	0.40694(2)	0.0263(1)
Fe2	0.13427(4)	0.39597(3)	-0.30844(2)	0.0238(1)
S1	0.42005(7)	1.19027(6)	0.20055(3)	0.0285(2)
S2	0.09861(7)	0.68102(6)	-0.16795(3)	0.0369(2)
O1	0.66470(18)	1.10242(15)	0.29116(9)	0.0330(6)
O2	-0.19877(18)	0.52450(15)	-0.19748(8)	0.0319(5)
C1	0.5164(3)	1.2441(2)	0.35384(12)	0.0223(7)
C2	0.5867(3)	1.2300(2)	0.43029(12)	0.0294(8)
C3	0.5096(3)	1.3062(2)	0.47808(13)	0.0342(8)
C4	0.3907(3)	1.3683(2)	0.43221(13)	0.0322(8)
C5	0.3947(3)	1.3312(2)	0.35528(12)	0.0262(7)
C6	0.0901(3)	1.0823(2)	0.35204(16)	0.0414(9)
C7	0.0940(3)	1.1107(3)	0.43022(17)	0.0509(11)
C8	0.2131(4)	1.0446(3)	0.47087(16)	0.0486(10)
C9	0.2848(3)	0.9730(2)	0.41775(15)	0.0389(9)
C10	0.2088(3)	0.9962(2)	0.34507(14)	0.0352(8)
C11	0.5534(3)	1.1701(2)	0.28723(12)	0.0253(7)
C12	0.5035(3)	1.0925(2)	0.13151(12)	0.0280(8)

C13	0.3634(2)	1.0018(2)	0.07649(11)	0.0213(7)
C14	0.2833(3)	1.0479(2)	0.01066(12)	0.0227(7)
C15	0.1650(3)	0.9614(2)	-0.04389(12)	0.0238(7)
C16	0.1273(2)	0.8295(2)	-0.03219(12)	0.0223(7)
C17	0.2060(3)	0.7831(2)	0.03359(12)	0.0236(7)
C18	0.3198(2)	0.8702(2)	0.09023(12)	0.0218(7)
C19	0.3236(3)	1.1911(2)	-0.00209(13)	0.0327(8)
C20	0.0822(3)	1.0112(2)	-0.11567(12)	0.0332(8)
C21	0.1722(3)	0.6385(2)	0.04391(14)	0.0388(9)
C22	0.3919(3)	0.8236(2)	0.16409(12)	0.0324(8)
C23	-0.0028(3)	0.7356(2)	-0.09114(12)	0.0303(8)
C24	-0.0709(3)	0.5610(2)	-0.22134(12)	0.0237(7)
C25	-0.0413(2)	0.5124(2)	-0.29613(11)	0.0221(7)
C26	0.0794(3)	0.5727(2)	-0.33742(12)	0.0251(7)
C27	0.0727(3)	0.4872(2)	-0.40366(12)	0.0302(8)
C28	-0.0515(3)	0.3742(2)	-0.40395(13)	0.0335(8)
C29	-0.1226(3)	0.3896(2)	-0.33796(12)	0.0276(7)
C30	0.3671(3)	0.4270(2)	-0.23766(14)	0.0346(9)
C31	0.3706(3)	0.3490(3)	-0.30464(16)	0.0501(11)
C32	0.2507(4)	0.2349(3)	-0.31137(17)	0.0590(11)
C33	0.1714(3)	0.2417(3)	-0.24864(17)	0.0516(10)
C34	0.2423(3)	0.3596(2)	-0.20282(13)	0.0364(9)

Table A.9. Atomic Coordinates for **8**

Atom	x	y	z	$U_{iso/equiv}$
Se1	0.82756(8)	0.19636(2)	0.51000(2)	0.0275(2)
Se2	0.92639(8)	-0.07043(2)	0.27105(2)	0.0322(2)
Fe1	0.92518(10)	0.29967(3)	0.66125(3)	0.0216(2)
Fe2	0.72101(11)	-0.10606(3)	0.09390(3)	0.0245(2)
O1	1.2946(5)	0.22086(14)	0.54973(14)	0.0344(11)
O2	0.5079(5)	-0.13086(14)	0.25188(15)	0.0334(11)
C1	1.0522(7)	0.22341(19)	0.6311(2)	0.0253(12)
C2	1.2128(8)	0.24817(19)	0.6786(2)	0.0281(16)
C3	1.0956(8)	0.25366(19)	0.7327(2)	0.0287(16)
C4	0.8665(8)	0.23223(19)	0.7198(2)	0.0285(16)
C5	0.8350(7)	0.21366(18)	0.6576(2)	0.0241(12)
C6	0.8910(9)	0.35473(19)	0.5876(2)	0.0338(17)
C7	1.0321(9)	0.38115(19)	0.6373(2)	0.0346(17)
C8	0.8957(8)	0.38467(19)	0.6888(2)	0.0341(17)
C9	0.6737(8)	0.36073(19)	0.6704(2)	0.0305(17)
C10	0.6692(8)	0.3418(2)	0.6079(2)	0.0340(17)
C11	1.1029(8)	0.21554(18)	0.5672(2)	0.0247(12)

C12	0.9911(8)	0.1779(2)	0.4367(2)	0.0296(17)
C13	0.9307(7)	0.11829(18)	0.41239(18)	0.0217(12)
C14	1.0728(7)	0.07075(19)	0.43122(19)	0.0228(14)
C15	1.0207(7)	0.01605(19)	0.40738(19)	0.0247(14)
C16	0.8207(7)	0.00746(19)	0.36598(19)	0.0234(12)
C17	0.6787(7)	0.05478(19)	0.34612(18)	0.0234(14)
C18	0.7295(7)	0.11026(18)	0.37022(19)	0.0229(12)
C19	1.2823(7)	0.0780(2)	0.4795(2)	0.0293(14)
C20	1.1881(8)	-0.0340(2)	0.4251(2)	0.0327(17)
C21	0.4682(7)	0.0456(2)	0.2985(2)	0.0294(14)
C22	0.5702(8)	0.1605(2)	0.3515(2)	0.0356(17)
C23	0.7589(8)	-0.05315(19)	0.3430(2)	0.0300(17)
C24	0.6917(8)	-0.12276(18)	0.2311(2)	0.0248(12)
C25	0.7605(7)	-0.14977(18)	0.17485(19)	0.0214(12)
C26	0.6038(8)	-0.18054(17)	0.1313(2)	0.0244(14)
C27	0.7245(8)	-0.19389(19)	0.0795(2)	0.0304(16)
C28	0.9562(8)	-0.17238(18)	0.0910(2)	0.0265(14)
C29	0.9807(7)	-0.14488(18)	0.1494(2)	0.0246(12)
C30	0.5900(10)	-0.0260(2)	0.1117(2)	0.0430(19)
C31	0.4390(9)	-0.0559(2)	0.0682(3)	0.0476(19)
C32	0.5592(9)	-0.0687(2)	0.0167(2)	0.0401(17)
C33	0.7841(9)	-0.0470(2)	0.0282(2)	0.0363(17)
C34	0.8067(9)	-0.0204(2)	0.0871(2)	0.0374(17)

Table A.10. Atomic Coordinates for **11**

Atom	x	y	z	$U_{iso/equiv}$
Fe1	0.07481(11)	0.12314(5)	0.30834(4)	0.0182(2)
Fe2	0.50350(12)	0.73964(5)	0.07092(4)	0.0230(2)
S1	0.49528(19)	0.20572(8)	0.55144(8)	0.0199(3)
S2	0.6216(2)	0.49545(8)	0.24823(7)	0.0221(3)
O1	0.0607(6)	0.2625(2)	0.5355(2)	0.0270(10)
O2	0.9671(6)	0.6246(3)	0.2240(2)	0.0375(12)
C1	0.0952(8)	0.1171(3)	0.4459(3)	0.0188(12)
C2	-0.1456(8)	0.1038(3)	0.4012(3)	0.0206(12)
C3	-0.1678(8)	0.0177(3)	0.3413(3)	0.0228(12)
C4	0.0559(9)	-0.0236(3)	0.3477(3)	0.0231(14)
C5	0.2216(8)	0.0381(3)	0.4119(3)	0.0197(12)
C6	-0.0124(10)	0.2505(4)	0.2384(4)	0.0335(17)
C7	-0.0489(9)	0.1643(4)	0.1793(3)	0.0321(16)
C8	0.1680(10)	0.1197(4)	0.1825(3)	0.0319(16)
C9	0.3407(9)	0.1776(4)	0.2448(4)	0.0341(17)
C10	0.2276(10)	0.2583(4)	0.2800(4)	0.0342(17)
C11	0.1870(8)	0.2012(3)	0.5117(3)	0.0194(12)
C12	0.5277(8)	0.3248(3)	0.6146(3)	0.0202(12)

C13	0.5083(8)	0.4159(3)	0.5551(3)	0.0178(12)
C14	0.6448(8)	0.4248(3)	0.4878(3)	0.0186(12)
C15	0.6421(8)	0.5075(3)	0.4323(3)	0.0182(12)
C16	0.8007(8)	0.5108(3)	0.3625(3)	0.0201(12)
C17	0.7744(8)	0.5857(3)	0.1910(3)	0.0234(14)
C18	0.6477(8)	0.6063(3)	0.1003(3)	0.0229(14)
C19	0.3983(9)	0.5899(3)	0.0645(3)	0.0230(14)
C20	0.3578(9)	0.6284(3)	-0.0240(3)	0.0266(14)

Table A.11. Summary of Crystal Data for [**15**]X_2

Formula	$C_{66}H_{64}BrCl_{13}P_4Pd_2S_2$
Formula Weight (*g/mol*)	1798.75
Crystal Dimensions (*mm*)	0.13 × 0.10 × 0.04
Crystal Color and Habit	colourless
Crystal System	monoclinic
Space Group	P 2_1/n
Temperature, K	150(2)
a, Å	17.4473(8)
b, Å	23.7638(11)
c, Å	18.3345(9)
α,°	90
β,°	103.015(2)
γ,°	90
V, $Å^3$	7406.5(6)
Min and Max 2θ for cell determination, °	4.50, 49.5
Z	4
F(000)	3600
ρ (*g/cm*)	1.613
λ, Å, (MoKα)	0.71073
μ, (cm^{-1})	1.676
Diffractometer Type	CCD area detector
Scan Type(s)	phi and omega scans
Max 2θ for data collection, °	52.84
Measured fraction of data	0.998
Number of reflections measured	154031
Unique reflections measured	15167
R_{merge}	0.1083
Number of reflections included in refinement	15167
Cut off Threshold Expression	I > 2sigma(I)
Structure refined using	full matrix least-squares using F^2
Weighting Scheme	$w=1/[sigma^2(Fo^2)+(0.1204P)^2]$ where $P=(Fo^2+2Fc^2)/3$
Number of parameters in least-squares	806
R_1	0.0538
wR_2	0.1194
R_1 (all data)	0.1167
wR_2 (all data)	0.1493
GOF	1.029
Maximum shift/error	0.002
Min & Max peak heights on final ΔF Map (e^-/Å)	-1.082, 1.754

Table A12. Atomic Coordinates for **[15]**X_2

Atom	x	y	z	$U_{iso/equiv}$
Pd1	0.18982(2)	0.17553(2)	0.44472(2)	0.0191(1)
Pd2	0.29838(3)	0.17642(2)	0.32294(2)	0.0197(1)
S1	0.27827(9)	0.24257(6)	0.41462(9)	0.0205(5)
S2	0.27510(9)	0.10831(7)	0.41069(9)	0.0247(5)
P1	0.10633(9)	0.24481(7)	0.46722(9)	0.0216(5)
P2	0.10632(9)	0.10618(7)	0.46776(9)	0.0220(5)
P3	0.32139(9)	0.10665(7)	0.24443(9)	0.0225(5)
P4	0.32388(9)	0.24707(7)	0.24653(9)	0.0212(5)
C1	0.3772(3)	0.2368(3)	0.4781(4)	0.028(2)
C2	0.3746(4)	0.1111(3)	0.4741(4)	0.036(3)
C3	0.3817(4)	0.2013(3)	0.5475(4)	0.032(2)
C4	0.3805(4)	0.1421(3)	0.5460(4)	0.031(2)
C5	0.3880(4)	0.1126(4)	0.6126(4)	0.045(3)
C6	0.3974(4)	0.1402(4)	0.6803(5)	0.051(3)
C7	0.3995(4)	0.1972(4)	0.6824(4)	0.052(3)
C8	0.3905(4)	0.2292(4)	0.6169(4)	0.042(3)
C9	0.0008(4)	0.2291(3)	0.4421(4)	0.029(2)
C10	-0.0222(4)	0.1755(3)	0.4787(4)	0.033(2)
C11	0.0011(4)	0.1213(3)	0.4429(4)	0.030(2)
C12	0.3966(4)	0.1235(3)	0.1930(4)	0.028(2)
C13	0.3779(4)	0.1766(3)	0.1446(3)	0.0292(19)
C14	0.3960(4)	0.2307(3)	0.1920(4)	0.026(2)
C15	0.1282(4)	0.2649(3)	0.5651(3)	0.0244(19)
C16	0.2009(6)	0.2567(5)	0.6086(5)	0.085(4)
C17	0.2216(7)	0.2747(6)	0.6825(5)	0.119(6)
C18	0.1673(6)	0.3004(4)	0.7136(5)	0.057(3)

Table A13. Summary of Crystal Data for [**16**]X_2

Formula	$C_{68}H_{66}Cl_{20}P_4Pd_2Se_2$
Formula Weight (*g/mol*)	2086.80
Crystal Dimensions (*mm*)	0.37 × 0.25 × 0.24
Crystal Color and Habit	yellow block
Crystal System	monoclinic
Space Group	P 2_1/c
Temperature, K	150(2)
a, Å	18.668(4)
b, Å	17.724(4)
c, Å	24.914(5)
α,°	90
β,°	93.11(3)
γ,°	90
V, Å^3	8231(3)
Number of reflections to determine final unit cell	9917
Min and Max 2θ for cell determination, °	4.58, 54.62
Z	4
F(000)	4136
ρ (*g/cm*)	1.684
λ, Å, (MoKα)	0.71073
μ, (cm^{-1})	2.088
Diffractometer Type	CCD area detector
Scan Type(s)	phi and omega scans
Max 2θ for data collection, °	54.976
Measured fraction of data	0.999
Number of reflections measured	35017
Unique reflections measured	18760
R_{merge}	0.0404
Number of reflections included in refinement	18760
Cut off Threshold Expression	I > 2sigma(I)
Structure refined using	full matrix least-squares using F^2
Weighting Scheme	$w=1/[sigma^2(Fo^2)+(0.1204P)^2]$ where $P=(Fo^2+2Fc^2)/3$
Number of parameters in least-squares	920
R_1	0.0585
wR_2	0.1523
R_1 (all data)	0.0934
wR_2 (all data)	0.1869
GOF	1.040
Maximum shift/error	0.001
Min & Max peak heights on final ΔF Map (e^-/Å)	-1.573, 2.619

Table A.14. Atomic Coordinates for [**16**]X_2

Atom	x	y	z	$U_{iso/equiv}$
Pd1	0.29782(2)	0.60402(2)	0.28507(2)	0.02323(12)
Pd2	0.14158(2)	0.51561(2)	0.27777(2)	0.02414(12)
Se1	0.17822(3)	0.64278(3)	0.31231(2)	0.02597(14)
Se2	0.23350(3)	0.53620(3)	0.21083(2)	0.02607(14)
P1	0.34817(7)	0.65851(8)	0.36206(5)	0.0266(3)
P2	0.40609(7)	0.55917(8)	0.25823(5)	0.0262(3)
P3	0.11463(7)	0.39929(8)	0.24196(5)	0.0261(3)
P4	0.05947(7)	0.50457(8)	0.34257(5)	0.0261(3)
C1	0.1282(3)	0.7049(3)	0.2537(2)	0.0321(12)
C1S	0.3431(4)	0.5698(4)	0.0021(3)	0.0605(19)
C2	0.1740(3)	0.6088(3)	0.1654(2)	0.0329(12)
C2S	-0.2414(5)	0.6005(4)	0.3036(3)	0.067(2)
C3	0.1761(3)	0.7351(3)	0.2125(2)	0.0319(12)
C3S	0.1386(4)	-0.0328(4)	0.3787(3)	0.0553(18)
C4	0.1984(3)	0.6887(3)	0.1707(2)	0.0305(12)
C4S	0.0028(4)	0.1831(4)	0.4173(3)	0.061(2)
C5	0.2415(3)	0.7191(3)	0.1325(2)	0.0363(13)
C5S	0.6325(3)	0.7629(4)	0.0113(3)	0.0494(16)
C6	0.2621(3)	0.7935(4)	0.1345(2)	0.0455(15)
C6S	0.5655(3)	0.4350(3)	0.4352(2)	0.0385(13)
C7	0.2397(3)	0.8396(4)	0.1753(3)	0.0434(15)
C8	0.1981(3)	0.8097(3)	0.2142(2)	0.0377(13)
C9	0.4310(3)	0.6151(3)	0.3902(2)	0.0296(11)
C10	0.4892(3)	0.6075(3)	0.3495(2)	0.0311(12)
C11	0.4755(3)	0.5415(3)	0.3112(2)	0.0305(11)
C12	0.0199(3)	0.3746(3)	0.2433(2)	0.0314(12)
C13	-0.0068(3)	0.3723(3)	0.3005(2)	0.0323(12)
C14	-0.0218(3)	0.4511(3)	0.3231(2)	0.0333(12)
C15	0.3711(3)	0.7575(3)	0.3524(2)	0.0327(12)
C16	0.3453(4)	0.7955(4)	0.3079(3)	0.0527(17)
C17	0.3634(5)	0.8712(4)	0.3017(4)	0.078(3)
C18	0.4059(5)	0.9091(5)	0.3402(4)	0.071(2)
C19	0.4306(4)	0.8707(4)	0.3840(3)	0.0540(18)
C20	0.4146(3)	0.7951(4)	0.3909(2)	0.0432(14)
C21	0.2901(3)	0.6576(3)	0.4186(2)	0.0310(12)
C22	0.2605(3)	0.7238(4)	0.4388(2)	0.0399(14)
C23	0.2179(3)	0.7204(4)	0.4824(2)	0.0463(16)
C24	0.2054(3)	0.6523(4)	0.5068(2)	0.0471(17)
C25	0.2337(3)	0.5860(4)	0.4870(2)	0.0452(15)
C26	0.2759(3)	0.5886(4)	0.4427(2)	0.0370(13)
C27	0.4471(3)	0.6277(3)	0.2145(2)	0.0292(11)
C28	0.4134(3)	0.6927(4)	0.1995(2)	0.0448(15)

C29	0.4459(3)	0.7460(4)	0.1686(3)	0.0536(18)
C30	0.5138(3)	0.7337(4)	0.1513(2)	0.0434(15)
C31	0.5480(4)	0.6680(4)	0.1654(3)	0.0576(19)
C32	0.5163(3)	0.6151(4)	0.1967(3)	0.0527(18)
C33	0.4039(3)	0.4703(3)	0.2207(2)	0.0285(11)
C34	0.3925(3)	0.4708(3)	0.1648(2)	0.0364(13)
C35	0.3896(3)	0.4036(4)	0.1371(2)	0.0408(14)
C36	0.3975(3)	0.3364(4)	0.1639(2)	0.0430(14)
C37	0.4063(3)	0.3348(3)	0.2193(2)	0.0433(14)
C38	0.4091(3)	0.4022(3)	0.2479(2)	0.0394(14)
C39	0.1332(3)	0.3924(3)	0.1708(2)	0.0297(11)
C40	0.0933(3)	0.4342(3)	0.1331(2)	0.0331(12)
C41	0.1073(3)	0.4309(3)	0.0793(2)	0.0375(13)
C42	0.1624(3)	0.3862(3)	0.0631(2)	0.0398(14)
C43	0.2041(3)	0.3443(3)	0.1003(2)	0.0390(14)
C44	0.1897(3)	0.3476(3)	0.1542(2)	0.0326(12)
C45	0.1640(3)	0.3217(3)	0.2753(2)	0.0278(11)
C46	0.1334(3)	0.2508(3)	0.2814(2)	0.0310(12)
C47	0.1721(3)	0.1938(3)	0.3069(2)	0.0382(13)
C48	0.2424(3)	0.2069(3)	0.3262(2)	0.0370(13)
C49	0.2728(3)	0.2771(3)	0.3204(2)	0.0377(13)
C50	0.2341(3)	0.3342(3)	0.2950(2)	0.0325(12)
C51	0.0253(3)	0.5942(3)	0.3661(2)	0.0286(11)
C52	-0.0318(3)	0.6301(3)	0.3382(2)	0.0372(13)
C53	-0.0555(3)	0.6982(4)	0.3559(3)	0.0450(15)
C54	-0.0239(3)	0.7326(3)	0.4006(3)	0.0442(15)
C55	0.0335(3)	0.6995(3)	0.4278(2)	0.0398(14)
C56	0.0575(3)	0.6293(3)	0.4108(2)	0.0332(12)
C57	0.0983(3)	0.4571(3)	0.4021(2)	0.0286(11)
C58	0.0583(3)	0.4458(3)	0.4477(2)	0.0368(13)
C59	0.0897(3)	0.4094(4)	0.4921(2)	0.0430(15)
C60	0.1595(3)	0.3844(3)	0.4919(2)	0.0429(14)
C61	0.1992(3)	0.3959(3)	0.4480(2)	0.0403(14)
C62	0.1687(3)	0.4323(3)	0.4035(2)	0.0334(12)
Cl01	0.61403(7)	0.59265(7)	0.60234(5)	0.0288(3)
Cl1	0.26777(14)	0.54248(18)	0.03562(10)	0.1073(10)
Cl02	-0.01520(7)	0.57171(8)	0.20141(5)	0.0311(3)
Cl2	0.39354(17)	0.49036(14)	-0.01182(10)	0.0995(9)
Cl3	0.39207(12)	0.63504(14)	0.04118(9)	0.0818(7)
Cl4	-0.2128(4)	0.5581(4)	0.3663(4)	0.0612(16)
Cl5	-0.2694(6)	0.5336(5)	0.2566(3)	0.138(5)
Cl6	-0.3060(4)	0.6650(4)	0.3125(3)	0.093(2)
Cl7	0.0979(4)	-0.0569(8)	0.4377(3)	0.182(5)
Cl8	0.1597(5)	-0.1116(4)	0.3514(3)	0.132(3)
Cl9	0.2163(5)	0.0215(4)	0.3963(3)	0.124(4)
Cl4A	-0.2187(8)	0.5741(9)	0.3694(5)	0.172(6)

Cl5A	-0.2230(4)	0.5272(5)	0.2628(3)	0.097(3)
Cl6A	-0.3307(4)	0.6269(6)	0.2974(5)	0.171(6)
Cl7A	0.1029(4)	-0.0023(3)	0.4362(2)	0.0827(19)
Cl8A	0.1149(4)	-0.1321(3)	0.3765(3)	0.108(2)
Cl9A	0.2272(4)	-0.0282(9)	0.3714(4)	0.223(8)
Cl10	-0.03218(18)	0.12585(14)	0.46868(11)	0.1070(9)
Cl11	0.08848(10)	0.21710(15)	0.43472(9)	0.0807(7)
Cl12	-0.05688(10)	0.25779(14)	0.40772(8)	0.0741(6)
Cl13	0.55615(9)	0.70597(12)	0.00333(9)	0.0710(6)
Cl14	0.65218(12)	0.80763(11)	-0.04891(7)	0.0654(5)
Cl15	0.70685(9)	0.70700(11)	0.03350(7)	0.0596(5)
Cl16	0.61528(9)	0.44852(10)	0.37719(6)	0.0494(4)
Cl17	0.58843(8)	0.50534(9)	0.48287(7)	0.0470(4)
Cl18	0.58257(9)	0.34465(9)	0.46185(6)	0.0466(4)

Table A.15. Summary of Crystal Data for [**17**]X_4

Formula	$C_{124}H_{120}Br_3Cl_{19}P_8Pd_4S_4$
Formula Weight (*g/mol*)	3325.07
Crystal Dimensions (*mm*)	0.193? × 0.184 × 0.094
Crystal Color and Habit	colourless prism
Crystal System	orthorhombic
Space Group	P b c a
Temperature, K	110
a, Å	17.875(7)
b, Å	26.862(10)
c, Å	26.933(11)
α,°	90
β,°	90
γ,°	90
V, $Å^3$	12932(8)
Number of reflections to determine final unit cell	9738
Min and Max 2θ for cell determination, °	5.3, 49.92
Z	4
F(000)	6640
ρ (*g/cm*)	1.708
λ, Å, (MoKα)	0.71073
μ, (cm^{-1})	2.080
Diffractometer Type	Bruker Kappa Axis Apex2
Scan Type(s)	phi and omega scans
Max 2θ for data collection, °	50.204
Measured fraction of data	0.979
Number of reflections measured	213930
Unique reflections measured	11459
R_{merge}	0.0698
Number of reflections included in refinement	11459
Cut off Threshold Expression	I > 2sigma(I)
Structure refined using	full matrix least-squares using F^2
Weighting Scheme	$w=1/[sigma^2(Fo^2)+(0.1046P)^2+122.3666P]$ where $P=(Fo^2+2Fc^2)/3$
Number of parameters in least-squares	793
R_1	0.0670
wR_2	0.1846
R_1 (all data)	0.0952
wR_2 (all data)	0.2191
GOF	1.119
Maximum shift/error	0.010
Min & Max peak heights on final ΔF Map (e^-/Å)	-1.631, 1.890

Table A16. Atomic Coordinates for [**17**]X_4

Atom	x	y	z	$U_{iso/equiv}$
Pd1	0.11183(3)	0.10066(2)	0.08786(2)	0.02764(19)
Pd2	-0.04304(3)	0.14635(2)	0.12441(2)	0.02616(18)
S1	0.01652(11)	0.14444(8)	0.04505(8)	0.0288(5)
S2	0.01438(11)	0.06704(8)	0.13640(7)	0.0273(4)
P1	0.20410(12)	0.13987(9)	0.04304(10)	0.0361(5)
P2	0.20027(12)	0.06064(8)	0.13493(9)	0.0312(5)
P3	-0.09727(12)	0.14238(8)	0.20093(8)	0.0285(5)
P4	-0.09913(12)	0.22087(8)	0.10603(9)	0.0300(5)
C1	-0.0238(4)	0.0497(3)	0.0082(3)	0.0283(18)
C2	-0.0227(4)	0.0148(3)	0.0474(3)	0.0273(17)
C3	0.0010(4)	-0.0336(3)	0.0385(3)	0.0285(18)
C4	-0.0503(4)	0.1012(3)	0.0143(3)	0.0307(18)
C5	-0.0499(5)	0.0293(3)	0.0985(3)	0.0320(19)
C6	0.2890(5)	0.1547(4)	0.0758(4)	0.046(2)
C7	0.3277(5)	0.1129(4)	0.1034(4)	0.048(3)
C8	0.2851(5)	0.0955(4)	0.1485(4)	0.041(2)
C9	-0.1917(5)	0.1677(3)	0.2047(3)	0.0295(18)
C10	-0.1972(5)	0.2228(3)	0.1879(3)	0.0336(19)
C11	-0.1932(5)	0.2283(3)	0.1314(3)	0.034(2)
C12	0.2309(5)	0.1035(4)	-0.0125(4)	0.044(6)
C13	0.1752(4)	0.0864(4)	-0.0443(4)	0.048(4)
C14	0.1940(5)	0.0576(4)	-0.0853(4)	0.066(5)
C15	0.2684(6)	0.0457(4)	-0.0945(4)	0.066(6)
C16	0.3241(5)	0.0628(5)	-0.0627(4)	0.059(5)
C17	0.3053(5)	0.0916(5)	-0.0218(4)	0.055(5)
C12A	0.2364(15)	0.1019(8)	-0.0032(10)	0.029(10)
C13A	0.1941(12)	0.0604(9)	-0.0160(10)	0.045(8)
C14A	0.2185(15)	0.0288(8)	-0.0534(10)	0.066(11)
C15A	0.2852(18)	0.0386(11)	-0.0781(10)	0.046(11)
C16A	0.3275(15)	0.0800(12)	-0.0653(12)	0.14(4)
C17A	0.3031(15)	0.1117(9)	-0.0279(12)	0.039(10)
C18	0.1752(5)	0.2000(4)	0.0191(4)	0.039(2)
C19	0.1726(5)	0.2102(4)	-0.0311(4)	0.046(2)
C20	0.1511(5)	0.2574(4)	-0.0468(4)	0.047(2)
C21	0.1326(5)	0.2938(4)	-0.0136(5)	0.050(3)
C22	0.1341(5)	0.2834(4)	0.0369(4)	0.046(2)
C23	0.1553(5)	0.2371(3)	0.0531(4)	0.040(2)
C24	0.2317(5)	0.0047(3)	0.1031(4)	0.037(2)
C25	0.1956(5)	-0.0100(5)	0.0590(5)	0.072(4)
C26	0.2235(7)	-0.0482(5)	0.0313(6)	0.080(5)
C27	0.2860(6)	-0.0742(4)	0.0484(5)	0.053(3)
C28	0.3219(7)	-0.0600(4)	0.0882(4)	0.060(3)
C29	0.2949(6)	-0.0195(4)	0.1170(4)	0.055(3)

C30	0.1703(5)	0.0421(4)	0.1967(3)	0.038(2)
C31	0.1520(5)	-0.0069(4)	0.2081(4)	0.044(2)
C32	0.1310(6)	-0.0182(5)	0.2567(5)	0.063(3)
C33	0.1287(6)	0.0183(6)	0.2932(4)	0.064(4)
C34	0.1454(6)	0.0661(6)	0.2811(4)	0.062(3)
C35	0.1654(6)	0.0783(4)	0.2335(4)	0.048(2)
C36	-0.1076(5)	0.0796(3)	0.2250(3)	0.0316(19)
C37	-0.1613(5)	0.0480(3)	0.2042(3)	0.0321(19)
C38	-0.1686(6)	-0.0002(3)	0.2205(3)	0.039(2)
C39	-0.1217(6)	-0.0183(4)	0.2575(4)	0.044(2)
C40	-0.0686(6)	0.0119(4)	0.2779(4)	0.049(3)
C41	-0.0592(5)	0.0613(4)	0.2617(3)	0.040(2)
C42	-0.0408(5)	0.1745(3)	0.2465(3)	0.037(2)
C43	-0.0733(6)	0.1972(4)	0.2881(4)	0.047(2)
C44	-0.0261(8)	0.2220(4)	0.3214(4)	0.061(3)
C45	0.0495(7)	0.2244(5)	0.3141(5)	0.064(3)
C46	0.0809(7)	0.2014(4)	0.2748(4)	0.057(3)
C47	0.0357(6)	0.1780(4)	0.2395(4)	0.046(2)
C48	-0.1129(5)	0.2293(3)	0.0402(3)	0.035(2)
C49	-0.1682(5)	0.2011(3)	0.0155(4)	0.037(2)
C50	-0.1751(5)	0.2042(4)	-0.0345(4)	0.041(2)
C51	-0.1262(6)	0.2324(4)	-0.0632(4)	0.051(3)
C52	-0.0710(6)	0.2594(4)	-0.0396(4)	0.045(2)
C53	-0.0639(5)	0.2579(4)	0.0118(4)	0.040(2)
C54	-0.0479(5)	0.2753(3)	0.1274(4)	0.036(2)
C55	-0.0752(6)	0.3237(4)	0.1223(5)	0.062(3)
C56	-0.0354(7)	0.3631(4)	0.1412(6)	0.074(4)
C57	0.0301(7)	0.3564(4)	0.1634(5)	0.063(3)
C58	0.0594(6)	0.3096(4)	0.1687(5)	0.059(3)
C59	0.0220(5)	0.2685(4)	0.1501(4)	0.041(2)
C1S	0.0523(6)	0.4249(4)	-0.0663(5)	0.056(3)
Cl1	0.03593(15)	0.37783(11)	-0.11058(11)	0.0556(7)
Cl2	0.01698(18)	0.40498(14)	-0.00712(12)	0.0720(9)
Cl3	0.0087(2)	0.48040(13)	-0.08390(16)	0.0803(10)
C2S	-0.5261(7)	0.3615(6)	0.1545(5)	0.076(5)
Cl6	-0.6086(3)	0.3821(2)	0.1264(2)	0.0886(16)
C2SA	-0.436(2)	0.3657(16)	0.1602(18)	0.085(15)
Cl6A	-0.3549(10)	0.3900(7)	0.1341(7)	0.117(5)
Cl4	-0.4844(3)	0.41106(17)	0.18517(17)	0.1003(13)
Cl5	-0.4699(3)	0.33697(14)	0.10815(15)	0.0872(11)
C3S	-0.2429(7)	0.3358(8)	0.2538(6)	0.062(10)
Cl7	-0.2683(4)	0.3779(2)	0.2995(4)	0.0722(19)
Cl8	-0.2993(6)	0.3418(3)	0.2018(5)	0.113(4)
Cl9	-0.1477(4)	0.3418(3)	0.2402(3)	0.073(2)
C3SA	-0.2141(10)	0.3314(12)	0.2828(7)	0.116(16)
Cl7A	-0.2351(8)	0.3652(4)	0.3360(4)	0.124(4)

Cl8A	-0.2675(9)	0.3513(4)	0.2329(6)	0.120(4)
Cl9A	-0.1183(6)	0.3285(4)	0.2709(6)	0.124(4)
Br2	0.2258(4)	0.2251(2)	0.18249(19)	0.0512(13)
Cl10	0.2149(11)	0.2130(6)	0.1844(7)	0.064(5)
Br1	-0.25216(6)	0.09950(4)	0.09088(4)	0.0466(3)

Table A.17. Summary of Crystal Data for **18**

Formula	$C_{73}H_{96}Cu_2N_4S_2$
Formula Weight (*g/mol*)	1220.73
Crystal Dimensions (*mm*)	0.323 × 0.207 × 0.119
Crystal Color and Habit	colourless block
Crystal System	monoclinic
Space Group	P 2_1/c
Temperature, K	293
a, Å	12.333(3)
b, Å	18.948(4)
c, Å	15.858(3)
α,°	90
β,°	112.28(3)
γ,°	90
V, $Å^3$	3429.1(14)
Number of reflections to determine final unit cell	9778
Min and Max 2θ for cell determination, °	5.6, 60.74
Z	2
F(000)	1304
ρ (*g/cm*)	1.182
λ, Å, (MoKα)	0.71073
μ, (cm^{-1})	0.723
Diffractometer Type	Bruker Kappa Axis Apex2
Scan Type(s)	phi and omega scans
Max 2θ for data collection, °	61.144
Measured fraction of data	0.999
Number of reflections measured	65891
Unique reflections measured	10494
R_{merge}	0.0440
Number of reflections included in refinement	10494
Cut off Threshold Expression	I > 2sigma(I)
Structure refined using	full matrix least-squares using F^2
Weighting Scheme	$w=1/[sigma^2(Fo^2)+(0.1045P)^2+1.6037P]$ where $P=(Fo^2+2Fc^2)/3$
Number of parameters in least-squares	361
R_1	0.0538
wR_2	0.1546
R_1 (all data)	0.0882
wR_2 (all data)	0.1883
GOF	1.093
Maximum shift/error	0.001
Min & Max peak heights on final ΔF Map (e^-/Å)	-0.756, 1.223

Table A.18. Atomic Coordinates for **18**

Atom	x	y	z	$U_{iso/equiv}$
Cu1	-0.27787(3)	0.63920(2)	0.66278(2)	0.02316(10)
S1	-0.26073(6)	0.58564(3)	0.78573(4)	0.02849(15)
N1	-0.20171(17)	0.73880(10)	0.55671(13)	0.0216(4)
N2	-0.37794(18)	0.70533(10)	0.48137(13)	0.0226(4)
C1	-0.0605(2)	0.51889(13)	0.90927(16)	0.0268(5)
C2	-0.0813(2)	0.45314(13)	0.94028(17)	0.0295(5)
C3	0.0186(2)	0.56639(14)	0.96898(17)	0.0296(5)
C4	-0.1737(3)	0.40464(17)	0.8771(2)	0.0466(8)
C5	-0.1213(2)	0.53812(15)	0.81004(17)	0.0323(6)
C6	0.0361(3)	0.63904(15)	0.9362(2)	0.0437(8)
C7	-0.2861(2)	0.69444(12)	0.56107(15)	0.0208(4)
C8	-0.2409(2)	0.77707(13)	0.47567(16)	0.0273(5)
C9	-0.3509(2)	0.75597(13)	0.42918(16)	0.0274(5)
C10	-0.0860(2)	0.74241(13)	0.62755(16)	0.0256(5)
C11	-0.0627(3)	0.79321(16)	0.69597(19)	0.0347(6)
C12	0.0490(3)	0.7930(2)	0.7643(2)	0.0476(8)
C13	0.1329(3)	0.7455(2)	0.7637(2)	0.0507(9)
C14	0.1079(3)	0.69574(19)	0.6954(2)	0.0436(7)
C15	-0.0032(2)	0.69314(15)	0.62519(18)	0.0309(5)
C16	-0.4877(2)	0.66885(13)	0.45651(16)	0.0256(5)
C17	-0.5098(2)	0.61186(14)	0.39591(16)	0.0286(5)
C18	-0.6174(3)	0.57716(15)	0.37285(19)	0.0366(6)
C19	-0.6968(3)	0.59891(18)	0.4091(2)	0.0455(8)
C20	-0.6725(3)	0.65403(19)	0.4688(2)	0.0456(7)
C21	-0.5665(2)	0.69044(16)	0.49532(19)	0.0338(6)
C22	-0.1112(4)	0.9193(2)	0.7181(4)	0.0742(13)
C23	-0.1560(3)	0.84356(17)	0.6993(2)	0.0420(7)
C24	-0.2023(4)	0.8191(2)	0.7714(3)	0.0592(10)
C25	0.0601(3)	0.63441(18)	0.5084(2)	0.0475(8)
C26	-0.0309(3)	0.63658(14)	0.5524(2)	0.0338(6)
C27	-0.0414(3)	0.56408(17)	0.5918(2)	0.0476(8)
C28	-0.4737(4)	0.5647(2)	0.2598(2)	0.0550(9)
C29	-0.4202(3)	0.58556(15)	0.3600(2)	0.0375(6)
C30	-0.3553(4)	0.5234(2)	0.4167(3)	0.0743(13)
C31	-0.6204(5)	0.8130(2)	0.5191(3)	0.0907(18)
C32	-0.5419(3)	0.75141(17)	0.5622(2)	0.0411(7)
C33	-0.5506(5)	0.7306(3)	0.6504(3)	0.0864(16)
C1S	0.4121(12)	0.6021(7)	0.8162(9)	0.106(4)
C2S	0.4216(6)	0.5554(3)	0.8930(4)	0.066(2)
C3S	0.3148(5)	0.5407(4)	0.8998(4)	0.089(3)
C4S	0.3115(5)	0.5014(4)	0.9728(5)	0.082(3)
C5S	0.4150(6)	0.4768(4)	1.0389(4)	0.092(3)

C6S	0.5218(5)	0.4915(5)	1.0322(5)	0.108(4)
C7S	0.5251(5)	0.5308(4)	0.9592(5)	0.070(2)

Table A.19. Summary of Crystal Data for **19**

Formula	$C_{72}H_{94}Cu_2N_4Se_2$
Formula Weight (*g/mol*)	1300.51
Crystal Dimensions (*mm*)	0.283 × 0.061 × 0.028
Crystal Color and Habit	colourless plate
Crystal System	monoclinic
Space Group	P 2_1/c
Temperature, K	110
a, Å	12.294(6)
b, Å	19.047(9)
c, Å	15.877(7)
α,°	90
β,°	111.530(12)
γ,°	90
V, Å^3	3459(3)
Number of reflections to determine final unit cell	9974
Min and Max 2θ for cell determination, °	5.08, 47.28
Z	2
F(000)	1360
ρ (*g/cm*)	1.249
λ, Å, (MoKα)	0.71073
μ, (*cm*$^{-1}$)	1.708
Diffractometer Type	Bruker Kappa Axis Apex2
Scan Type(s)	phi and omega scans
Max 2θ for data collection, °	47.848
Measured fraction of data	0.849
Number of reflections measured	53528
Unique reflections measured	5315
R_{merge}	0.1236
Number of reflections included in refinement	5315
Cut off Threshold Expression	I > 2sigma(I)
Structure refined using	full matrix least-squares using F^2
Weighting Scheme	$w=1/[sigma^2(Fo^2)+(0.1141P)^2]$ where $P=(Fo^2+2Fc^2)/3$
Number of parameters in least-squares	356
R_1	0.0509
wR_2	0.1433
R_1 (all data)	0.0973
wR_2 (all data)	0.1916

GOF	1.076
Maximum shift/error	0.001
Min & Max peak heights on final ΔF Map (e^-/Å)	-0.944, 0.817

Table A.20. Atomic Coordinates for **19**

Atom	x	y	z	$U_{iso/equiv}$
Se1	-0.27315(5)	1.08583(3)	0.28900(4)	0.0378(2)
Cu1	-0.28425(6)	1.14092(4)	0.16135(5)	0.0331(3)
N1	-0.2020(4)	1.2389(2)	0.0566(3)	0.0318(12)
N2	-0.3784(4)	1.2072(3)	-0.0182(3)	0.0342(13)
C1	-0.0602(5)	1.0184(3)	0.4100(4)	0.0360(15)
C2	-0.0810(6)	0.9533(3)	0.4425(4)	0.0401(16)
C3	0.0188(6)	1.0648(3)	0.4683(5)	0.0401(16)
C4	-0.1222(5)	1.0361(4)	0.3118(4)	0.0432(17)
C5	-0.1747(6)	0.9048(4)	0.3799(5)	0.054(2)
C6	0.0366(6)	1.1362(4)	0.4330(5)	0.058(2)
C7	-0.2891(5)	1.1953(3)	0.0610(4)	0.0309(14)
C8	-0.2397(6)	1.2768(3)	-0.0234(4)	0.0399(16)
C9	-0.3506(5)	1.2570(3)	-0.0707(4)	0.0381(16)
C10	-0.0867(5)	1.2419(3)	0.1271(4)	0.0349(15)
C11	-0.0634(5)	1.2925(4)	0.1938(4)	0.0414(17)
C12	0.0482(6)	1.2926(4)	0.2608(5)	0.060(2)
C13	0.1328(6)	1.2441(5)	0.2597(6)	0.064(2)
C14	0.1076(6)	1.1941(4)	0.1941(5)	0.055(2)
C15	-0.0043(5)	1.1908(4)	0.1234(4)	0.0416(17)
C16	-0.4892(5)	1.1709(3)	-0.0442(4)	0.0376(16)
C17	-0.5690(5)	1.1938(4)	-0.0058(5)	0.0497(19)
C18	-0.6752(6)	1.1578(4)	-0.0348(6)	0.067(2)
C19	-0.6993(6)	1.1033(4)	-0.0943(6)	0.062(2)
C20	-0.6163(6)	1.0802(4)	-0.1272(5)	0.0484(19)
C21	-0.5089(6)	1.1138(3)	-0.1035(4)	0.0400(17)
C22	-0.2005(7)	1.3204(5)	0.2723(6)	0.070(2)
C23	-0.1557(6)	1.3428(4)	0.1987(5)	0.053(2)
C24	-0.1113(8)	1.4188(4)	0.2131(7)	0.083(3)
C25	-0.0451(7)	1.0631(4)	0.0918(6)	0.062(2)
C26	-0.0331(6)	1.1345(4)	0.0521(5)	0.0497(19)
C27	0.0558(7)	1.1327(4)	0.0043(6)	0.065(2)
C28	-0.5637(9)	1.2331(6)	0.1492(7)	0.110(4)
C29	-0.5460(6)	1.2530(4)	0.0609(6)	0.063(2)
C30	-0.6115(10)	1.3171(6)	0.0162(8)	0.122(4)
C31	-0.3598(8)	1.0215(5)	-0.0805(7)	0.087(3)
C32	-0.4171(6)	1.0855(4)	-0.1363(5)	0.0509(19)
C33	-0.4643(8)	1.0670(5)	-0.2361(6)	0.082(3)

C1S	0.5319(11)	1.0401(9)	0.4466(11)	0.102(7)
C2S	0.5243(9)	1.0059(9)	0.5215(10)	0.146(10)
C3S	0.4154(12)	0.9908(7)	0.5251(8)	0.076(5)
C4S	0.3142(9)	1.0101(7)	0.4538(10)	0.092(6)
C5S	0.3218(12)	1.0444(8)	0.3788(9)	0.138(9)
C6S	0.4307(15)	1.0594(7)	0.3752(9)	0.137(9)

Table A.21. Summary of Crystal Data for **20**

Formula	$C_{67}H_{86}Cl_2Cu_2FeN_4S_2$
Formula Weight (*g/mol*)	1265.34
Crystal Dimensions (*mm*)	0.232 × 0.121 × 0.109
Crystal Color and Habit	yellow block
Crystal System	monoclinic
Space Group	P 2_1/c
Temperature, K	110
a, Å	20.836(8)
b, Å	9.596(4)
c, Å	16.941(5)
α,°	90
β,°	101.905(8)
γ,°	90
V, Å^3	3314(2)
Number of reflections to determine final unit cell	9929
Min and Max 2θ for cell determination, °	5.48, 58.0
Z	2
F(000)	1332
ρ (*g/cm*)	1.268
λ, Å, (MoKα)	0.71073
μ, (*cm*$^{-1}$)	1.036
Diffractometer Type	Bruker Kappa Axis Apex2
Scan Type(s)	phi and omega scans
Max 2θ for data collection, °	48.5
Measured fraction of data	0.994
Number of reflections measured	47566
Unique reflections measured	5323
R_{merge}	0.0483
Number of reflections included in refinement	5323
Cut off Threshold Expression	I > 2sigma(I)
Structure refined using	full matrix least-squares using F^2
Weighting Scheme	w=1/[sigma^2(Fo^2)+(0.1217P)^2+8.8608P] where P=(Fo^2+2Fc^2)/3
Number of parameters in least-squares	361

R_1	0.0680
wR_2	0.2016
R_1 (all data)	0.0818
wR_2 (all data)	0.2128
GOF	1.142
Maximum shift/error	0.001
Min & Max peak heights on final ΔF Map (e^-/Å)	-1.235, 1.856

Table A.22. Atomic Coordinates for **20**

Atom	x	y	z	$U_{iso/equiv}$
Cu1	0.74550(3)	0.21916(6)	0.54419(3)	0.0237(2)
Fe1	0.5000	0.5000	0.5000	0.0311(3)
S1	0.73456(6)	0.44035(14)	0.53554(8)	0.0291(3)
N1	0.76706(18)	-0.0636(4)	0.6140(2)	0.0190(8)
N2	0.74318(18)	-0.0661(4)	0.4843(2)	0.0197(9)
C1	0.6481(3)	0.4711(6)	0.4810(3)	0.0362(13)
C2	0.5997(3)	0.4722(6)	0.5348(3)	0.0312(12)
C3	0.5661(3)	0.3552(6)	0.5585(3)	0.0338(13)
C4	0.5254(3)	0.4036(7)	0.6094(3)	0.0373(14)
C5	0.5337(3)	0.5462(7)	0.6193(3)	0.0399(15)
C6	0.5799(2)	0.5935(7)	0.5741(3)	0.0348(13)
C7	0.7539(2)	0.0233(5)	0.5485(3)	0.0183(10)
C8	0.7639(2)	-0.2016(5)	0.5900(3)	0.0243(11)
C9	0.7495(2)	-0.2029(5)	0.5097(3)	0.0232(11)
C10	0.7829(2)	-0.0145(5)	0.6959(3)	0.0216(10)
C11	0.7341(2)	-0.0145(5)	0.7416(3)	0.0242(11)
C12	0.7514(3)	0.0335(6)	0.8203(3)	0.0331(13)
C13	0.8135(3)	0.0806(7)	0.8515(3)	0.0390(14)
C14	0.8609(3)	0.0799(6)	0.8053(3)	0.0358(13)
C15	0.8473(2)	0.0309(6)	0.7266(3)	0.0281(11)
C16	0.7302(2)	-0.0186(5)	0.4015(3)	0.0221(10)
C17	0.6667(3)	0.0295(6)	0.3664(3)	0.0291(12)
C18	0.6565(3)	0.0736(6)	0.2869(3)	0.0373(14)
C19	0.7060(3)	0.0695(7)	0.2441(3)	0.0439(15)
C20	0.7671(3)	0.0217(6)	0.2788(3)	0.0379(14)
C21	0.7813(3)	-0.0238(5)	0.3596(3)	0.0265(11)
C22	0.6201(3)	0.0656(8)	0.6943(6)	0.083(3)
C23	0.6647(2)	-0.0617(6)	0.7063(3)	0.0297(12)
C24	0.6400(3)	-0.1685(7)	0.7584(4)	0.0488(17)
C25	0.9175(4)	0.1798(9)	0.6566(5)	0.073(2)
C26	0.8995(3)	0.0306(7)	0.6765(3)	0.0396(14)
C27	0.9595(4)	-0.0514(12)	0.7175(5)	0.081(3)
C28	0.5565(3)	0.1294(8)	0.3765(5)	0.0561(18)
C29	0.6116(3)	0.0318(6)	0.4127(3)	0.0347(13)

C30	0.5816(3)	-0.1113(8)	0.4138(5)	0.0550(18)
C31	0.8941(3)	0.0559(7)	0.4222(4)	0.0500(16)
C32	0.8493(2)	-0.0687(6)	0.3975(3)	0.0289(12)
C33	0.8787(3)	-0.1715(8)	0.3450(5)	0.0564(19)
C1S	0.9218(8)	-0.0796(19)	1.0423(11)	0.072(4)
Cl1S	0.9445(4)	-0.2036(8)	1.0809(5)	0.0741(19)
Cl2S	0.9411(5)	0.0793(12)	1.0472(6)	0.109(3)
C2S	0.9218(8)	-0.0796(19)	1.0423(11)	0.072(4)
Cl3S	0.9784(6)	0.0270(14)	1.0232(8)	0.085(3)
Cl4S	0.9062(10)	-0.070(2)	1.1252(13)	0.143(6)

Table A.23. Summary of Crystal Data for **21**

Formula	$C_{71}H_{101}Cu_2FeN_4Se_2$
Formula Weight (*g/mol*)	1351.40
Crystal Dimensions (*mm*)	0.136 × 0.121 × 0.023
Crystal Color and Habit	yellow plate
Crystal System	monoclinic
Space Group	P 2_1/c
Temperature, K	110
a, Å	20.825(9)
b, Å	9.791(4)
c, Å	17.063(5)
α,°	90
β,°	102.294(8)
γ,°	90
V, Å^3	3399(2)
Number of reflections to determine final unit cell	9417
Min and Max 2θ for cell determination, °	5.42, 60.18
Z	2
F(000)	1414
ρ (*g/cm*)	1.320
λ, Å, (MoKα)	0.71073
μ, (*cm*$^{-1}$)	1.943
Diffractometer Type	Bruker Kappa Axis Apex2
Scan Type(s)	phi and omega scans
Max 2θ for data collection, °	48.498
Measured fraction of data	0.999
Number of reflections measured	75915
Unique reflections measured	5473
R_{merge}	0.0591
Number of reflections included in refinement	5473
Cut off Threshold Expression	I > 2sigma(I)
Structure refined using	full matrix least-squares using F^2

Weighting Scheme	$w=1/[sigma^2(Fo^2)+(0.0895P)^2+3.9308P]$ where $P=(Fo^2+2Fc^2)/3$
Number of parameters in least-squares	352
R_1	0.0549
wR_2	0.1589
R_1 (all data)	0.0669
wR_2 (all data)	0.1728
GOF	1.366
Maximum shift/error	0.001
Min & Max peak heights on final ΔF Map (e^-/Å)	-1.383, 1.613

Table A.24. Atomic Coordinates for **21**

Atom	x	y	z	$U_{iso/equiv}$
Se1	0.24089(2)	0.05890(5)	0.53843(3)	0.0212(2)
Cu1	0.24701(3)	0.28808(6)	0.54377(3)	0.0184(2)
Fe1	0.0000	0.0000	0.5000	0.0190(3)
N1	0.2665(2)	0.5661(4)	0.6111(2)	0.0184(9)
N2	0.2420(2)	0.5673(4)	0.4833(2)	0.0164(9)
C1	0.1484(3)	0.0295(6)	0.4803(3)	0.0252(11)
C2	0.1002(2)	0.0255(5)	0.5341(3)	0.0217(11)
C3	0.0671(3)	0.1392(6)	0.5589(3)	0.0241(11)
C4	0.0259(3)	0.0908(6)	0.6100(3)	0.0271(12)
C5	0.0343(3)	-0.0526(6)	0.6178(3)	0.0279(12)
C6	0.0803(3)	-0.0948(6)	0.5721(3)	0.0265(12)
C7	0.2532(2)	0.4817(5)	0.5472(3)	0.0159(10)
C8	0.2642(3)	0.7014(5)	0.5876(3)	0.0244(12)
C9	0.2488(3)	0.7024(5)	0.5078(3)	0.0238(12)
C10	0.2849(2)	0.5187(5)	0.6933(3)	0.0190(11)
C11	0.2361(3)	0.5168(5)	0.7393(3)	0.0219(11)
C12	0.2554(3)	0.4708(6)	0.8177(3)	0.0297(13)
C13	0.3178(3)	0.4252(6)	0.8487(3)	0.0346(14)
C14	0.3653(3)	0.4268(6)	0.8014(3)	0.0324(14)
C15	0.3487(3)	0.4745(5)	0.7223(3)	0.0242(11)
C16	0.2273(2)	0.5198(5)	0.4007(3)	0.0182(10)
C17	0.1641(3)	0.4738(5)	0.3675(3)	0.0215(11)
C18	0.1518(3)	0.4287(6)	0.2879(3)	0.0309(13)
C19	0.2008(3)	0.4306(6)	0.2448(3)	0.0347(14)
C20	0.2626(3)	0.4774(6)	0.2788(3)	0.0320(13)
C21	0.2782(3)	0.5234(6)	0.3583(3)	0.0244(12)
C22	0.1206(3)	0.4347(8)	0.6965(6)	0.068(3)
C23	0.1660(3)	0.5604(6)	0.7050(3)	0.0281(13)
C24	0.1422(3)	0.6685(6)	0.7558(4)	0.0411(16)
C25	0.4215(4)	0.3318(8)	0.6552(5)	0.056(2)

C26	0.4006(3)	0.4772(7)	0.6718(3)	0.0332(14)
C27	0.4600(4)	0.5607(10)	0.7110(5)	0.072(3)
C28	0.0537(3)	0.3737(6)	0.3821(4)	0.0377(14)
C29	0.1091(3)	0.4765(6)	0.4139(3)	0.0257(12)
C30	0.0796(3)	0.6182(7)	0.4115(4)	0.0465(16)
C31	0.3914(3)	0.4432(7)	0.4182(4)	0.0480(17)
C32	0.3474(3)	0.5686(6)	0.3957(3)	0.0302(13)
C33	0.3755(3)	0.6659(7)	0.3421(5)	0.0518(19)
C1S	0.5432(15)	0.294(3)	0.9458(18)	0.138(10)
C2S	0.5713(8)	0.4088(18)	0.9381(10)	0.151(6)
C3S	0.5238(6)	0.5230(13)	0.9738(7)	0.110(4)
C2S'	0.5713(8)	0.4088(18)	0.9381(10)	0.151(6)
C3S'	0.5238(6)	0.5230(13)	0.9738(7)	0.110(4)

Table A.25. Summary of Crystal Data for **24**

Formula	$C_{130}H_{178}Cu_4N_8O_3Se_4$
Formula Weight (*g/mol*)	2470.79
Crystal Dimensions (*mm*)	0.274 × 0.156 × 0.103
Crystal Color and Habit	yellow block
Crystal System	triclinic
Space Group	P -1
Temperature, K	110
a, Å	13.006(4)
b, Å	14.080(5)
c, Å	19.173(7)
α,°	71.160(15)
β,°	89.187(15)
γ,°	65.456(10)
V, $Å^3$	2993.2(17)
Number of reflections to determine final unit cell	9895
Min and Max 2θ for cell determination, °	4.7, 63.22
Z	1
F(000)	1290
ρ (*g/cm*)	1.371
λ, Å, (MoKα)	0.71073
μ, (cm^{-1})	1.972
Diffractometer Type	Bruker Kappa Axis Apex2
Scan Type(s)	phi and omega scans
Max 2θ for data collection, °	63.76
Measured fraction of data	0.991
Number of reflections measured	71877
Unique reflections measured	20161

R_{merge}	0.0440
Number of reflections included in refinement	20161
Cut off Threshold Expression	I > 2sigma(I)
Structure refined using	full matrix least-squares using F^2
Weighting Scheme	$w=1/[sigma^2(Fo^2)+(0.0881P)^2+0.0167P]$ where $P=(Fo^2+2Fc^2)/3$
Number of parameters in least-squares	821
R_1	0.0459
wR_2	0.1284
R_1 (all data)	0.0843
wR_2 (all data)	0.1610
GOF	1.121
Maximum shift/error	0.003
Min & Max peak heights on final ΔF Map (e^-/Å)	-1.614, 0.927

Table A.26. Atomic Coordinates for **24**

Atom	x	y	z	$U_{iso/equiv}$
Cu1	0.95357(3)	0.31371(3)	0.70478(2)	0.02466(8)
Cu2	0.76716(3)	0.48049(3)	0.71900(2)	0.02841(9)
Se1	0.96153(2)	0.47151(2)	0.72280(2)	0.02449(7)
Se2	0.78065(2)	0.38824(2)	0.62369(2)	0.02649(7)
N1	1.0565(2)	0.06724(19)	0.74562(13)	0.0294(5)
N2	1.1372(2)	0.1141(2)	0.81680(14)	0.0297(5)
N3	0.5371(2)	0.6560(2)	0.70782(15)	0.0303(5)
N4	0.6021(2)	0.5628(2)	0.82277(14)	0.0284(5)
C1	0.9602(2)	0.5394(2)	0.55890(15)	0.0252(5)
C2	0.8920(2)	0.5104(2)	0.52166(15)	0.0235(5)
C3	0.9343(2)	0.4718(2)	0.46348(14)	0.0245(5)
C4	0.9213(3)	0.5850(2)	0.61997(16)	0.0315(6)
C5	0.7770(2)	0.5200(2)	0.54008(17)	0.0311(6)
C6	1.0521(3)	0.1589(2)	0.75814(15)	0.0274(6)
C7	1.1420(3)	-0.0309(2)	0.79407(17)	0.0356(7)
C8	1.1929(3)	-0.0015(2)	0.83903(17)	0.0359(7)
C9	1.0102(5)	0.0757(5)	0.68091(18)	0.0310(16)
C10	1.0603(3)	0.0921(4)	0.6162(2)	0.0254(11)
C11	1.0045(3)	0.1067(4)	0.54967(18)	0.0323(13)
C12	0.8985(4)	0.1048(4)	0.5478(2)	0.0332(13)
C13	0.8484(4)	0.0884(4)	0.6124(3)	0.0340(14)
C14	0.9043(5)	0.0738(5)	0.6790(2)	0.0386(18)
C21	1.1657(8)	0.2095(7)	0.5739(4)	0.0340(16)
C22	1.1743(8)	0.0948(7)	0.6171(5)	0.0301(16)
C23	1.2618(8)	0.0066(7)	0.5885(5)	0.0386(17)
C24	0.7281(9)	0.1313(10)	0.7492(7)	0.083(4)

C25	0.8507(7)	0.0442(7)	0.7552(5)	0.0384(18)
C26	0.8675(9)	-0.0715(7)	0.7815(5)	0.056(2)
C9A	0.9845(5)	0.0741(6)	0.6816(2)	0.0196(14)
C10A	1.0328(4)	0.0765(5)	0.6163(3)	0.0302(17)
C11A	0.9739(4)	0.0801(4)	0.5548(2)	0.0299(14)
C12A	0.8665(4)	0.0814(5)	0.5587(2)	0.0339(16)
C13A	0.8182(4)	0.0790(5)	0.6240(3)	0.0350(18)
C14A	0.8771(5)	0.0753(6)	0.6854(2)	0.0284(15)
C21A	1.1364(9)	0.1920(8)	0.5645(6)	0.041(2)
C22A	1.1501(9)	0.0735(8)	0.6104(5)	0.034(2)
C23A	1.2306(8)	-0.0106(7)	0.5778(5)	0.0392(19)
C24A	0.6925(10)	0.1613(10)	0.7298(7)	0.066(3)
C25A	0.8163(8)	0.0777(8)	0.7514(6)	0.041(2)
C26A	0.8091(11)	-0.0350(10)	0.7932(7)	0.080(3)
C15	1.1637(3)	0.1800(2)	0.85049(18)	0.0319(6)
C16	1.2322(3)	0.2316(3)	0.81625(18)	0.0354(7)
C17	1.2543(3)	0.2960(3)	0.8498(2)	0.0444(8)
C18	1.2100(4)	0.3080(4)	0.9145(3)	0.0560(11)
C19	1.1443(4)	0.2547(4)	0.9476(3)	0.0535(10)
C20	1.1196(3)	0.1894(3)	0.9157(2)	0.0395(7)
C27	1.3784(8)	0.1141(7)	0.7573(5)	0.045(2)
C27A	1.4101(13)	0.1250(14)	0.7673(10)	0.088(6)
C28	1.2786(3)	0.2199(3)	0.7456(2)	0.0470(9)
C29	1.2927(4)	0.3206(4)	0.6960(3)	0.0682(14)
C30	0.9219(3)	0.2035(4)	0.9121(2)	0.0525(10)
C31	1.0448(3)	0.1321(3)	0.9504(2)	0.0461(8)
C32	1.0504(4)	0.1041(4)	1.0336(2)	0.0590(11)
C33	0.6325(2)	0.5692(2)	0.75346(16)	0.0270(6)
C34	0.4503(3)	0.7001(3)	0.7477(2)	0.0367(7)
C35	0.4917(3)	0.6409(3)	0.8196(2)	0.0379(7)
C36	0.5278(3)	0.7035(2)	0.62793(18)	0.0336(7)
C37	0.5739(3)	0.7809(2)	0.5991(2)	0.0366(7)
C38	0.5599(3)	0.8278(3)	0.5219(2)	0.0443(8)
C39	0.5040(3)	0.8003(3)	0.4764(2)	0.0451(9)
C40	0.4598(3)	0.7248(3)	0.5065(2)	0.0440(8)
C41	0.4706(3)	0.6741(3)	0.58346(19)	0.0382(7)
C42	0.6741(7)	0.4748(6)	0.8963(3)	0.0146(13)
C43	0.7585(7)	0.4885(5)	0.9298(3)	0.0233(15)
C44	0.8110(6)	0.4189(5)	1.0019(3)	0.0277(15)
C45	0.7790(6)	0.3356(6)	1.0405(3)	0.0356(19)
C46	0.6946(7)	0.3220(6)	1.0070(4)	0.0268(15)
C47	0.6421(6)	0.3915(6)	0.9349(4)	0.0166(14)
C42A	0.6649(8)	0.5028(7)	0.8877(4)	0.031(2)
C43A	0.7545(7)	0.5193(6)	0.9115(3)	0.0245(16)
C44A	0.8185(6)	0.4518(6)	0.9811(3)	0.0378(19)
C45A	0.7929(7)	0.3676(6)	1.0268(3)	0.041(2)

C46A	0.7033(8)	0.3510(7)	1.0030(4)	0.044(2)
C47A	0.6393(7)	0.4186(7)	0.9334(5)	0.040(3)
C48	0.5477(4)	0.8954(3)	0.6810(3)	0.0626(12)
C49	0.6335(3)	0.8116(3)	0.6496(2)	0.0464(9)
C50	0.7123(3)	0.8615(3)	0.6112(3)	0.0496(9)
C51	0.2932(7)	0.6436(7)	0.6013(5)	0.0389(16)
C52	0.4259(10)	0.5822(9)	0.6087(5)	0.0301(19)
C53	0.4598(5)	0.4947(5)	0.5743(4)	0.0381(14)
C54	0.7066(13)	0.6960(10)	0.8913(6)	0.040(2)
C55	0.7930(8)	0.5826(8)	0.8870(4)	0.0283(16)
C56	0.9119(7)	0.5610(7)	0.9139(5)	0.0387(16)
C57	0.4681(4)	0.3644(5)	0.9582(3)	0.0719(14)
C58	0.5484(3)	0.3811(3)	0.9024(2)	0.0456(8)
C59	0.6012(16)	0.2640(14)	0.8870(11)	0.078(5)
C51A	0.3108(8)	0.6266(8)	0.5675(5)	0.049(2)
C52A	0.4078(10)	0.6068(9)	0.6239(6)	0.0290(19)
C53A	0.4870(7)	0.4845(6)	0.6565(5)	0.0510(19)
C54A	0.6964(13)	0.7233(11)	0.8649(6)	0.043(2)
C55A	0.7798(10)	0.6130(8)	0.8596(5)	0.037(2)
C56A	0.9023(8)	0.5970(8)	0.8782(5)	0.0442(19)
C57A	0.4681(4)	0.3644(5)	0.9582(3)	0.0719(14)
C58A	0.5484(3)	0.3811(3)	0.9024(2)	0.0456(8)
C59A	0.5998(13)	0.3017(13)	0.8652(8)	0.063(4)
O1S	0.1766(2)	0.7497(2)	0.7473(2)	0.0605(8)
C1S	0.0669(6)	0.7761(5)	0.7012(4)	0.0376(14)
C2S	0.0244(6)	0.7066(6)	0.7581(5)	0.0474(18)
C3S	0.1310(6)	0.5981(6)	0.7930(4)	0.0422(16)
C4S	0.2274(7)	0.6317(6)	0.7827(4)	0.0343(14)
C1SA	0.1232(7)	0.7939(7)	0.6805(4)	0.0455(16)
C2SA	0.0699(7)	0.7222(6)	0.6716(4)	0.0456(16)
C3SA	0.1485(6)	0.6075(6)	0.7277(4)	0.0447(16)
C4SA	0.1772(9)	0.6418(8)	0.7882(6)	0.052(2)
O2S	1.4178(6)	-0.0545(6)	0.9644(4)	0.0768(19)
C5S	1.4132(15)	-0.0058(15)	1.0203(10)	0.093(5)
C8S	1.5265(10)	-0.0793(10)	0.9500(7)	0.079(3)
C7S	1.561(2)	0.005(2)	0.9606(14)	0.131(8)
C6S	1.4913(13)	0.0401(12)	1.0113(9)	0.100(4)

Table A.27. Summary of Crystal Data for **25**

Formula	$C_{34}H_{53}CuN_2OSSi$
Formula Weight (*g/mol*)	629.47
Crystal Dimensions (*mm*)	0.312 × 0.237 × 0.067
Crystal Color and Habit	colourless plate
Crystal System	monoclinic
Space Group	C 2/c
Temperature, K	110
a, Å	28.986(15)
b, Å	12.887(7)
c, Å	19.067(9)
α,°	90
β,°	92.619(12)
γ,°	90
V, $Å^3$	7115(6)
Number of reflections to determine final unit cell	9992
Min and Max 2θ for cell determination, °	5.02, 54.92
Z	8
F(000)	2704
ρ (*g/cm*)	1.175
λ, Å, (MoKα)	0.71073
μ, (cm^{-1})	0.733
Diffractometer Type	Bruker Kappa Axis Apex2
Scan Type(s)	phi and omega scans
Max 2θ for data collection, °	56.83
Measured fraction of data	1.000
Number of reflections measured	60384
Unique reflections measured	8905
R_{merge}	0.0771
Number of reflections included in refinement	8905
Cut off Threshold Expression	I > 2sigma(I)
Structure refined using	full matrix least-squares using F^2
Weighting Scheme	$w=1/[sigma^2(Fo^2)+(0.1000P)^2]$ where $P=(Fo^2+2Fc^2)/3$
Number of parameters in least-squares	348
R_1	0.0573
wR_2	0.1633
R_1 (all data)	0.1080
wR_2 (all data)	0.2016
GOF	1.195
Maximum shift/error	0.000
Min & Max peak heights on final ΔF Map (e^-/Å)	-0.733, 0.943

Table A.28. Atomic Coordinates for **25**

Atom	x	y	z	$U_{iso/equiv}$
Cu1	0.13409(2)	0.89331(3)	0.23739(2)	0.02657(15)
S1	0.13757(3)	0.92716(8)	0.34702(5)	0.0312(2)
Si1	0.18433(4)	0.81752(8)	0.39088(5)	0.0310(3)
N1	0.10298(9)	0.9416(2)	0.09415(14)	0.0239(6)
N2	0.15833(10)	0.8321(2)	0.09454(14)	0.0253(6)
C1	0.13103(12)	0.8846(3)	0.13860(17)	0.0245(7)
C2	0.11281(12)	0.9259(3)	0.02480(17)	0.0277(8)
C3	0.14785(13)	0.8568(3)	0.02453(18)	0.0288(8)
C4	0.06468(12)	1.0014(3)	0.11782(17)	0.0261(7)
C5	0.07237(13)	1.1024(3)	0.14264(19)	0.0317(8)
C6	0.03410(14)	1.1572(4)	0.1635(2)	0.0432(10)
C7	-0.00970(15)	1.1137(4)	0.1602(2)	0.0469(11)
C8	-0.01592(13)	1.0126(4)	0.13604(19)	0.0387(10)
C9	0.02111(12)	0.9546(3)	0.11484(18)	0.0308(8)
C10	0.19345(12)	0.7591(3)	0.11752(17)	0.0263(7)
C11	0.17975(13)	0.6589(3)	0.13624(18)	0.0319(8)
C12	0.21517(15)	0.5902(3)	0.1570(2)	0.0375(9)
C13	0.26055(15)	0.6182(3)	0.1590(2)	0.0394(10)
C14	0.27300(13)	0.7180(3)	0.14054(18)	0.0342(9)
C15	0.23943(13)	0.7915(3)	0.11942(17)	0.0287(8)
C16	0.13221(17)	1.1956(5)	0.2194(2)	0.0594(14)
C17	0.11977(13)	1.1523(3)	0.14632(19)	0.0325(8)
C18	0.12270(16)	1.2362(4)	0.0919(3)	0.0580(13)
C19	-0.02555(14)	0.8315(4)	0.0368(2)	0.0447(10)
C20	0.01422(13)	0.8421(3)	0.0914(2)	0.0346(9)
C21	0.00614(19)	0.7722(4)	0.1544(3)	0.0668(15)
C22	0.1224(2)	0.5261(4)	0.0907(3)	0.0720(16)
C23	0.12975(15)	0.6247(3)	0.1348(2)	0.0386(9)
C24	0.11367(19)	0.6079(5)	0.2085(3)	0.0654(15)
C25	0.28989(15)	0.9055(3)	0.0483(2)	0.0423(10)
C26	0.25357(13)	0.9013(3)	0.10265(19)	0.0311(8)
C27	0.26957(18)	0.9600(4)	0.1695(2)	0.0508(12)
C28	0.23217(14)	0.7843(3)	0.3327(2)	0.0421(10)
C29	0.20992(17)	0.8781(4)	0.4728(2)	0.0483(11)
C30	0.15415(17)	0.6937(3)	0.4118(2)	0.0462(11)
O1S	0.0539(5)	1.3530(10)	0.4354(6)	0.280(5)
C1S	0.0855(4)	1.3448(10)	0.3772(6)	0.175(5)
C2S	0.0834(4)	1.4169(9)	0.3459(7)	0.071(3)
C3S	0.0525(7)	1.4790(16)	0.3713(11)	0.149(8)
C4S	0.0165(7)	1.4271(15)	0.4147(10)	0.108(6)
C2SA	0.0484(4)	1.3832(9)	0.3078(6)	0.075(3)
C3SA	0.0179(7)	1.4497(14)	0.3274(9)	0.124(6)
C4SA	0.0257(16)	1.451(3)	0.4060(16)	0.28(3)

Table A.29. Summary of Crystal Data for **26**

Formula	$C_{34}H_{53}CuN_2OSeSi$
Formula Weight (*g/mol*)	676.37
Crystal Dimensions (*mm*)	0.554 × 0.545 × 0.274
Crystal Color and Habit	colourless block
Crystal System	monoclinic
Space Group	C 2/c
Temperature, K	110
a, Å	29.597(6)
b, Å	12.842(3)
c, Å	19.184(4)
α,°	90
β,°	93.196(5)
γ,°	90
V, $Å^3$	7280(3)
Number of reflections to determine final unit cell	9824
Min and Max 2θ for cell determination, °	4.94, 72.42
Z	8
F(000)	2848
ρ (*g/cm*)	1.234
λ, Å, (MoKα)	0.71073
μ, (cm^{-1})	1.659
Diffractometer Type	Bruker Kappa Axis Apex2
Scan Type(s)	phi and omega scans
Max 2θ for data collection, °	72.744
Measured fraction of data	0.999
Number of reflections measured	150833
Unique reflections measured	17704
R_{merge}	0.0414
Number of reflections included in refinement	17704
Cut off Threshold Expression	I > 2sigma(I)
Structure refined using	full matrix least-squares using F^2
Weighting Scheme	$w=1/[sigma^2(Fo^2)+(0.0729P)^2+2.5263P]$ where $P=(Fo^2+2Fc^2)/3$
Number of parameters in least-squares	367
R_1	0.0365
wR_2	0.1025
R_1 (all data)	0.0625
wR_2 (all data)	0.1284
GOF	1.081
Maximum shift/error	0.006
Min & Max peak heights on final ΔF Map (e^-/Å)	-0.955, 0.868

Table A.30. Atomic Coordinates for **26**

Atom	x	y	z	$U_{iso/equiv}$
Cu1	0.63374(2)	0.39498(2)	0.73481(2)	0.02243(5)
Se1	0.63523(2)	0.43562(2)	0.84863(2)	0.02755(5)
Si1	0.68600(2)	0.31872(3)	0.89197(2)	0.02638(8)
N1	0.60409(4)	0.44128(9)	0.59249(6)	0.0214(2)
N2	0.65864(4)	0.33196(9)	0.59324(5)	0.0215(2)
C1	0.63179(4)	0.38436(11)	0.63673(6)	0.0213(2)
C2	0.61354(5)	0.42564(12)	0.52333(7)	0.0246(2)
C3	0.64806(5)	0.35644(12)	0.52371(6)	0.0249(2)
C4	0.56672(4)	0.50141(12)	0.61597(7)	0.0245(2)
C5	0.57480(5)	0.60253(14)	0.64110(8)	0.0297(3)
C6	0.53755(6)	0.65791(17)	0.66296(9)	0.0398(4)
C7	0.49475(6)	0.6141(2)	0.66013(10)	0.0457(5)
C8	0.48799(5)	0.51342(18)	0.63614(9)	0.0391(4)
C9	0.52405(5)	0.45398(14)	0.61350(7)	0.0292(3)
C10	0.69305(5)	0.25878(11)	0.61715(7)	0.0227(2)
C11	0.73828(5)	0.29073(12)	0.61940(7)	0.0241(2)
C12	0.77092(5)	0.21767(13)	0.64161(8)	0.0303(3)
C13	0.75879(6)	0.11831(14)	0.66119(9)	0.0352(3)
C14	0.71384(6)	0.08950(13)	0.65888(9)	0.0343(3)
C15	0.67962(5)	0.15869(12)	0.63656(7)	0.0277(3)
C16	0.62362(8)	0.7302(2)	0.58398(12)	0.0524(5)
C17	0.62118(5)	0.65238(14)	0.64326(9)	0.0321(3)
C18	0.63384(8)	0.7036(2)	0.71351(11)	0.0507(5)
C19	0.51015(9)	0.2738(2)	0.65488(13)	0.0620(7)
C20	0.51668(5)	0.34186(15)	0.59112(9)	0.0333(3)
C21	0.47674(6)	0.33014(18)	0.53785(10)	0.0428(4)
C22	0.76757(9)	0.46017(17)	0.66771(10)	0.0458(5)
C23	0.75208(5)	0.40055(12)	0.60115(8)	0.0265(3)
C24	0.78832(7)	0.40179(15)	0.54760(9)	0.0367(3)
C25	0.61506(9)	0.1096(2)	0.70848(13)	0.0573(6)
C26	0.63074(6)	0.12438(14)	0.63454(9)	0.0351(3)
C27	0.62346(10)	0.0238(2)	0.59262(17)	0.0649(7)
C28	0.71263(8)	0.37880(16)	0.97326(10)	0.0443(5)
C29	0.65770(8)	0.19322(15)	0.91203(10)	0.0424(4)
C30	0.73178(6)	0.28948(16)	0.83173(10)	0.0381(4)
O1S	0.4418(3)	0.8406(7)	0.5627(4)	0.137(3)
C1S	0.4073(4)	0.8268(8)	0.6072(6)	0.122(3)
C2S	0.4126(4)	0.9208(8)	0.6469(6)	0.104(3)
C3S	0.4480(4)	0.9864(10)	0.6282(7)	0.148(4)
C4S	0.4766(4)	0.9146(9)	0.5802(7)	0.127(4)
O1SA	0.4531(3)	0.8838(7)	0.7018(5)	0.145(3)
C1SA	0.4203(5)	0.8695(14)	0.6464(7)	0.149(5)
C2SA	0.4459(9)	0.907(3)	0.5882(13)	0.36(2)

C3SA	0.4881(5)	0.9665(15)	0.6052(8)	0.168(6)
C4SA	0.4880(5)	0.9511(12)	0.6803(7)	0.172(6)

Table A.31. Summary of Crystal Data for **27**

Formula	$C_{30}H_{45}CuN_2SiTe$
Formula Weight (*g/mol*)	652.91
Crystal Dimensions (*mm*)	0.284 × 0.145 × 0.126
Crystal Color and Habit	colourless block
Crystal System	monoclinic
Space Group	P 2_1/n
Temperature, K	110
a, Å	9.789(3)
b, Å	21.443(11)
c, Å	15.580(6)
α,°	90
β,°	100.673(19)
γ,°	90
V, $Å^3$	3214(2)
Number of reflections to determine final unit cell	9369
Min and Max 2θ for cell determination, °	5.66, 72.0
Z	4
F(000)	1336
ρ (*g/cm*)	1.349
λ, Å, (MoKα)	0.71073
μ, (cm^{-1})	1.626
Diffractometer Type	Bruker Kappa Axis Apex2
Scan Type(s)	phi and omega scans
Max 2θ for data collection, °	65.0
Measured fraction of data	1.000
Number of reflections measured	109050
Unique reflections measured	11631
R_{merge}	0.0305
Number of reflections included in refinement	11631
Cut off Threshold Expression	I > 2sigma(I)
Structure refined using	full matrix least-squares using F^2
Weighting Scheme	$w=1/[sigma^2(Fo^2)+(0.0554P)^2]$ where $P=(Fo^2+2Fc^2)/3$
Number of parameters in least-squares	320
R_1	0.0249
wR_2	0.0836
R_1 (all data)	0.0328
wR_2 (all data)	0.0984
GOF	1.313
Maximum shift/error	0.004
Min & Max peak heights on final ΔF Map (e^-/Å)	-0.934, 1.210

Table A.32. Atomic Coordinates for **27**

Atom	x	y	z	$U_{iso/equiv}$
Cu1	0.35716(2)	0.69762(2)	0.26320(2)	0.01672(5)
Te1	0.29670(2)	0.71037(2)	0.40616(2)	0.02428(4)
Si3	0.23954(4)	0.59843(2)	0.42179(3)	0.02041(9)
N1	0.48086(11)	0.73624(6)	0.11515(8)	0.0153(2)
N2	0.40852(12)	0.64234(6)	0.09784(8)	0.0154(2)
C1	0.41565(13)	0.69118(7)	0.15373(9)	0.0149(2)
C2	0.51497(15)	0.71608(7)	0.03762(10)	0.0192(3)
C3	0.46944(14)	0.65672(7)	0.02653(10)	0.0196(3)
C4	0.50859(14)	0.79710(6)	0.15334(10)	0.0155(2)
C5	0.63408(14)	0.80670(7)	0.21128(10)	0.0181(3)
C6	0.65531(16)	0.86512(8)	0.24995(10)	0.0226(3)
C7	0.55559(17)	0.91172(8)	0.23201(11)	0.0246(3)
C8	0.43327(16)	0.90088(7)	0.17359(11)	0.0232(3)
C9	0.40674(13)	0.84323(7)	0.13251(10)	0.0185(3)
C10	0.35203(14)	0.58239(7)	0.11379(9)	0.0165(2)
C11	0.44572(14)	0.53445(7)	0.14388(9)	0.0182(3)
C12	0.38997(16)	0.47605(7)	0.15870(10)	0.0224(3)
C13	0.24696(17)	0.46718(8)	0.14449(11)	0.0254(3)
C14	0.15706(16)	0.51606(8)	0.11554(11)	0.0237(3)
C15	0.20612(14)	0.57486(7)	0.09925(9)	0.0185(3)
C16	0.7541(2)	0.73370(13)	0.32706(15)	0.0475(6)
C17	0.74307(15)	0.75534(8)	0.23304(11)	0.0247(3)
C18	0.8800(3)	0.77246(16)	0.2075(3)	0.0352(6)
C18A	0.8876(6)	0.7860(4)	0.2373(7)	0.043(2)
C19	0.15025(17)	0.82954(13)	0.11963(15)	0.0445(6)
C20	0.27074(15)	0.83177(8)	0.06973(11)	0.0233(3)
C21	0.24316(19)	0.88066(9)	-0.00221(11)	0.0312(4)
C22	0.66462(18)	0.53595(12)	0.25857(12)	0.0378(5)
C23	0.60257(14)	0.54444(7)	0.16163(10)	0.0209(3)
C24	0.67290(17)	0.50099(9)	0.10513(11)	0.0262(3)
C25	-0.03868(19)	0.62126(11)	0.08428(15)	0.0392(5)
C26	0.10903(14)	0.62855(7)	0.06498(10)	0.0215(3)
C27	0.09805(19)	0.63540(10)	-0.03370(13)	0.0345(4)
C28	0.36763(18)	0.54654(9)	0.38125(13)	0.0308(4)
C29	0.2397(3)	0.58140(10)	0.53934(13)	0.0443(5)
C30	0.06269(18)	0.57993(10)	0.35735(16)	0.0414(5)

Table A.33. Summary of Crystal Data for **28**

Formula	$C_{29}H_{40}Cl_4CuHg_{0.50}N_2S$
Formula Weight (*g/mol*)	754.32
Crystal Dimensions (*mm*)	0.325 × 0.205 × 0.108
Crystal Color and Habit	colourless block
Crystal System	monoclinic
Space Group	P 2_1/n
Temperature, K	110
a, Å	13.026(3)
b, Å	16.803(3)
c, Å	16.264(4)
α,°	90
β,°	106.93(3)
γ,°	90
V, Å^3	3405.6(14)
Number of reflections to determine final unit cell	9963
Min and Max 2θ for cell determination, °	5.32, 59.16
Z	4
F(000)	1524
ρ (*g/cm*)	1.471
λ, Å, (MoKα)	0.71073
μ, (cm^{-1})	3.279
Diffractometer Type	Bruker Kappa Axis Apex2
Scan Type(s)	phi and omega scans
Max 2θ for data collection, °	48.494
Measured fraction of data	0.997
Number of reflections measured	18008
Unique reflections measured	5492
R_{merge}	0.0380
Number of reflections included in refinement	5492
Cut off Threshold Expression	I > 2sigma(I)
Structure refined using	full matrix least-squares using F^2
Weighting Scheme	w=1/[sigma^2(Fo^2)+(0.0890P)^2+15.0081P] where P=(Fo^2+2Fc^2)/3
Number of parameters in least-squares	362
R_1	0.0518
wR_2	0.1454
R_1 (all data)	0.0658
wR_2 (all data)	0.1676
GOF	1.216
Maximum shift/error	0.001
Min & Max peak heights on final ΔF Map (e^-/Å)	-1.642, 3.273

Table A.34. Atomic Coordinates for **28**

Atom	x	y	z	$U_{iso/equiv}$
Hg1	0.5000	0.5000	0.5000	0.02055(18)
Cu1	0.37028(8)	0.44746(5)	0.32074(6)	0.0238(3)
S1	0.41883(16)	0.56265(11)	0.37105(13)	0.0266(5)
N1	0.2278(6)	0.3107(4)	0.2630(4)	0.0306(16)
N2	0.3783(6)	0.2963(5)	0.2348(5)	0.043(2)
C1	0.3234(7)	0.3470(5)	0.2714(5)	0.0295(19)
C2	0.2215(9)	0.2383(6)	0.2207(7)	0.046(2)
C3	0.3182(9)	0.2293(6)	0.2043(7)	0.053(3)
C4	0.1447(6)	0.3393(5)	0.2976(5)	0.0274(18)
C5	0.0665(7)	0.3878(6)	0.2447(6)	0.040(2)
C6	-0.0143(9)	0.4108(7)	0.2781(9)	0.061(3)
C7	-0.0181(8)	0.3890(8)	0.3575(10)	0.067(4)
C8	0.0623(9)	0.3396(7)	0.4094(8)	0.056(3)
C9	0.1471(7)	0.3139(5)	0.3802(6)	0.038(2)
C10	0.4901(8)	0.3093(6)	0.2319(7)	0.044(2)
C11	0.5006(9)	0.3503(7)	0.1619(8)	0.054(3)
C12	0.6076(9)	0.3640(9)	0.1596(9)	0.071(4)
C13	0.6912(10)	0.3363(9)	0.2237(10)	0.077(4)
C14	0.6768(10)	0.2959(9)	0.2918(10)	0.081(5)
C15	0.5716(9)	0.2788(8)	0.2992(8)	0.062(3)
C16	0.1169(13)	0.5023(7)	0.1650(11)	0.078(4)
C17	0.0740(10)	0.4151(7)	0.1575(8)	0.063(3)
C18	-0.0337(11)	0.4088(9)	0.0893(9)	0.085(4)
C19	0.2911(13)	0.2996(9)	0.5213(9)	0.090(4)
C20	0.2359(9)	0.2624(6)	0.4343(7)	0.051(3)
C21	0.1987(12)	0.1777(8)	0.4405(11)	0.089(4)
C22	0.3935(14)	0.4714(10)	0.0926(11)	0.089(5)
C23	0.4065(9)	0.3801(7)	0.0894(7)	0.055(3)
C24	0.4138(11)	0.3540(10)	0.0013(8)	0.080(4)
C26	0.5567(10)	0.2355(8)	0.3745(8)	0.066(3)
C25	0.633(2)	0.2803(13)	0.4567(16)	0.068(8)
C27	0.600(3)	0.1548(16)	0.361(2)	0.088(10)
C25A	0.552(2)	0.2788(17)	0.4540(19)	0.073(8)
C27A	0.623(3)	0.160(2)	0.408(2)	0.080(11)
Cl1S	0.7690(3)	0.4713(3)	0.4543(2)	0.0823(11)
C1S	0.8282(8)	0.4595(6)	0.5638(7)	0.049(3)
Cl2S	0.9476(2)	0.40317(18)	0.5888(2)	0.0600(8)
C2S	0.6283(9)	0.5919(8)	0.2732(8)	0.061(3)
Cl3S	0.5694(2)	0.6804(2)	0.2264(2)	0.0650(8)
Cl4S	0.7576(4)	0.5775(3)	0.2694(4)	0.0892(16)
Cl5S	0.6738(17)	0.5334(13)	0.2312(14)	0.087(5)

Table A.35. Summary of Crystal Data for **29**

Formula	$C_{34}H_{53}AgN_2OSSi$
Formula Weight (*g/mol*)	673.80
Crystal Dimensions (*mm*)	0.260 × 0.118 × 0.084
Crystal Color and Habit	colourless plate
Crystal System	triclinic
Space Group	P -1
Temperature, K	110
a, Å	10.196(2)
b, Å	12.625(3)
c, Å	16.038(5)
α,°	67.516(13)
β,°	79.534(12)
γ,°	71.104(9)
V, $Å^3$	1800.8(9)
Number of reflections to determine final unit cell	7964
Min and Max 2θ for cell determination, °	5.28, 60.0
Z	2
F(000)	712
ρ (*g/cm*)	1.243
λ, Å, (MoKα)	0.71073
μ, (cm^{-1})	0.677
Diffractometer Type	Bruker Kappa Axis Apex2
Scan Type(s)	phi and omega scans
Max 2θ for data collection, °	48.296
Measured fraction of data	0.968
Number of reflections measured	20047
Unique reflections measured	5584
R_{merge}	0.0395
Number of reflections included in refinement	5584
Cut off Threshold Expression	I > 2sigma(I)
Structure refined using	full matrix least-squares using F^2
Weighting Scheme	$w=1/[sigma^2(Fo^2)+(0.1093P)^2+6.4611P]$ where $P=(Fo^2+2Fc^2)/3$
Number of parameters in least-squares	361
R_1	0.0610
wR_2	0.1740
R_1 (all data)	0.0735
wR_2 (all data)	0.1945
GOF	1.141
Maximum shift/error	0.000
Min & Max peak heights on final ΔF Map (e^-/Å)	-0.983, 3.817

Table A.36. Atomic Coordinates for **29**

Atom	x	y	z	$U_{iso/equiv}$
Ag1	0.50887(4)	0.33595(4)	0.26100(3)	0.0265(2)
S1	0.27225(17)	0.34982(16)	0.27133(11)	0.0330(4)
Si1	0.1892(2)	0.4529(2)	0.35426(14)	0.0404(5)
N1	0.8123(5)	0.2117(5)	0.3125(3)	0.0244(11)
N2	0.8043(5)	0.3773(4)	0.2033(3)	0.0223(11)
C1	0.7230(6)	0.3080(5)	0.2569(4)	0.0218(13)
C2	0.9474(7)	0.2226(6)	0.2932(5)	0.0311(15)
C3	0.9432(6)	0.3249(6)	0.2248(4)	0.0298(15)
C4	0.7690(6)	0.1137(6)	0.3814(4)	0.0288(14)
C5	0.7382(7)	0.0315(6)	0.3548(5)	0.0350(16)
C6	0.6946(8)	-0.0618(7)	0.4229(5)	0.0451(19)
C7	0.6838(8)	-0.0709(8)	0.5128(6)	0.051(2)
C8	0.7144(8)	0.0109(7)	0.5363(5)	0.047(2)
C9	0.7585(7)	0.1064(6)	0.4712(4)	0.0341(16)
C10	0.7528(6)	0.4882(6)	0.1307(4)	0.0248(13)
C11	0.7584(6)	0.4846(6)	0.0435(4)	0.0273(14)
C12	0.7064(7)	0.5919(6)	-0.0239(5)	0.0344(16)
C13	0.6498(7)	0.6972(7)	-0.0069(5)	0.0389(17)
C14	0.6457(7)	0.6984(6)	0.0799(5)	0.0338(16)
C15	0.6984(6)	0.5933(6)	0.1503(4)	0.0278(14)
C16	0.6165(9)	0.0428(8)	0.2261(7)	0.056(2)
C17	0.7536(8)	0.0372(6)	0.2569(5)	0.0397(17)
C18	0.8724(8)	-0.0679(7)	0.2435(6)	0.0453(19)
C19	0.6622(9)	0.2562(10)	0.5506(8)	0.070(3)
C20	0.7907(7)	0.1956(7)	0.4996(5)	0.0386(17)
C21	0.9090(8)	0.1367(8)	0.5615(6)	0.054(2)
C22	0.6998(9)	0.3356(9)	0.0010(7)	0.059(2)
C23	0.8160(7)	0.3696(6)	0.0247(5)	0.0327(15)
C24	0.9343(8)	0.3764(7)	-0.0505(5)	0.0425(18)
C25	0.5429(9)	0.6163(10)	0.2864(7)	0.065(3)
C26	0.6934(7)	0.5953(7)	0.2449(5)	0.0353(16)
C27	0.7523(9)	0.6904(8)	0.2459(6)	0.053(2)
C28	0.2994(8)	0.4131(8)	0.4486(5)	0.0459(19)
C29	0.1579(10)	0.6168(8)	0.2896(7)	0.066(3)
C30	0.0198(9)	0.4207(12)	0.4076(7)	0.080(4)
O1S	0.3872(7)	-0.0221(6)	0.1117(5)	0.0663(17)
C1S	0.2715(11)	0.0124(10)	0.1690(7)	0.073(3)
C2S	0.1523(10)	0.0854(9)	0.1109(7)	0.062(2)
C3S	0.1850(11)	0.0300(12)	0.0388(8)	0.084(3)
C4S	0.3325(10)	-0.0482(9)	0.0496(8)	0.065(3)

Table A.37. Summary of Crystal Data for **30**

Formula	$C_{34}H_{53}AgN_2OSeSi$
Formula Weight (*g/mol*)	720.70
Crystal Dimensions (*mm*)	0.406 × 0.210 × 0.170
Crystal Color and Habit	colourless block
Crystal System	triclinic
Space Group	P -1
Temperature, K	110
a, Å	10.309(3)
b, Å	12.604(5)
c, Å	16.151(5)
α,°	68.375(15)
β,°	78.886(13)
γ,°	71.154(11)
V, $Å^3$	1839.9(10)
Number of reflections to determine final unit cell	9690
Min and Max 2θ for cell determination, °	5.2, 68.44
Z	2
F(000)	748
ρ (*g/cm*)	1.301
λ, Å, (MoKα)	0.71073
μ, (cm^{-1})	1.595
Diffractometer Type	Bruker Kappa Axis Apex2
Scan Type(s)	phi and omega scans
Max 2θ for data collection, °	48.498
Measured fraction of data	0.998
Number of reflections measured	25554
Unique reflections measured	5942
R_{merge}	0.0189
Number of reflections included in refinement	5942
Cut off Threshold Expression	I > 2sigma(I)
Structure refined using	full matrix least-squares using F^2
Weighting Scheme	$w=1/[sigma^2(Fo^2)+(0.0732P)^2+2.9145P]$ where $P=(Fo^2+2Fc^2)/3$
Number of parameters in least-squares	372
R_1	0.0333
wR_2	0.1028
R_1 (all data)	0.0382
wR_2 (all data)	0.1180
GOF	1.125
Maximum shift/error	0.001
Min & Max peak heights on final ΔF Map (e^-/Å)	-0.596, 1.614

Table A.38. Atomic Coordinates for **30**

Atom	x	y	z	$U_{iso/equiv}$
Ag1	0.51958(2)	0.32595(2)	0.26077(2)	0.01890(12)
Se1	0.27861(4)	0.33348(3)	0.26961(2)	0.02471(13)
Si1	0.19142(11)	0.44954(11)	0.35499(8)	0.0339(3)
N1	0.8197(3)	0.2099(3)	0.31037(19)	0.0191(6)
N2	0.8091(3)	0.3739(3)	0.20363(19)	0.0177(6)
C1	0.7305(3)	0.3039(3)	0.2573(2)	0.0169(7)
C2	0.9514(4)	0.2221(3)	0.2903(3)	0.0240(8)
C3	0.9456(4)	0.3251(3)	0.2233(3)	0.0236(8)
C4	0.7773(4)	0.1112(3)	0.3783(2)	0.0248(8)
C5	0.7617(4)	0.1058(4)	0.4676(3)	0.0312(9)
C6	0.7166(5)	0.0118(4)	0.5309(3)	0.0449(12)
C7	0.6874(5)	-0.0703(4)	0.5063(3)	0.0498(13)
C8	0.7042(5)	-0.0633(4)	0.4181(3)	0.0437(11)
C9	0.7506(4)	0.0285(3)	0.3506(3)	0.0313(9)
C10	0.7556(3)	0.4837(3)	0.1343(2)	0.0204(7)
C11	0.7010(4)	0.5873(3)	0.1565(3)	0.0264(8)
C12	0.6460(4)	0.6918(4)	0.0888(3)	0.0345(10)
C13	0.6470(4)	0.6915(4)	0.0038(3)	0.0390(11)
C14	0.7026(4)	0.5876(4)	-0.0166(3)	0.0348(10)
C15	0.7586(4)	0.4806(4)	0.0483(3)	0.0261(8)
C16	0.6604(6)	0.2616(7)	0.5421(6)	0.081(2)
C17	0.7909(4)	0.1976(4)	0.4959(3)	0.0367(10)
C18	0.9035(6)	0.1405(5)	0.5595(4)	0.0589(15)
C19	0.6409(5)	0.0360(4)	0.2213(4)	0.0489(13)
C20	0.7723(5)	0.0314(4)	0.2544(3)	0.0353(10)
C21	0.8906(5)	-0.0750(4)	0.2427(3)	0.0425(11)
C22	0.5523(6)	0.6053(6)	0.2956(4)	0.0586(15)
C23	0.6984(4)	0.5884(4)	0.2505(3)	0.0320(9)
C24	0.7592(6)	0.6834(5)	0.2513(4)	0.0492(12)
C25	0.7025(6)	0.3336(5)	0.0014(4)	0.0551(14)
C26	0.8159(4)	0.3676(4)	0.0255(3)	0.0304(9)
C27	0.9325(5)	0.3781(5)	-0.0497(3)	0.0412(11)
C28	0.0203(5)	0.4249(7)	0.4060(4)	0.0695(17)
C29	0.2987(5)	0.4120(4)	0.4477(3)	0.0389(10)
C30	0.1690(6)	0.6094(5)	0.2892(4)	0.0614(14)
O1S	0.3952(6)	-0.0210(5)	0.1155(4)	0.0962(15)
C2S	0.1612(6)	0.0899(5)	0.1124(4)	0.0645(15)
C1S	0.2849(8)	0.0212(8)	0.1755(5)	0.090(2)
C3S	0.1971(8)	0.0311(8)	0.0454(6)	0.094(2)
C4S	0.3326(8)	-0.0497(7)	0.0589(6)	0.088(2)

Table A.39. Summary of Crystal Data for **31**

Formula	$C_{70}H_{104}Ag_2HgN_4O_4S_2$
Formula Weight (*g/mol*)	1546.02
Crystal Dimensions (*mm*)	0.313 × 0.254 × 0.226
Crystal Color and Habit	colourless blcok
Crystal System	triclinic
Space Group	P -1
Temperature, K	110
a, Å	14.614(3)
b, Å	16.118(3)
c, Å	16.572(3)
α,°	88.030(8)
β,°	66.251(8)
γ,°	87.115(9)
V, $Å^3$	3567.8(11)
Number of reflections to determine final unit cell	9911
Min and Max 2θ for cell determination, °	5.9, 56.34
Z	2
F(000)	1580
ρ (*g/cm*)	1.439
λ, Å, (MoKα)	0.71073
μ, (cm^{-1})	2.795
Diffractometer Type	Bruker Kappa Axis Apex2
Scan Type(s)	phi scans
Max 2θ for data collection, °	56.648
Measured fraction of data	1.000
Number of reflections measured	31783
Unique reflections measured	31783
R_{merge}	?
Number of reflections included in refinement	31783
Cut off Threshold Expression	I > 2sigma(I)
Structure refined using	full matrix least-squares using F^2
Weighting Scheme	$w=1/[sigma^2(Fo^2)+(0.1116P)^2]$ where $P=(Fo^2+2Fc^2)/3$
Number of parameters in least-squares	776
R_1	0.0534
wR_2	0.1399
R_1 (all data)	0.0967
wR_2 (all data)	0.1954
GOF	1.075
Maximum shift/error	0.001
Min & Max peak heights on final ΔF Map (e^-/Å)	-2.435, 2.385

Table A.40. Atomic Coordinates for **31**

Atom	x	y	z	$U_{iso/equiv}$
Hg1	0.5000	0.5000	0.5000	0.02154(11)
Ag1	0.64107(4)	0.33048(3)	0.49483(4)	0.01993(14)
S1	0.53816(16)	0.42163(13)	0.60269(13)	0.0289(5)
N1	0.7332(5)	0.2456(4)	0.3137(4)	0.0197(13)
N2	0.8254(5)	0.2157(4)	0.3859(4)	0.0186(13)
C1	0.7388(5)	0.2560(4)	0.3929(5)	0.0183(15)
C2	0.8160(6)	0.1995(5)	0.2572(5)	0.0232(17)
C3	0.8740(6)	0.1801(5)	0.3027(5)	0.0239(17)
C4	0.6594(6)	0.2897(4)	0.2890(5)	0.0200(16)
C5	0.6802(6)	0.3710(4)	0.2576(5)	0.0194(16)
C6	0.6077(6)	0.4140(5)	0.2377(5)	0.0254(17)
C7	0.5208(7)	0.3784(5)	0.2465(6)	0.0285(19)
C8	0.5043(6)	0.2976(5)	0.2760(5)	0.0256(18)
C9	0.5742(6)	0.2505(5)	0.2975(5)	0.0213(16)
C10	0.8642(6)	0.2129(5)	0.4530(5)	0.0204(16)
C11	0.9102(6)	0.2831(5)	0.4641(5)	0.0219(16)
C12	0.9471(6)	0.2771(5)	0.5291(6)	0.0295(19)
C13	0.9380(7)	0.2061(5)	0.5807(6)	0.0311(19)
C14	0.8913(6)	0.1386(5)	0.5686(5)	0.0283(18)
C15	0.8538(6)	0.1404(5)	0.5038(5)	0.0223(16)
C16	0.7552(6)	0.4831(5)	0.3080(6)	0.0270(18)
C17	0.7759(6)	0.4116(5)	0.2458(5)	0.0244(17)
C18	0.8324(7)	0.4402(6)	0.1518(6)	0.035(2)
C19	0.4963(7)	0.1138(5)	0.2905(7)	0.036(2)
C20	0.5549(6)	0.1615(5)	0.3319(6)	0.0271(18)
C21	0.5027(7)	0.1597(5)	0.4341(6)	0.034(2)
C22	0.8953(9)	0.4401(5)	0.4620(7)	0.049(3)
C23	0.9233(6)	0.3606(5)	0.4068(6)	0.0279(18)
C24	1.0290(8)	0.3648(7)	0.3378(8)	0.066(4)
C25	0.7052(8)	0.0499(7)	0.5719(7)	0.051(3)
C26	0.8032(7)	0.0651(5)	0.4899(5)	0.0283(19)
C27	0.8740(7)	-0.0120(5)	0.4688(6)	0.036(2)
Hg2	1.0000	1.0000	0.0000	0.02834(13)
Ag2	0.86228(4)	0.83338(3)	0.01190(4)	0.02109(14)
S2	0.97704(19)	0.91351(14)	-0.09820(14)	0.0367(6)
N3	0.7697(4)	0.7498(4)	0.1941(4)	0.0178(13)
N4	0.6774(5)	0.7253(4)	0.1264(4)	0.0192(13)
C28	0.7621(6)	0.7632(4)	0.1158(5)	0.0191(15)
C29	0.6908(6)	0.7056(4)	0.2519(5)	0.0193(16)
C30	0.6326(6)	0.6900(5)	0.2098(5)	0.0212(16)
C31	0.8456(6)	0.7880(5)	0.2131(5)	0.0193(16)
C32	0.9345(6)	0.7430(5)	0.2001(5)	0.0199(16)
C33	1.0103(6)	0.7846(5)	0.2109(5)	0.0249(18)

C34	0.9956(6)	0.8682(5)	0.2360(5)	0.0273(19)
C35	0.9053(6)	0.9095(5)	0.2506(5)	0.0242(17)
C36	0.8282(6)	0.8709(5)	0.2408(5)	0.0202(16)
C37	0.6363(6)	0.7260(5)	0.0604(5)	0.0210(16)
C38	0.6610(6)	0.6600(5)	0.0013(5)	0.0229(16)
C39	0.6196(6)	0.6601(5)	-0.0605(6)	0.0300(19)
C40	0.5542(6)	0.7266(5)	-0.0630(6)	0.0297(19)
C41	0.5318(6)	0.7915(5)	-0.0047(6)	0.0277(18)
C42	0.5721(6)	0.7931(5)	0.0589(5)	0.0252(17)
C43	1.0054(7)	0.5988(5)	0.2190(6)	0.035(2)
C44	0.9497(6)	0.6514(5)	0.1726(5)	0.0239(17)
C45	1.0043(7)	0.6439(6)	0.0722(5)	0.033(2)
C46	0.7416(7)	0.9908(5)	0.1944(6)	0.033(2)
C47	0.7286(6)	0.9171(5)	0.2589(5)	0.0254(18)
C48	0.6784(8)	0.9449(6)	0.3533(6)	0.044(3)
C49	0.7004(9)	0.5051(6)	-0.0051(7)	0.046(3)
C50	0.7353(7)	0.5909(5)	0.0020(6)	0.034(2)
C51	0.8381(8)	0.6046(7)	-0.0720(8)	0.055(3)
C52	0.4392(9)	0.8790(9)	0.1781(10)	0.089(5)
C53	0.5474(7)	0.8670(5)	0.1214(6)	0.0310(19)
C54	0.5850(11)	0.9476(6)	0.0687(8)	0.062(3)
O1	0.6510(6)	0.4926(4)	-0.1982(5)	0.0436(17)
C1S	0.7304(9)	0.4666(7)	-0.2796(8)	0.064(4)
C2S	0.7383(9)	0.3748(8)	-0.2701(9)	0.067(4)
C3S	0.6340(9)	0.3519(7)	-0.2172(8)	0.054(3)
C4S	0.5856(8)	0.4273(7)	-0.1700(8)	0.047(3)
O2	0.8772(6)	-0.0493(5)	0.6992(5)	0.055(2)
C5S	0.8594(9)	-0.1304(7)	0.6819(8)	0.059(3)
C6S	0.764(2)	-0.152(2)	0.738(3)	0.102(14)
C6SA	0.8027(15)	-0.1697(12)	0.7666(14)	0.032(4)
C7S	0.7332(10)	-0.0953(8)	0.8157(8)	0.082(5)
C8S	0.8051(8)	-0.0266(6)	0.7839(7)	0.048(3)
O3	1.2610(5)	0.8035(5)	0.0871(5)	0.0509(19)
C9S	1.2779(7)	0.7296(6)	0.0382(7)	0.039(2)
C10S	1.2757(9)	0.7511(7)	-0.0490(7)	0.049(3)
C11S	1.2159(10)	0.8287(10)	-0.0316(10)	0.048(4)
C17S	1.280(2)	0.8419(16)	-0.0526(18)	0.024(6)
C12S	1.2411(9)	0.8690(7)	0.0374(7)	0.049(3)
O4	0.2179(8)	0.2632(6)	0.4641(6)	0.081(3)
C13S	0.1965(9)	0.2625(6)	0.5602(6)	0.043(2)
C14S	0.2496(7)	0.3222(6)	0.5754(5)	0.037(2)
C15S	0.2981(8)	0.3697(6)	0.5003(7)	0.045(3)
C16S	0.2486(7)	0.3535(6)	0.4404(6)	0.037(2)

Table A.41. Summary of Crystal Data for **32**

Formula	$C_{18}H_{31}CuN_2O_{0.50}SSi$
Formula Weight (*g/mol*)	407.14
Crystal Dimensions (*mm*)	0.371 × 0.268 × 0.170
Crystal Color and Habit	colourless block
Crystal System	monoclinic
Space Group	C 2/c
Temperature, K	110
a, Å	10.379(3)
b, Å	16.442(4)
c, Å	24.602(7)
α,°	90
β,°	94.930(13)
γ,°	90
V, $Å^3$	4182.7(19)
Number of reflections to determine final unit cell	9061
Min and Max 2θ for cell determination, °	4.96, 69.7
Z	8
F(000)	1728
ρ (*g/cm*)	1.293
λ, Å, (MoKα)	0.71073
μ, (cm^{-1})	1.206
Diffractometer Type	Bruker Kappa Axis Apex2
Scan Type(s)	phi and omega scans
Max 2θ for data collection, °	69.76
Measured fraction of data	1.000
Number of reflections measured	69222
Unique reflections measured	9133
R_{merge}	0.0344
Number of reflections included in refinement	9133
Cut off Threshold Expression	I > 2sigma(I)
Structure refined using	full matrix least-squares using F^2
Weighting Scheme	$w=1/[sigma^2(Fo^2)+(0.0760P)^2]$ where $P=(Fo^2+2Fc^2)/3$
Number of parameters in least-squares	242
R_1	0.0277
wR_2	0.0904
R_1 (all data)	0.0422
wR_2 (all data)	0.1205
GOF	1.175
Maximum shift/error	0.001
Min & Max peak heights on final ΔF Map (e^-/Å)	-1.366, 0.931

Table A.42. Atomic Coordinates for **32**

Atom	x	y	z	$U_{iso/equiv}$
Cu1	0.10771(2)	0.25809(2)	0.28518(2)	0.01559(5)
S1	0.09167(3)	0.19980(2)	0.19941(2)	0.01554(6)
Si1	0.20916(4)	0.26551(2)	0.14879(2)	0.01984(8)
N1	0.26991(10)	0.39750(6)	0.32542(4)	0.01729(18)
N2	0.30568(10)	0.29024(5)	0.37575(4)	0.01507(17)
C1	0.23226(11)	0.31854(6)	0.33099(5)	0.01615(19)
C2	0.36560(11)	0.41916(6)	0.36603(5)	0.01671(19)
C3	0.38717(11)	0.35023(6)	0.39874(5)	0.01527(19)
C4	0.47864(12)	0.34913(7)	0.44374(5)	0.0186(2)
C5	0.54907(14)	0.42006(8)	0.45447(6)	0.0241(2)
C6	0.52794(14)	0.48924(8)	0.42175(6)	0.0260(3)
C7	0.43678(13)	0.49047(7)	0.37709(5)	0.0222(2)
C8	0.31258(18)	0.48192(9)	0.24536(6)	0.0349(3)
C9	0.21233(14)	0.45150(7)	0.28216(6)	0.0257(3)
C10	0.13868(16)	0.52066(9)	0.30665(8)	0.0376(4)
C11	0.29328(14)	0.14140(7)	0.35992(6)	0.0246(2)
C12	0.29227(12)	0.21012(7)	0.40144(5)	0.0186(2)
C13	0.17249(15)	0.20910(8)	0.43292(6)	0.0265(3)
C14	0.37499(14)	0.27277(10)	0.18449(7)	0.0314(3)
C15	0.14114(16)	0.36891(9)	0.13144(6)	0.0306(3)
C16	0.21788(17)	0.20940(10)	0.08260(6)	0.0333(3)
O1S	0.4218(4)	0.0893(2)	0.50009(17)	0.0791(12)
C1S	0.3656(4)	0.0253(3)	0.5222(3)	0.0715(17)
C2S	0.4621(13)	-0.0440(5)	0.5282(5)	0.055(2)
C3S	0.5748(4)	-0.0153(3)	0.50378(19)	0.0478(9)
C4S	0.5404(10)	0.0672(5)	0.4801(4)	0.0532(19)

Table A.43. Summary of Crystal Data for **33**

Formula	$C_{80}H_{140}Cu_4N_8O_4Se_4Si_4$
Formula Weight (*g/mol*)	1960.35
Crystal Dimensions (*mm*)	0.600 × 0.032 × 0.032
Crystal Color and Habit	colourless needle
Crystal System	monoclinic
Space Group	P 2_1/c
Temperature, K	110
a, Å	20.371(5)
b, Å	21.812(5)
c, Å	21.819(6)
α,°	90
β,°	101.334(10)
γ,°	90
V, Å^3	9506(4)
Number of reflections to determine final unit cell	9676
Min and Max 2θ for cell determination, °	5.02, 58.5
Z	4
F(000)	4064
ρ (*g/cm*)	1.370
λ, Å, (MoKα)	0.71073
μ, (*cm*$^{-1}$)	2.512
Diffractometer Type	Bruker Kappa Axis Apex2
Scan Type(s)	phi and omega scans
Max 2θ for data collection, °	61.118
Measured fraction of data	1.000
Number of reflections measured	209634
Unique reflections measured	29090
R_{merge}	0.1031
Number of reflections included in refinement	29090
Cut off Threshold Expression	I > 2sigma(I)
Structure refined using	full matrix least-squares using F^2
Weighting Scheme	$w=1/[sigma^2(Fo^2)+(0.0930P)^2]$ where $P=(Fo^2+2Fc^2)/3$
Number of parameters in least-squares	958
R_1	0.0494
wR_2	0.1237
R_1 (all data)	0.1149
wR_2 (all data)	0.1713
GOF	1.033
Maximum shift/error	0.002
Min & Max peak heights on final ΔF Map (e^-/Å)	-1.391, 1.541

Table A44. Atomic Coordinates for **33**

Atom	x	y	z	$U_{iso/equiv}$
Cu1	0.60677(2)	0.55441(2)	0.23058(2)	0.02043(11)
Cu2	0.48228(2)	0.55682(2)	0.24439(2)	0.02007(11)
Se1	0.51842(2)	0.60357(2)	0.15099(2)	0.02053(9)
Se2	0.57349(2)	0.57591(2)	0.32906(2)	0.02395(10)
Si1	0.52706(7)	0.70098(6)	0.18659(6)	0.0284(3)
Si2	0.57503(7)	0.48399(7)	0.37702(6)	0.0342(3)
N1	0.67884(17)	0.47396(15)	0.15742(16)	0.0217(7)
N2	0.74740(16)	0.52138(14)	0.23038(15)	0.0185(7)
N3	0.37734(17)	0.47101(15)	0.18572(15)	0.0206(7)
N4	0.33948(17)	0.53576(15)	0.24509(16)	0.0214(7)
C1	0.6812(2)	0.51283(18)	0.20673(18)	0.0193(8)
C2	0.7430(2)	0.45838(18)	0.14893(19)	0.0224(8)
C3	0.7872(2)	0.48876(18)	0.19630(19)	0.0204(8)
C4	0.8563(2)	0.4830(2)	0.2015(2)	0.0280(9)
C5	0.8787(2)	0.4455(2)	0.1593(2)	0.0321(10)
C6	0.8342(3)	0.4148(2)	0.1124(2)	0.0329(11)
C7	0.7666(2)	0.42046(19)	0.1059(2)	0.0275(9)
C8	0.6052(2)	0.4727(2)	0.0521(2)	0.0322(10)
C9	0.6145(2)	0.45141(19)	0.12013(19)	0.0246(9)
C10	0.6085(3)	0.3823(2)	0.1273(2)	0.0342(11)
C11	0.8111(3)	0.6141(2)	0.2709(2)	0.0379(12)
C12	0.7715(2)	0.5595(2)	0.2863(2)	0.0262(9)
C13	0.8094(3)	0.5208(3)	0.3398(2)	0.0401(12)
C14	0.3967(2)	0.51714(18)	0.22745(18)	0.0205(8)
C15	0.3085(2)	0.46144(19)	0.1757(2)	0.0254(9)
C16	0.2838(2)	0.50275(19)	0.21392(19)	0.0219(8)
C17	0.2160(2)	0.5060(2)	0.2157(2)	0.0275(9)
C18	0.1742(2)	0.4669(2)	0.1761(2)	0.0312(10)
C19	0.1988(2)	0.4255(2)	0.1372(2)	0.0344(11)
C20	0.2663(2)	0.4220(2)	0.1361(2)	0.0304(10)
C21	0.4147(3)	0.4487(2)	0.0873(2)	0.0341(11)
C22	0.4265(2)	0.43721(19)	0.1572(2)	0.0254(9)
C23	0.4257(3)	0.3692(2)	0.1742(2)	0.0357(11)
C24	0.2980(2)	0.6400(2)	0.2593(2)	0.0344(11)
C25	0.3392(2)	0.5860(2)	0.2901(2)	0.0272(9)
C26	0.3175(2)	0.5651(2)	0.3493(2)	0.0343(11)
C27	0.5113(4)	0.7560(2)	0.1197(3)	0.0578(17)
C28	0.4644(3)	0.7177(3)	0.2347(3)	0.0576(17)
C29	0.6115(3)	0.7157(3)	0.2343(4)	0.067(2)
C30	0.4958(3)	0.4749(3)	0.4070(3)	0.0562(17)
C31	0.6477(3)	0.4793(4)	0.4424(3)	0.073(2)

C32	0.5788(4)	0.4203(3)	0.3217(3)	0.067(2)
Cu3	0.04234(2)	0.76534(2)	0.44752(2)	0.01989(11)
Cu4	-0.08845(3)	0.77168(2)	0.44051(2)	0.02332(12)
Se3	-0.02677(2)	0.85151(2)	0.39353(2)	0.02115(9)
Se4	-0.02942(2)	0.67780(2)	0.42712(2)	0.02251(10)
Si3	-0.03347(7)	0.81806(6)	0.29486(6)	0.0308(3)
Si4	-0.01254(7)	0.63678(5)	0.52416(6)	0.0271(3)
N5	0.14786(17)	0.83394(16)	0.53195(16)	0.0223(7)
N6	0.19008(17)	0.76531(15)	0.47937(16)	0.0207(7)
N7	-0.16220(17)	0.83114(16)	0.52750(16)	0.0234(7)
N8	-0.2278(2)	0.77347(19)	0.4618(2)	0.0370(10)
C33	0.1310(2)	0.78664(18)	0.49126(18)	0.0197(8)
C34	0.2164(2)	0.84387(19)	0.54538(19)	0.0218(8)
C35	0.2568(2)	0.8867(2)	0.5820(2)	0.0288(10)
C36	0.3252(2)	0.8827(2)	0.5838(2)	0.0300(10)
C37	0.3521(2)	0.8384(2)	0.5507(2)	0.0282(10)
C38	0.3126(2)	0.7956(2)	0.5134(2)	0.0243(9)
C39	0.2437(2)	0.79898(18)	0.51132(18)	0.0192(8)
C40	0.0944(3)	0.9351(2)	0.5356(3)	0.0408(13)
C41	0.0971(2)	0.8686(2)	0.5578(2)	0.0329(11)
C42	0.1083(3)	0.8611(3)	0.6284(2)	0.0417(13)
C43	0.2204(2)	0.7323(2)	0.3802(2)	0.0335(11)
C44	0.1933(2)	0.71318(19)	0.4370(2)	0.0247(9)
C45	0.2299(3)	0.6588(2)	0.4710(3)	0.0395(12)
C46	-0.1637(2)	0.79164(19)	0.4794(2)	0.0266(9)
C47	-0.2262(2)	0.83832(19)	0.5406(2)	0.0233(9)
C48	-0.2681(2)	0.8016(2)	0.4984(2)	0.0299(10)
C49	-0.3361(2)	0.7977(3)	0.4984(2)	0.0390(12)
C50	-0.3607(2)	0.8321(3)	0.5415(2)	0.0379(12)
C51	-0.3187(2)	0.8692(2)	0.5837(2)	0.0336(11)
C52	-0.2512(2)	0.8736(2)	0.5836(2)	0.0300(10)
C53	-0.1046(3)	0.9302(3)	0.5456(3)	0.0584(18)
C54	-0.1011(2)	0.8618(2)	0.5593(2)	0.0362(12)
C55	-0.0860(3)	0.8461(3)	0.6288(3)	0.0577(17)
C56	-0.2322(4)	0.7508(4)	0.3492(3)	0.0273(16)
C57	-0.2618(5)	0.7382(4)	0.4058(4)	0.0257(18)
C58	-0.2537(7)	0.6713(5)	0.4253(5)	0.042(3)
C56A	-0.2785(7)	0.7421(6)	0.3640(7)	0.040(3)
C57A	-0.2385(7)	0.7161(7)	0.4204(6)	0.026(3)
C58A	-0.2675(9)	0.6616(8)	0.4472(8)	0.035(3)
C59	-0.0910(5)	0.7546(4)	0.2696(4)	0.045(2)
C59A	-0.1240(13)	0.7735(12)	0.2770(14)	0.065(7)
C60	-0.0532(3)	0.8840(2)	0.2397(2)	0.0401(12)
C61	0.0511(4)	0.7879(3)	0.2845(3)	0.067(2)
C62	0.0568(3)	0.5793(3)	0.5333(3)	0.0505(15)
C63	-0.0908(3)	0.5979(3)	0.5364(3)	0.0491(15)

C64	0.0102(3)	0.6969(3)	0.5857(2)	0.0493(15)
O1S	0.39801(18)	0.69295(17)	0.44083(18)	0.0424(9)
C1S	0.4293(3)	0.7149(2)	0.3937(3)	0.0431(13)
C2S	0.5016(3)	0.7229(3)	0.4241(3)	0.0511(15)
C3S	0.5135(3)	0.6688(3)	0.4677(3)	0.0451(14)
C4S	0.4432(3)	0.6516(2)	0.4786(2)	0.0395(12)
O2S	1.13928(19)	0.58009(18)	0.3230(2)	0.0486(10)
C5S	1.0853(3)	0.6189(2)	0.2991(2)	0.0393(12)
C6S	1.0244(3)	0.5783(3)	0.2860(3)	0.0455(13)
C7S	1.0385(3)	0.5345(2)	0.3418(2)	0.0388(12)
C8S	1.1150(3)	0.5320(3)	0.3564(3)	0.0457(13)
O3S	0.6985(4)	0.3039(3)	0.2746(3)	0.118(2)
C9S	0.7536(5)	0.3438(5)	0.2641(5)	0.102(3)
C10S	0.8117(7)	0.3270(6)	0.3061(7)	0.156(5)
C11S	0.7863(6)	0.2948(6)	0.3588(6)	0.127(4)
C12S	0.7188(5)	0.2883(5)	0.3418(5)	0.100(3)
O4S	-0.2968(11)	0.6672(10)	0.5772(10)	0.175(7)
O4SA	-0.2444(12)	0.6140(11)	0.6061(11)	0.197(8)
C13S	-0.3224(7)	0.6093(6)	0.5959(6)	0.147(5)
C14S	-0.3279(6)	0.6205(5)	0.6626(5)	0.126(4)
C15S	-0.2682(5)	0.6561(5)	0.6887(5)	0.112(3)
C16S	-0.2391(8)	0.6843(8)	0.6299(8)	0.183(6)

Table A.45. Summary of Crystal Data for **34**

Formula	$C_{99.97}H_{151.94}Cu_{10}Hg_3N_{12}O_{5.49}S_8$
Formula Weight (*g/mol*)	3103.44
Crystal Dimensions (*mm*)	0.260 × 0.163 × 0.126
Crystal Color and Habit	yellow block
Crystal System	monoclinic
Space Group	P 2_1/n
Temperature, K	110
a, Å	17.820(4)
b, Å	34.856(4)
c, Å	21.289(4)
α,°	90
β,°	100.093(10)
γ,°	90
V, Å^3	13018(4)
Number of reflections to determine final unit cell	9478
Min and Max 2θ for cell determination, °	5.22, 57.32
Z	4
F(000)	6151
ρ (*g/cm*)	1.583
λ, Å, (MoKα)	0.71073
μ, (cm^{-1})	5.295
Diffractometer Type	Bruker Kappa Axis Apex2
Scan Type(s)	phi and omega scans
Max 2θ for data collection, °	72.908
Measured fraction of data	1.000
Number of reflections measured	561862
Unique reflections measured	63135
R_{merge}	0.1237
Number of reflections included in refinement	63135
Cut off Threshold Expression	I > 2sigma(I)
Structure refined using	full matrix least-squares using F^2
Weighting Scheme	$w=1/[sigma^2(Fo^2)+(0.1202P)^2]$ where $P=(Fo^2+2Fc^2)/3$
Number of parameters in least-squares	1308
R_1	0.0686
wR_2	0.1875
R_1 (all data)	0.1879
wR_2 (all data)	0.2464
GOF	1.038
Maximum shift/error	0.004
Min & Max peak heights on final ΔF Map (e^-/Å)	-3.139, 1.685

Table A.46. Atomic Coordinates for **34**

Atom	x	y	z	$U_{iso/equiv}$
Hg1	0.61876(2)	0.79120(2)	0.37337(2)	0.03301(6)
Hg2	0.80039(2)	0.80968(2)	0.59330(2)	0.04747(8)
Hg3	0.85009(2)	0.88704(2)	0.39687(2)	0.03743(7)
Cu0	0.74666(4)	0.83068(2)	0.45691(4)	0.03440(17)
Cu1	0.71018(4)	0.85206(2)	0.31073(4)	0.03528(17)
Cu2	0.65335(5)	0.76627(3)	0.51895(4)	0.0435(2)
Cu3	0.90320(5)	0.86747(3)	0.53661(4)	0.0454(2)
Cu4	0.64311(5)	0.90764(2)	0.38938(4)	0.03643(18)
Cu5	0.80891(5)	0.78570(2)	0.32950(4)	0.03682(18)
Cu6	0.58183(5)	0.83758(3)	0.51806(4)	0.03768(18)
Cu7	0.77801(5)	0.73055(3)	0.48374(4)	0.0424(2)
Cu8	0.75315(5)	0.90858(3)	0.55241(5)	0.0463(2)
Cu9	0.94006(5)	0.80242(3)	0.47061(4)	0.03895(19)
S1	0.67688(10)	0.79414(5)	0.28369(8)	0.0369(4)
S2	0.74354(10)	0.91089(5)	0.32979(9)	0.0400(4)
S3	0.75376(13)	0.74685(7)	0.58321(10)	0.0537(5)
S4	0.54990(10)	0.78327(5)	0.45614(9)	0.0410(4)
S5	0.81919(10)	0.78427(5)	0.43623(8)	0.0373(4)
S6	0.67061(10)	0.87444(5)	0.48088(8)	0.0380(4)
S7	0.96534(10)	0.86775(6)	0.45809(9)	0.0421(4)
S8	0.84667(12)	0.87168(7)	0.61738(10)	0.0565(5)
N1	0.4947(3)	0.91858(18)	0.3063(3)	0.0398(13)
N2	0.5536(3)	0.97284(16)	0.3236(3)	0.0406(13)
N3	0.8703(3)	0.74599(18)	0.2270(3)	0.0421(14)
N4	0.9040(3)	0.80544(19)	0.2333(3)	0.0409(13)
N5	0.5630(3)	0.84307(18)	0.6527(3)	0.0405(13)
N6	0.4684(3)	0.86939(17)	0.5916(3)	0.0393(13)
N7	0.7142(4)	0.66353(18)	0.4086(3)	0.0445(14)
N8	0.8305(4)	0.65385(18)	0.4555(3)	0.0512(16)
N9	0.8169(4)	0.9854(2)	0.5508(4)	0.0562(19)
N10	0.7274(3)	0.9863(2)	0.6074(3)	0.0501(16)
N11	1.0888(3)	0.76354(17)	0.4732(3)	0.0374(12)
N12	1.0444(3)	0.75309(16)	0.5604(3)	0.0336(11)
C1	0.5579(4)	0.9358(2)	0.3411(3)	0.0365(14)
C2	0.4504(4)	0.9449(2)	0.2668(3)	0.0448(17)
C3	0.4900(5)	0.9798(2)	0.2784(4)	0.0526(19)
C4	0.4614(6)	1.0130(3)	0.2449(5)	0.068(3)
C5	0.3951(7)	1.0092(4)	0.2017(6)	0.086(3)
C6	0.3575(7)	0.9749(4)	0.1911(5)	0.087(4)
C7	0.3848(5)	0.9411(3)	0.2244(4)	0.063(2)
C8	0.4859(4)	0.8564(2)	0.2513(4)	0.0486(18)

C9	0.4811(4)	0.8771(2)	0.3127(4)	0.0437(16)
C10	0.4045(5)	0.8701(3)	0.3334(5)	0.064(2)
C11	0.6645(5)	1.0084(2)	0.3017(5)	0.057(2)
C12	0.6070(5)	1.0038(2)	0.3481(5)	0.055(2)
C13	0.6441(6)	0.9982(3)	0.4159(5)	0.066(3)
C14	0.8680(4)	0.7779(2)	0.2620(4)	0.0426(16)
C15	0.9043(4)	0.7535(2)	0.1744(4)	0.0459(17)
C16	0.9269(4)	0.7909(2)	0.1786(4)	0.0441(17)
C17	0.9626(4)	0.8081(3)	0.1320(4)	0.0499(19)
C18	0.9742(5)	0.7844(3)	0.0813(4)	0.057(2)
C19	0.9499(6)	0.7465(3)	0.0767(4)	0.063(2)
C20	0.9152(5)	0.7300(2)	0.1229(4)	0.054(2)
C21	0.7539(6)	0.7053(2)	0.1972(5)	0.059(2)
C22	0.8375(5)	0.7081(2)	0.2381(4)	0.0482(19)
C23	0.8388(5)	0.6996(2)	0.3077(4)	0.053(2)
C24	0.8691(5)	0.8728(3)	0.2145(4)	0.056(2)
C25	0.9151(5)	0.8441(2)	0.2589(4)	0.0502(19)
C26	1.0004(5)	0.8546(3)	0.2761(5)	0.073(3)
C27	0.5346(4)	0.8497(2)	0.5905(3)	0.0372(14)
C28	0.5155(4)	0.8577(2)	0.6933(3)	0.0401(15)
C29	0.4559(4)	0.8739(2)	0.6527(4)	0.0412(16)
C30	0.3951(5)	0.8925(2)	0.6766(4)	0.0484(18)
C31	0.4025(5)	0.8926(2)	0.7432(4)	0.051(2)
C32	0.4645(5)	0.8761(2)	0.7833(4)	0.0486(19)
C33	0.5233(5)	0.8580(2)	0.7594(4)	0.0507(19)
C34	0.6134(6)	0.7819(3)	0.6992(5)	0.077(3)
C35	0.6327(5)	0.8205(3)	0.6729(4)	0.054(2)
C36	0.6930(5)	0.8416(3)	0.7184(5)	0.076(3)
C37	0.3736(7)	0.8508(3)	0.4992(5)	0.087(4)
C38	0.4143(5)	0.8825(3)	0.5326(5)	0.063(2)
C39	0.4564(8)	0.9141(3)	0.4995(6)	0.072(4)
C38'	0.4143(5)	0.8825(3)	0.5326(5)	0.063(2)
C39'	0.3971(18)	0.9154(9)	0.5170(16)	0.020(8)
C40	0.7722(4)	0.6791(2)	0.4482(4)	0.0434(16)
C41	0.7343(5)	0.6265(2)	0.3894(4)	0.0468(18)
C42	0.8075(5)	0.6209(2)	0.4185(4)	0.052(2)
C43	0.8490(5)	0.5874(2)	0.4088(4)	0.0513(19)
C44	0.8089(6)	0.5608(3)	0.3692(4)	0.062(2)
C45	0.7360(6)	0.5661(3)	0.3394(4)	0.061(2)
C46	0.6946(5)	0.5988(2)	0.3480(4)	0.055(2)
C47	0.6140(5)	0.6875(2)	0.3213(4)	0.053(2)
C48	0.6380(4)	0.6815(2)	0.3923(4)	0.0426(16)
C49	0.5793(5)	0.6604(3)	0.4230(5)	0.074(3)
C50	0.9687(7)	0.6644(4)	0.4712(6)	0.096(4)
C51	0.9024(5)	0.6596(3)	0.5021(4)	0.065(3)
C52	0.9092(8)	0.6291(3)	0.5522(5)	0.090(4)

C53	0.7621(4)	0.9628(2)	0.5704(4)	0.0501(19)
C54	0.8188(4)	1.0224(2)	0.5757(4)	0.051(2)
C55	0.7604(4)	1.0232(2)	0.6119(4)	0.0481(18)
C56	0.7465(5)	1.0557(2)	0.6457(4)	0.056(2)
C57	0.7918(5)	1.0873(3)	0.6412(5)	0.064(2)
C58	0.8487(5)	1.0869(3)	0.6053(5)	0.062(2)
C59	0.8644(5)	1.0540(3)	0.5726(6)	0.072(3)
C60	0.8614(6)	0.9930(3)	0.4464(5)	0.073(2)
C61	0.8681(5)	0.9691(3)	0.5098(5)	0.0614(19)
C62	0.9503(5)	0.9669(3)	0.5491(6)	0.072(2)
C63	0.5895(7)	0.9807(5)	0.5844(7)	0.115(4)
C64	0.6633(6)	0.9755(3)	0.6385(6)	0.074(3)
C65	0.6560(9)	0.9363(4)	0.6548(8)	0.086(4)
C64'	0.6633(6)	0.9755(3)	0.6385(6)	0.074(3)
C65'	0.724(2)	0.9552(10)	0.7047(17)	0.066(11)
C66	1.0276(4)	0.77136(19)	0.5034(3)	0.0346(13)
C67	1.1430(4)	0.7421(2)	0.5121(3)	0.0379(14)
C68	1.1152(4)	0.73540(19)	0.5677(3)	0.0367(14)
C69	1.1570(4)	0.7147(2)	0.6172(4)	0.0457(17)
C70	1.2266(5)	0.7006(2)	0.6095(4)	0.0518(19)
C71	1.2543(5)	0.7073(3)	0.5542(4)	0.056(2)
C72	1.2124(4)	0.7278(2)	0.5038(3)	0.0427(16)
C73	1.0871(6)	0.7499(3)	0.3618(4)	0.061(2)
C74	1.0920(5)	0.7785(3)	0.4102(4)	0.053(2)
C75	1.1571(5)	0.8064(2)	0.4131(4)	0.053(2)
C76	0.9819(5)	0.7199(3)	0.6418(4)	0.056(2)
C77	0.9936(4)	0.7573(2)	0.6078(3)	0.0423(16)
C78	1.0215(5)	0.7901(3)	0.6556(4)	0.058(2)
O1S	0.2183(4)	0.91543(19)	0.6032(4)	0.0746(19)
C1S	0.1770(6)	0.9122(3)	0.6548(5)	0.073(3)
C2S	0.1170(5)	0.8836(3)	0.6355(6)	0.082(3)
C3S	0.1398(5)	0.8621(3)	0.5811(4)	0.061(2)
C4S	0.2086(7)	0.8808(4)	0.5688(6)	0.104(4)
O2S	1.2890(5)	0.7317(3)	0.3623(4)	0.101(3)
C5S	1.3578(8)	0.7116(5)	0.3748(7)	0.139(5)
C6S	1.3947(8)	0.7188(4)	0.3177(7)	0.141(5)
C7S	1.3527(8)	0.7518(4)	0.2825(6)	0.118(4)
C8S	1.2968(9)	0.7620(4)	0.3218(8)	0.132(6)
O3S	0.8700(5)	0.4664(2)	0.3569(4)	0.099(2)
C9S	0.9082(7)	0.4338(3)	0.3377(6)	0.089(3)
C10S	0.8744(7)	0.3994(3)	0.3644(6)	0.100(4)
C11S	0.8026(7)	0.4132(4)	0.3847(9)	0.133(4)
C12S	0.8004(8)	0.4528(4)	0.3700(9)	0.130(4)
O4S	1.0062(11)	0.5471(4)	0.4921(9)	0.110(3)
C13S	1.0453(15)	0.5284(6)	0.4483(12)	0.110(3)
C14S	1.0638(15)	0.4906(7)	0.4772(14)	0.110(4)

C15S	1.0058(16)	0.4832(6)	0.5190(14)	0.110(3)
C16S	0.9674(15)	0.5192(6)	0.5207(14)	0.110(3)
O5S	0.2511(9)	0.8714(5)	0.2050(8)	0.208(5)
C17S	0.1879(12)	0.8895(5)	0.1665(11)	0.198(6)
C18S	0.1629(13)	0.8564(6)	0.1228(9)	0.205(6)
C19S	0.1670(11)	0.8254(5)	0.1708(11)	0.187(6)
C20S	0.2468(10)	0.8316(5)	0.2005(11)	0.183(5)
O6S	1.0041(11)	0.9120(6)	0.8150(13)	0.281(6)
C21S	0.9515(17)	0.9238(9)	0.8538(10)	0.281(6)
C22S	0.8815(12)	0.9257(9)	0.8041(15)	0.282(6)
C23S	0.9111(17)	0.9452(8)	0.7506(13)	0.282(6)
C24S	0.9801(17)	0.9216(9)	0.7509(12)	0.281(6)

Appendix 3 $^{77}Se\{^{1}H\}$ NMR Spectra of **2**, **4**, **6**, **8**, **10**, **12**

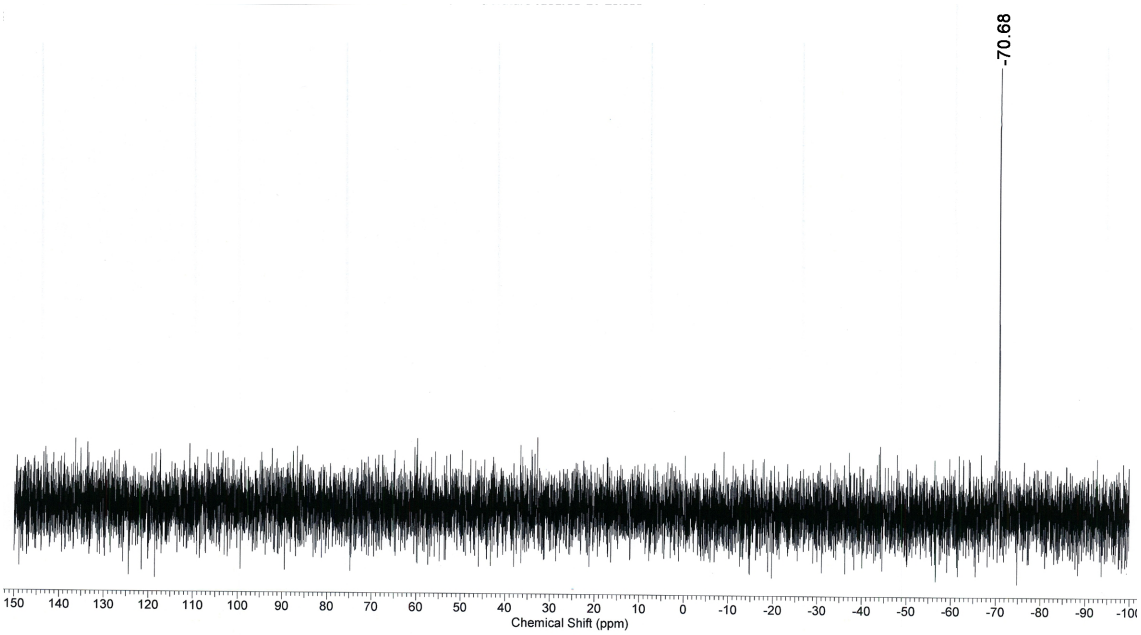

Figure A3.1. $^{77}Se\{^{1}H\}$ NMR spectrum of **2** ($CDCl_3$, 23 °C, 76.24 MHz).

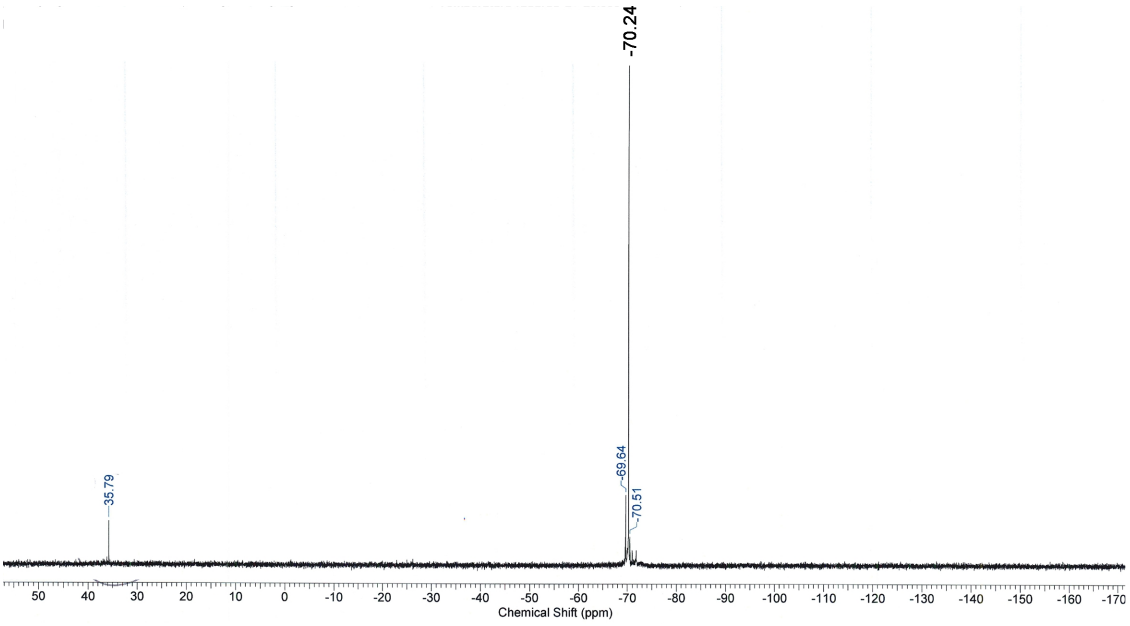

Figure A3.2. $^{77}Se\{^{1}H\}$ NMR spectrum of **4** ($CDCl_3$, 23 °C, 76.24 MHz).

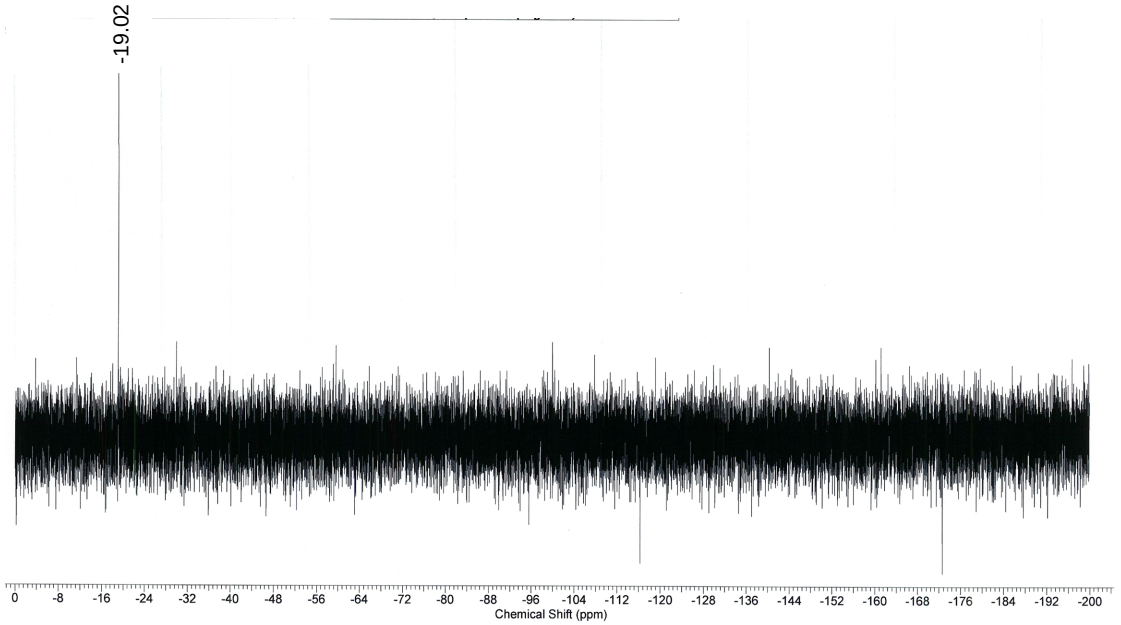

Figure A3.3. $^{77}Se\{^{1}H\}$ NMR spectrum of **6** ($CDCl_3$, 23 °C, 76.23 MHz).

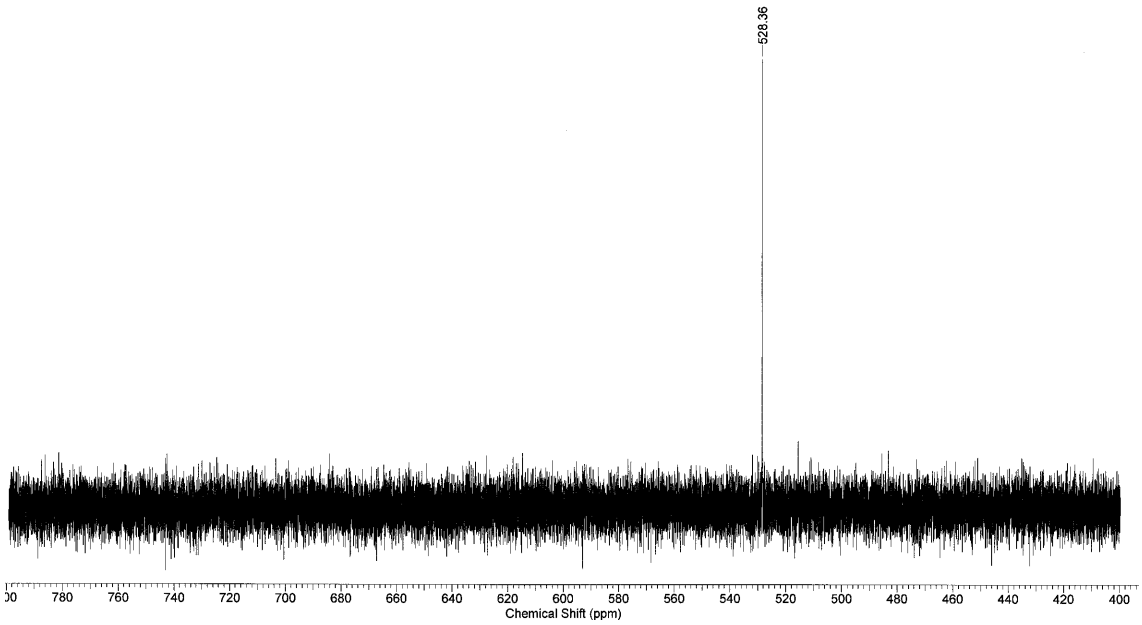

Figure A3.4. $^{77}Se\{^{1}H\}$ NMR spectrum of **8** ($CDCl_3$, 23 °C, 76.29 MHz).

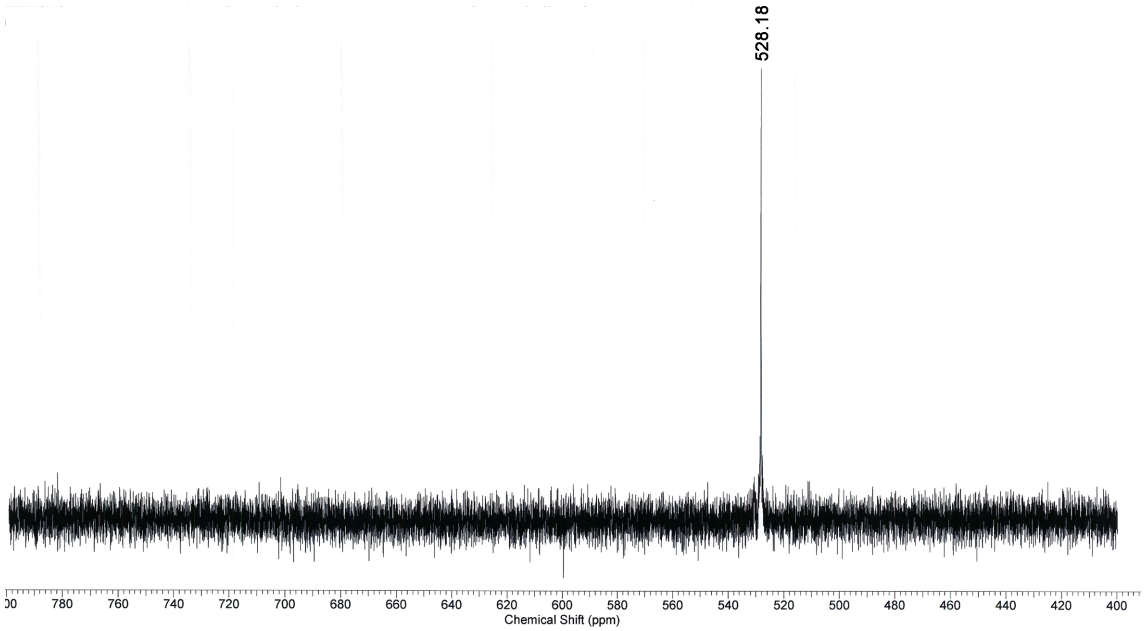

Figure A3.5. $^{77}Se\{^{1}H\}$ NMR spectrum of **10** ($CDCl_3$, 23 °C, 76.29 MHz).

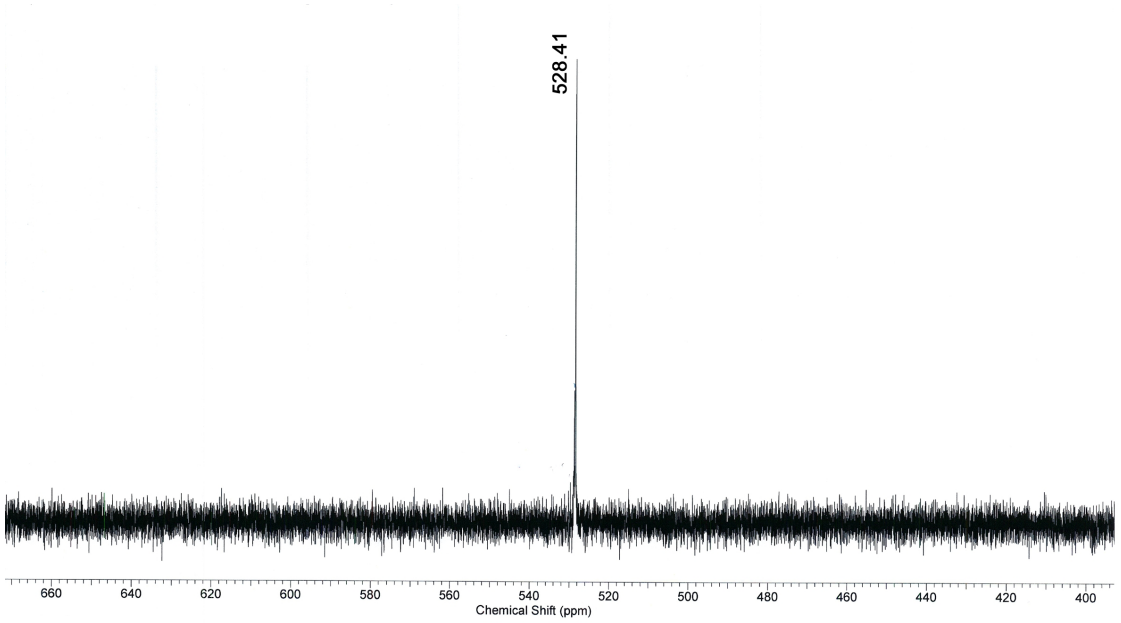

Figure A3.6. $^{77}Se\{^{1}H\}$ NMR spectrum of **12** ($CDCl_3$, 23 °C, 76.29 MHz).

Curriculum Vitae

Name: Mahmood Azizpoor Fard

Post-secondary Education and Degrees:

University of Tehran
Tehran, Iran
2002-2006 B.A.

The National University of Iran
Tehran, Iran
2007-2009 M.A.

The University of Western Ontario
London, Ontario, Canada
2011-2015 Ph.D.

Related Work Experience

Teaching Assistant
The University of Western Ontario
2011-2015

Crystallography Lab Technician
The University of Western Ontario
2013-2015

Publications:

2015 "NHC Stabilized Bis(trimethylsilyl)phosphido Complexes of Pd(II) and Ni(II)",
Madadi, M.; Khalili Najafabadi, B.; Azizpoor Fard, M.; Corrigan, J. F., *Eur. J. Inorg. Chem.,* Submitted, **2015**, 3094–3101.

2015 "Simple but Effective: Thermally Stable Cu-ESiMe$_3$ via NHC Ligation"
Azizpoor Fard, M.; Weigend, F.; Corrigan, J. F., *Chem. Commun.*, **2015**, *51*, 8361-8364.

2015 "Polydentate Chalcogen Reagents for the Facile Preparation of Pd_2 and Pd_4 Complexes",
Azizpoor Fard, M.; Willans, M. J.; Khalili Najafabadi, B.; Levchenko T. I., Corrigan, J. F., *Dalton Trans.*, **2015**, *44*, 8267-8277.

2015 "Functionalized Ag_2S Molecular Architectures - Facile Assembly of the Atomically Precise Ferrocene Decorated Nanocluster $[Ag_{74}S_{19}(dppp)_6(fc(C\{O\}OCH_2CH_2S)_2)_{18}]$",
Liu, Y.; Khalili Najafabadi, B.; Azizpoor Fard, M.; Corrigan J. F., *Angew. Chem., Int. Ed.*, **2015**, *54*, 4832–4835.

2014 Back Cover: New Polydentate Trimethylsilyl Chalcogenide Reagents for the Assembly of Polyferrocenyl Architectures, (Azizpoor Fard, M.; Corrigan, J. F., *Chem. Eur. J.* 23/**2014**) (page 7172)

2014 “New Polydentate Trimethylsilyl Chalcogenide Reagents for the Assembly of Polyferrocenyl Architectures”, Azizpoor Fard, M.; Khalili Najafabadi, B.; Hessari, M.; Workentin, M. S.; Corrigan, J. F., *Chem. Eur. J.*, 2014, *20*, 7037-7047.

2012 “Influence of ligand substituent on structural assembly and coordination geometry”, Khavasi, H. R.; Mehdizadeh Barforoush, M.; Azizpoor Fard, M., *CrystEngComm,* 2012, *14*, 7236-7244

2010 "π-π interactions affect coordination geometry", Khavasi, H. R.; Azizpoor Fard, M., *Cryst. Growth Des.*, **2010**, *10*, 1892-1896.

2010 "(1-Naphthylmethyl) ammonium chloride”, Salimi, A. R.; Azizpoor Fard, M.; Eshtiagh-Hosseini, H.; Amini, M. M.; Khavasi, H. R., *Acta Crystallogr. Sect. E.,* **2010**, *E66*, o509.

2006 "First catalytic application of metal complexes of porpholactone and dihydroxychlorin in the sulfoxidation reaction",

Rahimi, R.; Azhdari Tehrani, A.; Azizpoor Fard, M.; Mir Mohammad Sadegh, B.; Khavasi, H. R., *Catalysis Communications,* **2009**, *11*, 232-235.